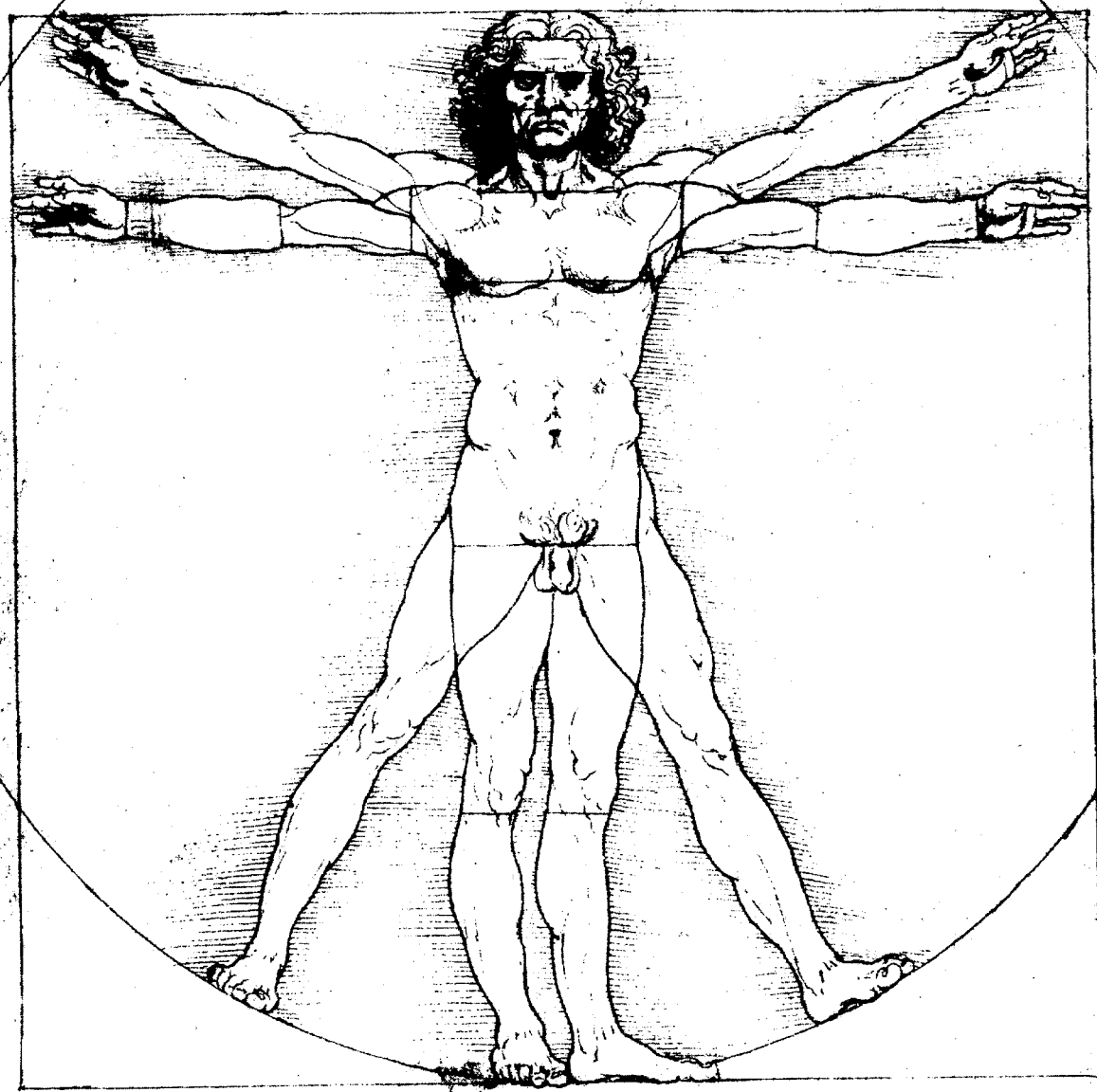


Handwritten text at the top of the page, likely bleed-through from the reverse side. It contains several lines of cursive script, possibly in a historical or scientific context.

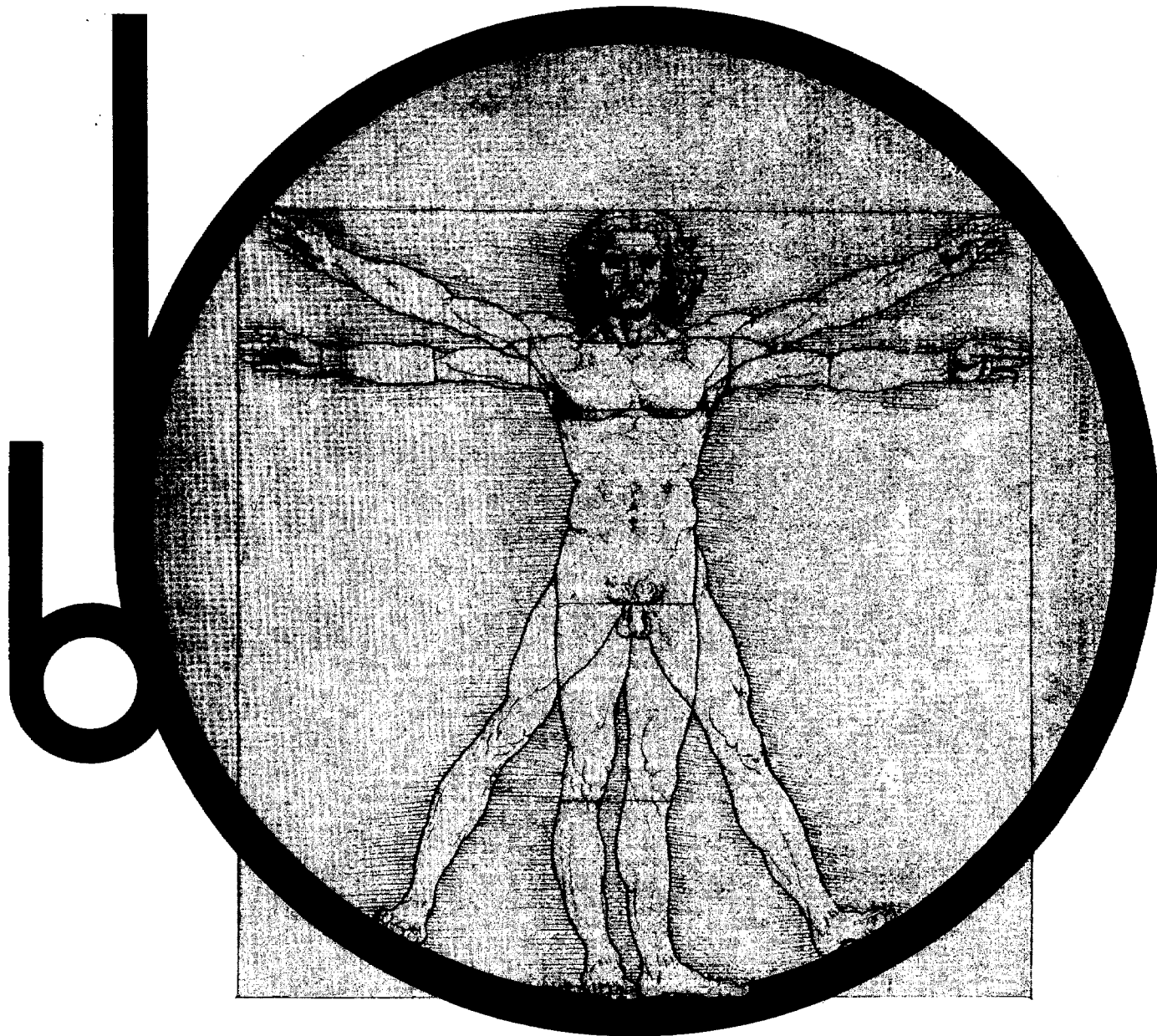
January 1968

# FERMILAB-NAL-DESIGN REPORT



Handwritten text below the Vitruvian Man drawing, likely bleed-through from the reverse side. It includes a horizontal line with tick marks above it, and several lines of cursive script.

Handwritten text at the bottom of the page, likely bleed-through from the reverse side. It contains several lines of cursive script, continuing the text from the previous block.



design report

**national  
accelerator  
laboratory**



# **national accelerator laboratory**

**Design Report January 1968**

**Universities Research Association**

**Under the Auspices of the**

**United States Atomic Energy Commission**

PAAP4430

## **Preface**





## PREFACE

This report is directed at a variety of readers; in some instances it will be an interested layman, in others it might be a new employee of the Laboratory. In any case, the object of the report is to explain exactly and precisely what it is that we are planning to build. It is divided into seven major parts of which the first (Part A) contains three chapters that describe the National Accelerator Laboratory and the proposed proton accelerator in non-technical terms.

The design report is the result of the efforts of members of the National Accelerator Laboratory and of visitors to the Laboratory since work on the new design started on June 15, 1967. Because so many people have contributed in such varying degrees to the design, it is impossible to give proper credit to them. In general, the report has been prepared on the basis of rough drafts submitted by the person in charge of the particular phase of the work. A list of principal contributors to the work described in each chapter of the report is given under the chapter heading. The name of the head of the section responsible for the work, or of the person submitting the first draft, has been underlined. A second list is given of people who have been more peripherally concerned, for example, by visits to the Laboratory or by participation in the Summer Study. An attempt has also been made to identify the contribution of others by giving references in the text. Many of the people whose names have been listed but not underlined have not participated in the writing of the report and therefore cannot be responsible for the material contained herein. This procedure does not properly acknowledge the very broad contribution of many, if not most, of the people in the Laboratory. In particular, the work of T. L. Collins and Lee Teng has been so extensive that for simplicity their names have not been added to more than one list.

Architectural-engineering work and cost estimates associated with conventional structures have been performed by DUSAF, a joint venture of four firms: Daniel, Mann, Johnson and Mendenhall; the Office of Max O. Urbahn; Seelye Stevenson Value & Knecht, Inc.; George A. Fuller Company.

Engineering work and cost estimates associated with technical components were performed for the National Accelerator Laboratory by William M. Brobeck and Associates.

The major responsibility for preparation and editing of this report was carried by F. T. Cole. We have shared with him the responsibility for final editing.

Robert Rathbun Wilson

Edwin L. Goldwasser

## TABLE OF CONTENTS

### A. General Discussion

1. Introduction
2. Purpose and Character of the Laboratory
3. Summary of the Report

### B. Detailed Description of the Accelerator

4. Main-Synchrotron Lattice and Orbits
5. Main-Synchrotron Magnet System
6. Main-Synchrotron Vacuum System
7. Main-Synchrotron Accelerating System
8. Main-Synchrotron Enclosure
9. Booster Accelerator
10. Linear Accelerator
11. Monitoring and Control System
12. Radiation and Shielding

### C. Provisions for Experimental Use

13. Beam-Extraction and Transport System
14. Experimental Areas and Programs

### D. Physical Plant

15. Physical Plant

### E. Costs and Schedules

16. Construction Cost Estimate and Schedule
17. Estimates of Operating Program

### F. Provisions for Future Expansion

18. Provisions for Future Expansion,

Appendix - Accelerator Parameters

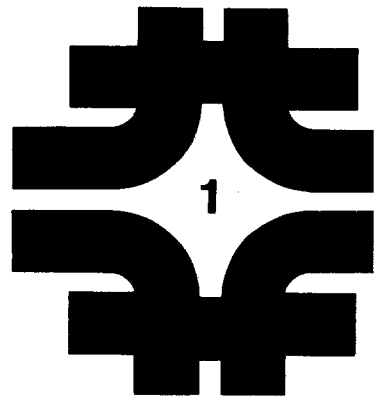
## General Discussion

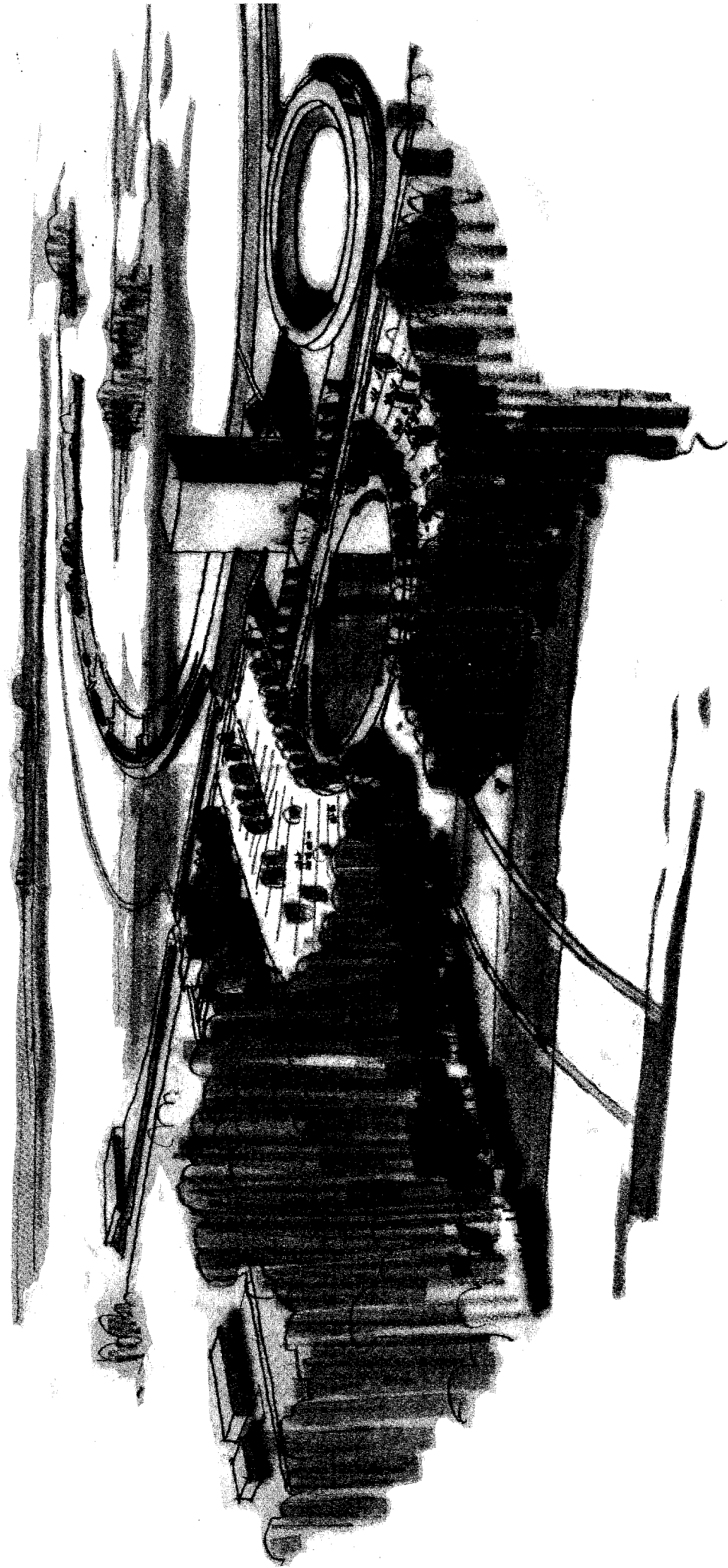
1. Introduction

2. Purpose and Character of the Laboratory

3. Summary of the Report

# Introduction





The National Accelerator Laboratory

## 1. INTRODUCTION

After almost a decade of intensive effort and study on the part of American scientists, of the Joint Committee on Atomic Energy of the United States Congress and of the United States Atomic Energy Commission, initial steps toward construction of a major new laboratory have been authorized by the Congress and the President of the United States. A national facility is projected, for which the world's most powerful proton accelerator will be constructed. Much of the background and motivation for this project has been described in a series of hearings before the Joint Committee on Atomic Energy of the U. S. Congress.<sup>1,2,3</sup> In these, witnesses have developed the idea that this instrument will enable physicists to probe more deeply into the structure of matter than ever before. It can be expected with confidence that the limits of our knowledge of the physical world will be greatly enlarged.

The National Accelerator Laboratory, shown opposite in artist's concept, will be constructed during the next few years in DuPage and Kane Counties, about 30 miles west of Chicago, on a 6,800 acre site which will be donated by the State of Illinois. The principal scientific instrument of the Laboratory will be a proton synchrotron of 200 BeV energy designed for an intensity of  $5 \times 10^{13}$  protons per pulse or  $1.5 \times 10^{13}$  protons per second. The most prominent part of the accelerator will be a ring of magnets which will be 1-1/4 miles in diameter.

A unique feature of the design of the accelerator is its flexibility. Should higher levels become desirable, the peak proton energy can be raised to more than 400 BeV - perhaps to as much as 500 BeV - without extensive modification of the accelerator and without seriously interrupting the current research program. It is this interesting aspect of the design that helps to assure that the Laboratory will be able to maintain this country's traditional position in the forefront of high-energy physics research.

This design report gives our solutions to the problems of constructing a proton synchrotron and ancillary experimental facilities on the Illinois site. We are confident that the accelerator can successfully be constructed in this way and within our cost estimates. It should be emphasized, though, that as we go into the phase of detailed design we do, of course, expect to make improvements and refinements.

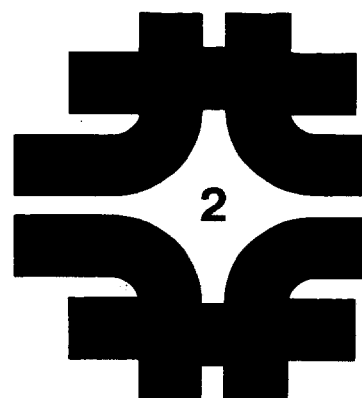
The work leading to the concepts outlined in this report has been done at the headquarters of the National Accelerator Laboratory at Oak Brook, Illinois, in the Summer and Fall of 1967. That plans of such complexity could be developed so swiftly is due to the intense interest and hard work of many high-energy physicists in the U.S. and abroad. Many of our concepts of the experimental areas has been derived from the CERN 300 BeV utilization study <sup>4</sup> generously provided by them. We have also leaned heavily on the CERN 300 BeV design study<sup>5</sup>. Of course, most basic of all to this study was the thorough exploration of the many facets and problems of the project carried out by the Lawrence Radiation Laboratory <sup>6</sup>, University of California, Berkeley. The cooperation of the Lawrence Radiation Laboratory in the present plans for the accelerator is gratefully acknowledged.

References:

1. High Energy Physics Program: Report on National Policy and Background Information, Joint Committee on Atomic Energy, Congress of the United States, (89th Congress), February, 1965.
2. High Energy Physics Research. Hearings before the Subcommittee on Research, Development, and Radiation of the Joint Committee on Atomic Energy, Congress of the United States (89th Congress), March 2, 3, 4 and 5, 1965.
3. AEC Authorizing Legislation, Fiscal Year 1968, Hearings before the Joint Committee on Atomic Energy, Congress of the United States (90th Congress) (Including Hearings Before the Subcommittee on Research, Development and Radiation on Management and Scope of the Proposed 200 BeV Accelerator, February 15 and 16, 1967).
4. ECFA (European Committee for Future Accelerators) Report 1967, CERN/ECFA 67/13, May, 1967.
5. Report on the Design Study of a 300 GeV Proton Synchrotron, CERN Report AR/Int. SG/64-15, Nov., 1964.
6. 200 BeV Accelerator Design Study, University of California, Lawrence Radiation Laboratory Report UCRL - 16000, June 1965.

# **Purpose and Character of the Laboratory**

- |  |     |
|--|-----|
| 1. Background of the High-Energy<br>Physics Program  | 2-1 |
| 2. Problems of High-Energy Physics   | 2-2 |
| 3. The Role of the Universities and<br>the Staff of the<br>National Accelerator Laboratory | 2-3 |
| 4. Organization  | 2-5 |





## 2. PURPOSE AND CHARACTER OF THE LABORATORY

### 1. Background of the High-Energy Physics Program

The proton synchrotron described here is a major step in the progressive construction of machines designed to accelerate protons to higher and ever higher energies. The first accelerator typical of this series was the cyclotron of E. O. Lawrence, invented in the early Thirties, by the use of which many of the properties of the nucleus of the atom were explored. In this kind of research, protons are first accelerated to high speed and then are directed at a target consisting of the material to be studied. By measuring how the protons are deflected at various angles in the collisions that occur with the atoms of the material, it is possible to deduce the form and structure of the atoms - even though they are invisible in the normal sense of the word. In this way, by directing particles at thin foils, Rutherford discovered that the atom has a nucleus. By similar experiments with particles of higher energies, physicists found that the nucleus itself has an inner structure, being made up of more fundamental particles, protons and neutrons.

The higher the energy of the bombarding protons, the more detail it is possible to discern in the structure of these particles. One can think of an accelerator and its detecting equipment as though it were a huge microscope; then its resolving power is proportional to the energy of the accelerator. Thus the high-energy protons produced by an accelerator allow us to examine and measure the properties of particles and, among other things, to see if they really are fundamental or whether they in turn are made of other more basic particles.

As the first exploration of the nucleus was made, it was felt that the fundamental particles were very simple. There seemed to be only three kinds: neutrons and protons that exist in the nucleus and electrons that exist in orbits, or better, in cloud-like formations, in the space around the nucleus. However, as the energy of the proton beams was raised, it was found that this picture was much too simple. All sorts of new particles such as mesons were produced in the collisions that occurred, for example, between the protons of the beam and the target protons. Furthermore, it was found that the proton itself changed its form - sometimes changing into a neutron but sometimes changing into more esoteric and complex structures. By now, instead of reaching the simple explanation of all matter in terms of a few particles, we have found more than 100 "fundamental particles", more than the number of chemical elements, about 100, that were to be explained by them in the first place.

That nature is more complex than first expected is a challenge rather than a disappointment. In building higher energy accelerators to study these complexities, all kinds of exciting and fundamental discoveries have been made. Not only have various kinds of new elementary particles been observed, but also new physical laws have been discovered while old laws have been observed to be violated.

It is interesting to compare the study of the very small with the study of the very large in nature. In both fields, the studies are being pushed vigorously, and both require a high degree of sophisticated instrumentation. The nuclear physicists see "in" about as many orders of magnitude in distance as astronomers see "out". The physicists' discovery of a world of sub-particles can be matched by the astronomers' discovery of quasars - tremendously distant and fantastically energetic objects.

In previous studies of the nucleus, physicists were able to understand why the stars shine and how matter is made. Today, a new mechanism for an intense release of energy is part of current theoretical conjectures about the possible formation of protons and neutrons from some still more fundamental particles, called quarks. The probability is small that an understanding of the mysteriously dense energy source of the quasars can be explained in terms of quarks, but it is almost certain that other phenomena almost as interesting will be related by an eventual understanding of the nature of fundamental particles.

This is not to imply that benefits will be forthcoming from this study that are the equivalent of those that came from previous nuclear research. Nevertheless, pure science, the search for understanding, is as important for its effect on the minds of men as it is for its eventual contributions to his standard of living. Man's effort to achieve a better comprehension of the world in which he lives will continue to have a profound effect not only on his philosophy, not only on his well-being, but also on his whole social organization.

## 2. Problems of High-Energy Physics

We would like to have answers to many questions. Among them are the following:

Which, if any, of the particles that have so far been discovered, is, in fact, elementary, and is there any validity in the concept of "elementary" particles?

What new particles can be made at energies that have not yet been reached? Is there some set of building blocks that is still more fundamental than the neutron and the proton?

Is there a law that correctly predicts the existence and nature of all the particles, and if so, what is that law?

Will the characteristics of some of the very short-lived particles appear to be different when they are produced at such higher velocities that they no longer spend their entire lives within the strong influence of the particle from which they are produced?

Do new symmetries appear or old ones disappear for high momentum-transfer events?

What is the connection, if any, of electromagnetism and strong interactions?

Do the laws of electromagnetic radiation, which are now known to hold over an enormous range of lengths and frequencies, continue to hold in the wavelength domain characteristic of the subnuclear particles?

What is the connection between the weak interaction that is associated with the massless neutrino and the strong one that acts between neutron and proton?

Is there some new particle underlying the action of the "weak" forces, just as, in the case of the nuclear force, there are mesons, and, in the case of the electromagnetic force, there are photons? If there is not, why not?

In more technical terms: Is local field theory valid? A failure in locality may imply a failure in our concept of space. What are the fields relevant to a correct local field theory? What are the form factors of the particles? What exactly is the explanation of the electromagnetic mass difference? Do "weak" interactions become strong at sufficiently small distances? Is the Pomeranchuk theorem true? Do the total cross sections become constant at high energy? Will new symmetries appear, or old ones disappear, at higher energy?

These are some of the questions before elementary-particle physics; there is good reason to believe that they can be clarified by experiments at higher energies than those available in present-day accelerators. Although these are the problems that today appear to be the "right" ones to investigate, the best questions have undoubtedly not yet been asked. Only further experimental investigation with an instrument such as we are building will give us the insight to ask them. Nature in the past has always surprised us. It is probable that, as we take the step up to an energy of 200 BeV, more surprises await us.

### 3. The Role of the Universities and the Staff of the National Accelerator Laboratory

Like most significant areas of basic research in the United States, elementary-particle physics has its foundations in the nation's institutions of higher learning. The relationship between higher education and research is fundamental to both. Research flourishes only in a hospitable environment in which the value of scientific contributions

is recognized and in which communications between the fields of knowledge are open and easy. This climate automatically exists at a university where the active participation of students and faculty in research is an essential ingredient of the educational process.

The large size of the accelerator precludes its being located at any single university. However, the National Accelerator Laboratory, as is the case with the other national laboratories, should benefit from its close relations with the universities. The laboratory will be managed by an association of universities, and the larger part of the research will be carried out by the faculty and students of the universities. Great care will be taken in the management of the laboratory to insure that its facilities will be operated in such a way as to make them available to any qualified scientist and his students.

In order to discharge its responsibility to provide an environment where scientific discoveries are likely to be made, the laboratory will need a staff of competent scientists and engineers. The experience, understanding and enthusiasm of men of this kind are often associated with their involvement in research activities. For this reason, it is essential that the National Accelerator Laboratory have its own research program in high-energy physics. In quality it should be second to none; in quantity, it should be matched to the overall requirements of the facility. The resident staff that will carry on this research activity will provide continuity to the research program connected with the accelerator. These scientists may be expected to contribute to the development of facilities that will meet the needs of the research program of the universities and of the laboratory. It is estimated that a reasonable sharing of the research program between resident and visiting scientists requires that the resident group be staffed so as to be able to conduct about twenty-five percent of the laboratory's total program.

In order to optimize the productivity of this new laboratory, a policy will be established through which the creation of the required large and complex experimental instruments and facilities will be encouraged and, at the same time, their availability for the use of outside groups will be assured. Physicists who work at the National Accelerator Laboratory will be expected to recognize that together with the privilege of carrying on their own research endeavors with the aid of large and complex instruments comes a share of the responsibility for the overall program. University-based scientists devote about half their time directly to research and the other half to education, both of graduate and undergraduate students. Similarly, research scientists at NAL, while devoting about half their time directly to their research programs, will in general be expected to invest the other half in the development, operation and improvement of a truly excellent set of laboratory facilities. It is in this spirit that the staff of the National Accelerator Laboratory is being recruited and organized.

#### 4. Organization

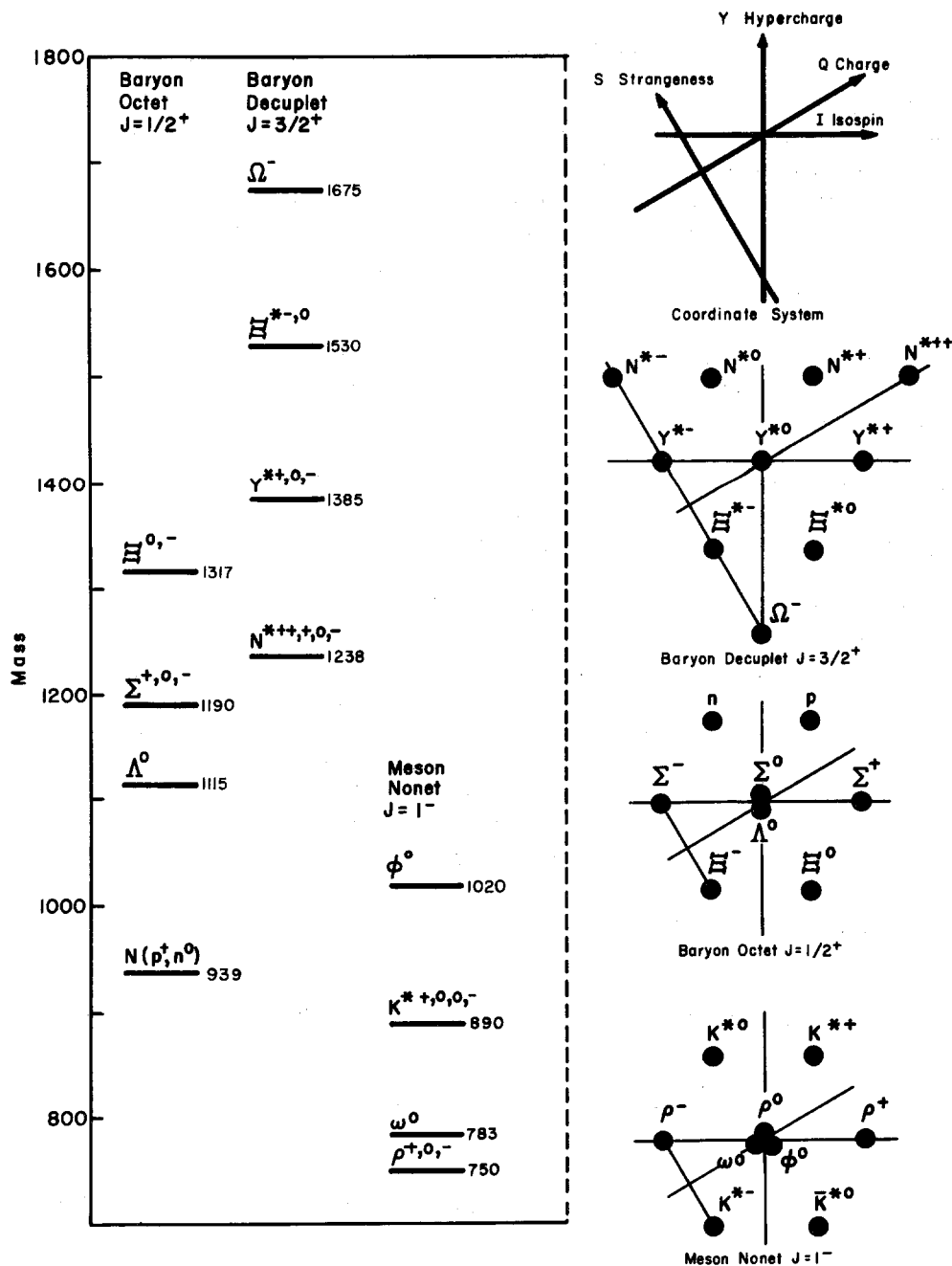
Since the high-energy physics program has its roots in the nation's universities, it is appropriate that the prime contractor for the new accelerator laboratory be a national group of universities comprising a major portion of the country's competence in high-energy physics research. Accordingly, Universities Research Association (URA) was incorporated in 1966. Today, URA's membership includes 47 of the leading universities in the United States and one in Canada.

Universities Research Association, Inc. is governed by a Board of Trustees whose members are selected by the Council of Presidents of the URA member institutions. Fifteen Board members represent 15 geographical regions into which the country has been divided so that there is the widest possible area representation. These 15 positions are divided among scientists with competence in high-energy physics and university officers with competence in administration.

In addition, the Board of Trustees includes several members-at-large, men with broad backgrounds and experience in industry and public affairs. The Chairman of the Board of Trustees is Dr. Henry DeWolf Smyth, and the President of the corporation, selected by the Board of Trustees, is Dr. Norman F. Ramsey, Higgins Professor of Physics at Harvard University, Cambridge, Massachusetts. On February 6, 1967, the Board of Trustees of the Universities Research Association selected Professor Robert Rathbun Wilson of Cornell University to be the Director of the new National Accelerator Laboratory. Under Dr. Wilson's direction, the National Accelerator Laboratory organization has been in the process of formation since the spring of 1967.

Recognizing the importance of the counsel of experienced senior members of the high-energy physics community, Dr. Wilson has appointed a Physics Advisory Committee with members drawn from universities and national laboratories in the east, the mid-west and the west. The National Accelerator Laboratory Users Organization has organized itself and has elected an Executive Committee which will govern the operation of that group. Much of the communication between the Laboratory and its potential users will be through this executive committee and its chairman.

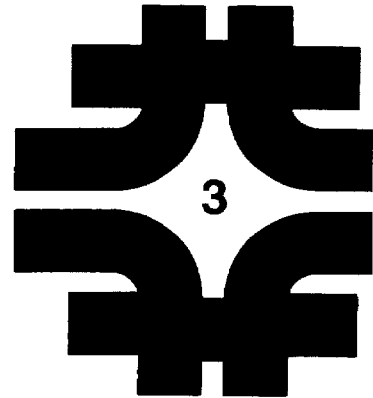
Through the intelligent use of the administrative and advisory apparatus that has been established and described herein, the National Accelerator Laboratory can become a uniquely effective research center, sensitively responsive to the needs of the broad community of scientists upon whose effort the success of the Laboratory must hinge.



**Figure 2-1 — Particle Classifications** The above graph shows some of the regularities that become evident when various properties of the particles are plotted. On the left are mass spectra for some groups of particles. On the right are regular patterns that occur when the properties of charge, isospin, strangeness, and hypercharge are plotted for the same groups. The existence of the  $\Omega^-$  was predicted from this graph and later verified by experiment.

## Summary of the Report

1. General Description	3-1
2. The Accelerator System	3-2
2.1 The Main Accelerator	3-3
2.2 The Booster Accelerator	3-9
2.3 The Linear Accelerator	3-9
2.4 The Cockcroft-Walton Accelerator	3-10
2.5 Beam Extraction	3-10
2.6 Control System	3-10
2.7 Radiation and Shielding	3-11
3. Experimental Program	3-11
4. Support Facilities	3-12
5. Costs and Schedules	3-13
6. Possible Future Expansions	3-14



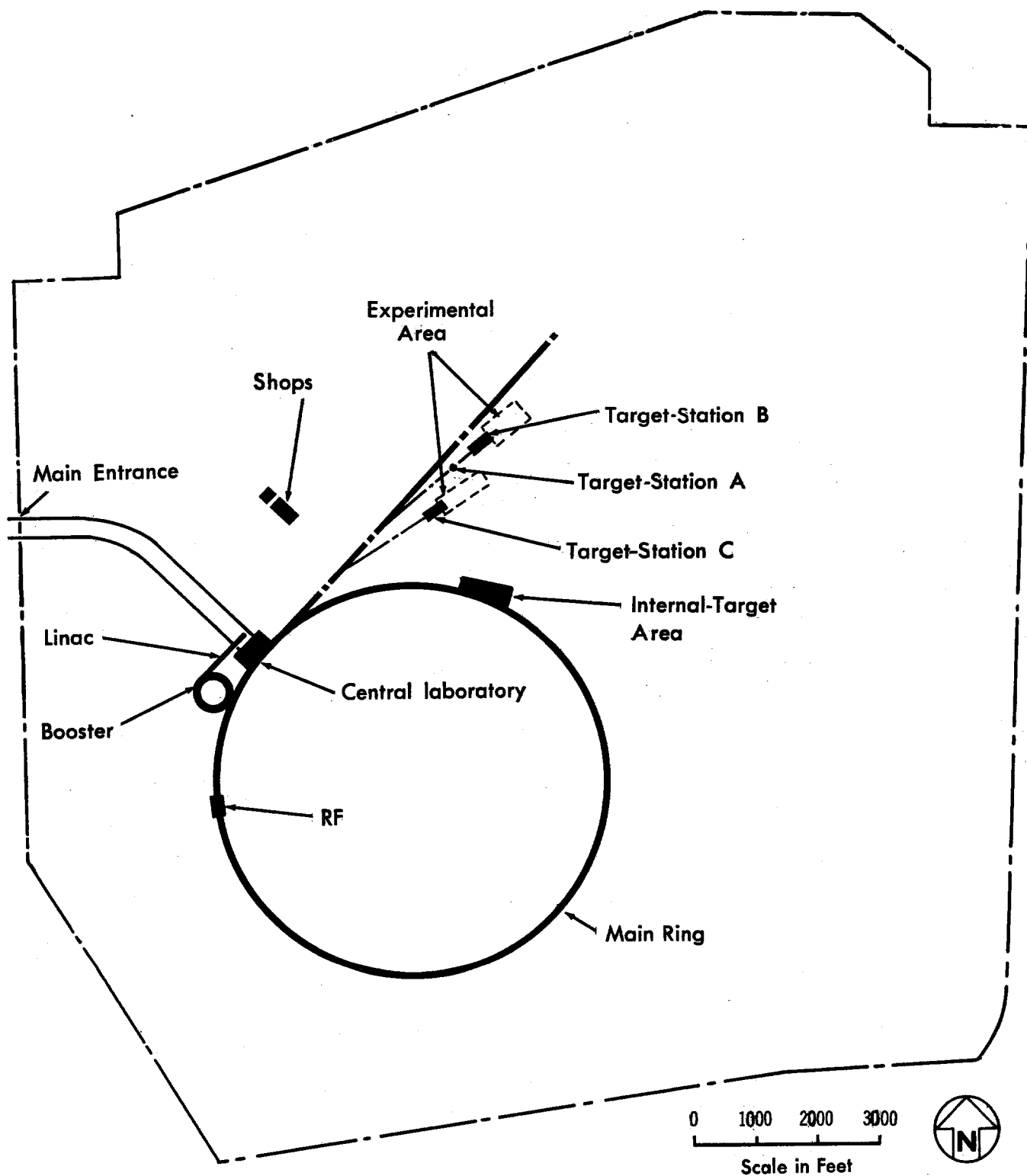


Figure 3-1 — Site Arrangement



### 3. SUMMARY OF THE REPORT

#### 1. General Description

The projected National Accelerator Laboratory is shown in an outline plan on the site in Fig. 3-1. For purposes of discussion, the Laboratory can be broken down into three elements:

- (i) The accelerator, in which protons are speeded up to full energy, then extracted and transported to targets.
- (ii) The experimental areas, in which experiments are performed with the primary beam of protons or with secondary beams of other particles produced when the protons strike targets.
- (iii) The support facilities, that is, laboratories, shops, and offices. Here the preparation of experiments and analysis of their results are carried out, as well as maintenance and development of the accelerator, theoretical research, and the housekeeping functions of the laboratory.

The accelerator is in the form of a large ring located in the southwest quadrant of the site, as can be seen in Fig. 3-1. During acceleration, the protons travel around this ring in a clockwise direction, gaining energy on each revolution as they pass through the "rf" or accelerating system. At full energy, the proton beam is extracted from the accelerator and transported to the target stations shown.

The smaller ring appended to this large ring on its northwest side is the booster accelerator, from which protons are injected into the main ring. The linear accelerator, often called the "linac", which is shown as a straight line in the plan, injects protons into the booster. The linear accelerator includes a small preaccelerator. Close to all these accelerators is the central laboratory building, a high-rise structure. The control center for the entire accelerator is located in this central laboratory. Heavy shops and warehouses are approximately a half mile away toward the experimental areas.

An important aspect of the design of the laboratory is the concentration of injection, booster, acceleration, and extraction functions close to one another and close to the central laboratory. This concentration is important economically, because it avoids the duplication of laboratory and office space that would inevitably occur in a spread-out facility. It is also important for efficiency, because it will promote easy communication between the different groups involved in operation and research. The high-rise laboratory is

believed to be no more expensive than the same space spread out in many lower buildings.

The sheer size of experimental areas for 200 BeV\* physics means that they cannot all be close to each other or to the accelerator. The heavy shops and warehouses have been located to give communication with both the accelerator and experimental areas.

The main beam-extraction point is also close to the central laboratory. Proton beams are transported from there northeast toward the experimental areas, where they are split off from the main transport run and guided to targets. The accelerator has been located toward one corner of the site so that, in the future, it will be possible to extend this beam run to additional experimental areas beyond those shown; these can be built later if circumstances justify expansion of the research program. An internal-target area is also planned for experiments at low beam intensities, but practically all of the research program will make use of extracted proton beams.

## 2. The Accelerator System

Four separate accelerators will be used to accelerate protons to an energy of 200 BeV in the accelerator designed at the National Accelerator Laboratory. They play the following roles:

- (i) Protons are generated in an ion source and accelerated to an energy of 750 keV in a Cockcroft-Walton preaccelerator, which is a relatively small device located at the beginning of the linear accelerator.
- (ii) Protons are accelerated from 750 keV to an energy of 200 MeV in a linear accelerator approximately 500 feet long.
- (iii) At 200 MeV, the protons are injected into the booster accelerator, which carries them to an energy of 10 BeV. The booster is a rapid-cycling synchrotron approximately 500 feet in diameter.
- (iv) At 10 BeV, the protons are injected into the main accelerator, a synchrotron of 6562 feet (1.24 miles) diameter, and accelerated to full energy. Initially, this energy will be 200 BeV, but more power supplies can be added later to increase the peak energy of the accelerator to 400, or possibly even 500 BeV. This additional acceleration will still take place in the main accelerator. After reaching maximum energy the protons are then extracted and transported to the experimental areas.

\*The eV (electron-volt) is a unit of energy for particles in accelerators. A BeV is a billion (1,000,000,000) eV, an MeV is a million (1,000,000) eV, and a keV is a thousand (1,000) eV. A proton passing through a potential difference of 1,000 volts will gain 1,000 eV (1 keV) in energy. In Europe, a BeV is called a GeV.

## 2.1 The Main Accelerator.

The Separated-Function Design. The magnets of a synchrotron have two functions. Their first function is bending, that is, providing a magnetic force to curve the protons' paths so that they go around the ring. On each traversal of the circumference, the protons are accelerated by the rf accelerating system.

The second function of the magnets is focusing. Protons travel very large distances around the circle during acceleration. For example, in the main accelerator, the first group of protons injected will travel approximately 500,000 miles in reaching 200 BeV. Any error in aiming at injection or any imperfection in the magnetic field, even though immeasurably small, would cause the beam to stray far from the circle during this large distance if the magnets did not automatically provide focusing forces to pull the beam back toward the circle.

In most synchrotrons built up to now, these two functions of bending and focusing are performed by a single set of magnets. The poles of these magnets are shaped to give a variation in field across the vacuum-chamber aperture, and it is these field variations that provide the focusing action. This kind of design can be called a "combined-function" synchrotron.

In contrast, a "separated-function" synchrotron has two kinds of magnets, one for each function. The "bending magnets" guide the proton beam around the circle. Their fields do not vary across the aperture and they make no contribution to the focusing. The "quadrupoles", or "focusing magnets", a separate set, provide the focusing action, but make no contribution to the bending.

A combined-function design has the advantage that all parts of the circumference occupied by magnets produce bending as well as focusing. For a given peak magnetic-field strength, it tends to be more compact. That is, because a larger fraction of the circumference is devoted to bending, the circle can be smaller in radius. But in fact, the "flat-field" bending magnets of a separated-function design can be pushed to considerably higher peak magnetic fields, which also makes a smaller circle. In a large synchrotron, the compactness that can be realized through a combined-function design is outweighed by the compactness that comes with the use of the higher magnetic fields possible in a separated-function design and the latter gives a smaller, more economical synchrotron.

It is interesting to note that different considerations apply in different cases. For example, if a rapid cycling rate is desired for a synchrotron, eddy-current problems require the use of a special kind of steel in its magnets. This steel cannot give high magnetic fields with reasonable power dissipation. The peak field strength is therefore limited, and the greater theoretical compactness of the combined-function design then dominates, with the result that such a

synchrotron can be more efficiently designed as a combined-function accelerator. The booster accelerator, a rapid-cycling synchrotron, is an example of a combined-function design.

The main accelerator is a separated-function synchrotron, in accordance with the discussion above. It has flat-field bending magnets and separate quadrupoles for focusing the proton beam. Figure 3-2 shows the "apertures", the cross-sectional areas of the vacuum chamber in which protons travel. The poles of the magnets are indicated by the shaded areas. In a strong-focusing accelerator, the proton beam is large in the horizontal and vertical dimensions at different locations on the accelerator's perimeter. Economies can therefore be made in the bending magnets by utilizing two different magnet shapes, one large horizontally and small vertically, and the other small horizontally and large vertically. These two kinds of bending-magnet apertures are shown in Fig. 3-2. The focusing-magnet aperture, also shown, is 5 inches wide and 2 inches high, larger than either of the bending-magnet apertures. Protons must be contained within this area during the entire course of acceleration.

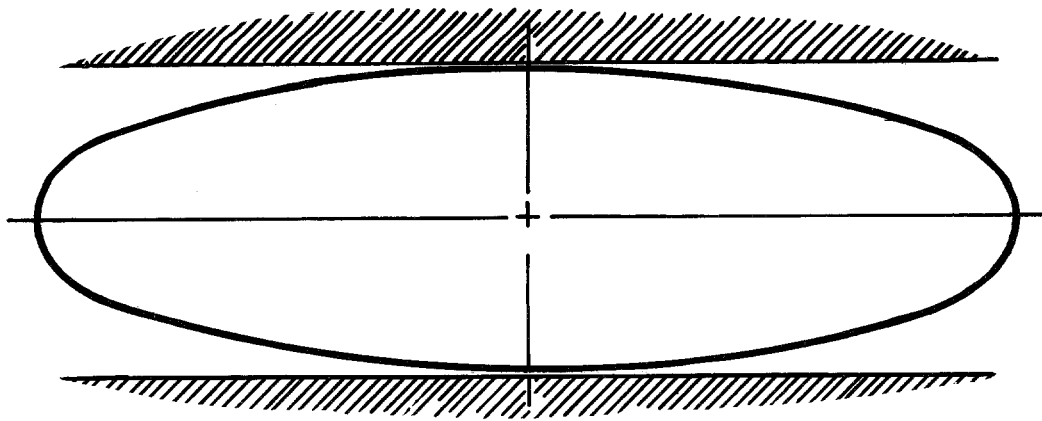
Some principal parameters of the main accelerator are collected in Table 3-1.

Table 3-1. Parameters Of The Main Accelerator

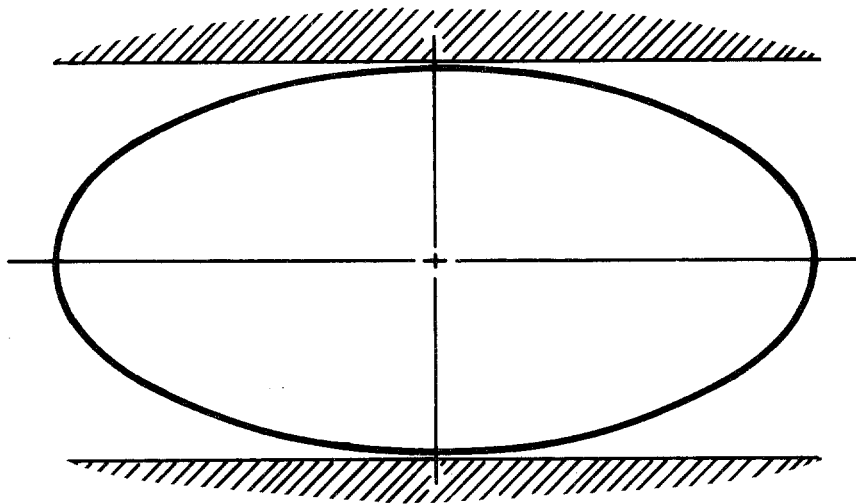
Energy	200 BeV
Injection Energy	10 BeV
Radius	1000 meters = 3,281 feet
Circumference	6283 meters = 20,610 feet = 3.9 mi.
Design Intensity	$5 \times 10^{13}$ protons per second
	$1.5 \times 10^{13}$ protons per second

The bending and focusing magnets are all to be made from 1/16-inch steel laminations, 25 inches wide and 14 inches high. It is planned to assemble them in I-beams for support. The bending magnets are each approximately 20 feet long and weigh 10 tons, while the quadrupoles are approximately 7 feet long and weigh 3 tons. Quadrupoles will be spaced every 100 feet, with four bending magnets in each space between. The magnets will be supported on jacks and a stretched-wire system under the magnets is planned to give the precise alignment needed, obviating the need for massive foundations.

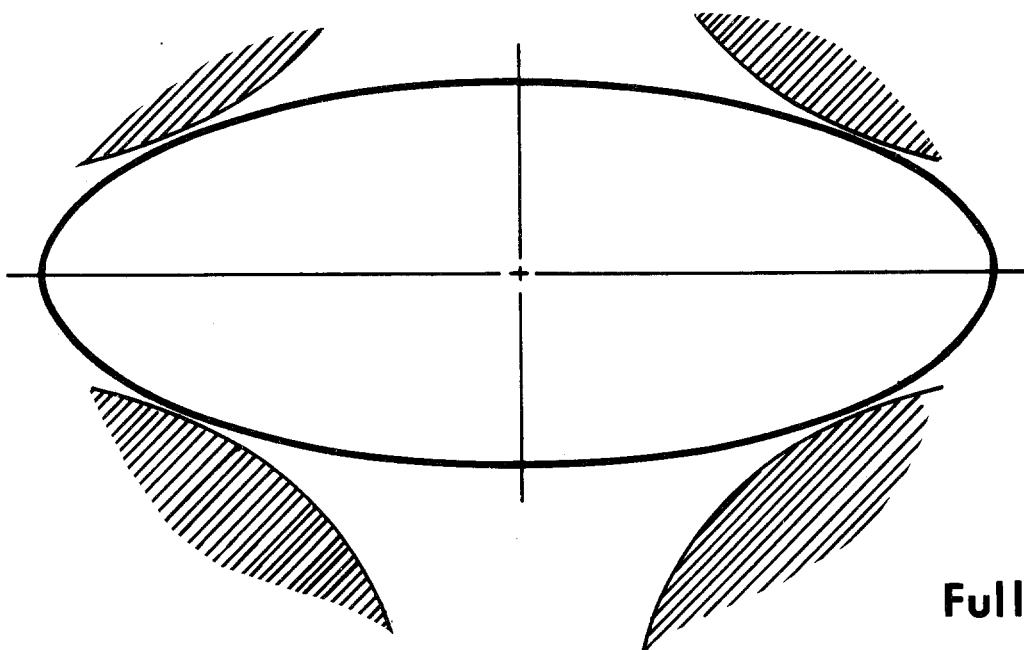
The vacuum chamber will be fabricated from stainless-steel tubes. It is planned to place high-vacuum pumps every 50 feet around the ring, but space is left for more frequent pumps, should some special applications require lower operating pressures.



Narrow-Gap  
Bending Magnet



Wide-Gap  
Bending Magnet



Quadrupole

**Full Scale**

Figure 3-2 — Main-Synchrotron Apertures

The entire accelerator is housed in an enclosure of horse-shoe shaped cross section, covered with earth for radiation shielding. The enclosure will be precast in 10-foot sections, assembled in a cut, and covered with earth. The thickness of earth cover planned varies from a minimum of 22 feet to a maximum of 30 feet over areas like the extraction point, where higher radiation levels inside the enclosure are expected. A cross section of the enclosure is shown in Fig. 3-3. It is 10 feet wide at the widest point and 8 feet high at the center. Every 100 feet along its length and at all the medium and long straight sections discussed below, a larger cross section is used to allow utility and personnel access and space for special equipment. Special houses are designed for extraction and internal-target areas. As can be seen in Fig. 3-3, the magnet ring is placed close to the outside enclosure wall to leave space inside for vehicles. Maintenance in high radiation-level areas will be carried out from shielded cabs.

Investigations have shown that it may be possible to do away with the motor-generator sets and flywheels used in most proton synchrotrons. Without motor-generators, better electrical filtering is needed. There is no appreciable cost saving from doing away with motor-generators, but they have been a source of serious trouble and long shutdowns in many accelerators; it is therefore believed that it may be of advantage to avoid the use of such sets.

Long Straight Sections. Long regions containing no magnets are needed in the main accelerator for the accommodation of components for injection of protons from the booster, for components of the rf accelerating system, and for extraction of full-energy beams. These "straight sections" are introduced in a number of positions around the main accelerator. The circumference is divided into six parts, each an arc of 60 degrees. Each of these 60-degree arcs has a "medium straight section", with about 60 feet of uninterrupted free length, and a "long straight section" with about 170 feet of uninterrupted free length. The medium straight sections are formed simply by omitting three of the four bending magnets between two adjacent quadrupoles. The long straight sections are formed by replacing four bending magnets and two quadrupoles with a special sequence of bending magnets and quadrupoles.

One medium straight section is utilized for injection, while one long straight section is utilized for extraction, one for the internal-target area, and one for the rf accelerating system. The arrangement of these functions around the ring is shown in Fig. 3-1.

Four more medium straight sections are utilized for clean-up targets, to localize beam losses. The remaining straight sections are reserved for possible future expansions of the research programs centering around the accelerator.

We are considering injection in the same long straight section used for extraction. In that case, the medium straight-section location might be changed to optimize clean-up.

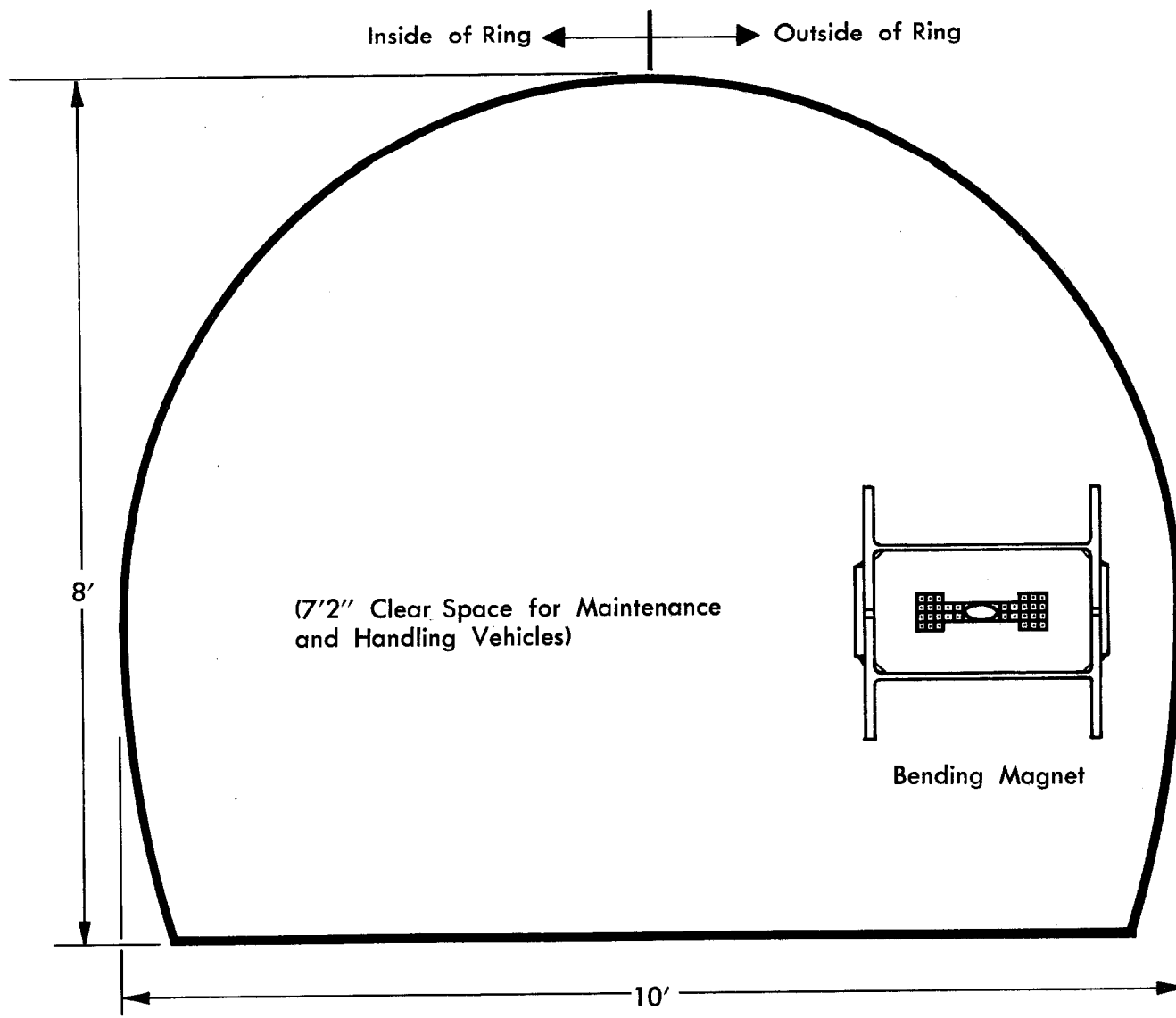


**Figure 3-3 — Main-Synchrotron Enclosure and Magnet**

Acceleration Cycle. Figure 3-4 is a graph of the acceleration cycle of the main accelerator. Thirteen successive pulses of 10 BeV protons from the booster synchrotron are injected and stored in orbit around the circumference of the main accelerator. This injection takes 0.8 second. When the ring has been filled, acceleration takes place in the next 1.6 seconds. At the full energy of 200 BeV, the beam can be extracted rapidly, as shown in the upper graph, or slowly, up to an interval of 1 second, while the guide field is held constant. This "flat-top" is graphed in the lower part of Fig. 3-4. After all the beam is extracted, the guide field falls to its injection value in 0.6 second, after which the cycle begins again. The total acceleration cycle then takes between 3 and 4 seconds, depending on the extraction mode being used. The extraction mode chosen will depend on the needs of the particular experiments being performed.

Figure 3-4 also gives the acceleration cycles that would be used for acceleration to 400 BeV, with more power supplies added. All the times are doubled from the 200 BeV cycle. Then twice as many pulses can be injected from the booster; the acceleration to 400 BeV takes twice the time of that to 200; the protons can be extracted over twice the flat-top, and the guide field returned to the injection value in 1.2 seconds rather than 0.6 second, so that the number of particles per second and the relative flat-top time remain the same as at 200 BeV. The option of doubling the pulse rate at the 200 BeV level will be kept open.

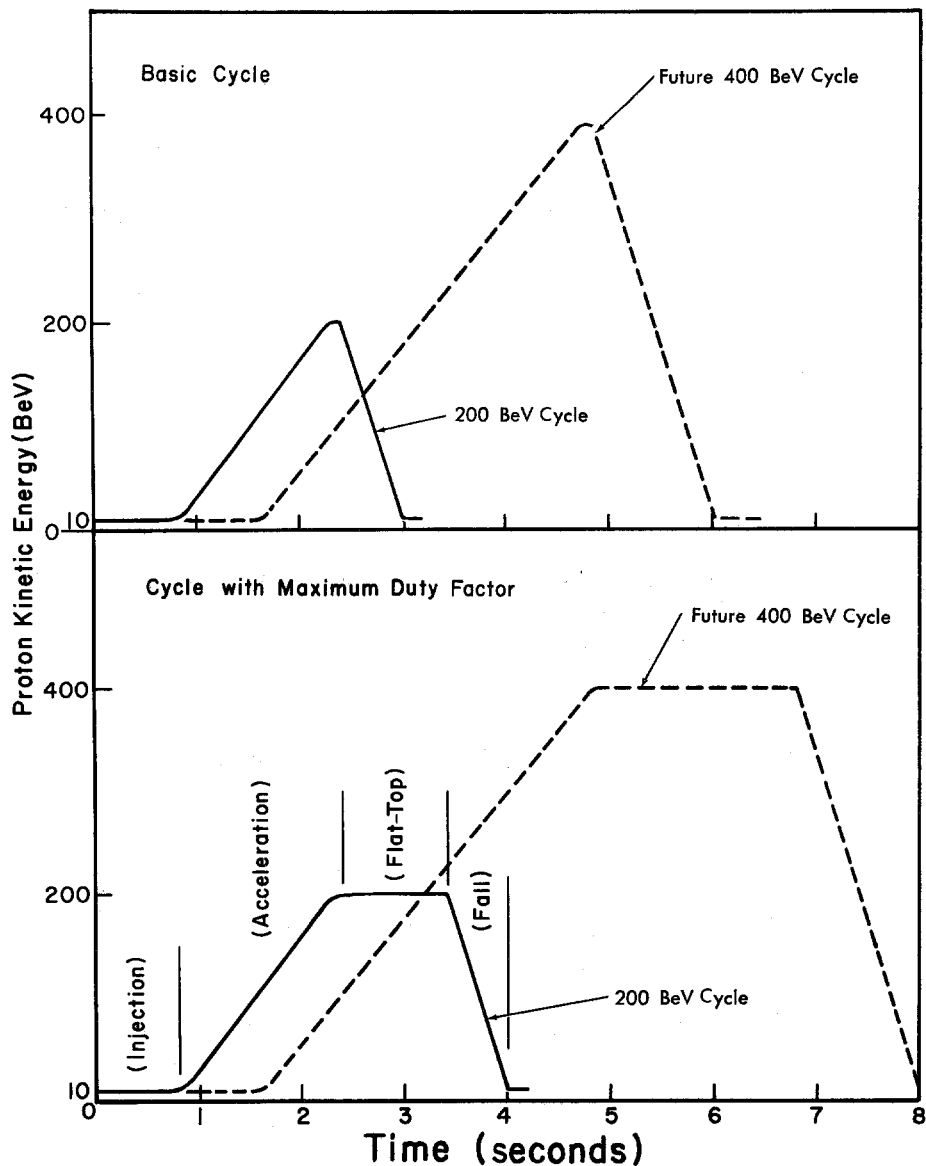


Figure 3-4 — Acceleration Cycles



2.2 The Booster Accelerator. Protons are injected into present-day synchrotrons directly from a linear accelerator. If protons were injected into the main ring of a 200 BeV synchrotron from a conventional linear accelerator, serious problems would arise from the very low injection guide fields in the main ring. Beam losses would result, and, at best, the accelerator would not operate reliably. On the other hand, a linear accelerator of energy high enough to avoid these problems would be extremely costly. The booster accelerator can provide protons at the desired energy and intensity much more economically.

The booster synchrotron is approximately 500 feet in diameter. It will accelerate protons to 10 BeV at the rate of 15 pulses per second. It is a combined-function design, but in many other respects it is similar to the main synchrotron. It will be housed in the same kind of enclosure, with a continuous equipment gallery above. Earth shielding will keep radiation levels in the gallery below permissible tolerance levels.

In order to inject thirteen pulses into the main accelerator in 0.8 second, the booster accelerates at a repetition rate of 15 cycles per second. This rapid rate does not pose any new technical problems; the Princeton-Pennsylvania Accelerator has a comparable cycling rate for protons and many electron synchrotrons accelerate at much higher rates (for example, 60 cycles per second at the Cambridge and Cornell Accelerators). The option of doubling the booster repetition rate will also be kept open.

There are no plans for a separate experimental area at the booster synchrotron. It is believed that there are enough accelerators capable of providing 10 BeV protons to exploit research opportunities at that energy and that final testing of 200 BeV equipment will be better done in the planned 200 BeV experimental area themselves, rather than in a separate 10 BeV experimental area at the booster.

2.3 The Linear Accelerator. A linear accelerator is a source of a more intense beam than a synchrotron, but is more expensive at the same energy. It provides an efficient injector into the booster synchrotron, whereas a synchrotron injector for the booster would have difficult technical problems.

In a proton linear accelerator protons are accelerated by the electric fields that appear between drift tubes. These cylindrical drift tubes shield the protons from the radio-frequency electric field when it is in the direction to decelerate them. Each drift tube along the accelerator is individually shaped to match the proton speed at its position.

The 200 MeV linear accelerator is quite similar in design to the new injector now being constructed for the AGS Conversion Program at the Brookhaven National Laboratory. It is expected that some joint work can be done by the two groups and that economies will result from the similarity.

The linear accelerator is to be approximately 500 feet long. It is divided into nine cavities of copper-clad steel, each a cylinder about 50 feet long and 3 feet in diameter. These cavities contain altogether 286 drift tubes. Radio-frequency power equipment will be located alongside the tanks in an equipment bay.

2.4 The Cockcroft-Walton Accelerator. The linear accelerator is fed from a 750 keV Cockcroft-Walton preaccelerator. The source of protons, which is an electrical arc in hydrogen gas, is located in the high-voltage electrode of the Cockcroft-Walton voltage supply. Protons from the source are accelerated directly from this electrode to the ground electrode. This accelerator is a well-proven design that will be obtained from private industry.

2.5 Beam Extraction. The extraction system will take full-energy beams from the accelerator either rapidly or slowly, depending on the needs of particular experiments, and transport them through a shielded enclosure to the experimental areas.

The extraction process begins when the beam is kicked from its normal orbit. The kick sends the beam into special magnets that bend it away from the accelerator. These magnets are designed with a septum, a thin copper foil carrying a sheet of current and located to keep the special magnet's field enclosed, so that it does not perturb protons in nearby orbits during acceleration. Some protons will strike the septum and be lost, but the system is designed to keep these losses down to approximately 1%.

Additional septum magnets are utilized to deflect the extracted beam from its transport line to any target station. These magnets in effect split the beam between different targets, so that variable fractions of the beam can be simultaneously used at different targets.

2.6 Control System. The control system is the nerve center of the accelerator, monitoring the status of its components, protecting against faults and programming its operation.

The control systems of most present accelerators utilize individual wiring and manual controls for each component. A system of this kind for this accelerator would be very expensive, because of the large number of components, and would require a larger number of operators. It is planned instead to transmit data from the accelerator, and commands to it, by a multiplex system, which transmits many different signals in turn over the same wires. The signals will be sent to monitoring and control computers that will store data and present to the operator only what he needs. The planned control system is similar in many respects to that of the new Cornell 10 BeV electron synchrotron. Further development work on control systems is being carried out at the Lawrence Radiation Laboratory, using the injection system of the Bevatron for practical tests.

2.7 Radiation and Shielding. The accelerators will be covered with earth shielding in order to keep the radiation levels at permissible levels outside the enclosures. This radiation is generated by protons that are lost from the beam and strike surrounding objects. These lost protons also generate radioactivity in accelerator components and enclosures that continues after shutdown. Even though the radiation outside the enclosures during operation can be made as small as desired by shielding, residual radiation inside would greatly hinder maintenance and servicing of the accelerators.

It is planned that shielded enclosures for servicing will be provided. In addition, residual radiation levels can be kept down by operational policy. Operation at high intensity will not be allowed under conditions where beam loss occurs. Vigorous efforts to understand the reasons for beam loss must be made, in order that the accelerator realize its full intensity capabilities.

### 3. Experimental Program

The planning of such a large facility must be based upon judgments of the amount of research that will be done with the accelerator and of how this research will be done. Experimental areas and support facilities must be large enough and be designed with enough flexibility to meet the needs of the program.

It is judged that a resident staff of appropriate size will carry out about one-quarter of the research program in the National Accelerator Laboratory, while three-quarters will be carried out by outside user groups.

There will be approximately 200 visiting experimentalists present at any one time, some involved in the preparation of experiments, some in the actual taking of data, and some in the analysis of these data.

It is estimated that in 1975, when the research program at the National Accelerator Laboratory is in full swing, that there will be about 2,000 Ph.D. physicists active in high-energy physics in the United States. Two-thirds of these will participate in experiments, while the remainder will be engaged in theoretical work. About one-fourth of this total national research program in high-energy physics will be centered at the new laboratory. We judge, by extrapolation from present work, that there will be an immediate need for seven secondary-particle beams to support research using electronic-detection methods. Using these beams, approximately twenty major experiments could be performed each year. There are also being planned two separated-particle beams for use with bubble chambers, and beams of mu-mesons and neutrinos with which to study electromagnetic and weak interactions.

The experimental areas around the accelerator are planned to support a program of this magnitude.

The design includes four target stations, which have some individual specialized purposes. Experimental techniques in high-energy physics change rapidly and it is therefore important that the areas be designed to be as flexible as possible to accommodate these changing techniques. It is also important to emphasize that the plans for experimental areas will be subjected to continuing review during the next several years by the Laboratory and by the University physicists who will do experiments in them.

The four target stations are shown in Fig. 3-1. Their purposes are as follows:

- (i) Target-Station A. This station is designed for low interaction rates, about  $10^{11}$  interactions per second. This low rate means that most of the proton beam can be transported through the station to Station B farther downstream.
- (ii) Target-Station B. This station is designed to produce a large number of secondary beams. These beams are to be of moderate intensity and will not include beams at 0 degrees (in the direction of the incident proton beam). The greatest bulk of the research work will probably be carried out here.
- (iii) Target-Station C. This station is very similar in overall design to Station B, but is specifically planned for secondary beams produced at or near 0 degrees, to yield secondary particles of the highest momentum and intensity. It includes special bending magnets for this purpose.
- (iv) Internal-Target Area. This station will use targets placed directly in the circulating beam in the main accelerator. It will be used only at very low intensities, in order to avoid generation of radioactivity in the accelerator. The internal-target area is planned in such a way that it could be later converted to another beam-extraction point, should this be justified by experience. It may also be used during construction and installation as a staging area for main-accelerator components.

#### 4. Support Facilities

Central Laboratory. Because of the advantages in communication discussed at the beginning of this summary, as many as possible of the light laboratories, shops and offices will be collected in a single high-rise structure. Laboratories and offices for visitors and resident staff, computer and film processing facilities, medical and eating facilities, and the control center for the accelerator will be located here. The building is planned to have a total of approximately 420,000 gross square feet.

Shops and Warehouses. Approximately 50,000 square feet of heavy laboratory and assembly area, 50,000 square feet of fabrication shops, 60,000 square feet of warehousing and miscellaneous minor buildings totalling about 5,000 square feet are planned. These are grouped about halfway between the central laboratory and the experimental areas.

In addition, electric-power distribution, cooling and domestic water distribution, storm and sanitary sewers, fencing and erosion-control grading are planned. These are described in Chapter 15.

## 5. Costs and Schedules

The construction cost of the National Accelerator Laboratory is estimated to be \$248,300,000, not including \$1,705,000 of construction-planning and design funds already expended. Table 3-2 gives a breakdown of these estimated costs.

Table 3-2. Construction Cost Estimate Summary  
(all amounts in millions of dollars)

1.	Construction Costs		
a.	Technical Components	65.5	
b.	Conventional Facilities	78.8	
c.	Standard Equipment	<u>10.2</u>	
	Subtotal		154.5
2.	EDIA (Engineering, Design, Inspection and Administration)		
a.	Technical Components (25%)	16.4	
b.	Conventional Facilities (17.5%)	<u>15.7</u>	
	Subtotal		32.1
3.	Contingencies		
a.	Technical Components (25%)	20.4	
b.	Conventional Facilities (15%)	14.1	
c.	Standard Equipment (10%)	<u>1.0</u>	
	Subtotal		35.5
4.	Escalation (Approximately 14%)		
a.	Technical Components	11.5	
b.	Conventional Facilities	13.3	
c.	Standard Equipment	<u>1.4</u>	
	Subtotal		<u>26.2</u>
	Total		\$248.3 MM

This estimate does not include the equipment needed for physics experiments with secondary beams.










It is planned to have the accelerator in operation by June 30, 1972. The research program will begin modestly at that time and will increase rapidly in size as accelerator operation becomes more routine and reliable. It has been estimated that the Laboratory will have a population of approximately 2,000 people by 1975 and that its operation will involve a budget of approximately \$60M per year (1967 dollars).

#### 6. Possible Future Expansions

A number of expansions in capability of the accelerator and experimental facilities can be envisioned. Care has been taken in the design to assure that these expansions will not be precluded in the future. The possible expansions include:

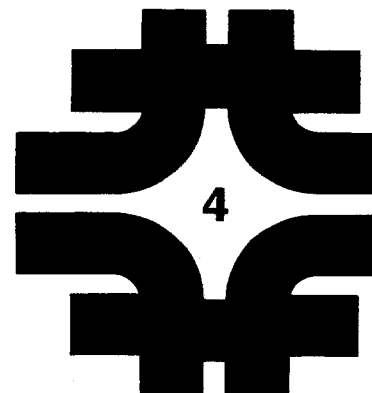
- (i) Increase of peak energy. The peak energy can be increased from 200 to 400 BeV without any loss in intensity or slow-extraction capability, by the addition of more power supplies. All equipment inside the accelerator enclosure is designed to be adequate for 400 BeV. The peak energy can be increased even more, up to a limit of approximately 500 BeV set by magnet saturation, with some loss in intensity. The cost at a later date of the conversion from 200 to 400 BeV is estimated to be approximately \$30M (in 1967 dollars).
- (ii) Increase of intensity. The useful intensity can be increased by a significant factor, perhaps as much as an order of magnitude, by increasing the repetition rate, by compensating space-charge detuning, and by improving extraction efficiency. The present shielding is designed to be adequate for increases both in energy and intensity.
- (iii) Expansion of existing experimental facilities. Secondary beams can be added at existing target stations. New target stations can also be added by extending the extracted-beam transport further and introducing more switching stations. A second extracted proton beam can also be constructed; the internal-target area is designed for this possible use.
- (iv) Beam bypass. The full-energy beam could be extracted from the main ring at the internal-target straight section, bent around a separate track outside the accelerator, and brought back into the main ring two straight sections downstream. This bypass could be used for further experimental beams or for the storage rings discussed in (v) and (vi) below.
- (v) It will be possible to construct a small storage ring between the bypass and the main accelerator. This ring can be used to study colliding-beam interactions between protons stored in it and protons in the main accelerator.
- (vi) A set of intersecting storage rings as large as the main accelerator could also be fed from the bypass to study colliding-beam interactions at the full energy of the accelerator. Space has been left on the site for both the bypass and the intersecting storage rings.

# Detailed Description of the Accelerator

- 4. Main-Synchrotron Lattice and Orbits 
- 5. Main-Synchrotron Magnet System 
- 6. Main-Synchrotron Vacuum System 
- 7. Main-Synchrotron Accelerating System 
- 8. Main-Synchrotron Enclosure 
- 9. Booster Accelerator 
- 10. Linear Accelerator 
- 11. Monitoring and Control System 
- 12. Radiation and Shielding 

# Main-Synchrotron Lattice and Orbits

1. Introduction	4-1
2. Considerations in the Choice of Lattice	4-2
3. Description of the Lattice	4-4
3.1 Normal Cell	4-4
3.2 Superperiodicity	4-6
3.3 Medium Straight Sections	4-6
3.4 Long Straight Sections	4-6
4. Error and Misalignment Tolerances	4-9
4.1 Closed-Orbit Errors	4-10
4.2 Focusing Errors	4-11
5. Aperture Considerations	4-13
6. Auxiliary Magnets	4-15
7. Space-Charge Limits	4-15
References	4-15





#### 4. MAIN-SYNCHROTRON LATTICE AND ORBITS

A. A. Garren, A. W. Maschke, L. Smith, L. C. Teng

##### 1. Introduction

The lattice of a synchrotron is the order of arrangement of magnets around the ring. These magnets serve two distinct functions. The first function is to bend the particles to travel around the ring in the neighborhood of an ideal closed orbit. The higher the particle energy, the stronger the required bending action, measured in terms of field strength multiplied by total length of magnets around the ring. The second function is to focus the particles. The focusing action is obtained by introducing proper gradients in the fields of the magnets. To produce certain desired focusing actions, these field gradients are determined by the lattice structure.

Focusing is needed in an accelerator because particles are emitted from the source over a finite area and with a distribution of velocities due to random thermal motion in the source. Because this randomness can not be removed, most particles of the beam are not injected exactly on the ideal closed orbit. To keep them in the neighborhood of the closed orbit, focusing must be provided. Focusing is also required because in a real accelerator the magnetic fields possess small imperfections that would cause particles to stray far from the closed orbit if focusing were not present.

The highest energy to which particles can be accelerated in a synchrotron is determined by the maximum field and gradient that the magnets can provide. For this accelerator, it was decided to provide in the design for initial operation at 200 BeV, but to build in the capability for a later increase of energy to at least 400 BeV. This is to be done by building a magnet lattice for 400 BeV, but initially only exciting the magnets to 9 kG to accelerate protons to 200 BeV. For the conversion, sufficient additional power supplies would be installed to excite the magnets to 18 kG, to permit acceleration to 400 BeV.

An alternative scheme has been proposed<sup>1</sup> in which only the magnets required for 200 BeV operation at full excitation are originally installed, and additional magnets are added later when the conversion is carried out. The argument for the latter approach is that the initial construction cost is smaller, and the capability would exist to take advantage of new technology in the conversion.

The main advantage of the scheme adopted is that the shutdown time during the conversion will be greatly reduced. In addition, the 200 BeV accelerator will use less power, the focusing properties of the ring are

changed much less at conversion, and the design constraints implicit in making two compatible lattices are removed.

With either approach, a greater premium is placed on building a ring of minimum circumference than would be done if operation at one energy only were intended, for one wishes to minimize the additional initial cost of providing the second-stage capability.

The remaining sections of this chapter describe factors influencing the choice of lattice, a description of the specific lattice designed, the orbit response to field errors and misalignments, the magnet aperture required and the limitations on intensity.

## 2. Considerations in the Choice of Lattice.

A significant lattice choice is between the combined-function concept on the one hand, in which bending and focusing are carried out in the same gradient magnets, and the separated-function concept, in which the bending and focusing functions are carried out in different magnets. Since the zero-gradient bending magnets of a separated function synchrotron can reach higher fields with adequate quality than the gradient magnets of a combined-function synchrotron, it is possible to design the former with a smaller circumference than the latter. In the plan to operate initially at 200 BeV, it is desirable that the capability for later energy increase be included with as little increase in circumference as possible. Design of specific 400 BeV lattices at NAL and similar comparisons elsewhere <sup>1,2,3,4</sup> have confirmed this difference between separated and combined-function synchrotrons.

The separated-function design also permits a wider range of adjustment of the focusing properties to be carried out with the cell quadrupoles, rather than by auxiliary ones. For these reasons, and because of other considerations having to do with the practical construction of magnets a separated-function design has been chosen.

A synchrotron lattice may be divided conceptually into two parts. The larger portion is made up of repetitive identical sequences of magnets and drift spaces called cells. A smaller portion consists of of special sequences containing extra long, magnet-free drift spaces for injection, acceleration, and beam extraction. These special sequences must be designed to be compatible with the focusing characteristics of the normal cells. We will first discuss the choice of the normal-cell structure.

Three types of separated-function cell structures have been investigated for the design of this synchrotron: FODO, FOFDFOOD, and OOFDFOO, where in the discussion of this section F and D refer respectively to horizontally focusing and defocusing quadrupoles, and O refers to sets of zero-gradient bending magnets. (A full notation for the adopted lattice is given in the parameter list of Table 4-1.)

The FODO structure focuses the beam with the greatest economy of quadrupoles. For this structure, the space between quadrupoles is more than adequate for the medium-length straight sections to be included in a cell. Hence, these medium straight sections may be formed by simply omitting some of the bending magnets between two consecutive quadrupoles of an otherwise normal cell. On the other hand, the long straight section required is too long and special arrays must be provided.

The FOOFDOOD or doublet cells for the accelerator could be about twice as long as the FODO cells. In this case both the medium and long straight sections may be formed by omitting magnets from half-cells. Thus all quadrupoles are identical and structure resonances weaker than in the FODO case, but the doublet structure requires appreciably greater total quadrupole length than the FODO.

The OOFDFOO or triplet structures studied also have adequately long cells. As with the doublet, both the medium and long straight sections can be made by simply omitting bending magnets. Another advantage of the triplet may be a lessened sensitivity to certain types of misalignment. However, this structure is also more costly in terms of quadrupoles than the FODO, and rather large vertical apertures would be required in the D quadrupoles.

The FODO structure has been selected for the accelerator, primarily because of its modest quadrupole requirement, but also because the special arrays containing the long straight sections are most favorable for extraction.

For the FODO separated-function synchrotron, three methods of providing the long straight sections were considered. The simplest was to omit the bending magnets from two successive half-cells, to produce a straight section of adequate length, but with a quadrupole in the center. This solution provides a very simple lattice, but the central quadrupole would complicate some internal-targeting experiments, the orbit characteristics of this arrangement make extraction more difficult, and the excursion of off-momentum particles is rather large.

Another straight-section type designed was a symmetric insertion at the center of an F quadrupole. This structure had the form O'FDOODFO', where the O' contain bending magnets and the OO do not. This structure provides a more nearly circular beam cross-section in the straight section, which is advantageous for the rf accelerating cavities, and it gives the smallest deviation of off-momentum particles.

The most favorable structure for extraction is an antisymmetric array, O'FDOOFDO', which replaces half a normal cell, from the center of an F to the center of the succeeding D quadrupole. The momentum deviation is intermediate between the two other types discussed above. Because of its superior properties for extraction, this structure is utilized in the design adopted.

### 3. Description of the Lattice

Discussion of the lattice can be subdivided into three parts:

(i) the normal cell structure, (ii) the superperiodicity and (iii) the specific design of the long straight sections. These parts are, of course, not independent. In the design work, they have been fitted together under the constraints that a ring of 1000 m (3,280.8 ft) radius should accelerate protons to 400 BeV with a bending field of 18 kG, and that the long straight-section magnet sequences match the focusing properties of the cells. The choice of exactly 1000 meters was arbitrary, but the design work has demonstrated that it provides the basis for an entirely feasible and efficient lattice. Furthermore, small changes in radius would make changes in cost so small as to be negligible compared with the uncertainties in any cost estimate.

**3.1 Normal Cell.** The normal cell, which is shown in Fig. 4-1, contains eight bending magnets and two quadrupoles, one horizontally and one vertically focusing. It is almost 200 feet in total length. There are 84 normal cells around the circumference of the main synchrotron, not including those cells containing the long and medium straight sections discussed below.

The length and gradient of the quadrupole are such as to reduce the amplitudes of oscillation of the particles to the smallest value possible in a cell of the length chosen. Had a shorter cell length been chosen, the oscillation amplitude would have been less, but the greater number of gaps between magnets would have increased the circumference. Minimum amplitude occurs in this type of lattice (FODO) when the particles execute about one-fifth of an oscillation in each cell.

It is desirable to build bending magnets as long as is technically feasible, in order to reduce the fraction of circumference used for straight sections that do not add to the bending. A length of approximately 20 ft is judged to keep the problems of magnet assembly and alignment manageable. It is also desirable to keep most of the straight sections between magnets as short as possible to give the largest amount of bending per unit length. The normal cell chosen provides a 1-ft space between magnet yokes. This space will contain only coil ends and connections, vacuum flanges, and pumpout manifolds. Fig. 6-1 in the discussion of the vacuum system shows a 1-ft straight section with the equipment contained in it. All the power and water connections to both adjacent magnets are in this straight section, as well as welded vacuum flanges and a pumpout manifold. A beam-position detector is also shown, inserted in the pumpout manifold.

Most auxiliary equipment, such as correcting magnets, will be located in the 7-ft straight sections, spaced at intervals of approximately 100 feet. The position of these straight sections, immediately after the quadrupole magnet, has been chosen to facilitate beam extraction.



3.2 Superperiodicity. The lattice of the main ring is divided into six identical superperiods, each containing one long straight section, one medium straight section, and sixteen cells, of which fourteen are normal. The medium straight section consists of the gap produced by removing three consecutive magnets from one of the cells. The long straight section is included in an array of magnets and quadrupoles that replaces one-half a normal cell (from an F to a D quadrupole).

The choice of the number of superperiods was influenced by the following considerations. Enough long and medium straight sections should be provided for immediate requirements and to provide reasonable flexibility for future needs. Too many straight sections would add unnecessarily to the circumference. However, it is undesirable to have too small a number of superperiods, because this makes the structure resonances very close.

The focusing properties of the lattice cause the particles to execute approximately sinusoidal oscillations about the closed orbit in each of the two directions perpendicular to the particle motion. The number of such oscillations per revolution in the horizontal plane of the closed orbit is called  $\nu_x$  and if the vertical direction the number is called  $\nu_z$ . For this synchrotron,  $\nu_x$  and  $\nu_z$  have been chosen to have nearly the same value,  $\nu_x = \nu_z = \nu = 20.25$ . The choice of the values takes account of the following:

The betatron phase advance through the cells should be about  $2\pi/5$  to minimize the betatron amplitudes. The phase advance through the long straight section is determined by the matching conditions and the straight-section drift length required. Finally,  $\nu$  should be chosen to avoid, so far as possible, low-order structure resonances caused by super-periodicity and to minimize the deviations of off-momentum particles. The chosen  $\nu$  value, 20.25, satisfies these criteria.

3.3 Medium Straight Sections. The seventh cell of each superperiod has the second, third, and fourth bending magnet omitted, as shown in Fig. 4-1. This provides a field-free length of 63.75 ft. Injection from the booster synchrotron will be located in medium straight section A; medium straight sections B, C, D and E will contain scrapers to clean up the beam during extraction. All are long enough for possible future developments, e.g., addition of more rf cavities, extraction of low-energy beams.

3.4 Long Straight Sections. The first half of the tenth cell of each superperiod is replaced by a sequence of bending magnets and two quadrupole doublets, with a clear space of almost 170 ft between the doublets. This half-cell replacement is shown in Fig. 4-1; it consists of the array of elements between the quadrupoles QFE and QDE as shown. The latter replace half-length cell quadrupoles. This particular method<sup>1,5</sup> of achieving a long drift space is especially effective in a FODO lattice. The particular dimensions chosen for the replacement array were designed to facilitate extraction.

Three long straight sections are required for beam extraction, the rf acceleration system, and the internal-target area. Three others may be used for additional extracted beams or for the beam bypass discussed in Chapter 18. Table 4-1 gives a Summary of the main-ring lattice parameters. Figure 4-2 shows the momentum-width and beam-width functions through a superperiod.

Table 4-1. Main-Accelerator Lattice Parameters

Physical Dimensions

		<u>Length</u>
A. Normal Cell (C)		
Elements in Normal Cell		
Bending Magnet (B1 or B2)		19 ft 11 in.
Quadrupole Focusing Magnet (QF or QD)		7 ft
Minimum Separation between Magnets (S)		1 ft
Short Straight Section (SS)		6 ft 11 in.
Cell Structure: (QF)SS(B1)S(B1)S(B2)S(B2)S (QD)SS(B2)S(B2)S(B1)S(B1)S		
Cell Length		195 ft 2 in.
Number of Normal Cells		84
B. Cell with Medium Straight Section (M)		
Length of Medium Straight Section (MS)		63 ft 9 in.
Cell Structure: (QF)SS(B1)MS (QD)SS(B2)S(B2)S(B1)S(B1)S		
Cell Length		195 ft 2 in.
Number of Cells with MS		6
C. Cell with Matched Long Straight Section (L)		
Matching Elements in Cell		<u>Length</u>
Bending Magnet (B1 or B2)		19 ft 11 in.
End Quadrupole Magnet (QFE or QDE)		3 ft 10 in.
Outer Quadrupole Magnet (QFO or QDO)		9 ft 9 in.
Inner Quadrupole Magnet (QFI or QDI)		11 ft 10.9 in.
End Straight Section next to QFE(FS)		31 ft
End Straight Section next to QDE(DS)		4 ft 2 in.
Separation between Outer and Inner Quadrupole Magnets (TS)		4 ft 10.44 in.
Long Straight Section (LS)		169 ft 4.68 in.
Cell Structure:		
(QFE)FS(B1)S(B1)S(B1)S(QFO)TS(QDI)LS (QFI)TS(QDO)SS(B2)S(B2)S(B2)S(B2)DS (QDE)SS(B2)S(B2)S(B1)S(B1)S		
Cell Length		508 ft 2.25 in.
Number of Cells with LS		6

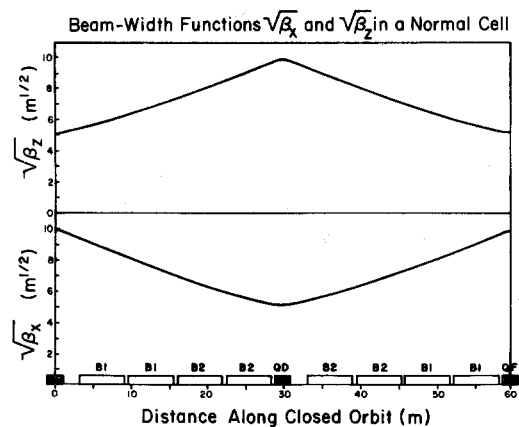
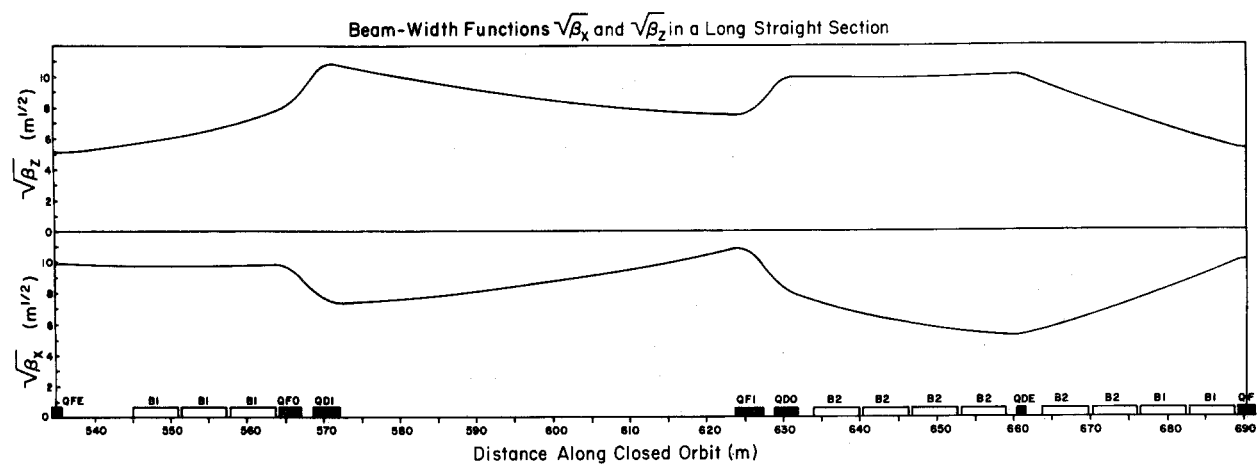
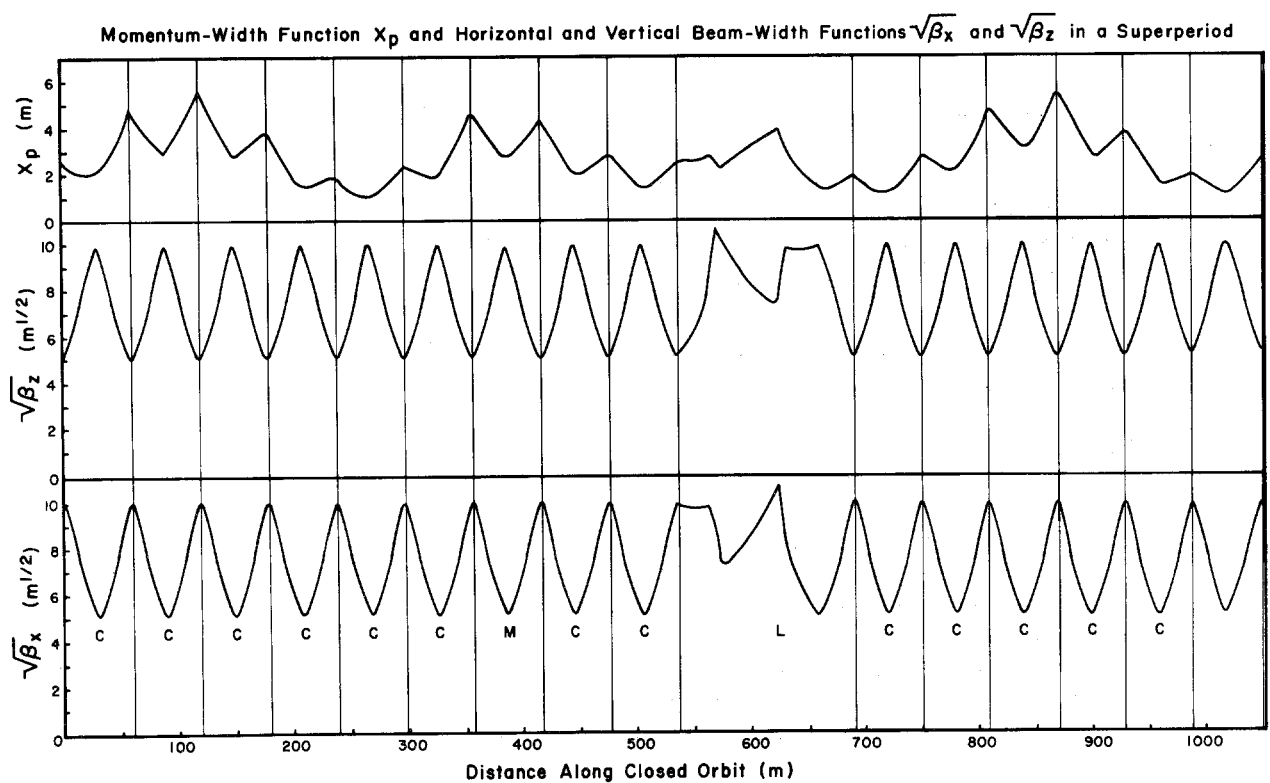


Figure 4-2 — Main-Ring Orbit Functions



D. Superperiod		
Structure	C-C-C-C-C-C-M-C-C-L-C-C-C-C-C-C	
Length	3,435.0 ft	8.25 in. (1047.2 m)
Number of Superperiods	6	
E. Circumference of Main Ring	20,614.1 ft	(6283.2 m)
F. Radius of Main Ring	3,280.8 ft	(1000.0 m)

#### Orbit Parameters

Injection Kinetic Energy ( $T_i$ )	10 BeV
Injection Revolution Frequency ( $f_i$ )	47.54 kHz
Final Kinetic Energy ( $T_f$ )	200 BeV
Final Revolution Frequency ( $f_f$ )	47.71 kHz
Radius of Curvature in Bending Magnets ( $\rho$ )	742 m
Betatron Oscillation Number	
Horizontal ( $\nu_x$ )	20.23
Vertical ( $\nu_z$ )	20.27
Betatron-Oscillation Phase Advance per Normal Cell	
Horizontal ( $\nu_x$ )	70.90°
Vertical ( $\nu_z$ )	71.04°
Betatron Oscillation Phase Advance per Cell with Long Straight Section	
Horizontal ( $\phi_x$ )	150.56°
Vertical ( $\phi_z$ )	150.75°
Transition Kinetic Energy ( $T_t$ )	17.38 BeV

#### Magnetic Field Parameters

At Injection Kinetic Energy ( $T_i=10\text{BeV}$ )	
Field strength in Bending Magnet ( $B_i$ )	0.490 kG
Field gradient in all quadrupole magnets ( $B_i$ )	6.81 kG/m
At Final Energy ( $T_f=200\text{ BeV}$ )	
Field strength in Bending Magnet ( $B_f$ )	9.03 kG
Field gradient in all Quadrupole Magnets ( $B_f$ )	125.6 kG/m
At Final Energy ( $T_f = 400\text{ BeV}$ )	
Field strength in Bending Magnet ( $B_f$ )	18.02 kG
Field gradient in all Quadrupole Magnets ( $B_f$ )	250.5 kG/m

### 4. Error and Misalignment Tolerances

Design, fabrication, and alignment imperfections and errors of magnets in the main-accelerator ring will always exist. In general, the effects of these imperfections and errors on the proton beam can be classified into two major categories: The first category of errors causes a distortion in the closed orbit of the proton beam around the ring, thereby requiring more space in the vacuum chamber to accommodate the beam. Although most of the closed-orbit distortion caused by these

imperfections and errors can in time be eliminated by moving elements and by using auxiliary magnets installed in the ring, these effects should be analyzed in the design. To this category of errors belong: (i) magnetic-field and length errors in the bending magnets, (ii) rotational misalignments of bending magnets about the longitudinal axis, (iii) horizontal and vertical misalignments of the quadrupole focusing magnets, and (iv) stray fields at injection.

The second category of errors causes deviations of the focusing actions from the design values. To this category belong: (i) systematic deviation of the horizontal magnetic-field gradient in the bending magnets from the design value of zero, (ii) systematic deviation of the field gradient of the quadrupole focusing magnets from the design value, (iii) random errors in the field gradient of the quadrupole magnets, and (iv) rotational misalignments of the quadrupole magnets about the longitudinal axis.

**4.1 Closed-Orbit Errors.** Typically, the maximum expected displacement of the closed-orbit distortion due to an error of the first category can be expressed as the root-mean-square magnitude of the error multiplied by the beam-width functions  $\sqrt{\beta_x}$  or  $\sqrt{\beta_z}$  at the point in question and an amplification factor. Following the work of Laslett<sup>6</sup> and Keil<sup>7</sup>, we use an amplification factor corresponding to 75% probability that the displacement will be less than the amount given. For the three types of errors above, we have:

- (i) Field error in bending magnet:  $A_x = 194\sqrt{\beta_x} (\Delta B/B)^{rms}$   
 Length error in bending magnet:  $A_x = 194\sqrt{\beta_x} (\Delta L/L)^{rms}$   
 where  $(\Delta B/B)^{rms}$  is the rms field error,  $\beta_x$  is expressed in m,  $(\Delta L/L)^{rms}$  is the rms length error and  $A_x$  is given in cm.

- (ii) Rotational error of bending magnet:

$$A_z = 194\sqrt{\beta_z} (\Delta\theta)^{rms}$$

where  $(\Delta\theta)^{rms}$  is the rms rotational angle in radians,  $\beta_z$  is expressed in m, and  $A_z$  is given in cm.

- (iii) Transverse displacements of quadrupole magnet. Exact evaluation of this type of error depends on the details of the alignment procedure. Assuming the displacement errors in individual quadrupoles to be uncorrelated, we have

$$A = 5.68\sqrt{\beta_x} (\Delta X)^{rms}$$

$$A = 5.68\sqrt{\beta_z} (\Delta Z)^{rms}$$

where  $(\Delta X)^{rms}$  and  $(\Delta Z)^{rms}$  are respectively the horizontal and the

vertical rms displacement errors and both  $\beta_x$  and  $\beta_z$  are expressed in m.

- (iv) The magnitude of the stray field is difficult to estimate, but since it is relatively easy to compensate its effects, we will omit it here.

For tolerances  $(\Delta B/B)^{rms} = 5 \times 10^{-4}$ ,  $(\Delta L/L)^{rms} = 5 \times 10^{-4}$ ,

$(\Delta \theta)^{rms} = 0.5 \times 10^{-3}$  rad, and  $(\Delta X)^{rms} = (\Delta Z)^{rms} = 0.01$  cm;

and using the largest values of  $\beta_x = 97$  m,  $\beta_z = 60$  m

in bending magnet B1, and  $\beta_x = 56$  m,  $\beta_z = 98$  m in magnet B2,

we find the total closed-orbit displacements at the 75% confidence level in B1 and B2 given in Table 4-2.

Table 4-2. Closed-Orbit Displacements

	<u>B1</u>	<u>B2</u>
$A_x$	1.46 cm (0.58 in.)	1.11 cm (0.44 in.)
$A_z$	0.87 cm (0.34 in.)	1.11 cm (0.44 in.)

Within the aperture of the vacuum chamber,  $2A_x$  of the full horizontal aperture and  $2A_z$  of the full vertical aperture will be taken up by the closed-orbit distortion and will not be available for containment of the beam widths. The effects of these imperfections and errors can be trimmed out by corrections based on beam observations and the full aperture of the vacuum chamber can be made available for containment of the beam, which will enable the main accelerator to accelerate a beam of higher intensity than the design value.

4.2 Focusing Errors. Errors of the second category affect only the focusing of the beam. These effects can further be classified in two types. The first two errors in this category modify the focusing strengths and may cause  $\nu_x$  or  $\nu_z$  to be at resonant values.

- (i) The change in  $\nu$  (either  $\nu_x$  or  $\nu_z$ ) due to a systematic deviation of the magnetic field gradient in the bending magnet from zero value is given by

$$\Delta \nu = 25 \frac{B'}{B},$$

where B is the field strength in kG and B' is the field gradient of the bending magnet in kG/m. For  $\nu$  to avoid the nearest integral and half-integral values, we must have

$$|\Delta\nu| < 0.25 \quad \text{or} \quad \left| \frac{B'}{B} \right| < 0.01 \text{ m}^{-1}$$

- (ii) The change in  $\nu$  due to a systematic deviation of the field gradient in the quadrupole magnet from design value is given by

$$\Delta\nu = 23 \frac{\Delta B'}{B'}$$

Again, for  $|\Delta\nu| < 0.25$ , we must have

$$\left| \frac{\Delta B'}{B'} \right| < 1.1\%$$

The last two errors in this category give rise to instability for certain ranges of  $\nu$  values.

This formula can also be used to estimate the tolerance on tracking of separate bending-magnet and quadrupole power supplies. For a  $\Delta\nu < 0.02$ , the relative difference in currents  $\Delta I/I$  must be less than 0.1%.

- (iii) For random errors in the field gradient of the quadrupole magnets, the half-integral resonance  $\nu = 41/2$  (where  $\nu$  denotes either  $\nu_x$  or  $\nu_z$ ) is excited.

The range  $\Delta\nu$  of unstable  $\nu$  values and strength, expressed as the rate of growth of the oscillation amplitude A on resonance are given by

$$\Delta\nu = 9.5 (\Delta B'/B')^{\text{rms}}$$

$$\frac{1}{A} \frac{dA}{dn} = 15 (\Delta B'/B')^{\text{rms}}$$

where n denotes the number of revolutions around the ring. For the easily attainable tolerance of  $(\Delta B'/B')^{\text{rms}} = 10^{-3}$ , the width and growth rate on resonance are only 0.009 and 1.5% per turn so that the region could easily be traversed if desired.

In addition, this type of error causes an increase in the beam-width factor (either  $\beta_x$  or  $\beta_z$ ). The root-mean-square increase  $(\Delta\beta/\beta)^{\text{rms}}$  is given by  $(\Delta\beta/\beta)^{\text{rms}} = 24 (\Delta B'/B')^{\text{rms}}$

For  $(\Delta B'/B')^{\text{rms}} = 10^{-3}$ , we get only a 2.4% increase in  $\beta$  or a 1.2% increase in beam width, which is entirely negligible. It may be pointed out that random errors in the field gradients of the bending magnets have similar effects on the orbit. Because of the rigid requirement in (i) above on systematic deviation of the field gradient from zero, the random error is necessarily small and its effects can be shown to be smaller than those of the quadrupoles given here.

- (iv) For random rotational misalignments of the quadrupole magnets about the longitudinal axis, the coupling resonances

$\nu_x + \nu_z = 41$  and  $\nu_x - \nu_z = 0$  are excited. The widths and growth rates on resonance are given approximately by

$$\Delta\nu = 38 (\Delta\theta)^{\text{rms}}$$

$$\frac{1}{A_z} \frac{dA_x}{dn} = 30 (\Delta\theta)^{\text{rms}}; \quad \frac{1}{A_x} \frac{dA_z}{dn} = \pm 30 (\Delta\theta)^{\text{rms}}$$

where in the last equation the + and - signs refer to the resonances  $\nu_x + \nu_z = 41$  and  $\nu_x - \nu_z = 0$  respectively. Again for the easily attainable tolerance of  $(\Delta\theta)^{\text{rms}} = 0.5$  mrad the width and growth rate are only 0.019 and 1.5% per turn.

### 5. Aperture Considerations

The horizontal widths of the four bending magnets on either side of a horizontally focusing quadrupole magnet (QF) need to be larger than those of the four bending magnets on either side of a vertically focusing quadrupole magnet (QD). On the other hand, the vertical width of the aperture of the four bending magnets on either side of a horizontally focusing quadrupole magnet (QF) can be smaller than that of the four bending magnets on either side of a vertically focusing quadrupole magnet (QD). In order to minimize cost, therefore, two types of bending magnets with different apertures will be built. Bending magnets type B1 with smaller vertical aperture and larger horizontal aperture will be installed on either side of the horizontally focusing quadrupole magnets, and bending magnets type B2 with larger vertical aperture and smaller horizontal aperture will be installed on either side of the vertically focusing quadrupole magnets.

In addition to the beam widths due to betatron oscillations, the following allowances in aperture must be provided

	<u>Horizontal</u>	<u>Vertical</u>
Vacuum-chamber wall thickness	2 x 0.05 in.	2 x 0.05 in.
Sagitta of orbit arc in straight magnet	0.24 in.	0
Beam width due to momentum spread ( $\Delta p/p = \pm 10^{-3}$ )	2 x 0.22 in.	0
Total	0.78 in.	0.10 in.

The ratios of the horizontal and vertical beam widths in B1 and B2 due to betatron oscillations are respectively

$$\frac{\text{max. } \sqrt{\beta_x} \text{ in B1}}{\text{max. } \sqrt{\beta_x} \text{ in B2}} = 1.32$$

and

$$\frac{\text{max. } \sqrt{\beta_z} \text{ in B1}}{\text{max. } \sqrt{\beta_z} \text{ in B2}} = 0.75$$

The aperture chosen for magnet B1 is 5 in. by 1.5 in. The allowances and beam-width ratios given above then lead to a required aperture for magnet B2 of 3.98 in. by 1.95 in. which is rounded off to 4 in. by 2 in.

In choosing the aperture for a synchrotron, the considerations are:

- (i) The aperture must be large enough to contain the widths of the injected beam and all necessary allowances with suitable safety factors to ensure a high probability of success of guiding a beam around the ring even with the distortions of the closed orbit uncorrected.
- (ii) The aperture must be large enough so that the space-charge limit (See Section 7 below) of the beam intensity is well above the desired value.
- (iii) The aperture should be adequate for the necessary maneuvering of the beam for extraction at peak energy.

For synchrotrons at energies of hundreds of BeV, the last requirement is by far the most demanding. Detailed study of the operation of the resonant-extraction scheme employed for this accelerator led to the above choice of aperture.

As calculated in Sec. 4 above, with the specified tolerances in field errors and misalignments, the expected initial distortions of the closed orbit are given in Table 4-2. When these distortions are subtracted from the full aperture, the effective clear aperture corresponds to horizontal and vertical phase-space acceptances of  $1.57 \pi$  cm-mrad and  $0.15 \pi$  cm-mrad respectively. Even these reduced acceptance values are more than adequate to accommodate the beam injected from the booster, which has horizontal and vertical emittances of  $0.3 \pi$  cm-mrad and  $0.12 \pi$  cm-mrad, respectively. Of course, in time the effects of these magnetic field errors and misalignments can be eliminated by using the trimming magnets installed in the main accelerator and the full horizontal and vertical acceptance of  $2.98 \pi$  cm-mrad and  $0.56 \pi$  cm-mrad will then be available to the beam.

## 6. Auxiliary Magnets

Several kinds of auxiliary magnets will be installed for various special purposes. They are listed below:

- (i) Closed-Orbit Deflecting Magnets. These are for the purpose of correcting horizontal or vertical distortions of the closed orbit. One such magnet, 1 ft in length with a maximum field of  $\pm 3$  kG will be installed in one 7-ft straight section of each normal cell.
- (ii) Trim Quadrupoles. These are used for the purpose of controlling the rate of change of  $\nu$  value to provide uniform beam spill during resonant extraction. One such magnet, 0.5 ft in length with a maximum gradient of  $\pm 7$  kG/m, will be installed in each 7-ft straight section.
- (iii) Sextupoles. These will be used to compensate for undesired sextupole field components caused by remanent fields or saturation. One sextupole, 1 ft in length with a maximum field second-derivative of  $\pm 2000$  kG/m<sup>2</sup>, will be installed in each 7-ft straight section. They are strong enough to compensate saturation effects well beyond 400 BeV.

## 7. Space-Charge Limits

This subject has been discussed extensively in other documents<sup>8,9</sup> and so requires only brief mention here. Incoherent space-charge limits have been calculated using the formulas of Laslett<sup>9</sup>, including image effects of extended beams. The result, assuming that the aperture is filled and that a  $\nu$  shift of 0.5 is allowed, is  $3 \times 10^{14}$  protons per pulse. If the beam size is assumed to be limited by closed-orbit deviations and the  $\nu$  shift is limited to 0.25, then the space-charge limit decreases to approximately  $10^{14}$  protons per pulse, twice the design intensity.

Several coherent effects give limits of the same magnitude. It is expected that these coherent oscillations can be damped by feedback systems, so that these effects should not impose any ultimate limitation on intensity.

### References:

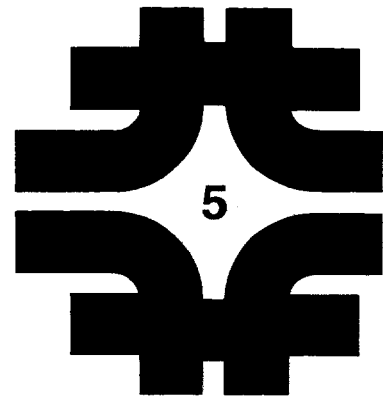
1. A. A. Garren, G. R. Lambertson, E. J. Lofgren, L. S. Smith, Extendible - Energy Synchrotrons, Nucl. Inst. and Methods, 54, (1967), 223.
2. M. G. White, Preliminary Design Parameters for a Separated-Function Machine, Princeton Internal Report, March 3, 1953.
3. T. L. Collins, A Proposal for a Separated-Function 1000 BeV Proton Synchrotron, Brookhaven National Laboratory Report IA-4, Aug. 3, 1961
4. G. T. Danby, Proceedings of the VI International Conference on High Energy Accelerators, CEA, Cambridge, Mass., Sept. 1967, (to be published).

5. A. A. Garren, Design of Long Straight Sections for Synchrotrons, Proceedings of the V International Conference on High Energy Accelerators, CNEN, Rome, 1966, p. 22
6. L. J. Laslett, Computational Results Concerning the Maximum Displacement of a Closed Orbit for One and Two Transverse Degrees of Freedom, University of California Lawrence Radiation Laboratory Report UCID - 10158, May, 1965.
7. E. Keil, A Monte Carlo Investigation of Closed-Orbit Distortions in AG Synchrotrons, CERN Report AR/Int. SG/65-3, Feb. 10, 1965
8. 200 BeV Accelerator Design Study, University of California Lawrence Radiation Laboratory Report UCRL-16000, (June, 1965), Chapter IV.
9. L. J. Laslett, On Intensity Limitations Imposed by Transverse Space Charge Effects in Circular Particle Accelerators, Brookhaven National Laboratory Report BNL-7534, July 19, 1963, p.324.



# Main-Synchrotron Magnet System

1. Introduction	5-1
2. Magnetic-Field Design and Computations	5-3
2.1 Bending Magnets	5-3
2.2 Focusing Magnets	5-5
3. Magnet Fabrication	5-7
3.1 Magnet Yokes	5-8
3.2 Magnet Coils	5-10
4. Power and Water Distribution	5-13
4.1 Choice of Systems and Materials	5-13
5. Main Magnet Power Supply	5-14
5.1 Bending-Magnet Power Supply	5-14
5.2 Focusing-Magnet Power Supply	5-16
5.3 Power Source	5-16
6. Magnet Support and Alignment	5-18
References	5-22



## 5. MAIN-SYNCHROTRON MAGNET SYSTEM

H. G. Blosser, W. M. Brobeck, R. Cassel, J. W. DeWire,  
R. C. Juergens, E. Malamud, I. J. Polk (BNL), R. Yamada

C. G. Dols (LRL), J. H. Dorst (LRL), M. Foss (Carnegie-  
Mellon), R. A. Kilpatrick (LRL), W. R. Winter (Wisconsin)

### 1. Introduction

The function of the magnet system in a circular particle accelerator is to provide bending of particles around a closed path, in order that they can traverse the accelerating system many times, and focusing of particles around the closed path, in order that they do not stray from the magnet aperture and be lost. In this separated-function design, bending and focusing are done by two different sets of magnets; this chapter will therefore describe the design of both these types, the "bending magnets" and the "quadrupoles" or "focusing magnets."

In a synchrotron, the closed path of the particles is the same at all energies. The magnetic field must increase in time as the particles are accelerated to keep them on the same path. The magnet power supply must then produce energizing currents for the magnets that also increase in time. In addition, the magnet yokes must be built of laminated steel in order that eddy currents do not distort the magnetic fields.

The bending magnets of the separated-function synchrotron are approximately 20 feet long. Each of the steel yokes contains approximately 4,000 1/16-inch thick laminations, each 25 inches wide and 14 inches high. They will be held in place by a steel I-beam supporting structure. The steel yoke of each bending magnet will have a total weight of approximately 10 tons. The quadrupoles utilize the same size laminations, 25 by 14 by 1/16 inch, but the whole magnet yoke is 7 feet long, and weighs approximately 3.5 tons. The coils will be fabricated of copper bars approximately 1 inch square in cross section. There are two types of bending magnets with different apertures (called B1 and B2) to fit the oscillations of the beam. In both kinds of magnets, the coils are located on either side of the particle aperture. The upper coils are bent up at the ends of the magnets and the lower coils down to clear the vacuum-chamber section that extends out from the aperture to join the adjacent chamber section.

Digital computation has been utilized in the design of the magnet pole faces, using the programs developed at the Lawrence Radiation Laboratory. In addition, a modeling program is in progress to test assembly methods and magnetic features not covered by computation.

The magnet power supply may not include large motor-generator sets, which have been used for energy storage on most previous large proton synchrotrons. Instead, the electric-power network supplying the site will be used for energy storage. Without motor-generators, more extensive filtering and power-factor correction is needed. There is therefore no appreciable saving from doing away with motor-generators, but it is believed that the present design will avoid many of the malfunctions and consequent lost time for repairs that have occurred in other accelerators.

Table 5-1 summarizes the parameters of the primary magnet system.

Table 5-1. Magnet-System Parameters

<u>Bending Magnets</u>	<u>B1</u>	<u>B2</u>	
Total Number	384	384	
Aperture	1-1/2 x 5	2 x 4	in. <sup>2</sup>
Length	239	239	in.
Outside Dimensions	25 x 14	25 x 14	in. <sup>2</sup>
Number of Turns	12	16	
Unit Core Weight	10.7	10.4	tons
Unit Coil Weight	0.85	1.1	tons
<u>Focusing Magnets</u>			
Total Number	180		
Pole Shape	xy = 1.35		sq. in.
Length	84		in.
Outside Dimensions	25 x 16		in. <sup>2</sup>
Turns per Pole	14		
Unit Core Weight	4.1		tons
Unit Coil Weight	0.4		tons
<u>Bending-Magnet Excitation</u>	<u>200 BeV</u>	<u>400 BeV</u>	
Peak Field	9	18	kG
Peak Current	2350	5000	A
Number of Power Supplies	24	48	
Peak Voltage to Ground	450	450	
Peak Power	55	189	MW
Average Power	15	68	MW

### Focusing-Magnet Excitation

Peak Field Gradient	125	250	kG/m
Peak Current	620	1300	A
Peak Voltage to Ground	300	300	V
Peak Power	4.3	16	MW
Average Power	1.3	5.9	MW

---

In addition to the primary magnets, the system will include a number of small secondary correction magnets to cancel small field errors and to aid in beam extraction.

## 2. Magnetic-Field Design and Computations

2.1 Bending Magnets. It is particularly advantageous in the flat-field bending magnets to consider an "H-magnet" design, with magnetic return paths on both sides of the aperture, rather than a "C-magnet", with a return on only one side. The H-magnet is smaller and therefore less expensive at the same field performance. On the other hand, the C-magnet offers the advantage of easy access to the vacuum chamber for repairs in place. Because of the problems of residual radioactivity, no repairs in place will be done on this accelerator. Instead, entire magnets and other components will be replaced by spares, an operation that can be carried out without undue radiation exposure. The easy accessibility of a C-magnet is therefore of little significance in this case, and an H-magnet design is therefore planned.

Conventionally, the current-carrying coil for energizing an H-magnet is wound separately around the top and the bottom poles, leaving unoccupied the space on either side of the poles, where the radiation level is high and the possibility of radiation damage to the coil insulation material is great. Instead, for maximum efficiency in the use of the coil and the yoke, we have designed the coil to fill the entire space on either side of the poles, including that between the poles on either side of the vacuum chamber. There are therefore coils in the gap between the magnet poles. Beam stops will be used to prevent lost beam from striking the coils.

To excite the two types of bending magnets to the same field strength, the ampere-turns of the coils should be in the ratio of the vertical gaps, that is, 0.75. In order to connect these two types of magnets in series, the turns ratio of their coils should therefore be 0.75. Magnet B1 is designed to have a 12-turn coil, and the coil for magnet B2 has 16 turns.

For the separated-function design, these bending magnets should provide a magnetic field uniform across the width of the gap occupied by the vacuum chamber. At low field strengths, when the permeability of iron is very large, the flat poles will give uniform magnetic fields, provided that the poles are sufficiently wide and the pole faces flat

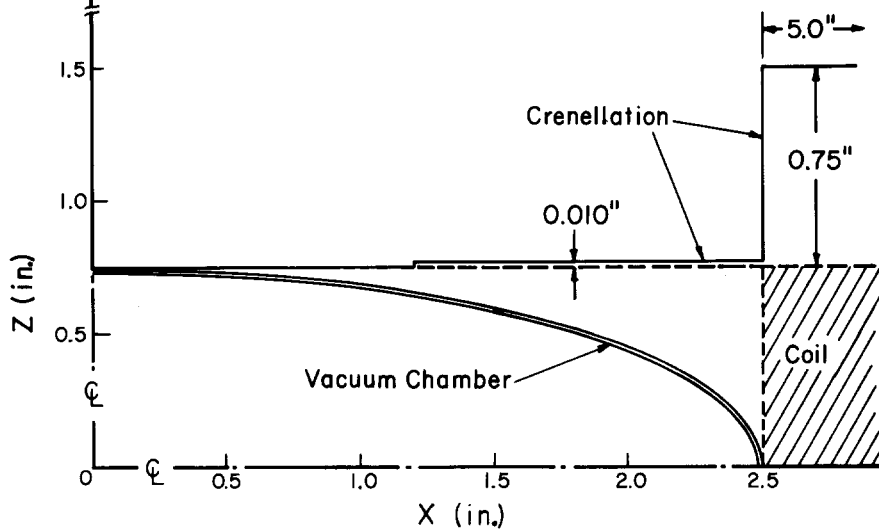
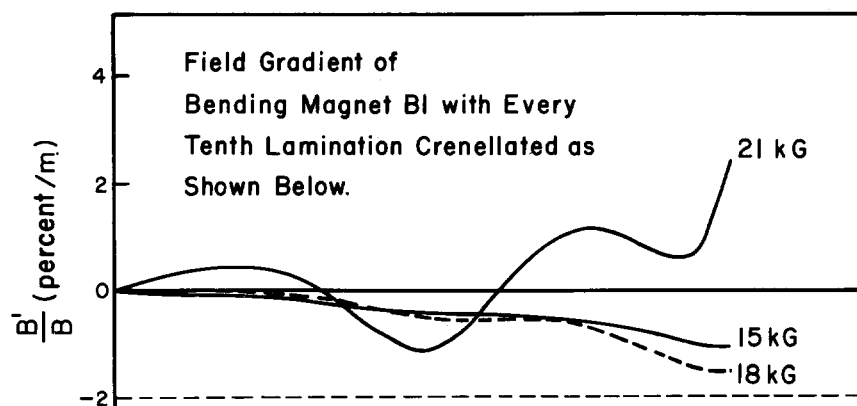
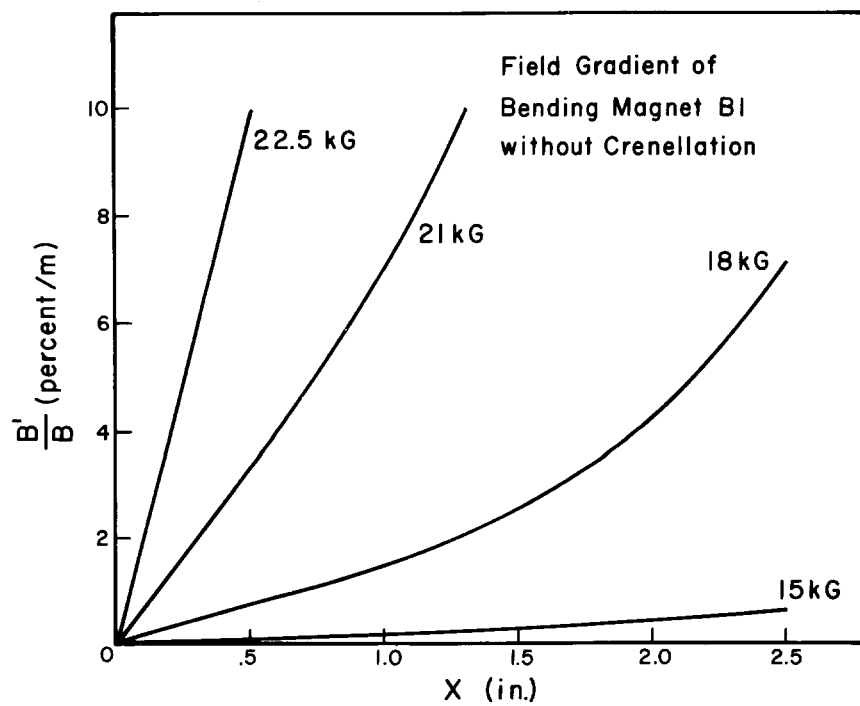


Figure 5-1 — Magnetic Field Plots

and parallel to each other. At high field strengths, when parts of the yoke iron are driven into saturation, the magnetic field will become nonuniform across the gap. Modifications on the details of the coil cross sections and the magnet pole faces must therefore be made to keep the field uniform. The studies and design for this modification have been performed using the CDC 6600 computer and the magnetic field computation programs, SIBYL<sup>1</sup>, LINDA<sup>2</sup>, and TRIM<sup>3</sup>, developed at the Lawrence Radiation Laboratory. The effects of saturation of iron and the resulting nonuniformity in field as computed by these computer programs for magnet B1 are shown in Fig. 5-1. Here the relative field gradient  $k = B' / B$  is plotted as a function of radial distance  $x$ . To restore the field uniformity at high field strengths, the average saturation behavior of the pole face must be modified. This is done by shaping the edges of specific evenly spaced laminations at the face of the pole, a technique known as "pole-face crenellation." The effect on the field shape for a specific configuration of crenellation is also shown in Fig. 5-1. In this case, the pole face edge of every tenth lamination is cut back 0.010 in. from  $x = 1.2$  in. to  $x = 2.5$  in. and cut back 0.75 in. from  $x = 2.5$  in. to the side of the coil window at  $x = 5.0$  in. These curves show that even with rather simple and crude crenellation, there is a remarkable improvement in the field uniformity at high field strengths. The field computations and design are still proceeding. The results obtained so far clearly indicate that good field uniformity within tolerance can be achieved up to at least 21 kG. With further refinement in the details of crenellation and coil cross section, it is likely that good field uniformity can be obtained up to 22 or even 22.5 kG.

A modeling program on the bending magnets is also in progress. As a first step, a 2-ft long section of a picture-frame type of H dipole bending magnet was constructed and tested. The purpose of this model is to study fabrication techniques and to test the validity of the computer programs for computing the magnetic-field excitation and shape.

This model has been energized up to a field strength of 18.1 kG, corresponding to a current of 10.4 kA or 83 kA-turns. The excitation curves giving the central magnetic field strength versus ampere turns and the field shape across the gap at several levels of excitation were measured. The excitation and field shape curves were also computed using the computer program TRIM. The agreement between computation and measurement is quite good all the way up to the maximum field strength obtained, which gives confidence in the use of the computer program for designing the magnets. In addition, the experience gained during construction of this model indicated that such a fabrication procedure can produce magnets of the required quality and can, with some modifications, be used to construct the bending magnets in the main accelerator.

**2.2 Focusing Magnets.** A quadrupole field is produced by a magnet with four poles shaped as hyperbolas. Four coils, one around each of the four

poles, are used to energize such a quadrupole magnet. Here, as in the bending magnets, the four coil slots are enlarged beyond the pole-tip region in order to reduce electric-power requirements.

In the separated-function design, focusing is completely separated from bending. To take advantage of this flexibility in the independent adjustment of these two actions, the quadrupole focusing magnets in the ring will be energized by separate power supplies from those for the dipole bending magnets.

At low magnetic-field strengths, the hyperbolic shape of the poles automatically produces the desired linear dependence of magnetic field on radial distance. The saturation of the yoke iron at high magnetic field strengths will again cause the magnetic field to deviate from the required linear dependence. These deviations can be reduced by proper location of the energizing coils, shaping of the poles, and the addition of crenellation to the yoke laminations. The design of the quadrupole magnet is also being studied using the computer program LINDA. The studies so far have indicated that with proper placement of the coils, without any pole-face shaping or crenellation, the field gradient can be made to fall within tolerance up to the value of 125 kG/m required for accelerating protons to 200 BeV.

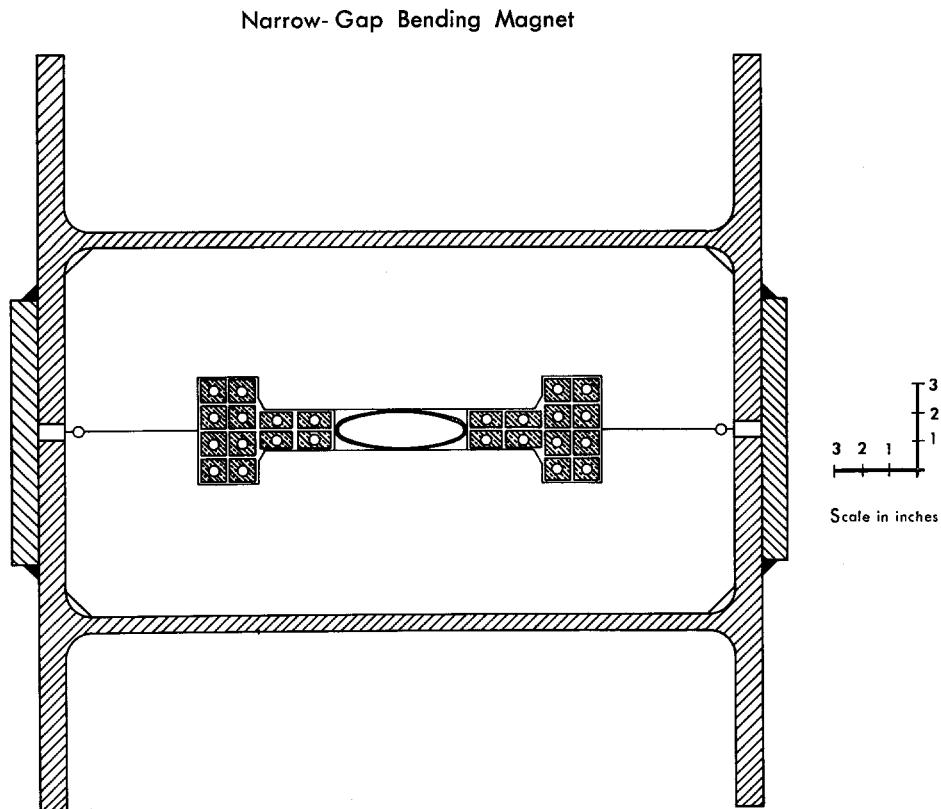


**Figure 5-2A — Main-Ring Bending Magnet**

A method of eliminating the undesirable octupole field component is to make the quadrupole magnet cross section symmetrical in the horizontal and vertical directions. For such a symmetric design, the octupole field is identically zero. Nevertheless, for economy in use of yoke iron, it is desirable to keep the outside vertical dimension of the magnet smaller than the horizontal dimension. This asymmetry between the vertical and the horizontal dimensions introduces an octupole field, but with proper placement of the coils, the octupole field can be reduced to well within allowable tolerance.

Computation and design of the focusing magnets are continuing. The present progress indicates that a magnetic field gradient within tolerance can be obtained at least up to the value of 250 kG/m required for accelerating protons to 400 BeV. Higher energy could be achieved with the same gradients by reducing the excitation of the quadrupoles relative to the bending magnets, thus reducing the  $\nu$  value.

### 3. Magnet Fabrication

The two bending magnets B1 and B2 and the quadrupole magnet are shown in cross section in Figs. 5-2 and 5-3. Fabrication of the yokes and coils of these magnets is discussed in this section. It is expected that the fabrication methods to be used for bending magnets and for quadrupoles will be similar. Although the quadrupoles have four-piece

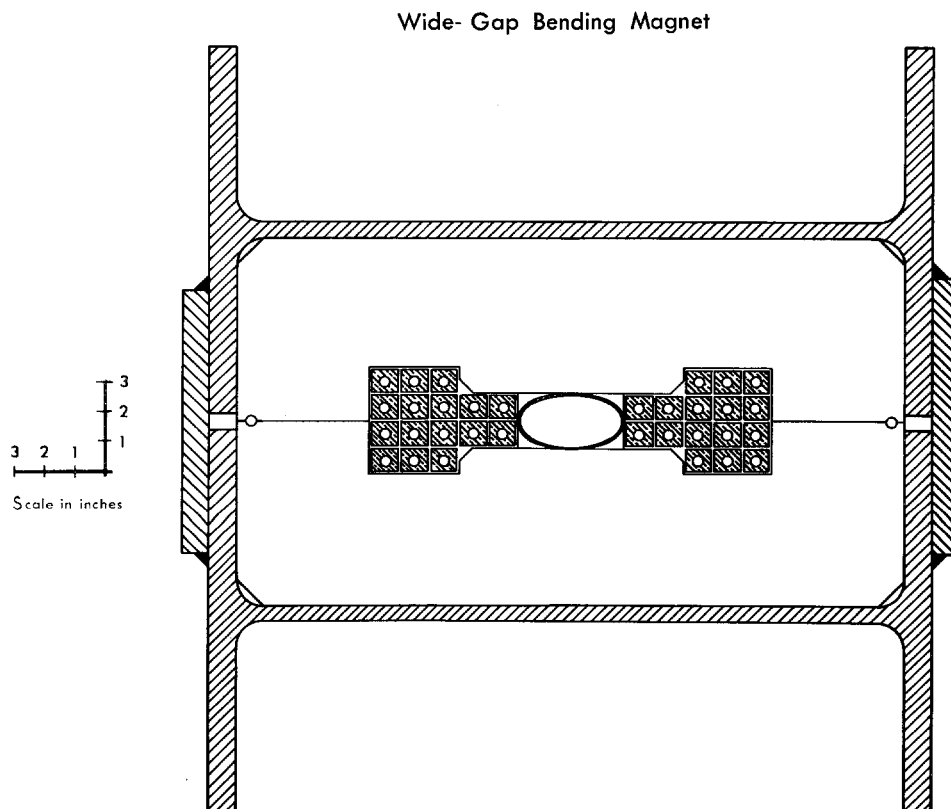


**Figure 5-2 B — Main-Ring Bending Magnet**



laminations, they are considerably shorter than the bending magnets and are, therefore, less affected by torsion and deflections in the structure.

### 3.1 Magnet Yokes

Choice of Steel and Lamination Thickness. The cross sections of the magnet yokes are designed to permit the operation of the magnets at very high fields by keeping the flux density in the steel quite uniform. To exploit this design fully, the steel must be capable of operation at the maximum possible induction. The characteristics of the steel at an induction of 18 kG and higher are of particular interest. The best performance at high induction is shown by mild steels of low carbon content. After the carbon content is reduced below about 0.1%, very little improvement in the high-field characteristics can be achieved by further reduction of the carbon level, but low coercive force is also desirable to minimize the residual field in the gap when the magnet has been cycled and the sextupole component at low field. Measurements on the 2-ft model magnet, which was fabricated from Grade 1010 steel having a coercive force of 3 Oersteds, showed a residual central-gap field of 30 G and a sextupole component of  $1.2 \text{ kG/m}^2$ . Such a sextupole term

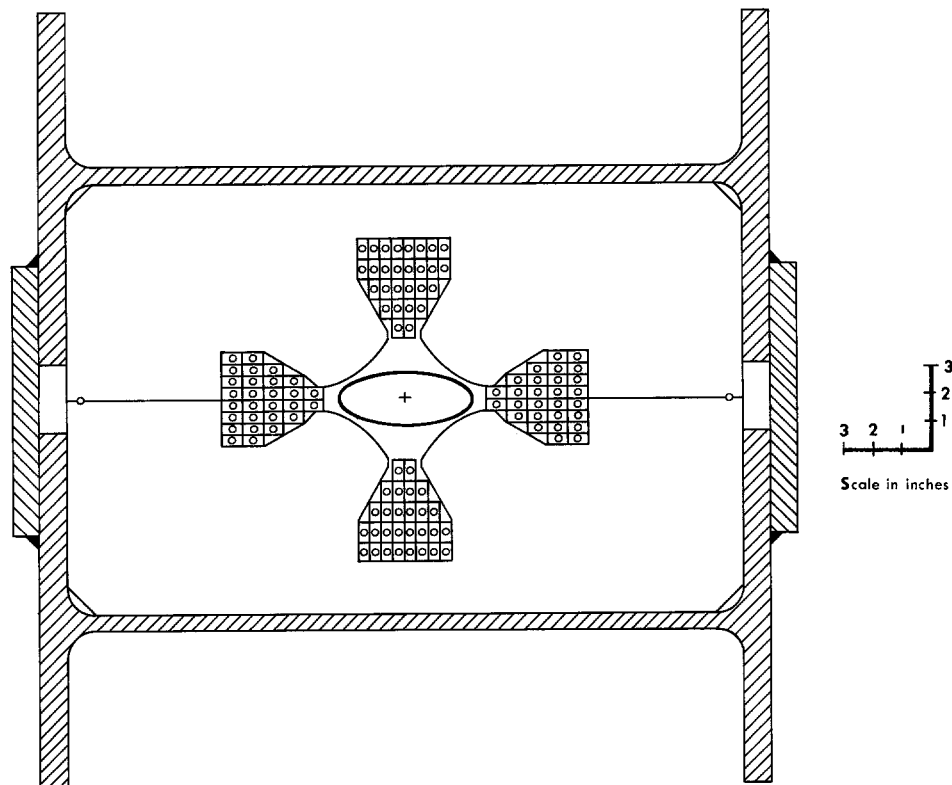


Figure 5-3 — Main-Ring Quadrupole

at injection would produce a shift in  $v$  of 0.36 for a proton off the central momentum by one part in  $10^3$ , approximately the largest momentum spread expected. This  $v$  shift is unacceptably large. Similarly, an rms variation of the central gap field of 0.5 G will produce an rms radial excursion of the closed orbit at injection of 0.8 cm. It is clear from these results that the use of steel with a lower coercive force will significantly reduce the amount of field correction required at injection.

Steel which is decarburized by open-coil annealing has a carbon content less than 0.005% and a coercive force of 1 Oersted or less. Furthermore, aging of such steel does not increase the coercive force. The use of decarburized steel should greatly simplify the correction of the guide field at injection.

Satisfactory magnet performance could be achieved with laminations up to one inch thick, but the decarburization of the steel can only be done efficiently with sheets of a thickness of 1/16 in. or less. The required precision of the pole contour can be maintained in the stamping process. A magnet design utilizing machined 1-in. plates is also being investigated.

Punching and Shuffling. To fabricate the bending magnets, approximately three million complete 1/16-in. laminations will be required. Since each lamination is split in the median plane, six million stampings must be made, half for B1 magnets and half for B2 magnets. Several commercial stamping firms have the facilities to make these stampings from one die set at a rate of several hundred thousand per week. The steel will be given a minimal inorganic insulating core plate, probably at the mill, and the steel will be supplied to the stamper in coils, unless it is found that adequate flatness cannot be achieved by this procedure. It will be fully annealed at the mill to develop optimum magnetic properties. No annealing is planned after stamping.

Several procedures can be used to obtain good uniformity of the magnetic field. Random shuffling of all the laminations prior to fabricating the magnets is neither feasible nor necessary, but it will be possible to include steel from several heats in each magnet without causing significant delay and added expense. Further mixing can be done by placing the magnets along several sectors of the ring simultaneously. The construction of the enclosure has been scheduled to make available widely separated sectors. Field measurements on each magnet can be used to determine where magnets can be placed to minimize low harmonic variations.

Yoke Assembly. The magnet cores will be fabricated in a manner indicated schematically by the cross sections in Figs. 5-2 and 5-3, where the structural support is made an integral part of the core. The absence of a separate support structure under the magnet provides additional space in the enclosure and makes it possible to develop a simple technique for replacing magnets. The two halves of the core

will be assembled separately and joined together after the coils have been inserted. Whether the cores will be welded or potted in the support structure will be determined after models have been made and studied. It appears to be quite feasible to make the magnet from a number of short blocks, perhaps welded into units 4 or 5 ft long. These units would then be assembled in an outside supporting structure.

**3.2 Magnet Coils.** The bending-magnet coils can be seen in cross section in Fig. 5-2, and the quadrupole coils in Fig. 5-3. The bending-magnet coil ends are shown in Fig. 5-4. Table 5-2 gives parameters of the bending-magnet coils and Table 5-3 parameters of the quadrupole coils.

Table 5-2. Tentative Parameters of Bending-Magnet Coils

	<u>B1</u>	<u>B2</u>	
Number of Turns	12	16	
Outside Dimensions of Copper Conductor	1.053 x 0.935 (8 turns) 1.350 x 0.685 (4 turns)	1.053 x 0.935 in. <sup>2</sup>	
Diameter of Cooling Hole	13/32	1/2	in.
Copper Area	0.826 0.766	0.759	sq. in.
Cooling Circuits	4	4	
Inductance	6.3	7.4	mH
Resistance	6.06	8.63	mΩ

	<u>200 BeV</u>	<u>400 BeV</u>	<u>200 BeV</u>	<u>400 BeV</u>	
Maximum Current Density	3060	6530	3160	6590 A/in. <sup>2</sup>	
Average Power	15.4	66.7	21.9	94.9 kW	
Temperature Rise per Pulse (no cooling)	0.2	1.8	0.2	2.0	°C
Cooling-Water Temperature Rise	6	16	6	16	°C
Total Water Flow	9.7	15.8	13.9	22.5	gpm
Pressure Drop across One Water Circuit	39	90	37	93	psi

**Choice of Material and Size.** The coils will be fabricated of a high-quality electrical-copper rectangular bar with a hole for cooling. In the B2 magnets all the copper will have the same cross section. In the B1 magnets, the four turns in the gap region will be of a different cross section than those in the outer window in order to match the desired core configuration. The copper bars will be obtained in the maximum possible lengths to keep the number of brazed joints as small as possible.

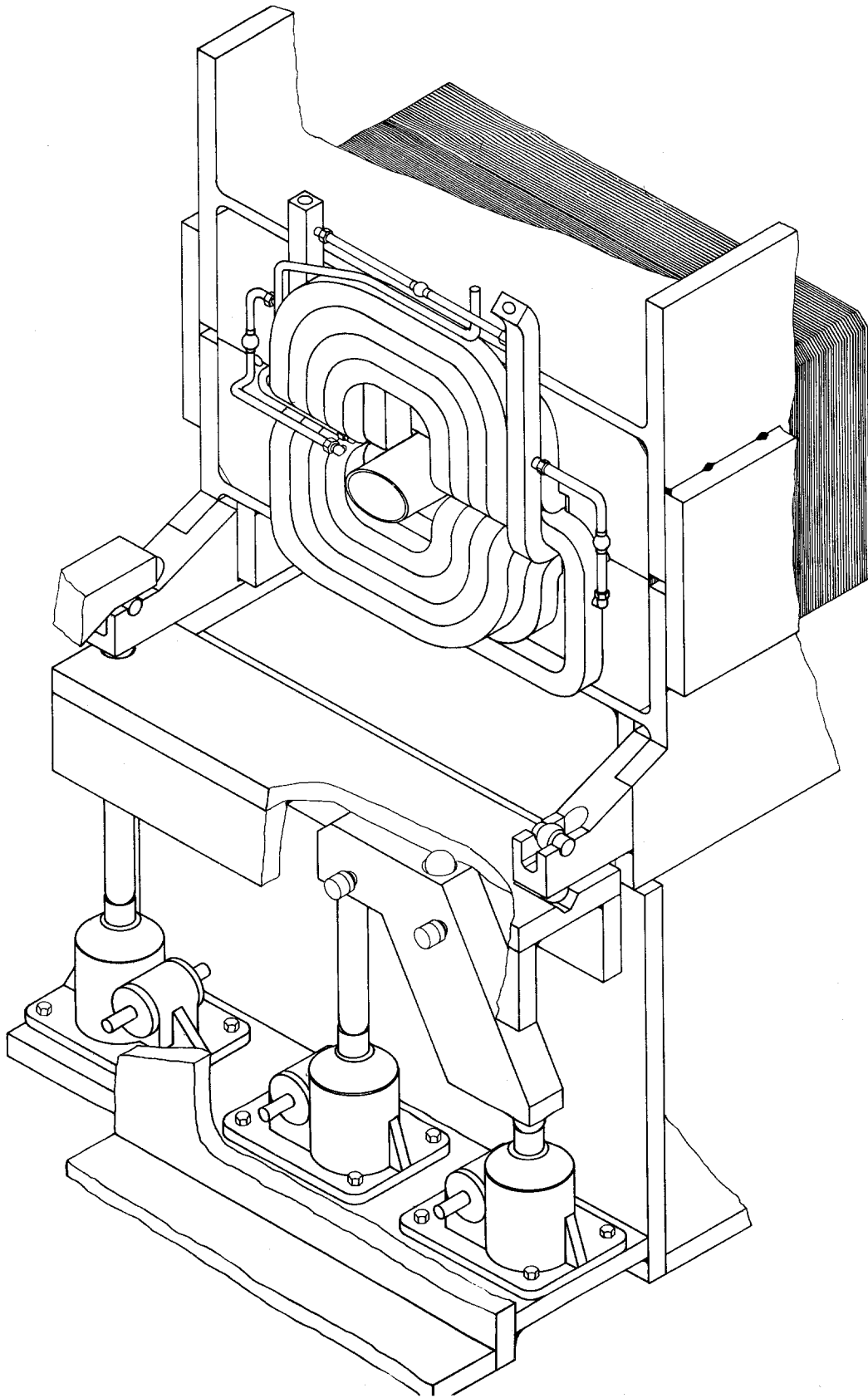


Figure 5-4 — Main-Ring Bending Magnet and Support System

Table 5-3. Tentative Parameters of Quadrupole Focusing-Magnet Coils

	<u>200 BeV</u>	<u>400 BeV</u>	
Turns per Pole	14		
Outside Dimensions of Copper			
Conductor	0.385 x 0.710		in. <sup>2</sup>
Diameter of Cooling Hole	1/4		in.
Copper Area	0.222		sq. in.
Inductance	19		mH
Resistance	35		m $\Omega$
Current Density	2790	5860	A/in. <sup>2</sup>
Average Power	5.9	26.0	kW
Cooling Circuits	8		
Cooling Water Temperature			
Rise	6	16	°C
Total Water Flow	3.7	6.2	GPM
Pressure Drop across One			
Water Circuit	32	80	psi

Fabrication of Ends and Joints. The geometry of the coil-end returns and connections is shown in Fig. 5-4. The copper conductors will be shaped by bending to form double layers of return windings above and below the gap against the end plates of the magnet cores. Bends of 1-in. inside radius have been made successfully on samples of copper bars similar to those to be used. The end plates will be beveled to accommodate the bends and permit the coil ends to lie flat on the end plates, providing an adequate clear space between magnets for insertion of pump manifolds and beam monitors.

Insulation. The selection of a suitable insulation for the coils can be made primarily on the basis of its resistance to damage by radiation, because the electrical requirements are rather modest. The potential above ground will not exceed 500 V, and the potential difference between adjacent turns will be less than 30 V, for either 200 BeV or 400 BeV operation.

An estimate of the expected radiation exposures can be made, using the beam losses listed in Table 12-1 and the measured radiation levels at the internal target of the Brookhaven AGS<sup>4</sup>. The magnet coils of the quiet areas of the main accelerator will be subject to dose rates no greater than  $10^7$  rads/year. No limitation of the useful life of these coils is expected. In the magnets near the extraction point, the magnitude of the radiation level will depend on the efficiency of beam extraction and the extent to which the cascade from interacting protons can be concentrated in beam scrapers. Calculations by Maschke<sup>5</sup> indicate that the radiation level on the magnet coils immediately downstream from the septum can be limited to about  $10^9$  rads/year, but it is possible that levels of about  $5 \times 10^9$  rads/year will be

encountered in localized areas.

Investigations of the effects of radiation on various insulating materials have shown that filled aromatic-epoxy resins are significantly more resistant to radiation than the polyester resins that have been used on previous accelerators.<sup>4,6,7,8</sup> Some insulators in this class should perform satisfactorily up to an accumulated irradiation of  $2 \times 10^{10}$  rads or perhaps somewhat more.<sup>9</sup> Further investigation of these materials is being carried out with the cooperation of the Argonne National Laboratory. The use of a fused vitreous insulating coating on the conductors is also being studied.

It is expected that the development of new insulating systems will continue through the construction period and will provide new designs for coils capable of giving longer lifetimes for these few magnets in areas of high radiation density. Alternative designs of magnets with provision for shielding the coils will also be developed.

Assembly of Core and Coil. Each coil will be fabricated in two halves in order to simplify the final assembly of the complete magnet. Each half-coil will be placed in a magnet half-core and potted in the core with epoxy to form a bonded unit. The two half-magnets will then be joined and assembled with the structural support. The half-cores and the half-coils will not be self-supporting and must be handled in supporting fixtures until they are completely assembled. This and other assembly methods are being investigated in the magnet-model program.

#### 4. Power and Water Distribution

4.1 Choice of Systems and Material. A system of tubular conductors will distribute both power and water to the bending magnets and water to the quadrupoles of the main accelerator. A separate bus system will distribute power to the quadrupoles. The system will be adequate to handle the power operation at 400 BeV with an 8-sec cycle and at higher energy provided the pulse rate is adjusted to maintain constant average power. With such a capability built into the system, it will be possible to increase the energy above the initial value of 200 BeV without making alterations in the main accelerator enclosure.

The combined bus bars and water manifolds must be capable of handling 68 MW average power, distributed from the power-supply system shown in Fig. 5-5, and must also carry the necessary water to carry away a 74 MW heat load. Two metal pipes (either copper or aluminum) will be on the outside wall of the enclosure just above the magnet structure (see Fig. 8-1). They must be mounted on insulators rated at the maximum voltage to ground, approximately 500 V. The two lines will be connected in series and will carry the magnet current in opposing directions to eliminate the large magnetic dipole that would result from a single-turn bus. Pairs of bending magnets will be connected in series with the lines in an alternating pattern by inserting

an insulating section in the line between the leads to the magnets. These insulating inserts must hold off the voltage drop across two magnets of about 80 V.

One of the pipe lines will be a water supply, the other a return. The flow required to limit the temperature rise in the magnets to 16°C at 400 BeV has a maximum of 365 gpm adjacent to each utility building and tapers to zero at the midpoints between houses. Water stops will be placed at the midpoints to isolate the separate pumping systems. Each bending magnet will have four parallel water circuits, each quadrupole two. Current and water connections to a pair of bending magnets are shown in Fig. 5-4.

The choice of metal for the bus piping has not been made. A considerable saving in cost (perhaps 50%) can be realized by using aluminum instead of copper, provided that the problem of electrolysis at the junctions with the copper coils can be solved. Some useful properties of two examples of piping material are listed in Table 5-4.

Table 5-4. Copper and Aluminum Bus Properties

	<u>4-in. Cu Tube</u> <u>(Type K)</u>	<u>4-in. Al Pipe</u> <u>(Sched. 40)</u>	
Outside Diameter	4.125	4.5	in.
Wall Thickness	0.134	0.237	in.
Wall Cross Section	1.680	3.174	sq. in.
Resistance per 1000 ft	4.58	4.40*	mΩ
Power Dissipation in Buses			
at 400 BeV	2.1	2.0	MW
Pressure Drop in 100 ft			
at 365 gpm	4.3	3.6	psi

\*Assumes Al alloy having a conductivity of 0.55 that of Cu.

## 5. Main Magnet Power Supply

The power supply is divided into two separate parts, the bending-magnet system and the quadrupole system. This arrangement allows for better tracking of the fields into saturation and allows greater flexibility in adjustment of the operating point of the synchrotron. Figure 5-5 is a schematic diagram of the entire supply.

5.1 Bending-Magnet Power Supply. The magnet ring bus consists of two loops connected in series. The currents are in opposite directions, thus avoiding the dipole field that would be produced by a single loop.

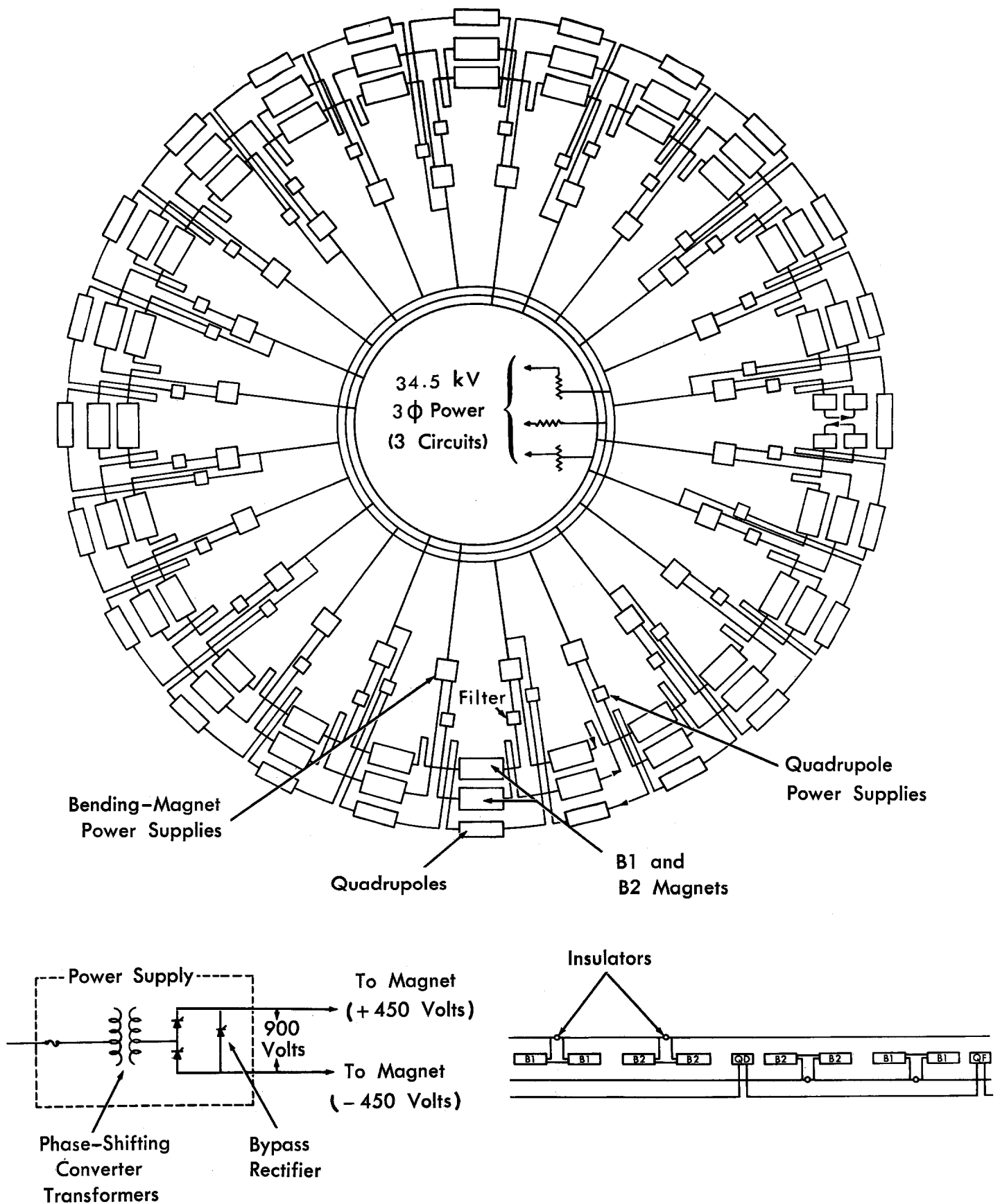


Figure 5-5 — Main-Synchrotron Magnet Power Supply



Each of the 24 utility buildings will have a power supply rated at 900 V peak at 2400 A dc, for 200 BeV excitation. Every other supply around the ring will be connected in series to one of the two loops; the others will be connected to the return loop.

To convert to 400 BeV, each existing supply will be paralleled by another equal supply. In addition, another equivalent supply will be connected in each utility building to the opposite loop, giving the entire power supply twice the voltage rating and four times the power rating. This type of connection maintains the low voltage to ground and the symmetry of the 200 BeV supply.

Each supply will be a rectifier of the controlled-thyristor type. The supplies will be phased with respect to each other to give an overall phase number greater than 72. Each rectifier will include a bypass thyristor to enable appropriate power supplies to be bypassed, reducing power requirements and reactive line power. Each supply will also include a passive filter to reduce the high-frequency ripple resulting from phasing back the rectifiers. The low frequency (less than 720 Hz) will be reduced by a feedback system.

5.2 Focusing-Magnet Power Supply. All the quadpoles are connected in series in one continuous loop. At 200 BeV, alternate utility buildings will contain a controlled-thyristor power supply rated at 580 V at 620 A dc. For 400 BeV, each power supply will be paralleled by an identical one and the remaining utility buildings will have comparable supplies connected into the same loop.

The supplies will be phased with respect to each other to give a phase number greater than 36. A passive filter across each supply will reduce high-frequency ripple.

The quadrupole field will be servo-controlled by the bending-magnet field to provide for tracking. During slow extraction, the quadrupole supply will be self-regulated to meet the stringent requirements of extraction.

5.3 Power Source. The magnet power supplies of existing proton synchrotrons all use motor-generators and static converters. Each motor generator set comprises an ac induction motor, a flywheel, and an ac generator which convert the ac into the long-duration power pulse required by the magnet. The converters act as rectifiers while power is going to the magnet and as inverters when power is returning to the generators.

Isolation of the converter from the incoming ac power line by the motor-generator and flywheel greatly reduces the variation in load on the line in spite of the wide swing in power flow to the magnet. The motor-generator also makes the power factor of the load seen by the power line reasonably high and independent of the power factor of the converter. The reactive power drawn by the inverter is supplied by the generator.

Operating experience with this system has been poor in some installations. Much mechanical trouble has occurred with the ac generators, due in most cases to the sudden and repetitive changes in torque during the cycle. These maintenance problems led to questioning the necessity for motor-generators between the power line and the converters for the 200 BeV magnet power supply.

Although the isolation from power-system disturbances provided by the motor-generator seems desirable, the fact is that neither CERN nor Brookhaven has been entirely successful in reducing the magnet-voltage fluctuation sufficiently to obtain a satisfactorily uniform external beam during flat-top extraction. It appears that some other approach will be needed to solve this problem.

The idea of directly connecting the converters to the power line is not new. In fact, the Rutherford Laboratory synchrotron operated many months in this manner after a generator failure. Studies have been made at Rutherford<sup>10</sup> and also at Argonne<sup>11</sup> of this arrangement.

This accelerator is more suited to direct connection than most machines for the following reasons:

- (i) It is located in a high-capacity electric power grid.
- (ii) The peak magnet power of about 54 MVA is moderate.
- (iii) The ratio of average to peak power of the site is high (Probably 0.8).

Accordingly, the problem of powering the 200 BeV magnet converters directly from the Commonwealth Edison system at Weston was investigated.

The following problems must be solved in this application:

- (i) The power system must be capable of supplying the necessary peak real and reactive power without excessive voltage fluctuation.
- (ii) The power system must be stable against oscillations excited by the pulse repetition rate.
- (iii) The accelerator must not be adversely affected by fluctuation in voltage. These fluctuations could originate in the power supply or in the power system to which it is connected.

The voltage-fluctuation limit to be met in problem (i) is approximately 1%. Voltage variation is primarily the result of changes in reactive power. The reactive power can be held satisfactorily low by limiting the degree to which the converter voltage is controlled by switching converters on and off. This method is practical because there are 24 converters used in the main-ring supply. In addition, power-factor correction capacitors can be switched in the same manner as

rectifiers. By this means, the reactive power can be held to a satisfactory level all times during the cycle.

The Commonwealth Edison Company has made a computer study of the effect of the pulsing load with the reactive power held to 22 MVAR, which can be easily done. This study showed a voltage fluctuation of about 0.45% and no signs of instability or oscillations. The company has stated that this load is acceptable.

The voltage-fluctuation requirements of the laboratory are no more restrictive than those of the power company for their other customers. As is customary, special regulation and filtering will be used where "quiet" ac service is required.

In regard to problem (iii), the production of sufficiently uniform magnet voltage, a multiple approach will be used. This will consist of the following:

1. Through the use of a large number of rectifiers, even though many are cut off for voltage control, the basic minimum ripple frequency will be held to 1080 cycles per second.
2. Passive filters will be used to reduce the peak-to-peak ripple voltage to 1% during the rise and the order of 0.2% during the flat top.
3. Active filters that apply a voltage to compensate the remaining ripple voltage will be used.
4. During the injection period, when the power required is only 82 kW, a separately regulated dc supply may be switched in.

#### 6. Magnet Support and Alignment

In order to make the alignment of the magnets independent of the settlement of the enclosure, the bending magnets and quadrupoles will be supported by means of adjustable jacks, as shown in Fig. 5-4. The ends of two successive magnets are hinged together and the hinged point is supported by means of a jack table. The jack tables and magnets are designed such that any magnet can be removed or replaced without disturbing the adjustment of the table or of the neighboring magnets. Furthermore, the position of each magnet will be determined by the supports in an absolute manner such that any magnet will assume the position of the magnet which it replaces. Each table is supported by three jacks and it is clear from Fig. 5-4 how relative motions of the jack can produce a vertical, a horizontal, or a tilt displacement.

The magnets rest on four points and because they are slightly flexible, the tilts of the two ends of the magnet are almost independent.

The quadrupole magnets which are placed around the ring at 100-foot intervals must be aligned more accurately than the bending magnets. Vertical or horizontal displacement of the bending magnets will not affect the orbit and will result only in an obvious loss of aperture equal to the displacement. The orbit is, however, sensitive to the tilt of a bending magnet, for this tilt will produce a horizontal component of the magnetic field that will cause a vertical orbit displacement. Each jack table will be adjusted so as to be level in the radial direction by the use of a spirit level, which can easily attain an accuracy of  $10^{-4}$  radians. The level will then be detected by an electrically sensitive device that can be monitored at the control center. The relative level of successive tables can be adjusted by means of an ordinary surveyor's level. It can be monitored by means of a stretched-wire method described below. It is also possible to install a liquid-leveling system that communicates a reference level to all points of the ring and that would combine the function of alignment and monitoring.

The closed orbit is sensitive to the positions of the quadrupoles; rms displacements of the order of  $\pm 0.01$  in. will produce rms orbit distortions of about  $\pm 1$  cm. Inasmuch as it is not planned to use piles or special foundation support underneath the jack tables, other than the concrete floor of the enclosure, it is especially desirable to be able to monitor almost continuously the positions of the magnets, and, if relative settlements or displacements are observed to occur, to be able to make compensatory motions.

A stretched-wire method has been chosen to align the quadrupoles (and the bending magnets at the same time) in the horizontal direction. A 0.004 in. steel wire is stretched from a point on jack-table A that supports one end of a quadrupole to the jack-table C of the next similar kind of quadrupole, which will be about 200 feet away. Because of the curvature of the orbit, the wire will lie about 20 inches within the circle at the midpoint, which is about 100 feet from each of the jack tables to which the wire is fastened. At this midpoint position, a jack table B supporting the opposite kind of quadrupole will be located. It is by accurately sensing and measuring the position of the wire at this table that an offset can be made and the relative positions of the three magnets can be determined. Then another wire is stretched from Table B to table D where the next similar quadrupole will be found. The offset is now sensed at table C and adjusted by moving the position of D with respect to tables A, B and C. Thus by stretching wires from each of the quadrupole support tables to the following similar table, the alignment can be propagated around the magnet ring.

The position of the wire at a particular table can be sensed by passing a small alternating current through the wire and by enclosing the wire with a ferrite core or frame on which four coils have been wound on opposite sides both vertically and horizontally. The coils on opposite sides are connected in opposition so that no signal is picked up when the wire is centered. When the wire is off center, a voltage

signal proportional to the displacement can be measured.<sup>12</sup> It is easy to detect a displacement considerably less than 0.001 inch by this method, so the problem becomes one of locating the ferrite core with respect to the magnets to the desired accuracy. It should be possible to work to an overall accuracy of 0.005 in. without excessive difficulty. L. J. Laslett has calculated<sup>13</sup> that an overall accuracy of  $\pm 0.01$  in. gives a 75% probability that the orbit deviations will be contained within a width of 1 in. A weight of six pounds seems adequate to stretch a wire 0.004 in. in diameter so that the sag in a distance of 200 ft is about 2 cm; care must be used that drafts do not produce a horizontal motion. Drafts can be avoided by locating the wires just under the flanges of the magnet or, if necessary, by shielding the wire by the use of tubing.<sup>14</sup>

The azimuthal positions of the magnets are far less sensitive. Thus, the tolerances are such that rms longitudinal displacements in the azimuthal direction of  $\pm 0.1$  in. correspond to a  $\pm 0.05$  in. rms displacement of the orbit. The quadrupoles can be put in position by means of an ordinary surveyor's tape. The distance between quadrupoles can be monitored by measuring the resistance of the stretched wires from support point to pulley, once they have been calibrated against a precision tape. The variation of length with temperature can be compensated for by measuring the resistance of the whole wire, from the support point to the weight.

Before the precise adjustment of the magnets that has been described above can be made, it will be a matter of practical necessity to have a rough survey made so as to know the approximate positions of the jack tables. A mekometer, or possibly several, will be used for this. The mekometer, which is a radar-laser device for determining distance, is capable of an accuracy of  $\pm 0.01$  in. in 150 ft and presumably of  $\pm 0.2$  in. or better in 1 km. As the floor of the enclosure is laid down, but before the top is put on, brass monuments can be fastened to the floor at positions corresponding to the tables. It should be possible to locate points on these monuments to about  $\pm 0.25$  in. by the use of four mekometers arranged in a square array within the circle. Another possibility is to use a single mekometer together with a precision theodolite, both at the center of the ring.

In order to keep the alignment of the magnets fixed in space, monuments will be placed at each end of the long straight sections and the stretched wire will start and end on indexed points attached to these monuments. Laslett computes<sup>13</sup> that the monuments must be located to an rms accuracy of 0.087 in. in order to attain a 75% probability that the orbit lies within a width of 1 in., ignoring transfer and wire errors. One of the piers at each long straight section will include an

inverted pendulum that will be attached to bedrock. These will be monitored from time to time to observe the stability of the piers. Two similar piers will be located at the booster ring and such piers will also be located along the external proton beam and at the experimental areas. A sketch of a pier with an inverted pendulum is shown in Fig. 5-6.

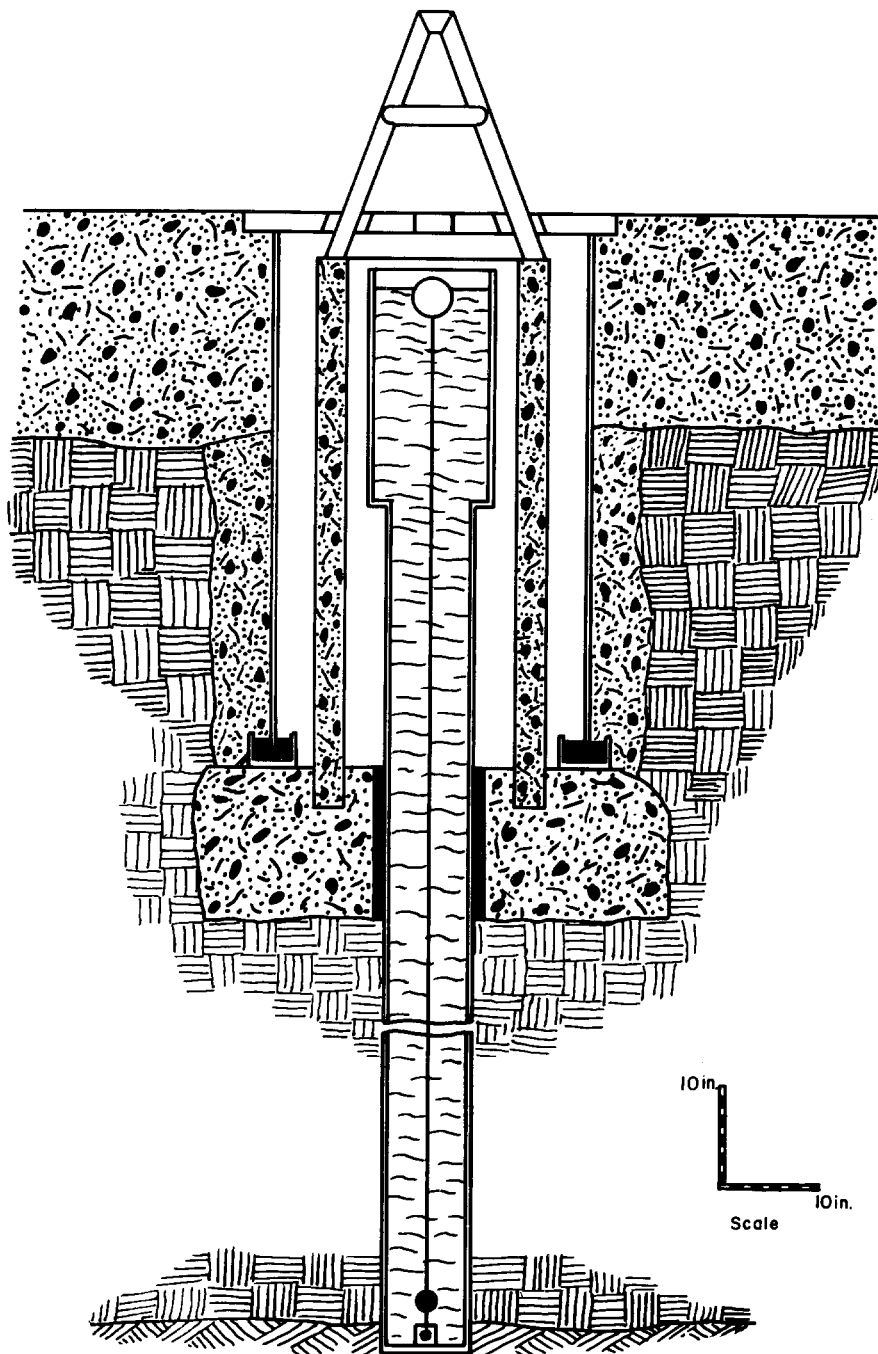


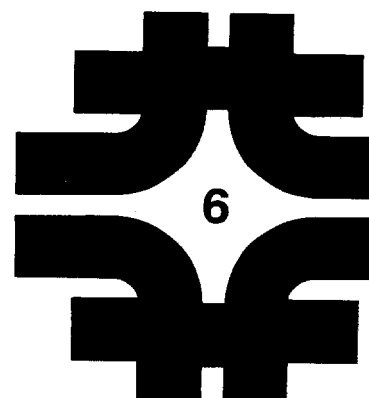
Figure 5-6 — Monument with Inverted Pendulum

References:

1. SIBYL was written by R. S. Christian, then of MURA.
2. LINDA was written by R. S. Christian.
3. TRIM was written by A. Winslow of LRL.
4. C. Lasky, private communication.
5. A. W. Maschke, NAL Note FN-100, Nov. 15, 1967.
6. G. Pluym and M. Van deVoorde.  
CERN Report ISR-MAG/67-3, Jan. 12, 1967.
7. H. Brechna, SLAC Report 40, Feb., 1965.
8. G. A. Foster, Argonne National Laboratory  
Report GAF-3, Dec. 1, 1967.
9. R. Sheldon and G. B. Stapleton, Rutherford Laboratory  
Report RHEL/R-152.
10. J. A. Fox, A Review of Static Power Supply Alternatives  
for the 300 GeV Accelerator Magnet System, Rutherford  
Laboratory Report, E/PS-DS/300 GeV/JAF-2, Dec., 1967.
11. A. Rohrmayer, Operation of Accelerators Directly Off the  
Utility System, IEEE NS-14, June, 1967, p. 849.
12. W. K. H. Panofsky and W. E. Marshall, SLAC Technical  
Note 65-74.
13. L. J. Laslett, private communication, Dec. 21, 1967.
14. W. H. Chamberlain, Alignment-Wire Errors due to  
Elastic, Magnetic and Wind Forces. University of  
California Lawrence Radiation Laboratory Report UCID  
2835, July 22, 1966.

# **Main-Synchrotron Vacuum System**

1. Introduction	6-1
2. Vacuum Chamber	6-1
3. Pumping System	6-2
4. Sector Valves	6-3
References	6-3





## 6. MAIN-SYNCHROTRON VACUUM SYSTEM

E. Malamud

G. M. Lee, W. R. Winter (Wisconsin)

### 1. Introduction

The path in which protons travel during acceleration must be evacuated to prevent loss of protons by collisions with the gas of the atmosphere. A closed vacuum chamber is pumped down to a pressure of  $10^{-7}$  torr or less, about one ten-billionth of atmospheric pressure. The beam travels in this vacuum throughout acceleration. At this pressure, less than 0.1% of the protons will be lost by gas-scattering collisions<sup>1</sup>.

The vacuum system will contain no organic materials because they are more easily damaged by radiation. With no organic materials in the system, it is not difficult to achieve the desired vacuum of  $10^{-7}$  torr with reasonable spacing of vacuum pumps. The possible future use of the synchrotron as a storage ring (discussed in Chapter 18) also makes it desirable to have very low pressure.

The vacuum chamber will be approximately elliptical in cross section to fit into the magnet apertures, as shown in Fig. 3-2. Most joints will be welded; quick-disconnect joints will be utilized where frequent disassembly is expected. The high vacuum will be achieved with sputter-ion pumps. Model sections have been tested with the planned pump spacing and the design pressure achieved.

### 2. Vacuum Chamber

The vacuum chamber will be all metal except for metal-ceramic rings inserted to insulate the chamber electrically; use of these materials avoids radiation damage. Welded joints will be used for most of the connections between sections of the 20,600-ft long chamber. These standing-edge joints can be made by welding machines<sup>2</sup> that fit in the 6-in. space between coil ends in the 1-ft straight sections. Between magnet units, in 1-ft straight sections, will be "T" sections containing bellows and pump arms. A 1-ft straight section with vacuum joints and manifold is shown in Fig. 6-1. A number of rewelds can be made. Where frequent disassembly is anticipated, for example, in the beam-extraction area, quick-disconnect flanged joints with metal gaskets will be used.

The outside dimensions of the chamber when evacuated are 5-in. by 1.5-in. in the B1 magnets and 4-in. by 2-in. in the B2 magnets. Seamless tubing will be formed with a die into the desired shape. The

installed tube will be prestressed between the poles by having the vertical dimension greater than the magnet gap; thus flexing during pumpdown and consequent loss of aperture will be avoided. This sheets of insulation top and bottom will prevent shorting of the laminations. The magnet gap will contract less than 0.002 inch during each magnet pulse. Fatigue produced in the chamber material by this cyclic stress is negligible.

The wall thickness will be 0.05 in. or less; the material will be chosen from one of the 300 series stainless steels. These steels are relatively low cost and have adequate resistivity ( $72 \mu\Omega$ -cm), so that eddy-current fields at injection can be kept below approximately 0.5 G. The fabricated vacuum-chamber sections must be annealed to insure a permeability close to unity.

The total vacuum chamber consists of the main-ring tube plus larger cross section pieces in the long and medium straight sections where acceleration, injection and extraction take place. The main-ring tube represents about one-fourth of the total system volume of  $60 \text{ m}^3$ , but over one-half of the total system surface area of  $1700 \text{ m}^2$ . The pumping speed of the tube is low; a 20-foot long B1 section has a conductance of only  $8 \text{ l/sec}$ .

### 3. Pumping System

Two ways of achieving low average pressure are the use of frequent pump spacing and reduction of surface outgassing rate from the chamber walls. In implementing the first, it is planned in the present design that the high-vacuum system will utilize approximately 400  $50\text{-l/sec}$  titanium sputter-ion pumps with an average spacing of 50 ft, or a pump every other bending magnet section. An alternative scheme being considered would have an even smaller pump, perhaps  $15 \text{ l/sec}$  between each two adjacent magnets, so that each bending magnet would be a self-contained modular unit. A 1- to 2-ft long pump connection will adequately isolate the pump magnet from the beam and the synchrotron magnet from the pump. Modeling studies now in progress will optimize pump spacing, pump size, and total cost of the high-vacuum system.

Various chemical cleaning recipes will be tested to reduce surface outgassing rates. It is already clear from preliminary results of these tests that the desired pressure can be achieved without baking.

Before turning on the sputter-ion pumps in a sector it is necessary to rough the system down to about  $10^{-5}$  torr. For this purpose six permanent forevacuum stations in utility buildings will be provided and connected via manifold and valve to the ring. Additional points in each sector will be provided with a valve and connection so that portable forevacuum pumps can be brought in and attached. After the system has pumped down far enough, these portable pumps can be removed from the tunnel. A forevacuum pump unit will be a combination of mechanical (15 cfm) and turbomolecular ( $260 \text{ l/sec}$ ) pumps. Pumpdown

of a sector from atmospheric pressure to approximately  $2-3 \times 10^{-6}$  torr will take about 1 hour. Another 5 hours will be required to reach a pressure of about  $10^{-7}$  torr.

Power for the sputter-ion pumps will be provided by supplies located in each utility building. The pump currents indicate local pressure and will be monitored individually and displayed centrally in the control room by the multiplex system. A vacuum map of the ring should be a sensitive indicator of difficulties with beam dynamics.

#### 4. Sector Valves

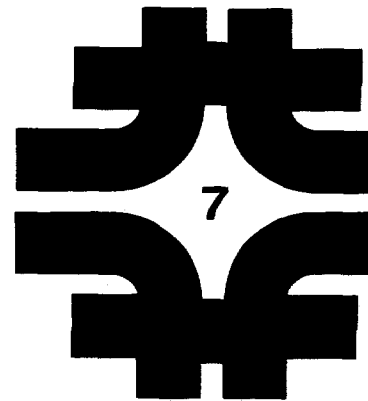
It will be necessary in the course of maintenance and repair to cycle certain segments of the machine between vacuum and atmospheric pressure. It is convenient, therefore, to use sector valves. A reasonable number of such valves is 12, i.e. one at each end of the long straight sections. The ring sectors thus isolated are still quite long and it will probably be desirable to add 6 more valves. These sector valves should not contain any organic material. An adequate solution is afforded by a metal-sealed valve with two gates, with a rough vacuum applied between gates. Special sections such as rf stations and the injection and extraction straight sections will have special pumping and valve arrangements to facilitate local isolation.

#### References:

1. A. A. Garren and W. A. S. Lamb, Vacuum Requirements for the Main Ring, University of California, Lawrence Radiation Laboratory Report, UCID - 10016, July, 1964.
2. N. Milleron, Some Recent Developments in Vacuum Techniques for Accelerators and Storage Rings, IEEE Trans. Nucl. Sci. NS-14, 794 (1967).

# Main-Synchrotron Accelerating System

1. Introduction	7-1
2. Choice of System	7-2
3. Choice of Frequency	7-3
4. Modular Arrangement of the RF System	7-5
5. Ferrite Tuner	7-5
6. Cavity Design	7-8
7. Transmission Lines	7-10
8. Beam-Control System	7-11
References	7-12



## 7. MAIN-SYNCHROTRON ACCELERATING SYSTEM

Q. A. Kerns, J. E. Katz (LRL), G. S. Tool, R. F. Tusting (LRL)

### 1. Introduction

Protons pass through the accelerating system and gain energy each time they make a circuit around the synchrotron. This energy is given to the protons by voltages appearing between two electrodes which are part of a resonant electromagnetic cavity. The electromagnetic fields in the cavity and the voltage across the electrode gap alternate at radio frequency in step with the protons' frequency of revolution so that the voltage is in the proper phase to accelerate (rather than decelerate) the beam.

As the protons gain energy, their frequency of revolution increases, and the frequency of the accelerating voltage must increase to stay in synchronism. This change in frequency is large in the booster, in which the protons' speed and revolution frequency almost double. It is much smaller in the main accelerator, because at the injection energy of 10 BeV, the protons are already travelling at 99.6% of the speed of light. At 200 BeV, protons will be travelling at 99.999% of the speed of light. Thus, the accelerating frequency must increase by approximately 0.4% as the protons go from 10 to 200 BeV. The synchrotron principle of McMillan and Veksler shows that particles will gain energy stably and not fall out of step with the changing frequency of the accelerating voltage.

The rf accelerating system of the main synchrotron has a total of sixteen resonant cavities. They are concentrated in the long straight section immediately upstream of the injection point. Only the cavities themselves are located in the accelerator enclosure. The ferrite tuners that change the frequency during acceleration and the amplifier system that generates the rf power are in a separate gallery shielded from the accelerator. The rf power is delivered to the enclosure by a coaxial transmission line going through the shielding. A cavity and its transmission line, ferrite tuner, and power-amplifier system form a module that operates independently; the accelerator can operate fully even if only fourteen of the sixteen modules are in operation.

Injection into the main synchrotron takes place with the rf voltage on. Protons from the booster are synchronized in phase with the main-ring rf and then injected into the main ring. After injection, acceleration is almost completely controlled by the beam; its phase is detected

and the accelerating frequency adjusted to keep the beam in the center of the vacuum chamber. This beam-controlled system is quite similar to those in existing accelerators, except that special precautions are taken to reduce the perturbation of the system caused by missing bunches.

The design of the rf accelerating system has evolved from the LRL 200 BeV design<sup>1</sup>. The number of cavities and rf power are both reduced because the acceleration time is longer and because the rate of acceleration is programmed to reduce rf power.

## 2. Choice of System

Several kinds of accelerating systems have been considered in discussions of the accelerator design, including two-stage arrangements employing ferrite-tuned cavities to cover the bulk of the tuning range and narrow-band cavities at high voltage for the later high-power stage of acceleration. With a two-stage system, it is also possible to consider a higher frequency in the second stage, because there is no frequency limitation caused by the presence of ferrite. But it would be difficult to match bucket shapes between the two frequencies and larger synchrotron-oscillation amplitudes would result. Even at the same frequency, narrow-band, high-voltage cavities would have significant perturbations when a missing bunch passes through. The narrow-band cavities could be used alone if the injection energy into the main ring were 30 BeV or higher, rather than the 10 BeV chosen. The additional cost of the higher-energy booster would, however, far outweigh any reduction in the cost of the rf system.

The intrinsic advantage of the two-stage system has been incorporated in the present ferrite-system design by means of a programmed magnet guide-field cycle with varying rates of change with energy. The magnet cycle includes a 0.1 sec region just after injection in which  $\frac{dB}{dt}$  increases linearly to its full value. In the rf accelerating system, there is a simultaneous linear rise of rf voltage during this 0.1 sec, leveling off at the full rf voltage, which is maintained for the high-power stage of acceleration. This guide-field program reduces the voltage required during the time when the power dissipated in the ferrite is largest. It is therefore possible to increase significantly the optimum operating voltage of each ferrite-tuned cavity. The synchronous phase angle, which is 0 degrees during the entire injection time, increases smoothly from 0 to 50 degrees during the 0.1 sec period and remains at 50 degrees up to the phase transition at approximately 17 BeV, when it is switched to 130 degrees. The selection of the 1.6 sec guide-field rise time, together with an individual cavity peak-voltage rating of 260 kV, and a 50 degree phase angle, enables the rf acceleration to be accomplished with a total of 16 cavities. Some relevant beam-dynamics parameters, energy gain per turn, peak voltage per turn and synchronous phase angle are plotted in Fig. 7-1.

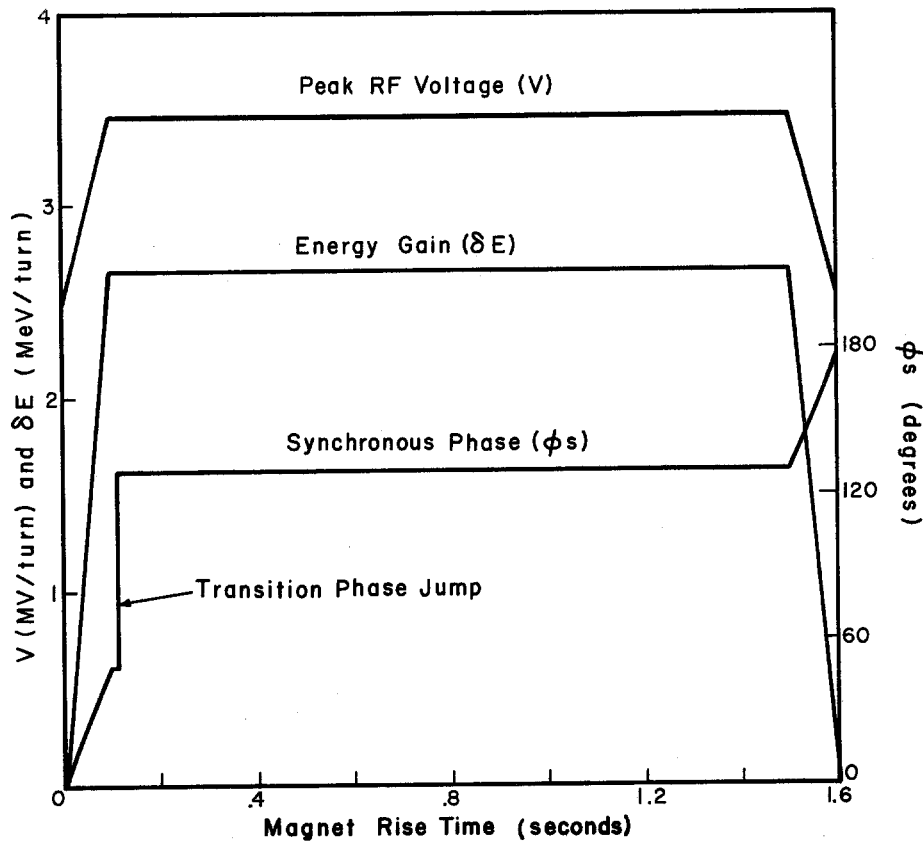


Figure 7-1 — Main-Ring Acceleration Parameters

### 3. Choice of Frequency

There are a number of arguments favoring a frequency of approximately 50 MHz. Among the most significant of these is the requirement of efficient beam transfer from booster synchrotron to main ring, most easily accomplished by a synchronized-frequency transfer of injector bunches into main ring buckets. This requires that the main-ring accelerator frequency at injection match the injector frequency at ejection. The choice of injector frequency tends to be restricted to frequencies below 100 MHz by the desire for a lower synchrotron-oscillation frequency in the injector, to avoid betatron-synchrotron coupling resonances.

A second argument favoring lower frequency is that of beam monitoring, control and servo regulation. A low frequency minimizes problems associated with signal-transport time delay in cables and amplifiers. Cavity rf amplitude and phase regulation under beam loading are particular concerns for the rf system that become less critical and less costly at lower frequency.

On the other hand, a choice of frequency much below 50 MHz would necessitate either increased capacitive loading of the rf cavities if they were to be fitted into the same straight-section length,

or increased straight-section length in proportion to rf wavelength. The present amount of capacitive loading is adjusted to give acceptable control-loop response under beam loading. A much larger amount would increase rf losses and the cost of the ferrite tuner.

Table 7-1 presents the major parameters of the system. Included is the beam shunt resistance  $R_b$ , defined in terms of the voltage gain per turn  $\delta V$  and the power absorbed by the beam  $P_b$  as  $R_b = (\delta V)^2/P_b$ .

Table 7-1. Acceleration Parameters

Injection Energy	10 BeV
Final Energy	200 BeV
Guide-Field Rise Time	1.6 sec
Maximum $\frac{dB}{dt}$	5.69 kG/sec
$\frac{d^2B}{dt^2}$ (Beginning and End of Rise)	56.9 kG/sec <sup>2</sup>
N (Beam Intensity)	$5 \times 10^{13}$ protons/pulse
Synchronous Phase	0° to 50°, programmed
Peak RF Voltage Per turn	3.47 MV
Maximum Synchronous Energy Gain per Turn ( $\delta E = e\delta V$ )	2.66 MeV
Beam RF Power ( $P_b$ )	1.01 MW
Average Circulating Beam Current	0.382 A
h (Harmonic Number)	1120
Injection Frequency	53.242 MHz
Final Frequency	53.439 MHz
Relative Frequency Change	0.37%
$R_b$ (Beam Shunt Resistance)	7 M

The considerations of cost, reliability, radiation resistance and flexibility have been kept in the foreground in the design. The present cavities are spaced as closely as is mechanically feasible, and the cavities themselves shortened somewhat, to reduce the straight-section length requirement.

The rf voltage during the injection filling time requires special attention, because of the problem of matching injector bunches to the main system. A relatively small voltage per turn (of the order of 1 kV) will give bucket phase-space areas in the main ring equal to the phase-space areas of bunches from the injector. Particles would then be lost in the transfer, because the bucket and bunch shapes would be different; the bunch would have much larger momentum spread than the bucket could contain. A voltage per turn of approximately 200 kV is required to just cover the maximum injected momentum spread.

With this voltage, synchrotron-oscillation amplitudes would be increased because the bucket and bunch shapes are not the same. In order to avoid the resulting waste of radial aperture, it is planned to



match bunch and bucket shapes at injection. This will require a voltage per turn of approximately 1.5 MV, corresponding to a bunching factor of 0.1. The rf system is consequently designed to provide this injection voltage with an adequate margin of safety.

#### 4. Modular Arrangement of the RF System

The total accelerating voltage will be supplied by 16 cavities in one long straight section. An individual cavity is shown in Fig. 7-2. A cavity, the transmission line delivering rf power to it from the rf gallery, and the ferrite tuner, power amplifier and rf drive system in the rf gallery comprise a module. Parameters of the modules are given in Table 7-2. Fig. 7-3 is a cross section of the accelerator enclosure and rf gallery, showing the arrangement of the equipment. The 16 modules operate independently, except that they utilize a common input from the beam-control system. The system can operate at its design energy, intensity, and repetition rate with only 14 of the 16 cavities operating. Automatic electronic switching is designed to give continuity of operation if a module goes out of service during acceleration. Any non-operating cavities in the ring, although detuned to present a low impedance to the beam, will extract energy from the beam. At design intensity, the energy per turn extracted by each non-operating cavity will be approximately 50 keV. This additional energy drain must be supplied by the operating cavities.

Table 7-2. Parameters of the Main-Synchrotron  
RF Accelerating System

Total Number of Cavities	16
Number of Cavities Required for Normal Acceleration at 3.47 MV/turn	14
Total Stored RF Energy (14 cavities operating)	12 J
Total Weight of Ferrite (16 x 175 lb)	2800 lb
Total Length of Accelerating Structure (16 cavities x 1.75 m/cavity)	28 m
Fraction of Circumference Occupied by RF	0.5%

#### 5. Ferrite Tuner

The natural bandwidth of the main-ring rf system is approximately 5 kHz. In order to track the required frequency change as the proton speed increases, it is necessary to tune the cavity system by 200 kHz or 40 bandwidths. The function of the ferrite tuner is to generate a controllable reactance for tuning the cavity from a distance, i.e., the upper end of the transmission line. Since the maximum cavity stored energy  $U_{cav}$  is 0.8 J and the relative frequency shift  $\Delta f/f$  is 0.37%, the tuner is required to provide controllable circulating energy of  $2\omega(\Delta f/f)U_{cav}$ , or about 2 MVA. Each tuner is a separate replaceable unit located in the rf gallery above the accelerator enclosure.

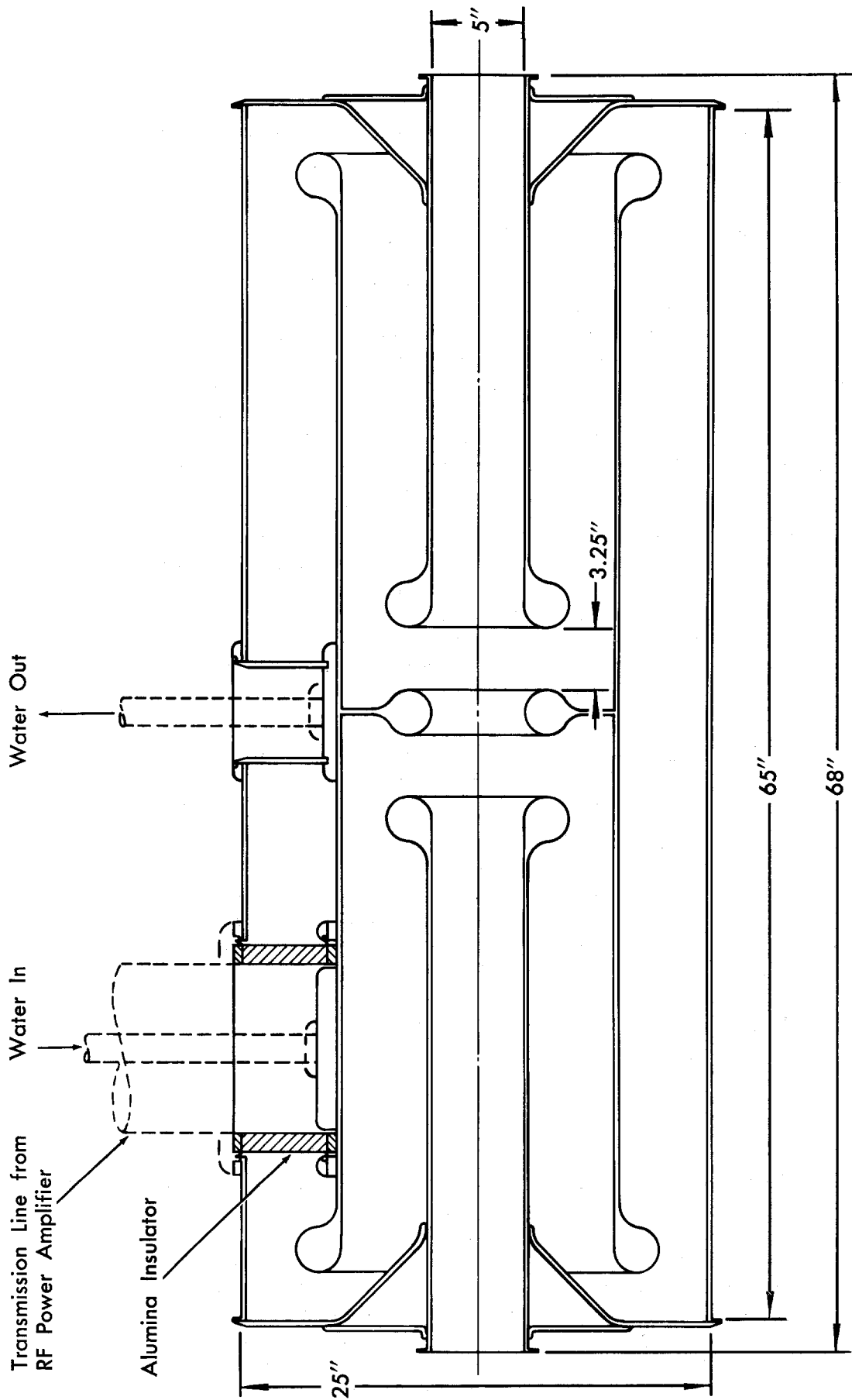


Figure 7 -2 — Main-Synchrotron Accelerating Cavity

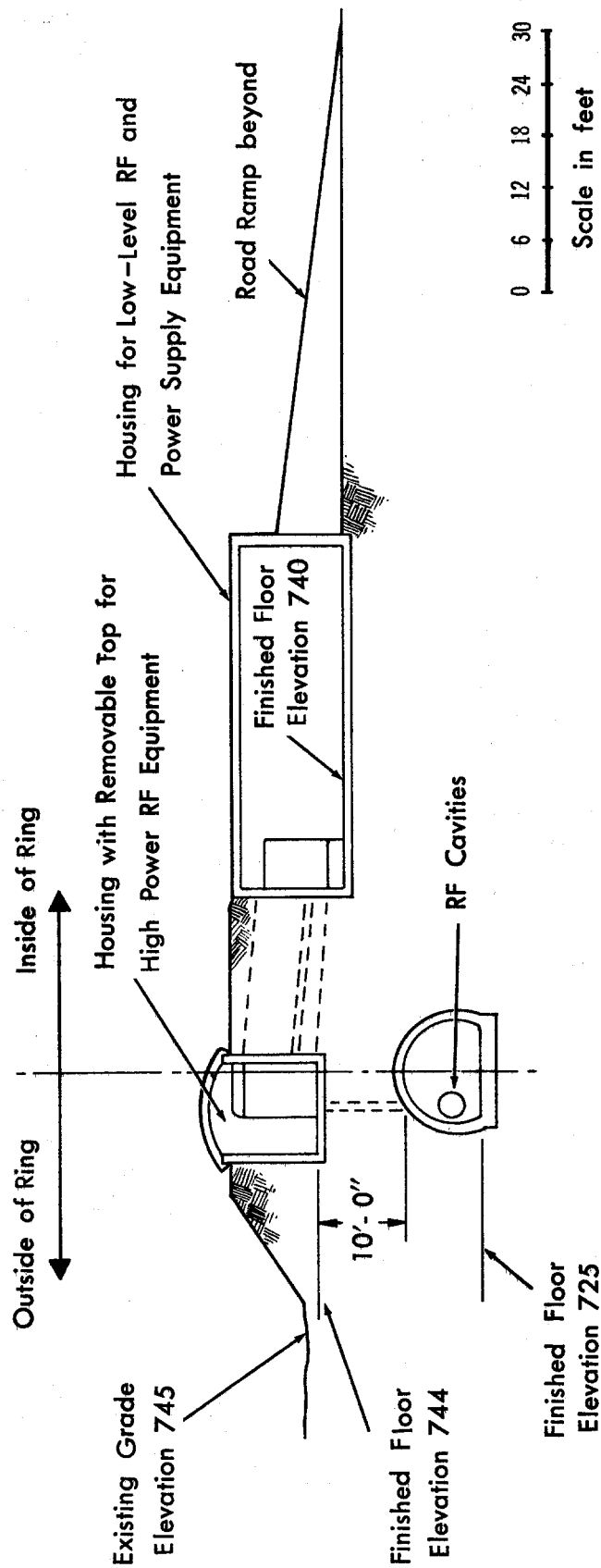


Figure 7 -3 — Main-Ring RF Housing

The tuner sketched in Fig. 7-4 is a short-circuited length of coaxial line loaded with ferrite near the short. The length of line, somewhat less than a quarter of a wavelength, serves to transform the low impedance seen at the ferrite location to a value suitable for parallel connection to the voltage maximum at the rf power tube anode, where the peak rf voltage rating is 20 kV. Near the short-circuited end of the line, the rf current maximum is 1,600A.

This current is shared by six ferrite-loaded stems, each carrying 270 A. For convenience in arranging the biasing windings, the stems are arranged like the spokes of a wheel. This multistem configuration permits the use of several smaller ferrite cores, with correspondingly lower peak bias current, rather than large cores, which to be equivalent would be 3 ft in diameter. Table 7-3 below lists the tuner characteristics when all 16 cavities are operating.

Table 7-3. Main-Ring Ferrite-Tuner Characteristics

Tuner Peak Voltage	17 KV
Tuner RF Peak Power Transfer	2 MVA
Transmission Line Length	0.75 m
Transmission Line Impedance	13
Number of Stems	6
Number of Rings Per Stem	8
Average Ferrite Power Density	0.7 W/cm <sup>3</sup>
Ferrite $\mu_{\Delta}$ at Injection	4
Ferrite $\mu_{\Delta}$ at Injection	2
Maximum Ferrite Power Loss	11 kW
Peak RF Flux Density	25 G
Ferrite-Ring Outer Diameter	6 in.
Ferrite-Ring Inner Diameter	4 in.
Ferrite-Ring Thickness	1 in.

## 6. Cavity Design

Each cavity is a standing-wave folded-coaxial resonator, 25 in. in diameter and 68 in. long. The individual cavity voltage is 255 kV peak with 14 of the 16 cavities operating. At the point where the transmission line is connected to the cavity structure, the voltage is 40 kV peak. A taper in the transmission line characteristic impedance provides a voltage transformation of 2:1 between the cavity in the enclosure and the power tube located in the rf gallery above the enclosure.

Table 7-4 gives individual cavity parameters when all 16 are operating. Fig. 7-5 shows cavity and tuner power, beam power, and ferrite flux as functions of time during acceleration.

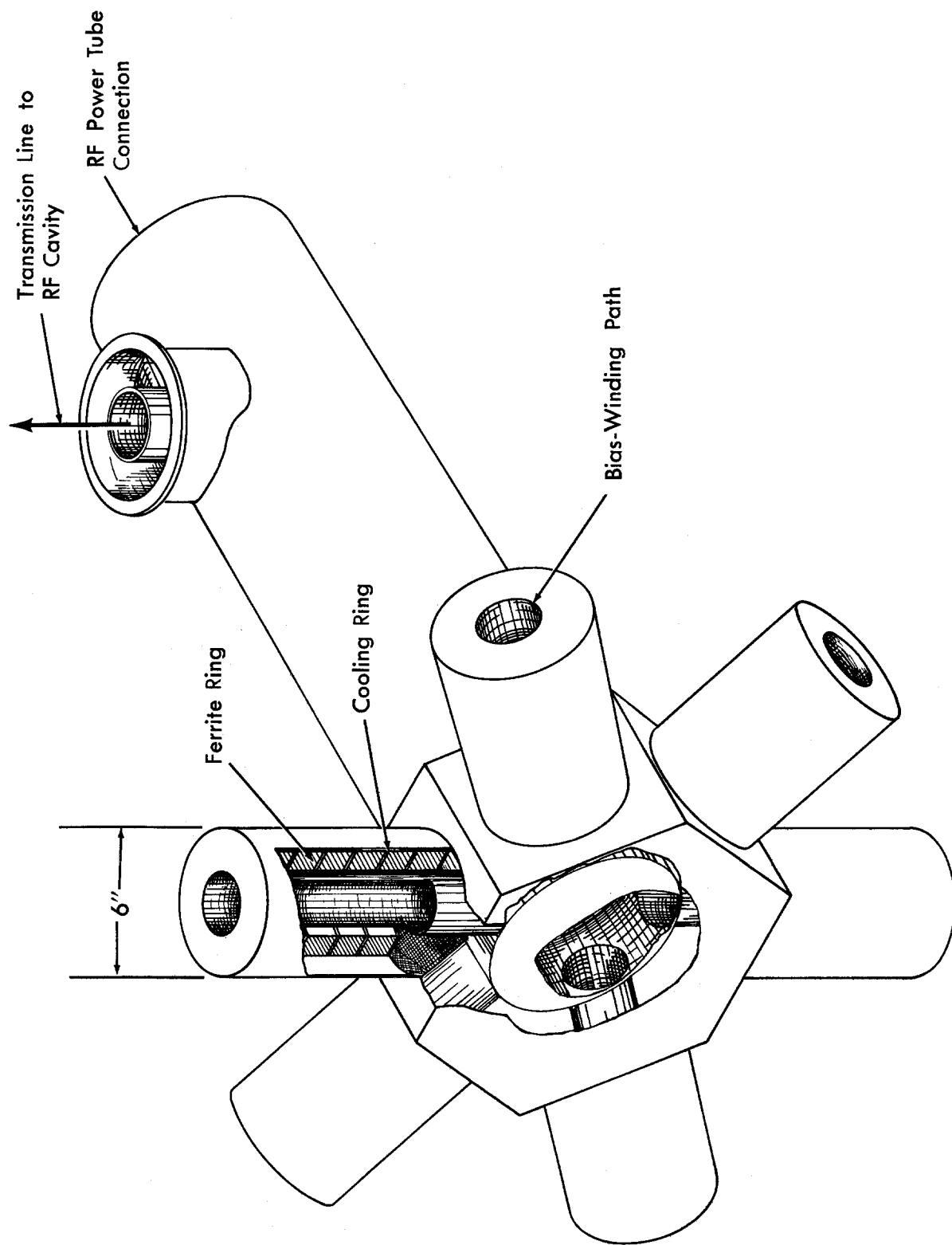


Figure 7-4 — Main-Synchrotron RF Ferrite Tuner

Table 7-4. Individual Cavity Parameters

Cavity Peak Voltage (Across two gaps per cavity)	217 kV
Axial Field Strength in Gap	$1.2 \times 10^6$ V/m
Cavity RF Current (At Current Maximum)	1600 A
Transmission-Line Voltage Tap	34 kV
Cavity and Transmission-Line Stored Energy	0.6 J

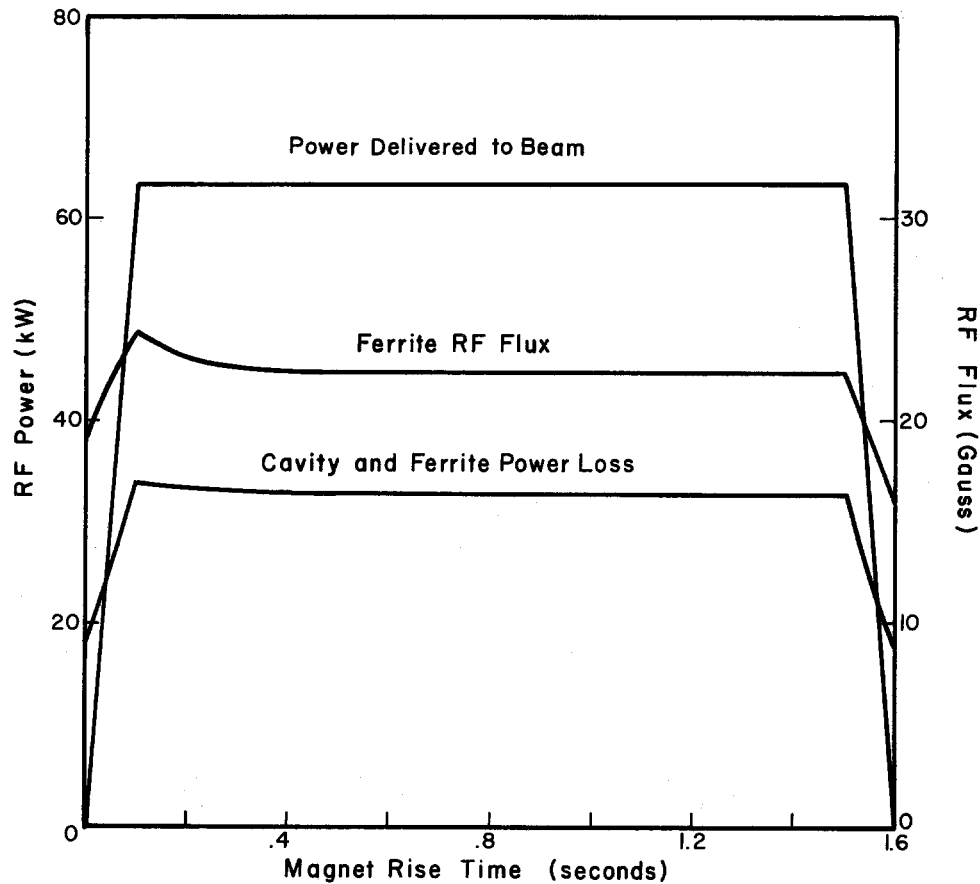


Figure 7-5 — Main-Ring RF Module Power during Acceleration

## 7. Transmission Lines

Coaxial transmission lines, 6-1/8 in. diameter, transmit rf power from the rf gallery to the cavities located in the accelerator enclosure. The electrical length of the lines is approximately  $3\lambda/2$ . Because of the 0.37% frequency variation, the lines cannot be precisely  $3\lambda/2$  throughout the entire accelerating cycle. The reactive effect is small and is absorbed by the tuner.

The transmission lines, in addition to transmitting power from tube to cavity, are used to effect a voltage stepup. By making the transmission-line impedance  $16 \Omega$  at the tube end and  $64 \Omega$  at the cavity end, a voltage multiplication of two is obtained. The benefit of line stepup is that the relative effect of leakage inductance at the cavity loop is less; that is, the tube is more tightly coupled to the cavity.

## 8. Beam-Control System

The beam will be used to control the phase and amplitude of the accelerating voltage. This beam-control system has three negative-feedback loops, a phase-lock loop, a radial-position control loop and a cavity-voltage regulation loop.<sup>2</sup> The first two loops, which follow systems used with outstanding success in many accelerators, act to match rf and proton-bunch phases and to keep the proton beam centered in the aperture. The new third loop is used to improve the response of the system to effects of high beam intensity.

The major part of the rf power input will go to accelerate the proton beam. Because of this high beam loading, gaps in the sequence of bunches passing through a cavity will impose large fluctuating loads, both real and reactive, on the rf system. These gaps will necessarily be present during the filling time, because of the sequential injection from the booster, and during acceleration, because of the non-integral ratio of main-ring and booster radii.

In an unregulated cavity subjected to variable beam loading, the voltage cannot attain a steady-state value, because the driving current is constant, but the load current fluctuates. A suitable regulator will, by changing the driving current, improve the transient regulation by a factor that may reach a value of approximately 100. For the parameters of this accelerating system, we estimate that the voltage variation can be limited to approximately 5% for 100% changes in beam loading.

Harmonic Voltages. The beam current pulses and the rf power-tube current pulses are narrow compared with an rf cycle and rather strong harmonic current excitation is therefore unavoidable. Nevertheless, the cavity system must not develop undue harmonic voltages; such voltage components would be undesirable because they would lower the power-tube efficiency, tend to precipitate sparking, and would alter the bucket shape seriously.

To this end, the transmission-line-cavity system is being studied carefully to avoid integer resonances. The goal is to maximize the driving point impedance at the fundamental frequency  $\omega$  and to locate impedance minima near the integer multiples of  $\omega$  by shifting the location of the network's poles and zeros. It appears that harmonic distortion of the accelerating voltage wave-form can be kept within a few percent by thus controlling the cavity mode spectrum.

Reference Signal Oscillator. The reference oscillator provides a continuous sine-wave signal despite gaps in the circulating beam. During passage of a gap, when no signal is available from the beam pick-up electrodes, the oscillator extrapolates the last previous signal, together with the rate of change of signal frequency. The use of nanosecond integrated circuits facilitates the construction of a compact, low-noise reference oscillator.

Output from the reference oscillator is the essential input to the phase-lock loop. In addition, during the ring-filling interval, the reference oscillator provides a phase datum for the synchronized transfer of beam from the booster.

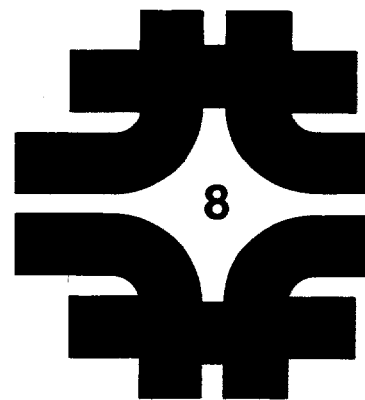
References:

1. 200 BeV Design Study, U. of Calif.  
Lawrence Radiation Laboratory Report UCRL-16000 (June, 1965)
2. Q. A. Kerns and W. S. Flood, Stabilization of Accelerating Voltage under High-Intensity Beam Loading. IEEE NS-12, June 1965, p. 58.



# **Main-Synchrotron Enclosure**

1. Introduction	8-1
2. Enclosure Design	8-1
3. External Structures	8-2
4. Enclosure Vehicles	8-3



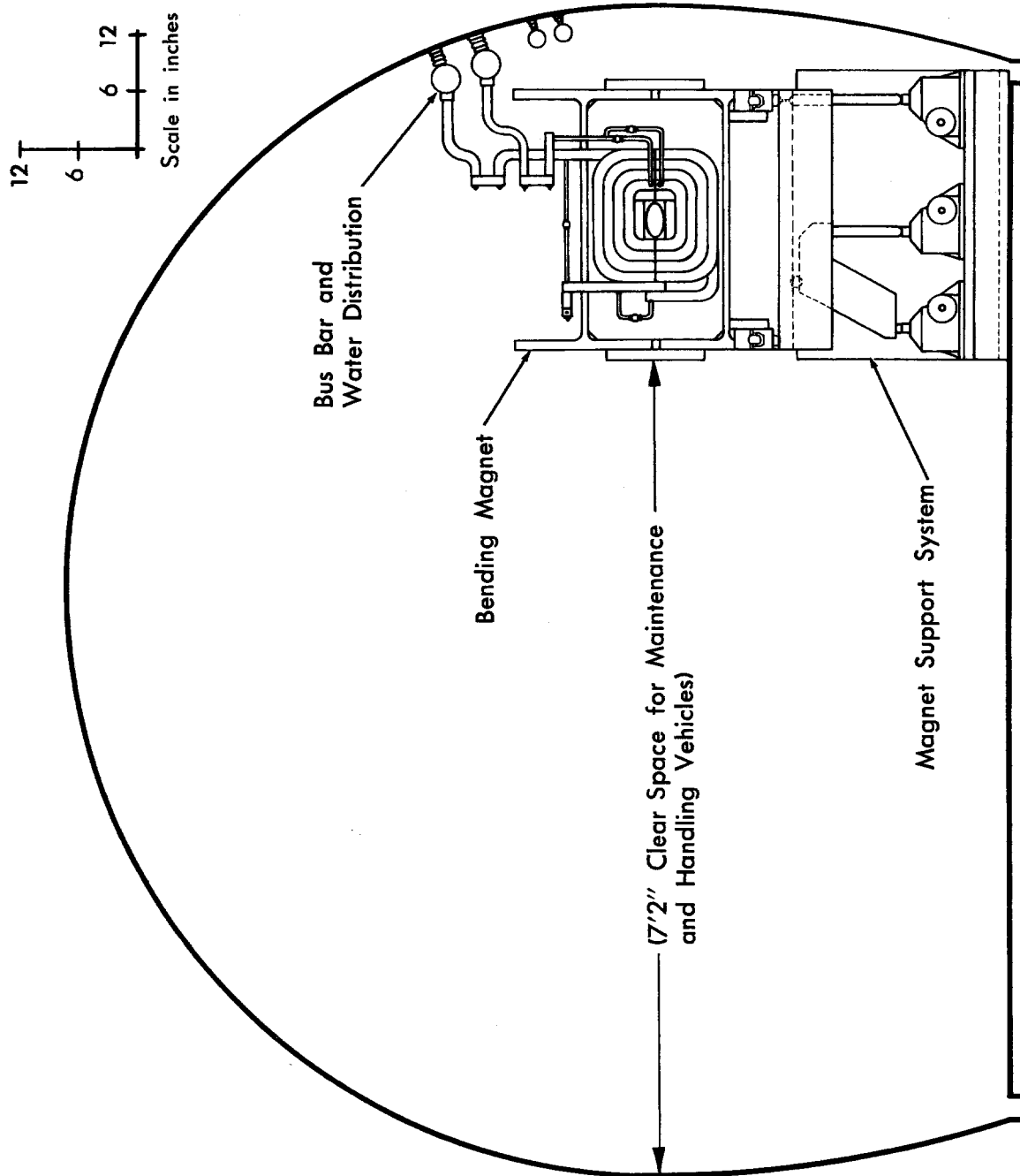


Figure 8-1 Main-Accelerator Enclosure Interior

## 8. MAIN-SYNCHROTRON ENCLOSURE

### 1. Introduction

The main synchrotron is housed in a ring-shaped enclosure approximately 20,600 feet in total length. The enclosure is to be constructed of prefabricated concrete sections mounted on a poured concrete slab. Radiation shielding is provided by earth cover. Special enclosures will be built at long straight sections to house particular functions.

Careful design work on the enclosure is of great importance, because it is a significant cost item. This design work has included examination of the functions to be carried out inside the enclosure, which must contain accelerator components, power and water distribution to them, control cabling, and space for servicing these components.

It is important to realize that the specialized functions of the accelerator, such as injection, acceleration and extraction, are collected in the straight sections. For approximately 90% of its circumference, the accelerator contains nothing but magnets and vacuum chamber. An enclosure with a small cross section, approximately 10 feet by 8 feet is planned for this section of the accelerator. Enlarged sections will be inserted at frequent intervals to provide space for the distribution of utilities and for radiation shields and equipment.

Special vehicles are planned for moving equipment and personnel and for providing a shielded environment for maintenance work in areas of high residual radiation.

The structural aspects of the enclosure are discussed in Chapter 15; this chapter will concentrate on the functional aspects.

### 2. Enclosure Design

Figure 8-1 shows a cross section of the standard enclosure that will house about 90% of the accelerator. It is 10 ft wide at its widest point, has a minimum floor width of 9 ft, and is 8 ft high at the center. The accelerator is located close to the outside wall, leaving an 86-in. clear space for vehicles and personnel at the elevation of the mid-plane of the accelerator, which is 36 in. above the floor. All connections to the accelerator will be accessible from this corridor.

Also shown in Fig. 8-1 are the pipes carrying the power and cooling water to the magnets, and the magnet support jacks. Since the pipes will be at potentials up to 500 V above ground, they will be supported

on insulators attached to inserts in the outside wall of the enclosure and enclosed by a protective insulating cover. The drive mechanisms for the support jacks will be located facing the corridor, where they can be engaged and operated by a remotely controlled mechanism. With this system, it will be possible to make small adjustments in magnet alignment with the accelerator in operation and observe the effects of magnet movements on the location of the beam.

Cable trays for control wiring will be mounted on the wall above the manifolds. Additional wall space is available for mounting small conduits for lighting and convenience outlets and piping for pneumatic controls of vacuum valves.

At each 7-ft straight section in the normal magnet lattice, spaced about 100 ft apart, the enclosure will be enlarged by inserting a special precast section with a cross section larger by 1 ft. These enlarged sections will be 12 ft wide at the widest point and 9 ft high at the center. The additional space provided by these enlargements will make it possible to install special magnets or other devices in the straight sections without cutting into the clear corridor. Utilities will be brought into the enclosure at these enlarged sections in order to use the extra overhead clearance for crossing from the inner side of the enclosure to the outer wall.

The same enlarged section will be installed along the entire length of each medium straight section to provide space for the shielding associated with beam scrapers and for various beam-control magnets. In medium straight-section A, the profile will be further modified by the conjunction of the enclosure for the beam transport between the booster and the main accelerator.

Long straight sections C, D, E and F will be housed in 12-ft enlargements that are placed off center with the inner wall flush with that of the standard enclosure. The extra 2-ft space between the beam line and the outer wall will provide more clearance around the RF cavities in straight section F. In the other straight sections it will accommodate special beam-handling magnets and will simplify modifications associated with possible future development of the accelerator.

Long straight sections A and B will be enclosed by special buildings designed for the extraction of the beam and the use of an internal target. These buildings are shown in Figs. 15-3 and 14-2.

### 3. External Structures

The utilities for the main accelerator will be distributed through 24 utility buildings spaced uniformly along the inside perimeter of the ring. These buildings, each about 2,000 sq ft in area, will contain the magnet power supplies, cooling-water pumps and heat exchangers, vacuum-pump power supplies, ventilation equipment, and circuitry for control multiplexing and transmission. Six of the utility buildings will contain

additional equipment associated with cooling towers that will be located nearby. Each building will be connected to the accelerator enclosure by a narrow corridor, to provide access by personnel to the accelerator and space for utility runs. The corridors will be offset and of sufficient length to reduce radiation in the utility buildings during accelerator operation to a level that is safe for occupancy by technical staff. The utility buildings are of a form that can be enlarged while the accelerator is operating.

Special entrances for vehicles will be located at the long straight sections. Each will include a small garage at ground level and a curved ramp leading to the accelerator enclosure.

#### 4. Enclosure Vehicles

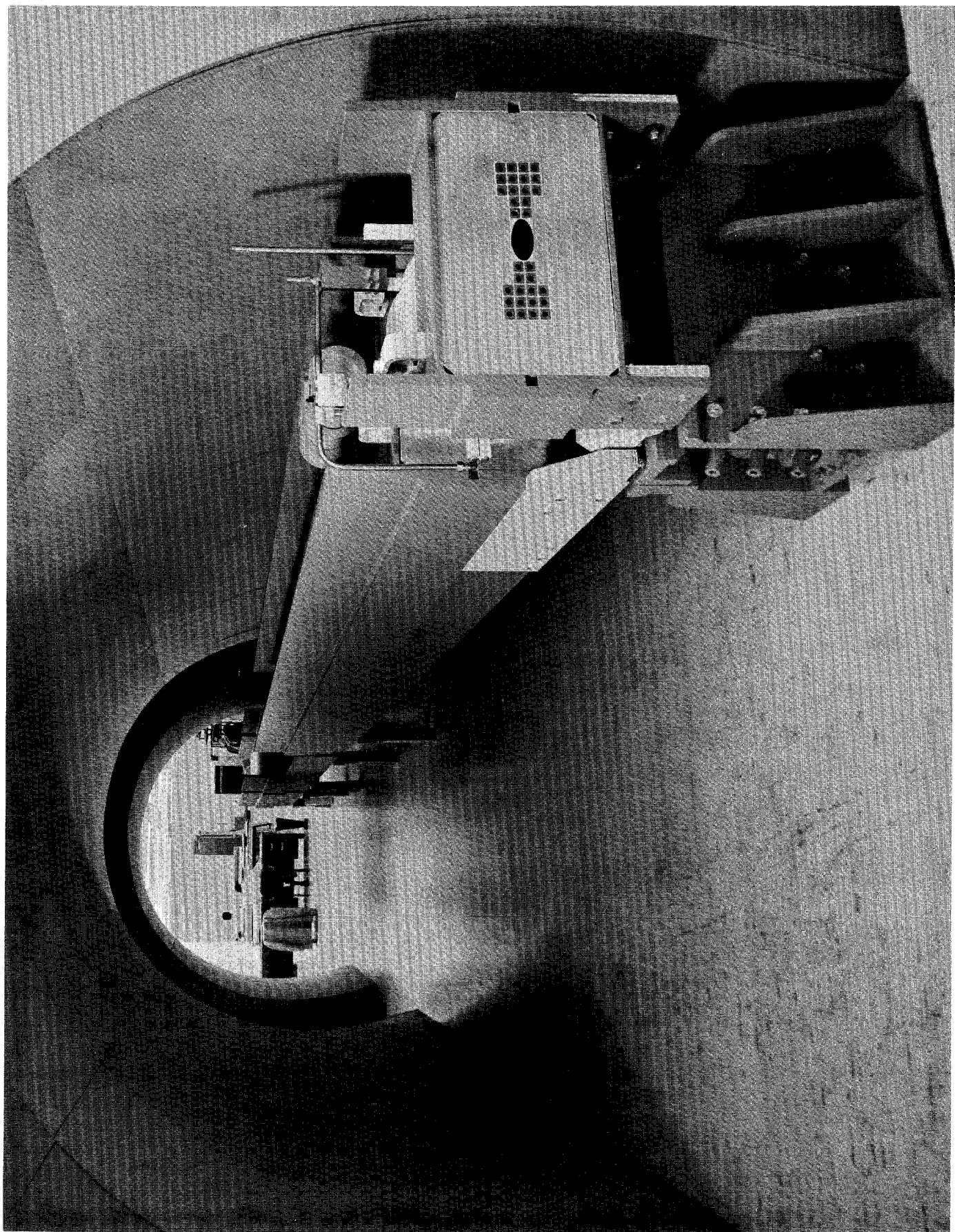
Special vehicles will be developed for installing accelerator components in the enclosure and for performing various maintenance operations on the accelerator. We have investigated vehicles using a rail system in the enclosure. This system has several difficulties. The rails must be installed in the enclosure before an accurate survey can be made and are therefore subject to positioning errors relative to accelerator components that will complicate their use. In addition, the rails will cost several hundred thousand dollars and will interfere with drainage of the enclosure.

We have therefore also investigated wheeled vehicles running directly on the enclosure floors. Discussions with suppliers of industrial handling equipment have indicated that vehicles weighing over 20 tons can be constructed using available polyurethane wheels and battery-driven motors. It appears that such vehicles will be able to climb grades too steep for railed systems, which will simplify the design of vehicle accesses.

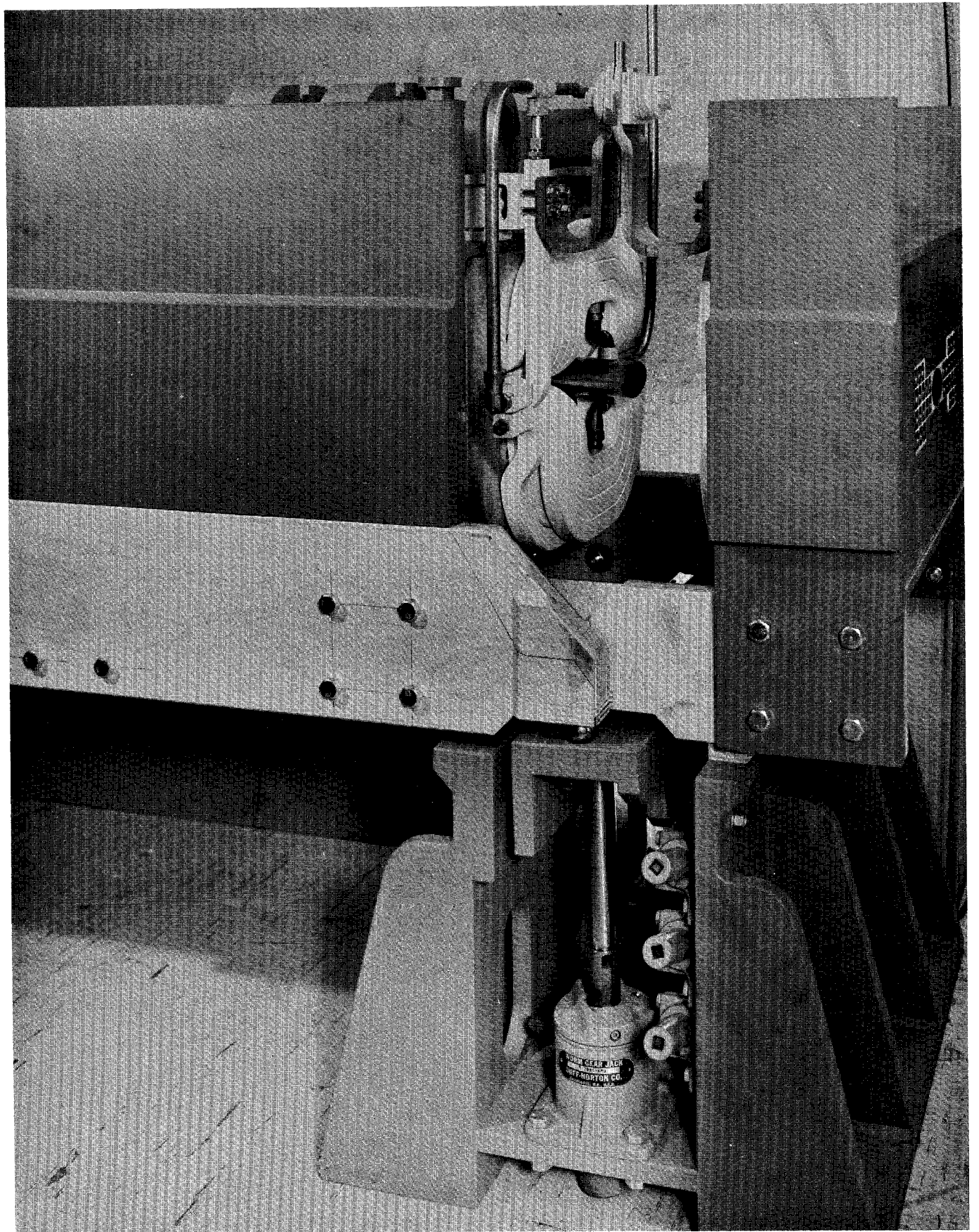
One of the vehicle systems under consideration would utilize an available flat bed capable of being driven from either end and remotely controllable. Various equipment could be mounted on this flat bed.

Vehicles will range in size and complexity from a simple tool-and-parts vehicle to one for handling bending magnets and possibly a shielded vehicle for use in areas of high residual radiation. They will be guided by pilot wheels that engage a guide rail mounted on the floor adjacent to the magnet support structures. The vehicle for installing magnets will have a gross weight of about 20 tons. A shielded vehicle having the same gross weight could provide a useful working space and a reduction of the radiation level by a factor approximately 100.

A full-scale model of a section of the enclosure has been built to test many design features. Photographs of the model and of the 1-ft straight section between magnets are shown on the next two pages.

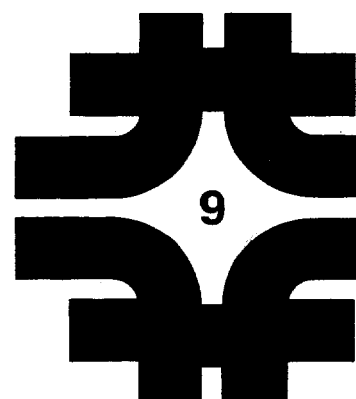






# Booster Accelerator

1. Introduction	9-1
2. Choice of Booster Type	9-2
3. Fast-Cycling Booster Synchrotron	9-4
3.1 General Description	9-4
3.2 Orbit Dynamics	9-5
3.3 Guide-Field Magnets	9-15
3.4 Magnet Power Supply	9-18
3.5 Booster-Synchrotron Acceleration System	9-22
3.6 Beam Manipulation and Observation	9-27
4. Linac to Booster Beam Transfer	9-28
4.1 General Description	9-28
4.2 Beam-Transport Arrangement	9-28
4.3 Beam-Transfer Monitoring	9-28
4.4 Booster Injection	9-30
5. Booster to Main Ring Beam Transfer	9-30
5.1 General Description	9-30
5.2 Bunch Synchronization	9-31
5.3 Booster Beam Extraction	9-32
5.4 Beam-Extraction Components	9-34
5.5 Beam-Transport Arrangement	9-35
5.6 Booster-Beam Monitoring	9-35
5.7 Injection into the Main Ring	9-36
6. Booster Synchrotron Services	9-36
6.1 Booster Vacuum System	9-36
References	9-39





## 9. BOOSTER ACCELERATOR

R. Billinge, R. Cassel, A. A. Garren, E. L. Hubbard, Q. A. Kerns,  
S. C. Snowdon, G. S. Tool, A. van Steenbergen

J. M. Peterson (LRL), R. Avery (LRL), E. D. Courant (BNL),  
H. Reich (CERN)

### 1. Introduction

A major difference between accelerator designs to produce proton energies over 100 BeV and existing proton synchrotrons is the use of a booster accelerator. The Brookhaven, CERN, and Russian accelerators inject protons directly from linear accelerators into the main synchrotrons, whereas all designs for new accelerators of 100 BeV or more proton energy plan to inject from linear accelerators into boosters, which carry protons to energies of the order of 10 BeV. At this energy, the protons are injected into the main accelerator.

If protons were injected into the main accelerator directly from a linear accelerator at an energy of several hundred MeV, the guide field in the accelerator would be so low at injection that remanent magnetic fields and eddy currents would cause undesirable guide-field distortions. In addition, the beam intensity in the main accelerator would be drastically limited by space-charge effects.

It would be possible to extend the linear accelerator to an energy of several BeV to circumvent the low-field problems, but the cost of such a linear accelerator would be at least as large as that of a 10 BeV booster synchrotron. The 10 BeV booster would give greater ultimate proton intensity. Thus the booster-synchrotron concept offers distinct technical advantages.

There are several possible types of booster synchrotron. Their relative advantages are discussed in the next section. The type chosen is a "rapid-cycling" synchrotron. In this type, more than one pulse of accelerated protons is injected from the booster into the main ring; the booster acceleration cycle is much more rapid than that of the main synchrotron.

The booster accelerates protons to 10 BeV at the rate of 15 pulses per second. It injects 13 pulses into the main ring in 0.8 second, while the main-ring guide field is held constant. The main ring is 13-1/3 times larger than the booster, and 13 pulses therefore leave a small gap in the distribution of protons around the main ring. Methods of coping with this gap are included in the main-synchrotron accelerating

system design and are discussed in Chapter 7.

## 2. Choice of Booster Type

The subject of booster types has received extensive study in the CERN and LRL design studies. Studies were continued on a number of types as part of the work leading to the design presented in this report.<sup>1-5</sup> The varieties studied include the rapid-cycling booster, a slow-cycling booster whose radius is a fraction of the main-ring radius, a slow-cycling booster of the same radius as the main accelerator and located in the main-ring enclosure<sup>7</sup>, and a combination of a small rapid-cycling booster injecting into a slow-cycling booster<sup>8,9</sup>, again of fractional main-ring radius. As a potential initial stage, for limited-intensity operation only, direct injection from the linear accelerator into the main ring was also considered<sup>10</sup>; this would be augmented by later construction of a booster accelerator.

The slow-cycling booster has the advantage of greatly simplified rf requirements and magnet-system power supply. In the case of the fractional main-ring radius slow-cycling booster, it requires, however, that multiple-turn ejection be used in order to fill the total main-ring circumference during the injection process. Of the order of 10 to 15 turn ejection would be required in this particular case. The resonant "fast-slow" or "deca-turn" ejection has recently been extensively studied at LRL and at BNL in relation to a slow-cycling booster study<sup>6</sup> for a possible higher energy injector for the AGS.

A disadvantage of the slow-ejection technique is that it can cause intensity variations during the ejection process and variations in transverse phase-space projection of the ejected beam during the multiple-turn ejection process. This process has been studied and some corrections seem possible, but beam-intensity modulation in the main ring should be expected; it would definitely limit the intensity that could be achieved with the final accelerator. In addition, the interchange of horizontal and vertical transverse phase space between booster synchrotron and main ring would be required. A significant advantage is, of course, that no injection dwell time is required for the main ring; injection into the main ring would take place within a time of approximately 25  $\mu$ sec.

An alternative is a slow-cycling booster of the same radius as the main synchrotron and located in the same enclosure. Its magnet structure could be very simple, but the required injection field of this booster would be uncomfortably low. In this case, single-turn ejection would suffice, eliminating the problems of beam phase-space variation that arise in the multiturn-ejection process. This alternative looked attractive in a first approach, notwithstanding the low injection field, and some study has been devoted to it. It soon became clear that problems could be expected from synchrotron-betatron oscillation coupling. Specifically, because of the large radius of this booster, the synchrotron-oscillation wave number  $\nu_s$  would be of the order of

unity unless the accelerating frequency were reduced to a low value. With such a high  $\nu_s$  value, the multiplicity of betatron resonant stopbands would be severe in the  $\nu$ -value domain of interest, making this booster design hazardous.

A careful reevaluation of the synchro-betatron coupling problem<sup>11-12</sup> led to the criterion that the maximum  $\nu_s$  value should be kept, if possible, below a value of 0.1. (The stopbands arising from the synchro-betatron coupling effect have been observed in some storage rings<sup>13</sup>.)

Because of the  $\nu_s$  problem, the undesirably low injection field of a large-radius booster, and the lower maximum intensity obtainable, this approach was not pursued further.

Similarly, the idea of placing a 10 BeV storage ring in the main-accelerator enclosure, as suggested by D. A. Swenson (LASL), has been considered. This storage ring could be used to reduce the booster cycle time by a factor 3 or 4 and to eliminate the main-ring injection time. This option was rejected mainly because of the interferences in construction between the storage ring and the main ring, the complexity of adding a third ring, and the undesirably low magnetic field in the storage ring.

Another difficulty of the fractional main-ring radius slow-cycling booster is the ultimate intensity requirement of the total accelerator. The slow-cycling booster must contain in one acceleration cycle the total charge required in the main ring. Thus the space-charge limit of the booster must be equal to that of the main ring, which would demand high injection energy in the slow-cycling booster. Therefore, an alternative was considered in which the linear accelerator would inject into a so-called "supercharger" ring, of small diameter, which would be fast cycling, and this in turn would inject into the slow-cycling booster. In this fashion the necessary intensity goal could be obtained. As another option, initially only the slow-cycling booster would be constructed, for operation with reduced intensity. At a later stage, the supercharger ring would be added in order to reach the desired goal.

The greater complexity of two booster accelerators in sequence made this combination an undesirable one, although sufficient study was devoted to it to evaluate injection and ejection energies of the various accelerators and the associated intensity capabilities and space-charge limitations.

As another initial option, again with limited initial goals, direct injection from the linear accelerator into the main ring was considered. The booster synchrotron would be added at a later stage in order to reach the ultimate intensity goal. Difficulties could be expected because the associated  $\nu_s$  value in the main ring would be of the order of unity. Moreover, this was not such an attractive system economically since the frequency modulation of the rf system in the main ring would have to be extended in order to cope with this initial low-energy injection.

Finally, the rapid cycling synchrotron was reevaluated and its choice as the best injector for the main synchrotron reaffirmed, notwithstanding the greater complexities of the required rf system and resonant power-supply system for the magnet.

The desirable values for booster-injection and main-ring injection energy were restudied, as these pertain to booster and main ring space-charge limits, desirable injection fields, frequency modulation of the main-ring system, and so forth. Earlier cost studies done at LRL showed that a broad cost minimum exists if the booster has a final energy between approximately 5 BeV and 12 BeV. Furthermore, the linear-accelerator design is closely related to the 200 MeV linear-accelerator construction for the Brookhaven AGS conversion program. As a consequence, the final energy of the linear accelerator crystallized at 200 MeV. Related to this and optimum main-synchrotron parameters, a final energy of the booster of 10 BeV was chosen.

The total cost of the booster accelerator is sharply sensitive to the filling time of the main ring. After consideration of the related parameters, especially the filling time of the main ring, a value of 15 cycles per second was selected.

For reasons to be discussed below, a nominal final booster accelerating frequency of 50MHz has been adopted. A maximum  $\nu_s$  value of 0.1 results. Addition of a second-harmonic rf component <sup>14</sup> could be used to reduce this maximum value of  $\nu_s$  by 30 to 50%.

### 3. Fast-Cycling Booster Synchrotron

3.1 General Description. There is no plan to use the booster for purposes other than injection into the main accelerator. As a consequence, in determining the radius of the booster, it is only necessary to take into account the long straight-section requirements for the acceleration system, for ejection, and for injection. No allowance need be made for optional slow or fast ejection possibilities. Efficient filling of the booster circumference with bending magnets is therefore possible. Even with a booster of radius as low as 62.5 meters, it would be possible to obtain the desired proton ejection energy of 10 BeV. On the other hand, a small-radius booster would require a higher repetition rate in order to maintain a fixed main-ring filling time, since this time is proportional to the ratio of the radii of the main ring to booster. The peak rf voltage required per turn is almost independent of the booster radius for a fixed main-ring filling time, but a small-radius booster requires higher fields in the bending magnets, which is more costly, because of higher stored energy, and allows less straight-section space. In fact, an LRL study showed that when booster ejection energies over a wide range around 7 BeV were considered the cost was a minimum when the injector synchrotron employed peak magnetic fields of approximately 8 kG. This suggests employing a booster synchrotron with a somewhat larger radius and lower repetition rate, maintaining the same main-ring injection time. Indeed, a 100-meter radius booster syn-

chrotron injector was seriously considered and studied in detail for some time. The  $\nu_s$  value would have been significantly in excess of 0.1 and this radius was therefore considered to be an upper limit for a desirable booster synchrotron. Consideration of these designs led to a choice of 75 meters for the booster radius.

The ratio of booster radius to main ring radius is then 13.33, a non-integral number. It is planned that the final accelerating frequency in the booster will be equal to the main-ring injection frequency and that synchronous transfer of booster bunches into main-ring rf buckets will be employed. Therefore, with simple one-turn ejection from the booster and single-turn injection into the main ring, perfect filling of the main ring could only be accomplished if the ratio of radii were an integral number. The possibility of multiturn ejection from the booster and multiturn injection into the main ring, as a potential future option, demands that the ratio of radii be non-integral and, depending on the mode of multiturn transfer, the desirable ratio should be between 13.0 and 13.5. With a booster radius of 75 meters, that is, a main-ring to booster radii ratio of 13.33 and with single-turn ejection, only about 2% of the available buckets in the main ring will remain unfilled.

**3.2 Orbit Dynamics.** Many lattice structures were examined for the booster synchrotron and compared with respect to straight-section characteristics, the symmetry of rf-cavity distribution, the phase advance per cell and between straight sections, the value of the transition energy, the choice of the  $\nu$  value and its remoteness from the nearest resonant stopband, the ease of ejection and other relevant criteria such as peak magnetic field, aperture, stored energy, number of major components, and so on.

A minimum long straight-section length of 5 meters is necessary for booster ejection and is consistent with all other straight-section requirements, although with this length only one rf cavity can be accommodated per straight section. A  $\pi/2$  insertion was considered but not adopted, because it would have produced a more crowded and inefficient structure. Lattices with straight sections long enough that two or even three rf cavities could be located in one long straight section were also considered and abandoned for the same reason. With the requirement of inserting at least 18 rf cavities and the need for 3 straight sections for injection and ejection, the number of cells desired in the structure was taken to be 24.

The betatron frequency  $\nu$  is determined from considerations of aperture size, transition energy, extraction problems, the number of lattice cells, and nonlinear resonances. For minimum aperture, a phase advance of approximately 90 degrees per cell is desirable. This phase advance is also convenient for extraction, in that it permits the kicker and septum magnets to be in adjacent long straight sections with the optimum separation. The cell number of 24, determined largely by straight-section requirements, then suggests a  $\nu$  value near 6. Considerations of nonlinear resonances for a 24-cell lattice suggest,

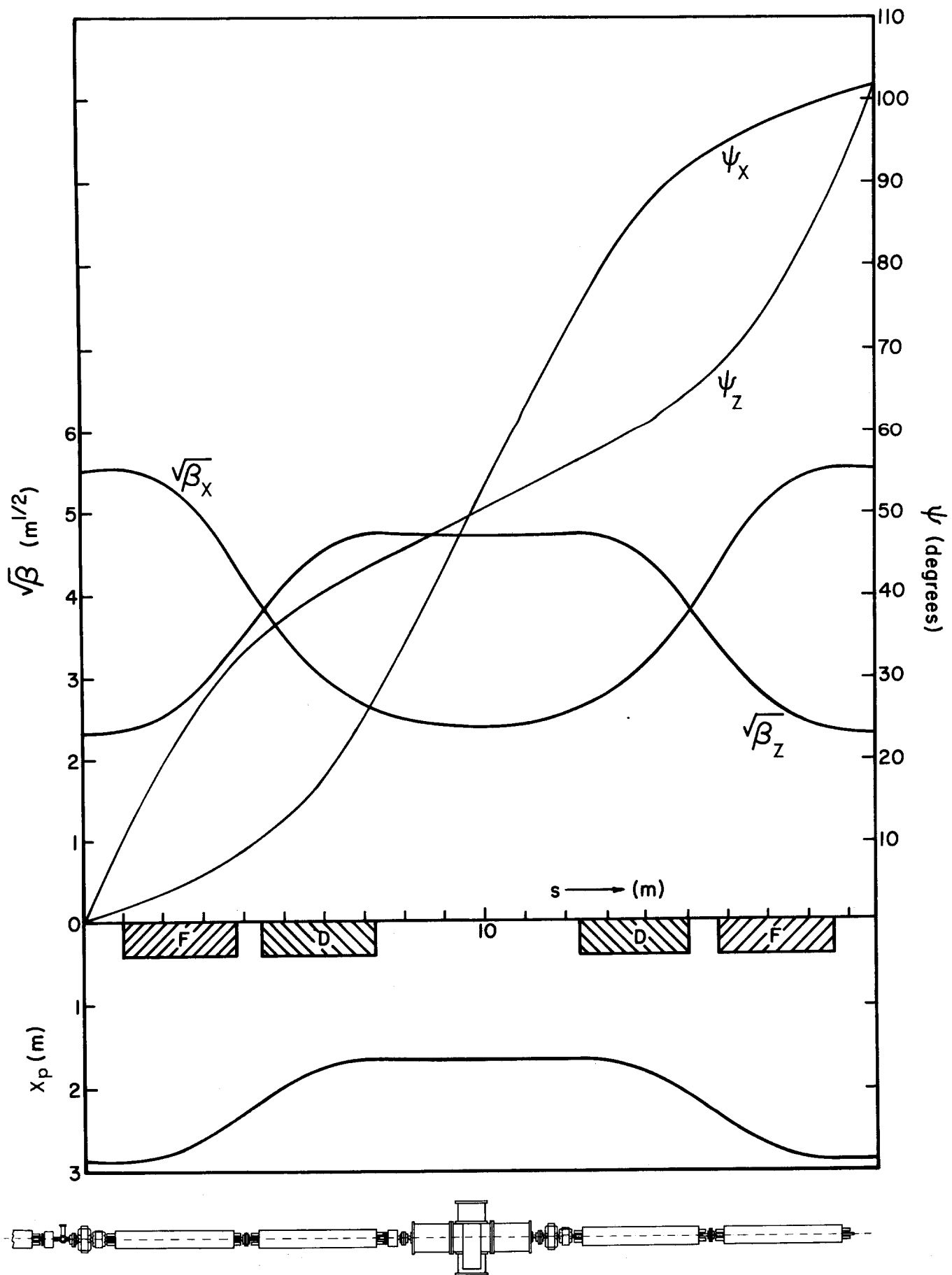


Figure 9-1 — Booster Lattice Orbit Functions

however, that  $\nu$  values close to 6, 8, or 12 should be avoided if possible, and that splitting the radial and vertical  $\nu$  values by 1 or 2 is dangerous with respect to nonlinear resonances.

In the usual lattices, the transition energy  $\gamma_t$  (in units of the proton rest mass) is approximately equal to  $\nu_x$ , which imposes another constraint on its choice. It is possible to construct a lattice such that  $\gamma_t$  and  $\nu_x$  are well separated<sup>15</sup>, which in this case would allow  $\gamma$  to be placed above the output energy of the booster ( $\gamma(10 \text{ BeV}) = 11.7$ ). Although such an arrangement would be convenient in some respects, the disadvantages of this stratagem outweigh its potential advantages.

A transition energy close to the ejection energy is undesirable because of the relatively large momentum spread that occurs near transition, and because of the small frequency of phase oscillations, which is undesirable for synchronous bunch transfer to the main ring. A low  $\gamma_t$  value is also undesirable because of the small amount of adiabatic damping that takes place before the beam passes through transition.

These considerations led to the choice of 6-3/4 for the nominal horizontal and vertical betatron frequencies.

For the booster, fast beam extraction will be used. Studies of horizontal versus vertical ejection indicated a strong preference for vertical ejection from the booster. Some lattice structures are superior to others with respect to the important problem of beam extraction.

The booster lattices examined include separated-function synchrotron structures with singlet, doublet, or triplet focusing, combined-function structures of the FOFDOD and FOFDOOD types, and some "hybrid" structures made up of flat-field bending magnets and combined-function magnets. A combined-function FOFDOOD structure has been adopted. It provides the simplest structure with the smallest number of major components and still satisfies all the criteria discussed above.

The preference for a combined-function booster structure comes about because the circumference and the final energy of the booster were determined by other factors, as indicated above. Consequently, the most economical structure could be obtained by using the best filling factor and minimum peak field for the booster magnet structure. The general arrangement of the cell structure is shown in Fig. 9-1, which also indicates the distribution of the major components and gives the betatron-amplitude and momentum-compaction functions. Booster synchrotron and beam-transfer parameters are given in Table 9-1.

The 24 cells of the FOFDOOD lattice are identical, so that there is no superperiodicity, an attractive feature. In some of the alternative lattice arrangements studied, a superperiodicity between 6 and 10 was typically obtained, leading to a closer proximity of the chosen  $\nu$

value to resonant stopbands. An attempt was made to satisfy the criterion suggested by A. W. Maschke that the  $\nu$  value should be chosen so that all resonances up to 3rd order are removed from the diamond of interest and from its integral boundaries, permitting only a fourth-order resonance at the integral boundary. For the case at hand, with 24 cells and a  $\nu$  of 6-3/4, a fourth-order structure resonance exists at  $\nu = 6$ , thereby satisfying this criterion.

With the choice of cell number and  $\nu$  value, the phase advance per cell is determined. A value of  $\phi = 101^\circ$  is obtained, which, with the location of the long and short straight sections in the structure, allows for insertion at suitable locations of correcting magnets for closed-orbit corrections. Furthermore, with the preferred location of the septum magnet in the ejection long straight section, the phase advance between kicker and ejection magnet will be approximately  $\pi/2$ .

It is also desirable to locate correcting sextupoles at locations where  $\beta_x$  is significantly larger than  $\beta_z$  and vice versa. This is done in the present lattice by providing a short 2-meter straight section. This serves not only for sextupoles, but also for trim quadrupoles, skew quadrupoles, and pick-up electrodes. Space is also available in the long straight section for correcting elements, since the rf cavity requires only about 3 out of the 5 meters available.

Because of the location of the D and F magnets around centers of symmetry of the lattice cell, it is possible to use two identical D magnets with one aperture and two identical F magnets with a different aperture.

Table 9-1. Booster-Synchrotron and Beam-Transfer Parameters

#### GENERAL

##### Summary of Booster Parameters

Output energy	10 BeV
Input energy	0.2 BeV
Transition energy	4.48 BeV
Beam intensity	$3.8 \times 10^{12}$ protons/pulse
Orbit radius	75 m
Magnetic radius	43.7 m
Focusing type	Alternating gradient
Lattice type	FOFDOOD, combined function
Cycling rate of magnet	15 Hz
Guide field at injection	490 G
Peak magnetic guide field	8.32 kG
Betatron oscillation wave number	$\nu_x = 6.75$ $\nu_z = 6.75$
Number of lattice cells	24 (identical)
Injector accelerator	200 MeV linac



### Nominal Intensity Parameters

Proton beam intensity	$3.8 \times 10^{12}$
Lowest calculated space-charge limit, incoherent transverse space-charge defocusing	$8.6 \times 10^{12}$ protons/pulse
Typical injection operational mode	75 mA, 4 turns
Charge injected into main ring, (13 booster cycles)	$5.0 \times 10^{13}$ protons

### Beam Transfer Parameters

Injector transverse emittance area	$\pi$ cm-mrad
Transverse emittance area, after stacking (nominal)	
horizontal	$5\pi$ cm-mrad
vertical	$2\pi$ cm-mrad
Booster transverse emittance area at ejection (nominal)	
horizontal	$0.3\pi$ cm-mrad
vertical	$0.12\pi$ cm-mrad
Injector momentum spread after debuncher ( $\Delta p/p$ )	$\pm 1.1 \times 10^{-3}$
Booster momentum spread for bunched beam at injection	$\pm 2.5 \times 10^{-3}$
Bunching factor	0.44
Longitudinal phase space area at injection	2.22 eV-sec
Bucket area at injection	3.00 eV-sec
Booster momentum spread at ejection	$\pm 0.9 \times 10^{-3}$
Booster bunching factor at ejection	0.14

### FURTHER BOOSTER PARAMETERS

#### Orbit Parameters

Betatron wavelength	69.8 m
Betatron amplitude function, gradient magnets,	
$\beta_F$ (max), horizontal	30.8 m
$\beta_F$ (max), vertical	11.6 m
$\beta_D$ (max), horizontal	15.5 m
$\beta_D$ (max), vertical	22.6 m
Momentum compaction, $X_p$ per ( $\Delta p/p$ )	
max. (F)	2.9 m
max. (D)	2.1 m
Phase advance per cell	0.28 ( $2\pi$ )
Synchrotron oscillation wave number, (max.)	0.1

Revolution period, at injection	2.78 $\mu$ sec
at ejection	1.58 $\mu$ sec

### Cell Structure

Cell length	19.63 m
Number of gradient magnets per cell	4
Long straight-section length	5 m
Short straight-section length	2 m
Intermagnet straight section length	0.6 m
Circumference factor	1.72

### Aperture Requirements

Vacuum envelope, internal dimensions,  
gradient magnets:

F, horizontal	5.5 in.
F, vertical	1.75 in.
D, horizontal	4.0 in.
D, vertical	2.5 in.

#### Long straight section

horizontal	2.25 in.
vertical	2.5 in.

#### Magnet gap,

F, vertical	2.25 in.
D, vertical	3.0 in.

### Magnet System

Number of gradient magnets	48 (D), 48 (F)
Effective length of F unit	2.86 m
Effective length of D unit	2.86 m
Cross section of each magnet	25 x 18 in.
Profile parameter, $B' / B$ in F unit	$2.36 \text{ m}^{-1}$
Profile parameter, $B' / B$ in D unit	$-2.48 \text{ m}^{-1}$
Number of correcting sextupole components	24
Number of tune-correcting quadrupoles	24
Number of skew-quadrupole elements	48
Number of closed-orbit deflectors	48

### Magnet Power Supply

Magnet excitation	sinusoidal biased resonant circuit
Number of resonant sections	24
Nominal maximum current	2,100 A
Peak magnet stored energy	1.6 MJ
Magnet power dissipation, average	1.5 MW
Total power supply (distributed-choke system) losses:	
ac	1.1 MW
dc	1.9 MW
Peak voltage to ground	1.6 kV

### Booster Acceleration System

Frequency range	30.26 - 53.24 MHz
Harmonic number	84
Number of cavities	18
Maximum energy gain per turn	0.76 MeV/turn
Peak rf voltage	0.85 MV/turn
Maximum voltage per cavity (2 gaps)	48 kV
Peak total rf power	0.7 MW
Peak power to beam	0.3 MW

---

Design Intensity and Aperture Requirements. The design intensity in the main accelerator is  $5 \times 10^{13}$  protons per pulse and is to be achieved by injecting 13 pulses from the booster synchrotron. This requires that  $0.38 \times 10^{12}$  protons be accelerated in each booster cycle. In the main accelerator, the transverse incoherent space-charge limit suggests an ultimate intensity of about  $3 \times 10^{14}$  protons per pulse for a beam filling the entire aperture.

The aperture in the booster is determined by assuming a space-charge limit of about 1/13 of that of the main accelerator. These considerations, together with the parameters presented in Table 9-2, determine the magnet apertures. The nominal values are 2.25 by 6 inches for the F magnets and 3 by 4.5 inches for the D magnets. The vacuum chamber wall thickness is taken to be 0.25 inch.

If the available apertures could be fully employed for injected beam, the associated space-charge limit in the booster would be  $2 \times 10^{13}$  protons per pulse, which matches the calculated limit for the main ring. The combination of nominal linac beam emittance of  $\pi$  cm-mrad, the multiturn-injection process and some allowance for space-charge beam blowup immediately after injection lead to nominal beam emittance values of  $2\pi$  cm-mrad vertically, and  $5\pi$  cm-mrad horizontally. With these values, the calculated booster space-charge limit is  $0.8 \times 10^{13}$  protons per pulse, which is adequate compared with the design value of  $0.38 \times 10^{13}$  protons per pulse.

Table 9-2. Aperture Considerations in the Booster

	(Horizontal)	(Vertical)	
Acceptance area	10.6 $\pi$	4.2 $\pi$	cm-mrad
Beam emittance area, 200 MeV.	5.0 $\pi$	2.0 $\pi$	cm-mrad
Calculated space charge limit, "2 $\pi$ , 5 $\pi$ " beam,	0.84 x 10 <sup>13</sup>	protons	
Design charge per Booster cycle	0.38 x 10 <sup>13</sup>	protons	
<hr/>			
F Magnet:			
beam betatron amplitude	7.84	3.00	cm
phase-oscillation amplitude*	1.44	-	cm
sagitta, corrected for $\beta$ profile	1.47	-	cm
aperture allowance (table 9-3)	3.57	1.38	cm
vacuum-chamber allowance	<u>1.27</u>	<u>1.27</u>	cm
Total	15.59	5.65	cm
	6.14	2.22	in.
<hr/>			
D Magnet:			
beam betatron amplitude	5.58	4.24	cm
phase-oscillation amplitude*	1.06	-	cm
sagitta, corrected for $\beta$ profile	0.86	-	cm
aperture allowance (table 9-3)	2.54	1.94	cm
vacuum-chamber allowance	<u>1.27</u>	<u>1.27</u>	cm
Total	11.31	7.45	cm
	4.45	2.93	in.
<hr/>			
Nominal Magnet Apertures, F Magnet 6	2.25	in.	
, D Magnet 4.5	3	in.	
<hr/>			
* $\Delta p/p$ , bunched	$\pm 2.5 \times 10^{-3}$		
bunching factor	0.44		

Subsequent to matching the nominal space-charge limits of booster and main ring, the resultant aperture parameters were checked against minimum aperture allowances for misalignment errors, field errors, and gradient errors. The net allowances over the requirements for the emittance-limited beam parameters, sagitta allowance and synchrotron amplitude allowance are given in Table 9-3 and have been judiciously allocated to closed-orbit deviations and beam-growth allowance related to gradient errors. These aperture allowances would result if field-error tolerances are taken as 0.1%, magnet-tilt tolerances as 1 mrad

about the azimuthal axis, horizontal and vertical position tolerances as approximately 0.25 mm, and magnetic field-gradient errors as 1 %. Contributions due to random stray fields have not been taken into account. Their contribution to the closed-orbit allowance would add approximately 25% of the total value in Table 9-3.

The field-error and misalignment tolerances are somewhat larger than those to be expected with standard alignment procedures. Gradient errors not exceeding 0.2% can be obtained in a straightforward manner. Actually, it is intended to reduce significantly the indicated aperture allowances for closed-orbit errors by means of magnet adjustment and injection closed-orbit deflector magnets. This is particularly necessary because of the aperture required for placement of the ejection septum magnet within the injection aperture, the beam-scraper units and the injection orbits during the multiturn-injection process. These requirements can be satisfied. Near the ejection septum magnet, precise injection-orbit perturbation and control will be necessary, since the vertical ejection requirement adds locally from 0.8 to 1.0 cm to the "beam-only" injection vertical-aperture requirements.

Table 9-3. Aperture Allowances

<hr/>				
Closed-orbit errors (rms)				
	Horizontal	$\pm 1.4$	$\pm 1.0$	cm
	Vertical	$\pm 0.5$	$\pm 0.7$	cm
Gradient errors (rms)				
	Horizontal	$\pm 0.4$	$\pm 0.3$	cm
	Vertical	$\pm 0.1$	$\pm 0.2$	cm
<hr/>				

If it is desired to split the horizontal and vertical  $\nu$  values, additional aperture allowance is required. Typically, for  $\nu$  values of  $\nu_x = 6.1$ ;  $\nu_z = 6.9$ , approximately 0.9 cm horizontally and approximately 0.3 cm vertically extra aperture allowance would be required. It is clear that this could only be accomplished after reduction of the indicated aperture allowances to small values.

Orbit Corrections. Because of the coherent  $\nu$ -value depression as a result of space-charge defocusing forces, it is desirable to control the horizontal and vertical  $\nu$  values independently. This independent control is also necessary if splitting of the  $\nu$  values is required to reduce horizontal-vertical coupling effects. It has, therefore, been assumed that  $\nu_x$  and  $\nu_z$  should be independently variable between values of 6.1 to 6.9. This can be accomplished by means of tuning quadrupoles located at the upstream end of each long and each short straight section. For this case the tuning diagram is given in Fig. 9-2, where the relationships are plotted. The lens strength,  $\Delta_{FF}$  or  $\Delta_{DD}$ , is given by  $\Delta = (\ell \partial B / \partial x) / B\rho$ , and  $\ell$  is assumed to be 0.2 m.

$$\delta v_x = 11.25 \Delta_{FF} + 40.6 \Delta_{DD}$$

$$\delta v_z = -48.5 \Delta_{FF} - 13.35 \Delta_{DD}$$

A smaller number of tuning quadrupoles is possible, adding somewhat to beam aperture requirements. This is being evaluated.

It has often been found attractive to make the  $v$  value independent of momentum by deliberately including sextupole components made by shaping the gradient-magnet profile. In suppression of coherent oscillations, this is not necessarily desirable. Therefore, in addition to shaping the magnet pole profile, sextupole magnets will be added to the structure to provide for adjustments.

To suppress horizontal-vertical coupling due to the earth's magnetic field in the straight sections, it is desirable to provide for some skew-quadrupole component. This can be accomplished by means of additional skew-quadrupole magnets or by judicious rotation of some or all of the tuning quadrupole magnets.

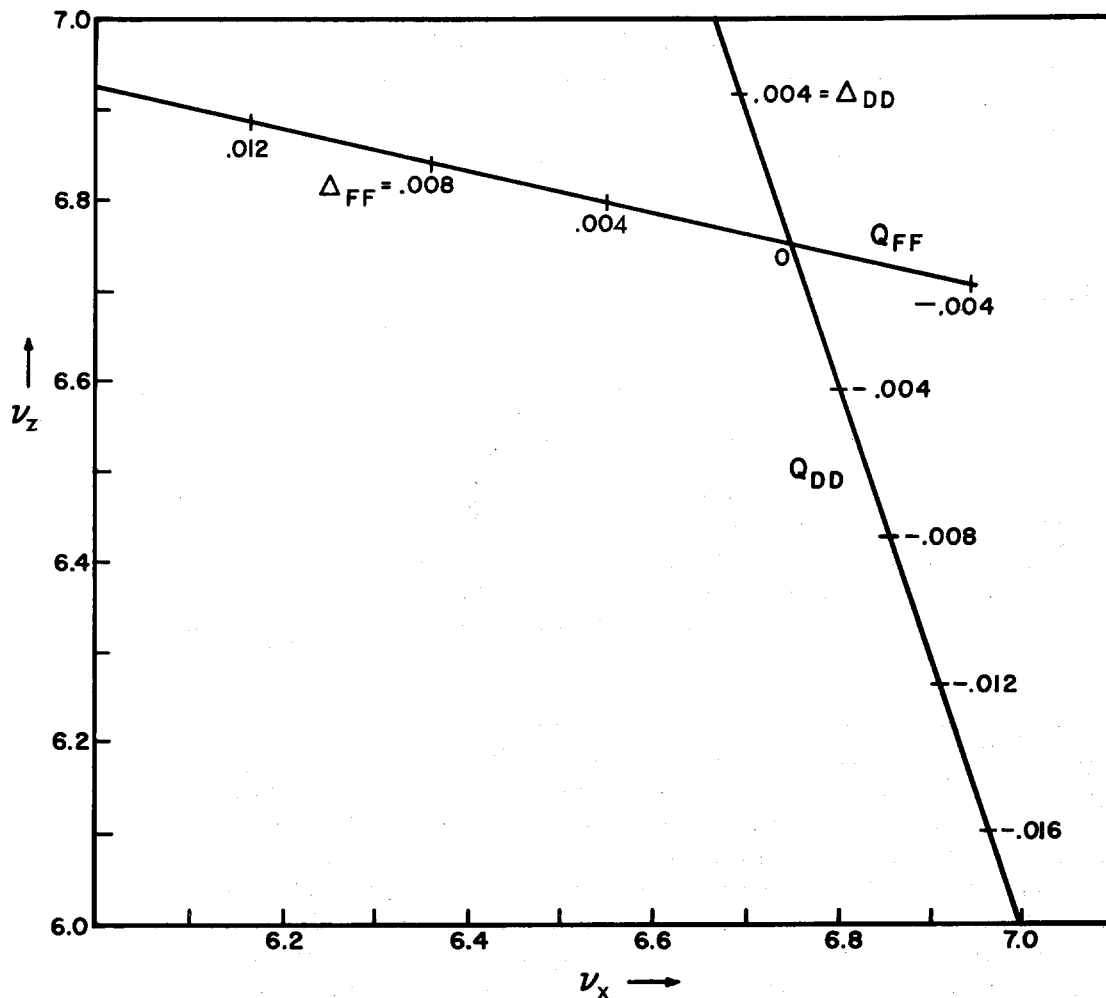


Figure 9-2 — Booster-Synchrotron Tuning Diagram

### 3.3 Guide-Field Magnets.

General Description. The magnet system is arranged in 24 cells. Each cell contains two mirror-image magnet assemblies. An assembly consists of an F magnet block and a D magnet block mounted on a common I-beam substructure. The individual magnet block is made by assembling H-frame transformer-iron laminations of the proper contour, as shown in Fig. 9-3. The length of each magnet block is 113 inches. The magnet block is powered with two coils, one around each upper and lower pole. There are two types of laminations, one for the F-block and one for the D-block. For excitation, four magnets, i. e., two D-F magnet pairs located on either side of the 2-meter straight section will be arranged in series and will form part of a unit cell of the resonant multisection power supply.

Magnet Core Design and Fabrication. The magnet core material is to be a silicon transformer steel laminated to about 22 gage (0.0310 in.) to reduce eddy currents. Each lamination will be stretcher leveled before the blanking-die operation. A subsequent shaving-die operation will assure precision contours. A core plate will be provided for each lamination to reduce stray core loss due to interlamination resistance and to prevent accidental shorts from developing in handling.

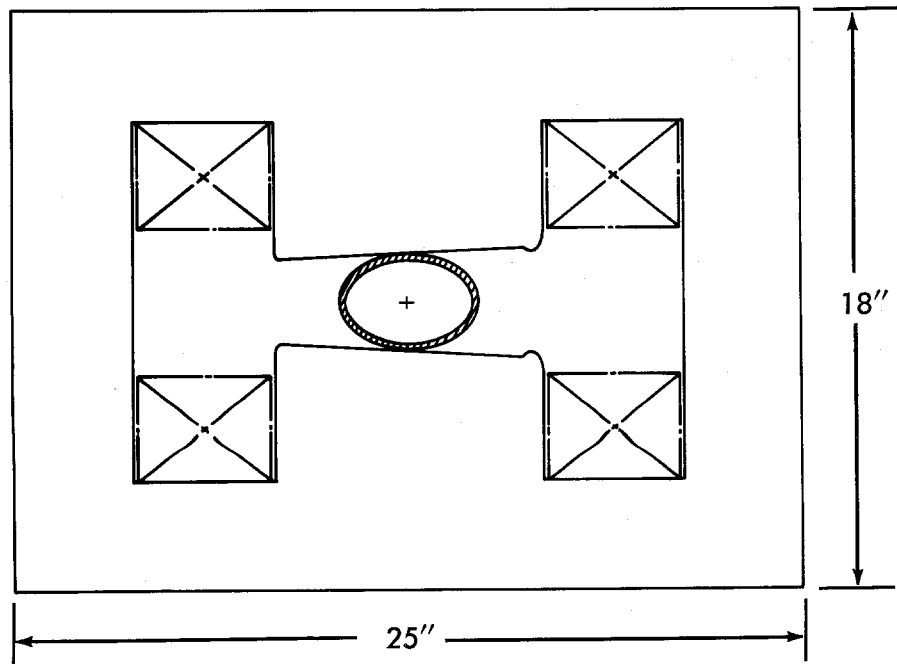
The core is straight stacked with laminations parallel. Normally, the sagitta allowance would be 0.92 in., but when account is taken of the change in beam profile due to betatron-amplitude variation with azimuth, this sagitta allowance reduces to 0.58 in. in the F magnet and 0.34 in. in the D magnet. Hence, the laminations are straight stacked instead of conforming to the local orbit curvature. The straight magnet block also has advantages for a possible thin-walled all-metal vacuum chamber.

The structure will be held together with welded bars and stainless steel-end plates that also contain specially machined laminations which form the transition from the magnet region to the straight-section region. Suitable adhesives will be employed to reduce interlamination shorts and to reduce the sound level.

A full-scale cross-section core block of reduced length will be constructed and tested during the development program. Magnetic properties will be confirmed in relation to computer calculations. In addition, the model will serve to test mechanical details.

Table 9-4 collects design parameters of the magnet system.

"D Magnet"



"F Magnet"

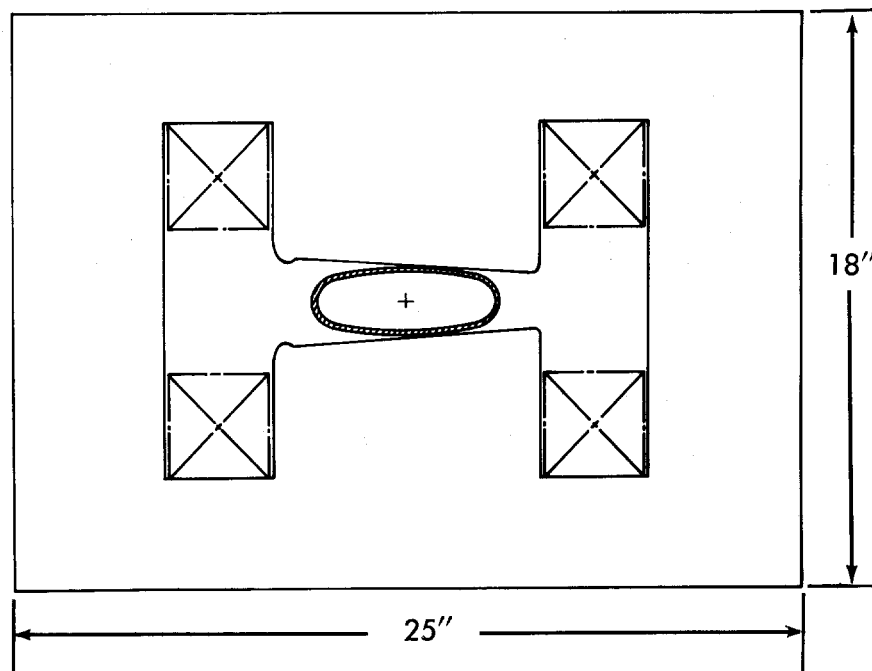


Figure 9-3 — Booster Magnet Cross Sections



Table 9-4. Booster-Synchrotron Magnet Parameters

Performance Parameters

Field at Center of Chamber

Injection	0.49 kG
Peak	8.32 kG

Field Gradients (Peak)

F - Magnet	19.9 kG/m
D - Magnet	-20.5 kG/m

Good-Field Region

F - Magnet	<u>+2</u> -3/4 in.
D - Magnet	<u>+2</u> in.

Magnet Core Weight

F - Block	5.2 tons
D - Block	5.2 tons
Number (F - Magnet)	48
Number (D - Magnet)	48
Total Weight	500 tons

Magnet Coil Weight (Copper)

F - Block	892 lbs
D - Block	1192 lbs
Total Weight	50 tons

Laminations (Tentative choice. Forms basis of calculations)

AISI Type No.	M-19
ESS Gage No.	22
Core Plate	2

Excitation

DC Bias Current	1100 A
Peak AC Current	1000 A
Turns (Top or Bottom in F)	9
Turns (Top or Bottom in D)	12

### Inductance

F - Block (Series Connected)	6.1 mH
D - Block (Series Connected)	8.7 mH

### Magnet Coil Resistance

DC	0.31 m $\Omega$ /turn
AC (Eddy-Current Effect Only)	0.36 m $\Omega$ /turn

---

Coil Design and Fabrication. The excitation coils will be made either of solid copper strands that form a cable around a hollow copper tube or of small cross-section hollow copper conductors. Economic considerations and ease of fabrication will form the basis of choice. In addition to the main excitation coils, other low-current windings will be installed to monitor magnet performance and to assist in closed-orbit control at injection and at high field.

The coil surrounding each pole of an F-magnet is subdivided into three layers each approximately 1-1/16 in. thick and weighing about 150 lbs. This permits assembly of the coil by inserting one layer at a time through the magnet window. Clamps will hold the coil securely. In the D-magnet, the coil around each pole is also divided into three layers each about 1-1/16 in. thick, but each weighing about 200 lbs. Assembly of the coil will proceed as with the F-block.

### 3.4 Magnet Power Supply.

Resonant Magnet System. Magnet excitation will be obtained by using a distributed series-resonant circuit with dc-biased sinusoidal excitation.\* This circuit consists of a number of series-connected magnet groups and associated resonant capacitors, with each capacitor connected in parallel with a winding of an energy-storage choke. Combining the choke in a transformer arrangement will allow the addition of ac power to make up for losses in the resonant circuit. All the primary windings of the chokes are connected in parallel to a primary ac source. By separating some of the secondary choke windings into two identical parts, a location is provided for insertion of dc bias power supplies. Since it is advantageous to keep the voltage to ground low, this has been done at six locations around the total circuit, with grounding provided only at one of these dc power supplies. The basic circuit is shown schematically in Fig. 9-4. Table 9-5 collects parameters of the power supply system.

\* Acknowledgment is made of contributions by R. Thomas (Brobeck and Associates) and H. Vogel (LRL).

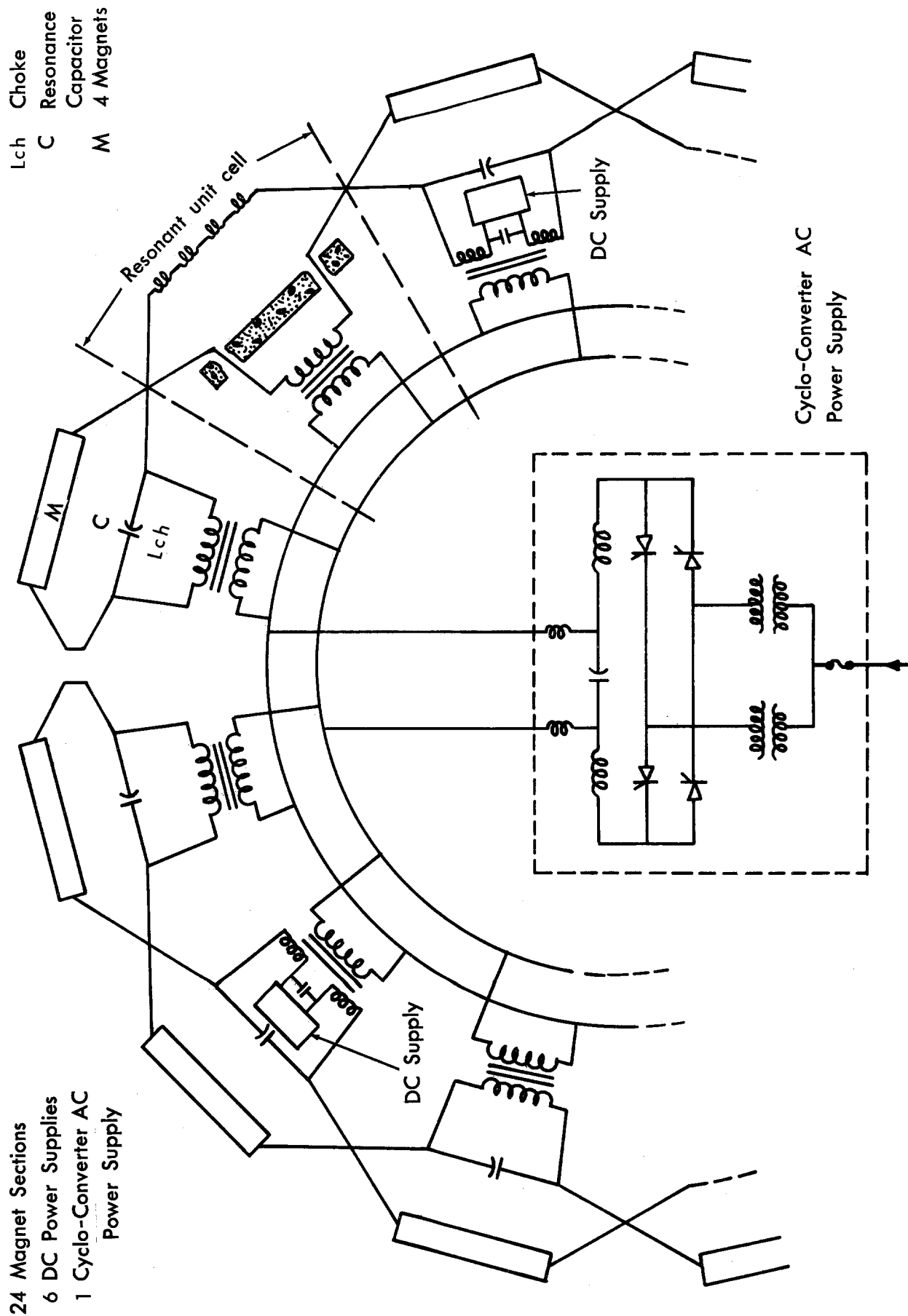


Figure 9-4 — Booster-Synchrotron Resonant Magnet Power Supply

Satisfactory excitation of individual magnets and circuit parameters could be obtained by arranging four magnets in series. A virtual ac ground exists at the central location of each four-magnet group. It is therefore only at the extremes of each unit cell that the peak ac voltage occurs. In the present case, this voltage will be 1.4 kV. Since the required dc bias will be distributed over six locations, approximately 200 V peak should be added, resulting in a peak magnet-coil-voltage-to-ground value of 1.6 kV, which is acceptable.

A problem connected with the multisection resonant circuit is the excitation of so-called "transmission-line modes." These standing waves, set up in what is essentially a low-loss transmission line of finite length  $2\pi R$ , where  $R$  is the radius of the booster synchrotron, can result in an inhomogeneous distribution of the magnet excitation current around the booster ring. These modes, being inherent in the basic circuit, are difficult to suppress. Factors contributing to the enhancement of the modes are variations in capacitor leakage currents, a finite number of power-input points, and nonlinearity of magnet self-inductance. Note, however, that leakage current variations may be "tuned" out. In addition, removal of the single-circuit ground connection will reduce the leakage current effect. This, however, is an undesirable solution from the point of view of safety.

Table 9-5. Booster Magnet Power-Supply Parameters

---

Magnet current at injection	124 A
Peak magnet current	2100 A
Bias current	1100 A
Magnet stored energy (max)	1.6 MJ
Magnet inductance	0.7 H
DC magnet coil resistance	0.8 $\Omega$
Number of magnets	96
Number of resonant cells	24
AC voltage per cell (rms)	2030 V
Max. voltage to ground	1600 V
Capacitance per cell	7260 $\mu$ F
Choke inductance per cell	0.03 H
Peak capacitor stored energy	720 kJ
Total choke stored energy	1.64 MJ
Total ac power losses	1.1 MW
Total dc power losses	1.9 MW
1. magnets:dc	980 kW
:ac	510 kW
2. chokes :dc	980 kW
:ac	510 kW
3. Capacitors ac	91 kW
Power-supply dc rating	2000 kW
Power-supply ac rating	1200 kW

---

In the unforeseen case that transmission-line modes could not be sufficiently suppressed, it would be a simple matter to correct for the resultant effects on the equilibrium orbit with the closed-orbit correction coils discussed below, since the estimated perturbation magnitude is such that it would be significant only near injection.

The bus bars for connecting the 24 magnet groups will be interlaced as indicated in Fig. 9-4 in order to avoid the generation of a single-loop dipole field around the ring circumference.

It is also important that each group of four magnets consists of two F and two D gradient magnets. This arrangement tends to reduce resultant gradient variations around the booster ring arising from minor variations between individual resonant circuit cells.

The chosen number of elementary circuit cells gives an economic optimum in relation to the number of circuit components and their ratings.

Component Design. To assure low voltages to ground from the magnets, the dc supply is subdivided into six power supplies. This also provides for an economical voltage rating of presently available thyristors.

For the central ac power supply, a "cyclo-converter" circuit will be used. This circuit has also been schematically indicated in Fig. 9-4. This type of circuit has become a practical solution for the booster resonant circuit power source because of the availability of suitable thyristors. The unfiltered output of the cycloconverter circuit has a large higher-harmonic content, but it is quite practical at this power level to use a circuit with 24-phase rectification, thereby decreasing the amplitude of the harmonics as well as increasing their frequency. Consequently, the necessary filter will be an inexpensive device.

The cycloconverter has the advantage that it is possible to drive the resonant circuit continuously during the whole magnetic-field cycle. This reduces the lower-frequency harmonic content, which is normally more difficult to attenuate.

As an option, decrease of the rate of rise of the magnetic field in the booster has been considered, especially during the early part of the cycle. This could reduce significantly the peak rf power required during the early part of the booster acceleration cycle. For beam transfer into the main ring, only a very short "flat-top" is required, and it is interesting to consider adding a second-harmonic component to the magnet excitation system, thereby providing a slower rate of rise during injection. The drive circuit discussed above lends itself suitably to the eventual adding of a second harmonic component.

A series of distributed chokes will be utilized, rather than a single central choke. The chokes and required capacitors will be distributed along the circumference of the equipment gallery, which is

located over the booster ring enclosure. From these locations, by means of short shield penetrations, the total circuit will be completed.

### 3.5 Booster Synchrotron Acceleration System.

General Considerations. The choice of the frequency in the accelerating system is influenced by many factors. The frequency must match that of the main ring (or be a subharmonic) for synchronous beam transfer. Cavity length and voltage specifications dominate the straight-section requirements and strongly influence the ring size and the lattice design. Considerations of synchronization and bunching factor favor high frequencies, whereas kicker-magnet problems, voltage requirements, phase-oscillation resonances, and beam-observation difficulties favor low frequencies. The technological state-of-the-art and costs also enter into the argument. The conclusion from the considerations is that a ferrite-tuned system with a final booster accelerating frequency of approximately 50 MHz will be suitable in all respects.

Performance Requirements. The voltage program during the acceleration cycle of the booster has three phases. The first is the trapping phase. The 200 MeV beam from the linac is injected in a nominal four turns; this beam debunches completely in approximately one revolution. Efficient adiabatic trapping of the beam is then accomplished by turning on the voltage linearly in about 50  $\mu$  sec to a final value of 200 kV per turn. At the end of this phase, virtually all of the beam has been trapped with negligible dilution in a stable phase area ("bucket") whose momentum width is about twice that of the beam from the linac.

The second is the acceleration phase of the voltage program and lasts 33 msec (1/30 second). Under conditions of constant bucket area and sinusoidal energy-gain variation, the necessary voltage rises to a maximum of 850 kV per turn just before the middle of the acceleration period and drops monotonically to a very low value at the end. The voltage waveform and other acceleration parameters are shown in Fig. 9-5.

During a 0.5 to 1 msec period at the end of the cycle, in the third phase, the voltage will probably be raised to its maximum value to synchronize the beam in the booster with the buckets in the main ring. This procedure is followed in the "phase-lock" method of synchronization.<sup>16,17</sup> If another method of synchronization were adopted, this part could be removed from the voltage program.

The frequency program of the system must, of course, follow the velocity change of the protons during acceleration. The frequency at injection is about 30 MHz (corresponding to a  $\beta$  of 0.566), and at ejection it is approximately 53 MHz ( $\beta = 0.996$ ).

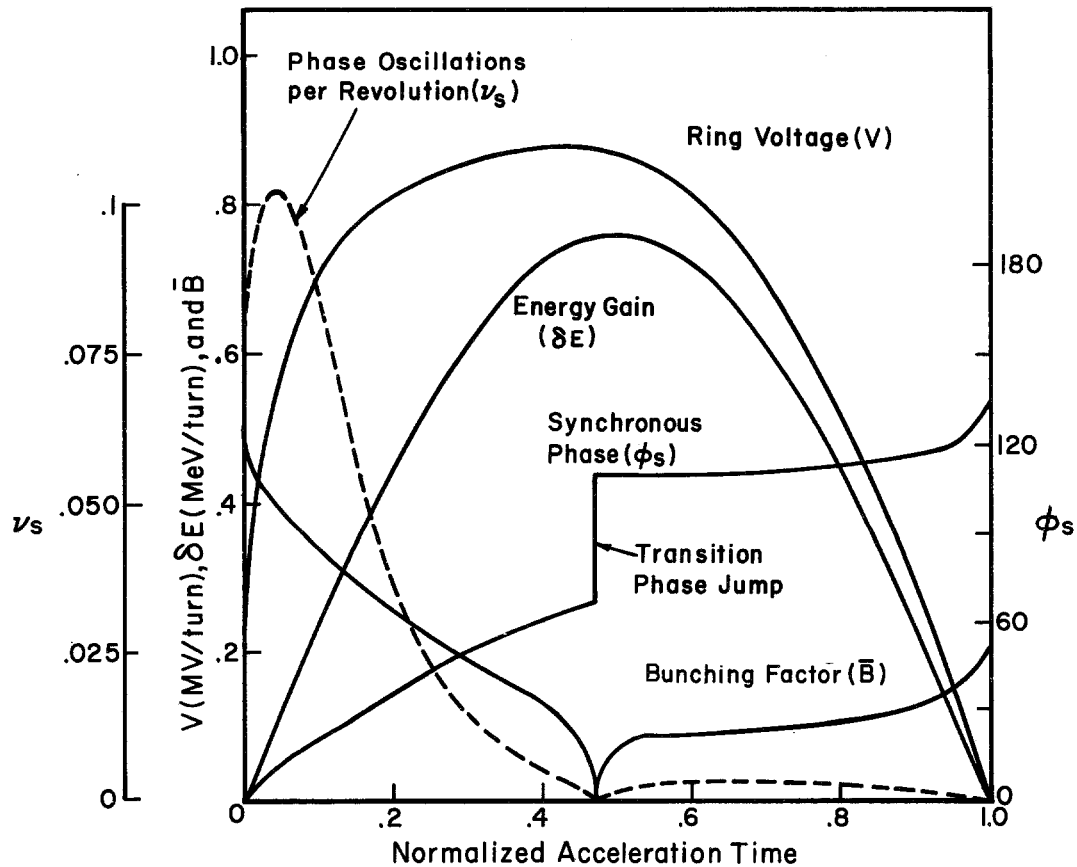


Figure 9-5 — Booster-Synchrotron RF Acceleration Parameters

At transition, which occurs near the middle of the acceleration period, the phase of the rf will be shifted to accommodate the change in stable phase. A "triple-switch" or a more complicated phase program<sup>18</sup> and possibly some modulation of the voltage may be incorporated to minimize the mismatch in longitudinal phase space that can occur at transition because of high beam intensity.

RF System Components. The rf system approach has been aimed at minimizing cost and straight-section length requirements while retaining flexibility of operation and reliability. The excellent performance record of ferrite tuning in numerous accelerator rf systems makes it a clear choice for achieving the frequency range with a minimum maintenance system. We are also considering mechanically tuned systems, whose design has been developed at CERN.

For a booster with radius of 75 m and cycling rate of 15 Hz, a maximum voltage per turn of 0.85 MV is required. At design intensity, the beam current at 10 BeV is 0.39 A, corresponding to  $3.85 \times 10^{12}$  protons circulating. The voltage program is based on an injected momentum spread  $\Delta p/p$  from the linac of  $\pm 1.1 \times 10^{-3}$ .

The rf system consists of 18 cavities distributed in straight sections around the injector synchrotron ring. The position of a cavity in the lattice is shown in Fig. 9-1.

The rf cavity shown in Fig. 9-6 contains two accelerating gaps connected by a 140-degree drift tube. The cavity is tuned by ferrite-loaded stems over a 1.76 to 1 frequency range.

The mechanical and overall power parameters of the accelerating structure are given in Table 9-6. Figure 9-7 shows individual module power as a function of time during acceleration.

The rf power tube is intimately connected to the cavity electrically, although readily replaceable. All other components of the amplifier chain are housed in the equipment gallery above the enclosure. As in the main-synchrotron rf system, a wide-band feedback loop serves to minimize phase and amplitude fluctuations of the cavity accelerating fields under beam loading.

Parameters of an individual cavity are given in Table 9-7.

---

Table 9-6. Parameters of Injector-Synchrotron Accelerating Structure

---

Total Number of Cavities	18
Cavity Length	2.4 m
Total Length of Accelerating Structure	43 m
Total Peak Power Delivered to Beam	300 kW
Total Peak Ferrite Losses	700 kW
Total Volume of Ferrite	2 m <sup>3</sup>
Total Weight of Ferrite	22,000 lb
Injection Frequency	30.2558 MHz
Ejection Frequency	53.2422 MHz
Harmonic Number h	84 (1120 in Main Ring)

---



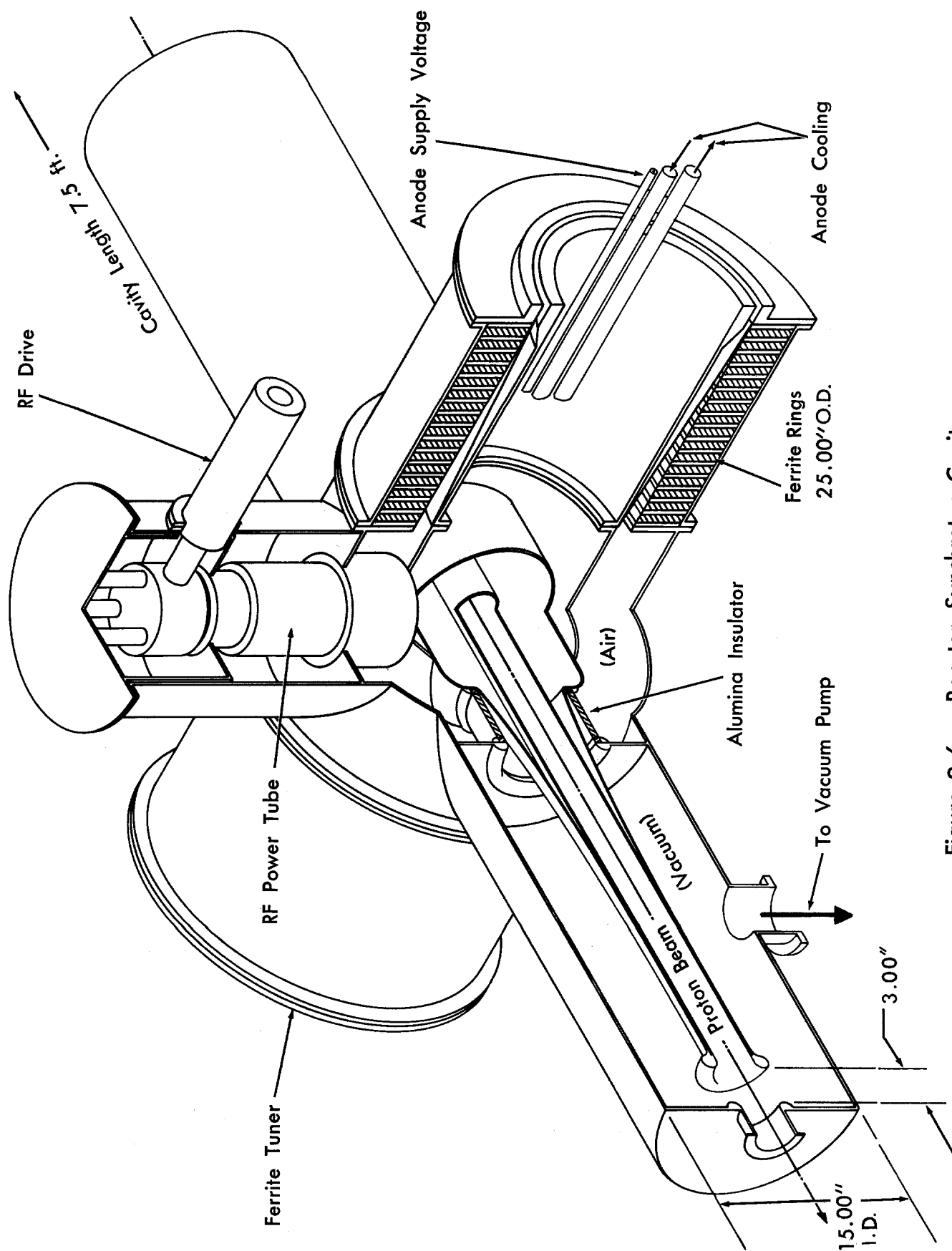


Figure 9-6 — Booster-Synchrotron Cavity

Table 9-7. Individual Injector-Synchrotron Cavity Parameters

Ferrite Tuners - Total for two tuners/cavity	
Ferrite Density	5 gm/cm <sup>3</sup>
Ferrite Weight	1200 lb
Ferrite Volume	110,000 cm <sup>3</sup>
Weight of Copper Cooling Rings	1,250 lb
Resistance of Bias Circuit at 30 cps, 23° C	8 μΩ
Maximum H	30 kA/m
Minimum H	4.5 kA/m
Ferrite μ <sub>Δ</sub> Injection	7.2
Ferrite μ <sub>Δ</sub> Ejection	1.5

RF Parameters

Cavity Peak Voltage (across 2 gaps/cavity)	48 kV
Axial Field Strength in Gap	0.32 MV/m
Cavity RF Current (at current maximum)	1200 A
Cavity Z <sub>0</sub> (tapers from 80 Ω at gap to 20 Ω at center)	60 Ω
H <sub>rf</sub> (at location of ferrite)	780 A/m
RF Stored Energy/Cavity at Maximum Voltage	0.03 J

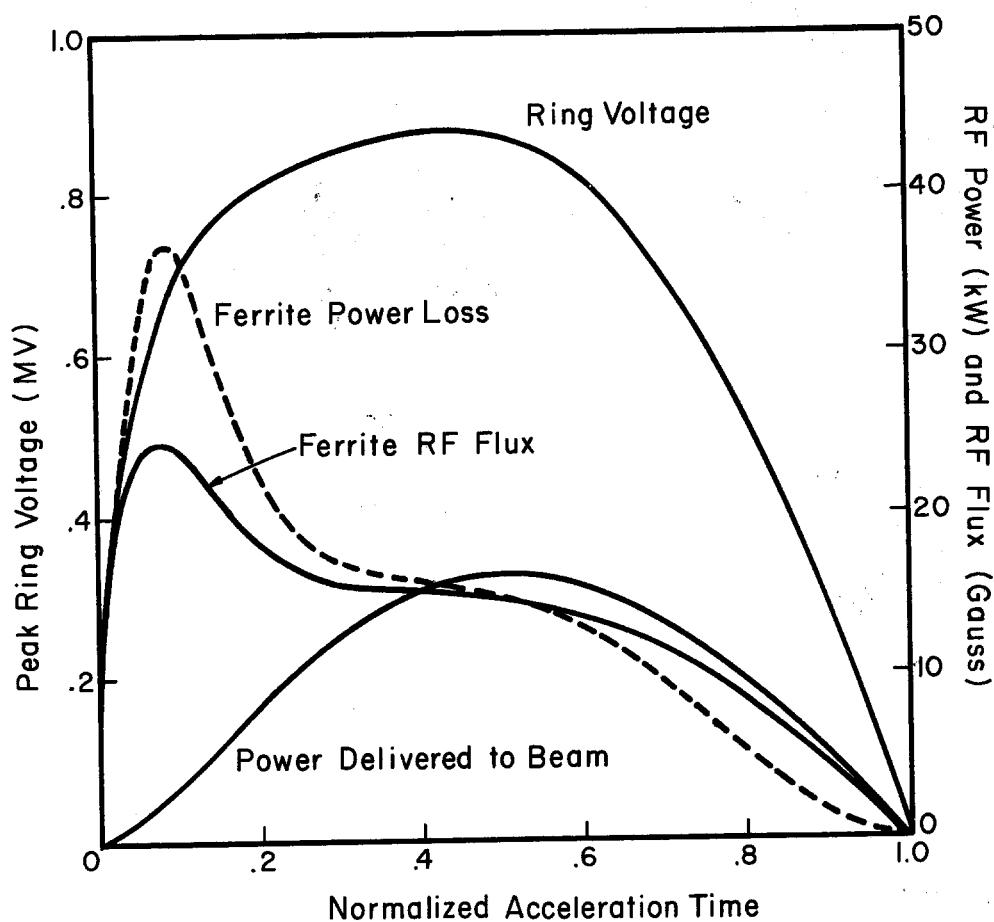


Figure 9-7—Booster-Synchrotron RF Power  
(for one module)

### 3.6 Beam Manipulation and Observation.

Beam Intensity and Position Monitoring. Beam-position sensors will be placed at frequent intervals around the booster lattice. With one sensor in the short (2-meter) straight section, and one in the long (5 meter) straight section, a total of 48 position sensors may be used. This provides for nominally 7 position detectors per betatron wave length, which is considered desirable. The beam-position units will also provide for a signal proportional to the total circulating charge in the booster. For transformer-type sensors, it may be desirable to resonate the coils to the circulating bunch frequency in order to obtain greater sensitivity. Because of the changing bunch separation in the booster, a wide-band coil system might have to be employed, with consequent lower sensitivity. It is intended to monitor all position sensors simultaneously, specifically for injection closed-orbit deviation, both in the vertical and the horizontal directions.

In addition to these units, a standard current transformer will be provided in the ring to measure the total injected charge immediately after and during the injection process, when, in essence, the beam has no time structure. This may be particularly useful in monitoring the injection efficiency and in providing additional calibration for the beam-position sensors.

Closed-Orbit Correction and Adjustment. With the information provided by means of the position sensors, injection closed-orbit corrections can be obtained in a straightforward manner. This is desirable in order to make most efficient use of the booster-synchrotron aperture and specifically in order to avoid the ejection-system aperture restriction. It may also be desirable to use beam scrapers during the injection process, depending on the mode of multiple-turn injection, in order to localize beam losses.

Closed-orbit correction coils will be placed around the booster lattice at the same intervals as the position sensors. Any local orbit deviation may then be corrected, typically with two or three bump coils. Even if nonlocal effects remain, complete correction of the injection equilibrium orbit can be obtained rapidly with a simple iterative process.

In addition to injection, closed-orbit corrections for optimum aperture usage, other adjustments will be necessary at injection due to the multiturn-injection process and to the ejection-component location, and during the beam-ejection process. It may also be desirable to manipulate the beam relative to the beam scrapers shortly before ejection in order to obtain a better defined beam for traversal through the ejection components.

#### 4. Linac To Booster Beam Transfer

4.1 General Description. Between the linear accelerator and booster synchrotron, a beam-transport length of approximately 100 m has been allowed for. A significant part of this length is required as drift space in combination with a beam-debuncher cavity, in order to reduce the beam momentum spread. Beam diagnostic measurements will also be done in this section. This includes momentum and momentum-spread analysis, beam-position and intensity monitoring and transverse phase-space analysis. The general layout is shown in Fig. 9-8, indicating the schematic arrangement of booster and beam-transfer lines.

Beam extraction from the booster takes place by means of vertical extraction. Since it is desirable to leave free access around the outside of the circumference of the booster, the injected beam will also be pitched downward from the linac beam level over the free space of the ring to the point of booster injection. Injection stacking will still, however, be done in horizontal phase space. This technique of vertical injection and horizontal stacking can be most suitably accomplished by means of a magnetic-septum inflector magnet, followed by a horizontally deflecting electrostatic septum device. This system leaves the outside of the ring clear for access.

4.2 Beam-Transport Arrangement. In the approximately 50-meter drift space between linac and debuncher cavity, six quadrupole doublets will be used for beam transport. Following the debuncher cavity, an achromatic transport system<sup>19</sup> will be used to provide a 6-meter parallel translation of the beam in the horizontal plane. This consists of two 12.5-degree bending magnets and five interposed quadrupole magnets. Near the center of the achromatic system, a horizontal beam waist is available so that the momentum spread of the beam can be limited with a defining slit system for booster diagnostic studies.

The horizontal translation system is followed by a sequence of quadrupole magnets, which are used to match the beam in transverse phase space to the acceptance of the booster. Following this, the beam is deflected downward to the level of the booster median plane by a second achromatic beam-transport system. The last magnet of this vertical deflection system will be located in the booster 5-meter injection straight section and will have a thin magnetic septum.

4.3 Beam-Transfer Monitoring. In order to evaluate the performance of the linear accelerator, and to tune the booster, it is essential to monitor beam intensity, position, and transverse and longitudinal beam phase-space properties. The first bending magnet of the horizontal achromatic system can be used as part of a momentum-analyzing system. For this purpose, the magnet-deflection polarity will be reversed, directing the beam into a beam-monitoring channel and beam dump. This monitoring will be done operationally on a continuous basis by using the linac beam pulses while beam acceleration is taking place in the main ring and no beam pulses for similar booster (10 BeV)

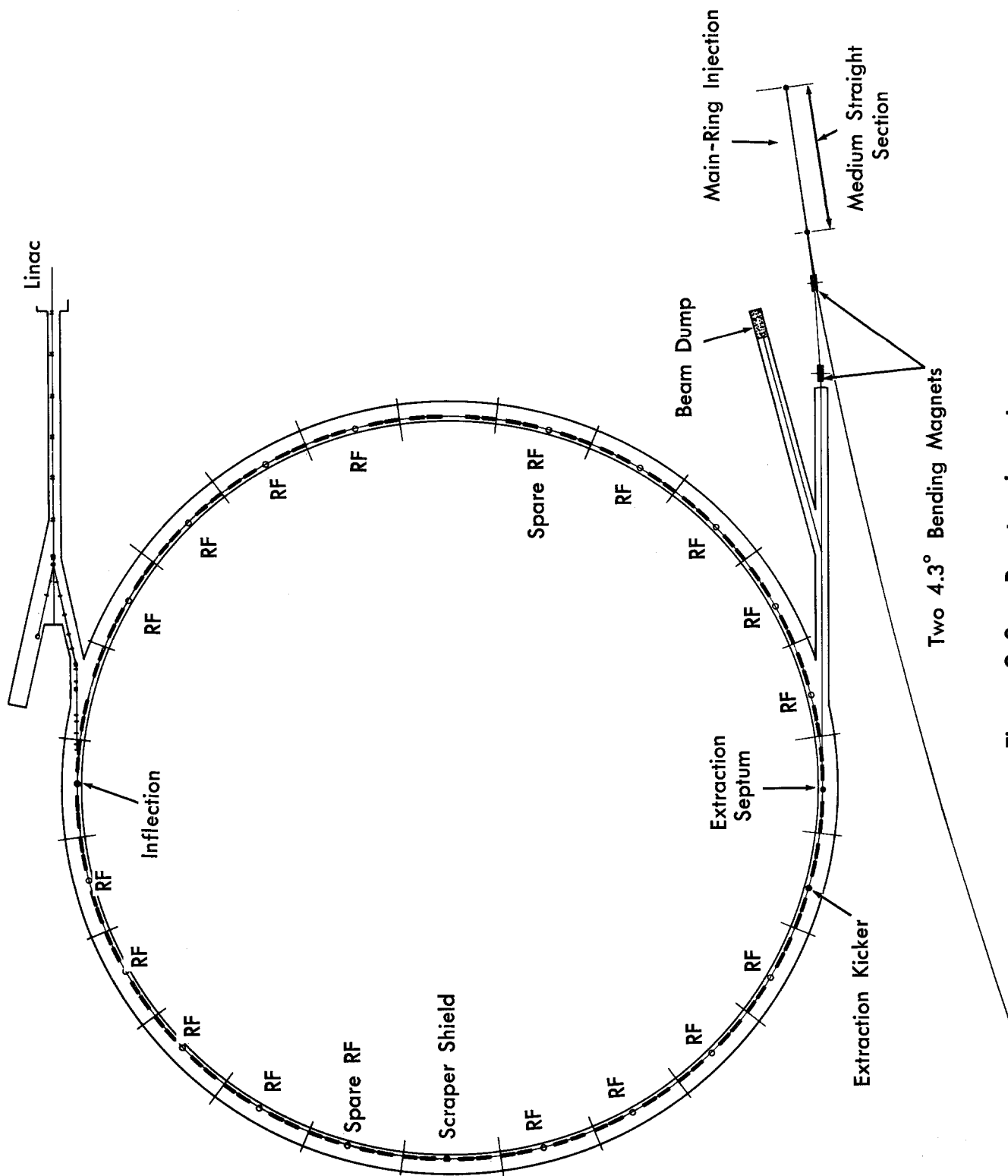


Figure 9-8— Booster Layout

monitoring are required. As a consequence, reversal of the first achromatic bending magnet polarity in a time of approximately 1 second will suffice. In addition, it is desirable, in order to avoid dispersion, to transport the beam in a straight line to a fast transverse phase-space analyzer of the type developed at Brookhaven<sup>20</sup>. It is straightforward to keep the first achromatic deflector magnet at zero current for one or more linac beam pulses during its sequence of polarity reversals.

In the deflected, momentum-analyzing mode, the beam momentum and momentum spread will be measured in a time duration of one beam pulse by means of a multichannel momentum-analyzing system also developed at Brookhaven for the 50 MeV beam-monitoring system.<sup>21</sup>

**4.4 Booster Injection.** Since approximately 225 mA-turns injection into the booster are required to achieve the main-ring design intensity of  $5 \times 10^{13}$  protons per pulse, a nominal 4-turn injection is required with a linac beam intensity of approximately 75 mA. Depending on the exact technique of the injection process, a larger number of turns with less linac beam intensity or vice versa may be desirable in order to achieve optimum booster beam intensity. Stacking will be done in horizontal phase space. The septum of the magnetic septum inflector will be located slightly within the booster injection aperture or immediately adjacent to it, depending on the exact injection technique to be used. In the latter case, the injection equilibrium orbit will be deformed in the injection straight section only during the process of injection. In the first case, a slowly decreasing half betatron-wavelength orbit bump will be used in a way similar to the multiturn-injection technique employed for the Brookhaven AGS. With this system, it would be desirable to maintain a horizontal betatron tune  $\nu_x$  of exactly 6.5 during the injection period. On the other hand, it has been found both computationally and experimentally that horizontal phase space can be filled satisfactorily with  $\nu_x$  values that are not half integral.<sup>22</sup> In this case, a significant fraction of the injected beam is lost during the injection process. This method has, however, the advantage that control of the booster synchrotron and linac injector are less critical.

## **5. Booster to Main-Ring Beam Transfer**

**5.1 General Description.** The beam-transfer system from booster to main ring involves not only the beam transport for physical transfer and matching of the booster ejected beam to the transverse acceptance of the main ring, but also the precise matching of longitudinal phase-space parameters by synchronous transfer of booster bunches into stationary buckets of the main ring. With synchronous transfer, the booster rf structure is preserved and injected with no longitudinal loss into the main ring. Synchronous transfer requires timing and manipulation to make the energy, spacing, and phase of the bunches simultaneously correct before the final process of extraction of the beam from the booster takes place.

The alternative system of debunching the beam in the booster at the time of ejection and then transferring this into the main ring with subsequent rebunching in the main ring is somewhat simpler, particularly in the precise parameters required for synchronization, but the trapping efficiency for this method has been estimated to be at maximum approximately 80%. The method also gives some dilution of longitudinal phase space. As a result, the synchronous transfer system has been adopted. This demands that the final booster frequency be equal to the main-ring frequency at injection.

The beam-transport system between booster and main synchrotron must not only match the booster ejection transverse phase space to the synchrotron transverse phase-space acceptance, but in addition must match the dispersive characteristics of the booster beam to that of the main ring at the point of injection into the main ring.

Vertical ejection will be used from the booster synchrotron. The beam will also be injected vertically into the main synchrotron. This has the advantage of greatly relaxing design requirements for the kicker magnets that are used for both ejection from the booster and injection into the main ring. This makes it possible to locate the booster synchrotron magnet at the inside of the enclosure, leaving the circumferential space outside of the magnets free for access.

In conjunction with the transfer system, a beam branch will be used leading to a beam dump. This branch will be used for beam momentum analysis and will provide facilities for transverse phase-space measurement. It is essential that all relevant parameters of the ejected beam from the booster be analyzed continuously in operation in order to provide the best possible beam for injection into the main synchrotron. It is expected that one or two booster synchrotron beam pulses will be used for this purpose outside the main-synchrotron injection period.

**5.2 Bunch Synchronization.** As protons in the booster approach 10 BeV near the end of each booster acceleration period, there will be a need to shift the phase of the bunches so that each will arrive at the center of an rf bucket when it reaches the main ring. The incoming bunches must have correct phase, as well as correct energy and frequency, in order to avoid beam loss, collective phase oscillations and eventual dilution in longitudinal phase space, and extra aperture requirements in the main ring.

Several workable methods <sup>16,17</sup> of bunch synchronization are under consideration. One method that appears attractive is the "phase-lock" method. The procedure is as follows:

The amount of required phase correction is determined by measurement about 0.5 millisecond before the peak of the booster magnet cycle, when the proton energy reaches 10 BeV and the magnet field is within 0.5% of its peak value. In the phase-lock method, the rf phase and amplitude are switched and held at such values that in one-fourth of a

phase oscillation the energy has deviated enough for a cumulative phase slippage equal to half the desired correction. The rf phase is then switched in an opposite sense and held at this value of phase for another one-fourth of a phase oscillation, during which the energy deviation is removed and the final accumulated phase slippage asymptotically approaches the desired phase correction. With the rf voltage raised to 825 kV per turn during this phase-correction period, the length of time to accomplish the correction is only 0.21 millisecond for the worst case (correction of  $\pm \pi$  radians). Making the correction period equal to half a phase-oscillation period ensures that the match of the bunch to the main ring bucket is not affected by the correction process. The radial excursion of the beam during this synchronizing process does not require additional aperture in the booster.

5.3 Booster Beam Extraction. The beam is ready to be extracted from the booster about 0.5  $\mu$ sec after the peak of the magnet cycle, when the energy goes through 10 BeV. The spacing between bunches also is correct if the beam is maintained on the central orbit in the vacuum chamber.

The method of fast extraction is a proven means of ejecting the 10 BeV beam from the booster with high efficiency and negligible phase space distortion. The main components involved are a kicker magnet and a septum magnet in the extraction straight section. The kicker magnet is switched on in a small fraction of a revolution (possibly in 16 nsec, the time between bunches) and deflects the beam vertically by 0.72 mrad to give an amplitude sufficient to clear the septum of the septum magnet a quarter wavelength downstream. The septum magnet, which is pulsed relatively slowly, deflects the beam another 100 mrad, which is sufficient to let the beam clear the magnet structure in this straight section and enter the transport line to the main ring. The deflection required of the fast kicker magnet is minimized by positioning the beam just prior to extraction as close as possible to the septum magnet by means of slow "bump" magnets. This extraction arrangement is shown in Fig. 9-9.

Use of the vertical plane for extraction, rather than the more customary horizontal direction, results in a much simpler kicker magnet. The amount of deflection is smaller because of the smaller beam size in the vertical direction. The kicker voltage is further reduced because of the smaller area in the kicker current loop, which here is in the vertical plane. These two effects reduce the kicker voltage about one order of magnitude below that for the horizontal case, whereas the kicker current is about the same for the two cases.

A kicker-magnet system with a total rise time (including jitter, switch rise time, and magnet filling times) of 16 nsec would be ideal. This time is sufficient to allow the kicker system to be turned on in the time between bunches, so that no beam need be scraped off in the septum nor sent in undesirable directions. Such a kicker system is



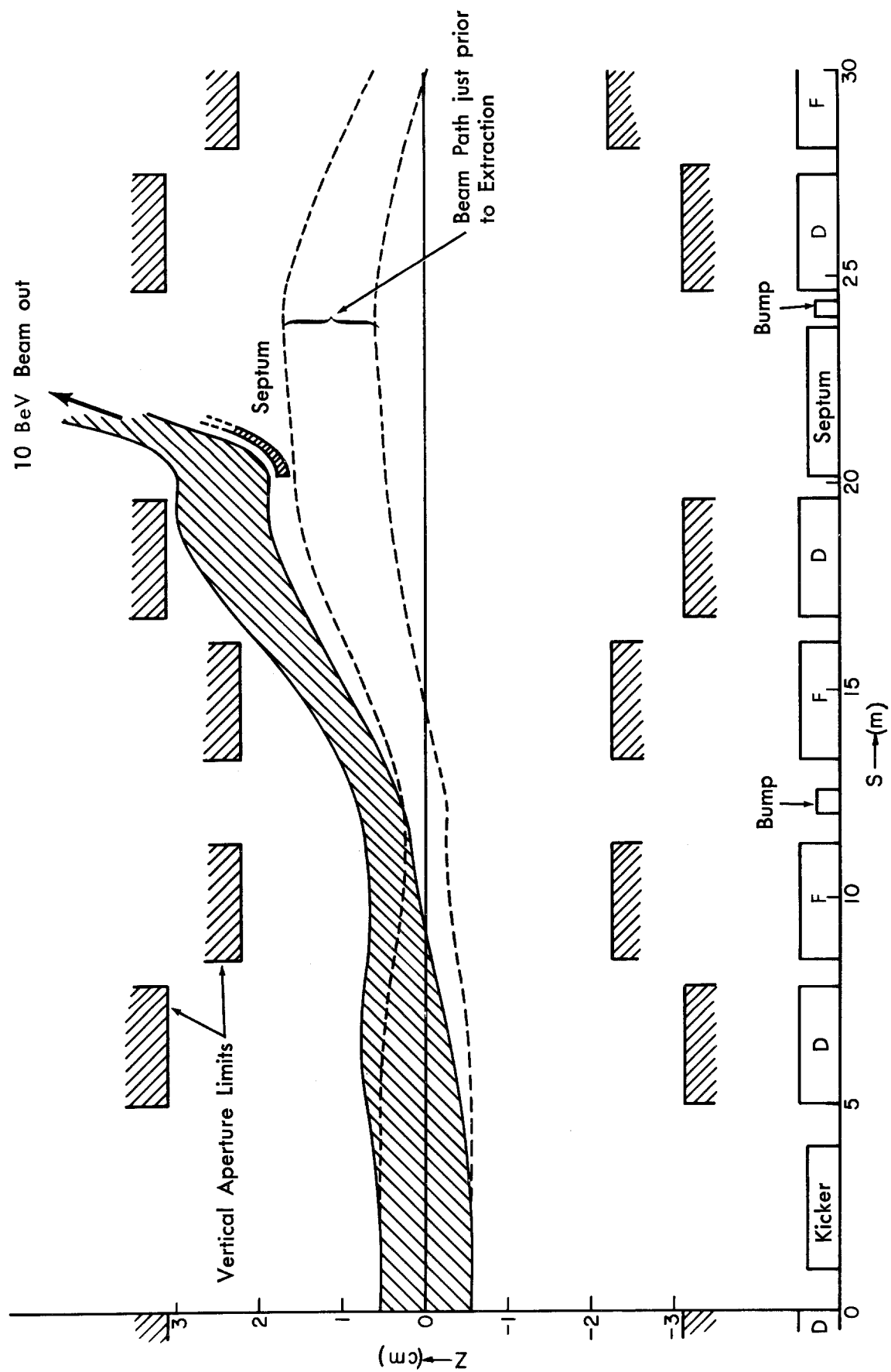


Figure 9-9 — Booster-Synchrotron Ejection

faster than any now in use, but a model has been built with 15-nsec total rise time at LRL. The principal development problem is obtaining adequate life time for the triggered spark gaps. Another possibility is to employ a 50-nsec rise-time system using deuterium thyratron switches, which would result in 2 lost bunches out of a total of 84 bunches. This 2.5% beam loss is not serious with respect to filling the main ring efficiently.

5.4 Beam-Extraction Components. The kicker magnet\* for the injector synchrotron will be made up of individually energized modules operated as push-pull pairs. Each module will be a transmission line short-circuited at one end to form a one-turn current loop. The impedance of the line will be  $90\ \Omega$ ; neither ferrite nor dielectric loading is required to achieve this value. The field distribution is determined by the conductor geometry.

Each module will be driven from an impedance-matched pulse line with triggered fast switches at both ends. The fast switch between the pulse line and the magnet will start the pulse, and hence must provide a low-jitter, short rise-time pulse. The fast switch at the far end of the line is switched on to terminate the pulse after all beam has been extracted and hence does not have to meet tight tolerances. In addition to conventional cables for the pulse lines, there will be two specially constructed pulse lines with a characteristic impedance that decreases going towards the far end of the pulse line in order to compensate for the pulse droop due to cable losses.

As presently conceived, septum extraction-magnet units with increasing septum thicknesses will be used in the extraction straight section in order to provide a beam path that clears the downstream gradient magnet. The total bend angle required is approximately 6 degrees, which could be achieved by three units as given in Table 9-8.

Table 9-8. Extraction Septum-Magnet Parameters

	<u>Unit 1</u>	<u>Unit 2</u>	<u>Unit 3</u>	
Magnetic Field	6.0	18.0	20.0	kG
Length, Effective	90	70	100	cm
Gap	1.5	1.5	2.0	cm
Septum Thickness	0.2	1.0	4.0	cm
Bend Angle	15	35	55	mrad

\* Acknowledgement is made of the contribution of A. Faltens and E. C. Hartwig (both of LRL).

5.5 Beam-Transport Arrangement. As presently conceived, the beam-transport line between the booster and main synchrotron will consist of a short transverse phase-space matching section following immediately after the booster ejection septum magnet, an "infinite" beam-transport system, an achromatic bending system, and, finally, a short matching section just preceding the injection septum magnet of the main ring. The first transport matching section is meant to adapt the beam to the optimum design parameters of the infinite transport section.

The total beam length between booster and synchrotron is approximately 120 m and use of an optimum transport-system design is desirable to reduce cost of the transport system. A simple FODO structure might be used for this particular purpose, and, although the final optimum system has not evolved as yet, the following set of parameters is illustrative: Distance between quadrupole magnets of 20 m; quadrupole-magnet gradient of 100 kG/m; quadrupole-magnet length, 0.5 m; nominal quadrupole-magnet aperture, 6 cm radius; phase advance per period, approximately  $\pi/2$ .

In order to bring the beam exactly over the equilibrium orbit of the main ring, an achromatic bending system involving two 4.3-degree bends is used. In addition, the achromatic system may also be utilized to match the dispersive properties of the ejected beam from the booster to the momentum-compaction function at the injection point into the main ring.

There will be a permanent shield wall between the booster and main ring in order to permit operation of the booster synchrotron during periods of main-accelerator downtime. This will allow booster-synchrotron studies without interference with corrective work or maintenance in the main ring enclosure.

5.6 Booster Beam Monitoring. For purposes of beam momentum and transverse phase-space analyses, the beam will be guided during one or more beam pulse periods through a beam branch leading to a beam analysis channel followed by a beam dump. This will be accomplished by locating a slow bump coil in the transfer line. This coil will provide sufficient kick to clear a thin slow-current-pulse septum magnet located downstream from the bump coil. This arrangement will then sequentially guide the beam into a dc spectrometer magnet. This magnet together with its associated analysing channel will give momentum and momentum spread analysis. In addition, in this branch, transverse phase-space measurements will be done with instrumentation similar to that indicated in the foregoing for the 200 MeV beam. Following this instrumentation, a beam dump is provided to dispose of the beam.

In the transfer line between booster and main ring, beam intensity and position monitors will be provided in addition to possible servo-driven corrective bending elements.

5.7 Injection into the Main Ring. Vertical injection into a medium straight section of the main ring lattice will be used for bringing the beam on to the injection equilibrium orbit. This will be accomplished with fast-kicker and septum magnets.

The medium straight section in the main ring has been arranged to provide for optimum vertical injection. Various injection arrangements were investigated prior to fixing the main-ring lattice. With the present arrangement, optimum vertical injection can be accomplished by locating a sequence of vertical bending septum magnets, similar to those used for ejection from the booster synchrotron, immediately following the bending magnet downstream from the horizontally focusing quadrupole magnet QF. By locating the fast injection kicker unit in the 7-foot straight section downstream from the horizontally defocusing quadrupole magnet QD, a sufficient distance between kicker and septum magnet is obtained for the injection process.

Some local orbit deformation is possible within the limits of the main-ring vertical phase-space acceptance and the booster-synchrotron beam emittance in order to bring the beam closer to the injection septum magnet during injection. Preliminary calculations<sup>10</sup> indicate that a kick of approximately 1 mrad is required for the fast kicker unit. Because of the non-integral ratio of radii of booster synchrotron and the main ring, a few empty buckets will exist between the sequence of "trains of bunches" injected into the main ring. This relaxes greatly the rise-time and fall-time parameters of the kicker unit.

## 6. Booster Synchrotron Services

6.1 Booster Vacuum System. Gas scattering at 200 MeV will be of no concern in the booster with a vacuum pressure in the range of  $10^{-5}$  to  $10^{-6}$  torr, but, because of possible coherent beam-oscillation phenomena, as observed on the CERN PS and Brookhaven AGS, it is desirable to set as a design goal a pressure of approximately  $5 \times 10^{-7}$  torr.

The vacuum system will be subdivided into twelve sectors, each containing two booster lattice cells. It is designed so that a single sector can be evacuated to a pressure of  $10^{-5}$  torr in an elapsed time of 30 minutes. This pressure is probably low enough so that the booster may be operated. The pressure continues to drop such that a pressure of less than  $5 \times 10^{-7}$  torr is reached in 24 hours. This rapid pumpdown time helps minimize lost time due to planned or unplanned vacuum shut-downs.

Vacuum Enclosure. Because of the high cost of increasing the magnet gap, the vacuum-chamber walls must be as thin as practicable. The vacuum chamber must also accommodate the time-varying fields of the gradient magnets without induction of excessive eddy-currents. Fortunately, there are several types of vacuum chambers that meet the foregoing criteria. A recent development has led to the possibility

of constructing a vacuum chamber by coating ( $\approx 0.130$ -in. thick) a thin-wall (0.005 in.) titanium-alloy tube with high-alumina ceramic. This is done by means of a plasma-spray technique.

An alternative vacuum chamber consists of short (18-in.) sections of fired high-alumina ceramic, joined by brazing and welding to form a length long enough for one gradient magnet. Vacuum chambers of this style have been built or studied at LRL<sup>23</sup> and elsewhere. The numerous joints, the brittleness and the minimal capacity for axial tension of this fired-ceramic approach, although acceptable, make it appear less attractive than the sprayed-ceramic approach.

A third alternative is use of the hot isostatic molding technique developed by Battelle Memorial Institute. This technique may permit molding of full-length (4 meters) high-alumina ceramic vacuum chambers as a single piece with close dimensional control. Cost and feasibility are still to be investigated.

Because of the high cost of the ceramic chambers and the necessary associated special techniques, the possibility of utilizing a stressed foil (0.005-in.) skin chamber is of great interest. This can be supported on frequent ribs with elliptical holes, as proposed for the European 300 GeV accelerator<sup>17</sup> or could be made an integral (though removable) part of the magnet structure by mechanical attachment to notches in the sides of the poles of the gradient magnets.

The vacuum tank in the long straight section of each cell will be an integral part of the rf cavity, inflector or other piece of equipment located there. Vacuum joints are located at each end of this tank to permit its removal without disturbing the adjacent gradient magnets.

Vacuum joints between the various sections will be welded joints<sup>24,25</sup>. In addition, quick-disconnect all-metal seal joints as developed at Berkeley and as constructed for the AGS conversion program will be utilized where frequent disassembly is expected.

Vacuum Pumping System. From the point of view of vacuum-system pumping-requirement calculations, the enclosure consists essentially of a vacuum tank about 3 meters long, located in the long straight section of each of the 24 lattice cells, with about 17 meters of a vacuum pipe connection between tanks.

The vacuum pumping system will also be constructed on a modular basis. A single getter-ion pump is attached to the straight section tank of each cell. Another getter-ion pump is located in the short straight section to improve rapid pumpdown. Even in the case of individual pump failure, the desired terminal pressure can be reached comfortably with, however, some sacrifice in pumpdown time.

Getter-ion pumps have been selected for their high reliability, ease of replacement, clean vacuum characteristics and relative invulnerability to radiation damage. Most getter-ion pumps will be rated at 140 liter/second pumping speed, with larger sizes used at locations of high gas loads.

Power supplied for the getter-ion pumps will be located in the equipment gallery outside the booster shielding fill and away from damaging radiation. Holding supplies will be installed for all getter-ion pumps, but starting supplies will be furnished for only three sectors of two cells each, in a manner similar to that planned for the AGS conversion<sup>26</sup>. Thus, only one-quarter of the getter-ion pumps can be started simultaneously, with the remaining quarters started sequentially. The saving in initial equipment cost and peak power demand are justified, since normally only a portion of the accelerator is let up to atmospheric pressure on most occasions. Only infrequently will the whole accelerator need to be pumped down concurrently.

Vacuum roughing equipment will also be located in the equipment gallery.

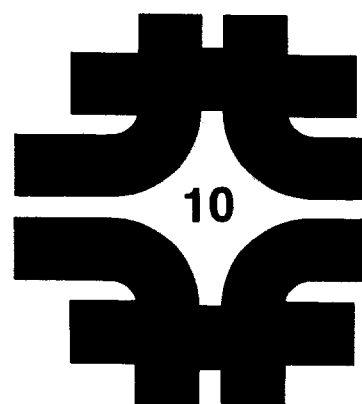
#### References:

1. E. D. Courant, A Separated Function Lattice for the NAL Booster, NAL Note FN-12, July 26, 1967.
2. R. Billinge, A Remodified LRL Booster, NAL Note FN-13, July 28, 1967.
3. L. C. Teng, Small Radius Separate Function Booster, NAL Note FN-20, August 4, 1967.
4. A. van Steenbergen and L. C. Teng, Preliminary Note on a Separate Function Booster, NAL Note FN-21, August 4, 1967.
5. L. C. Teng, Separate Function 10 BeV Booster, NAL Note FN-33, August 15, 1967.
6. Barton, Blewett, Courant, Maschke, Polk, Spiro, and Wheeler, "Design Study for a 1000 MeV Booster Synchrotron Injector for the BNL AGS", Brookhaven National Laboratory Report AADD-127, (1966)
7. G. Danby, F. E. Mills, Unpublished Study, NAL, 1967.
8. S. C. Snowdon, Slow Injection into 1000 m. Radius Accelerator, NAL Note FN-8, July 25, 1967.
9. S. C. Snowdon, Fast-Slow Booster Injection System, NAL Note FN-16, August 2, 1967.
10. A. van Steenbergen, Direct Injection into Main Ring, Vertical vs. Horizontal Injection, and Main Ring Injection, NAL Note FN-54, August 16, 1967.
11. L. Smith, Unpublished Study, NAL, 1967.
12. K. Symon, Unpublished Study, NAL, 1967.

13. Auslender, et al, The Appearance of Nonlinear Betatron Oscillation Resonances in the Storage Ring. Inst. Nucl. Phys., Siberian Div., Acad. Sci. USSR (1966).
14. R. Gram and P. Morton, Advantages of a Set of Second Harmonic rf Cavities, NAL Note FN-108, November, 1967.
15. E. D. Courant, Longitudinal Space-charge forces at Transition - Scaling Relations NAL Note FN-106, November 6, 1967.
16. 200 BeV Accelerator Design Study, Lawrence Radiation Laboratory Report UCRL-16000 (June, 1965).
17. Report on the Design Study of a 300 GeV Proton-Synchrotron, CERN/563 (Nov., 1964).
18. A. Sørenssen, The Triple Switch, MPS/Int., Mu/Ep 66-2 and Mu/Ep 67-2.
19. D. A. Swenson, Rev. Sci. Instr. 35, 608 (1964).
20. Th. J. M. Shuyters, R. Damm, and A. Otis, A. Single Pulse Transverse Phase Space Beam Analyzer, IEEE Trans. Nucl. Sci., NS-14, 1143 (1967).
21. Otis, Larson, Lockey, DeVito, and van Steenberg, AGS Injector Beam Monitoring System, IEEE Trans. Nucl. Sci., NS-14, 1116 (1967).
22. M. Q. Barton, Multiturn Injection into the AGS, Brookhaven Report AADD-57 (1964).
23. P. T. Clee and H. D. Hernandez, A Ceramic Vacuum Chamber for Fast-Cycling Synchrotrons, IEEE Trans. Nucl. Sci., NS-14, 794 (1967).
24. N. Milleron, Some Recent Developments in Vacuum Techniques for Accelerators and Storage Rings, IEEE Trans. Nucl. Sci., NS-14, 794 (1967).
25. J. M. Voss, Automatically and Remotely Welded and Removable Weld Flange Vacuum Joint, IEEE Trans. Nucl. Sci., NS-14, 1004 (1967).
26. T. Carides and J. G. Cottingham, Economical Powering of a Large Multiplicity of Sputter-Ion Pumps, IEEE Trans. Nucl. Sci., NS-14, 863 (1967).

# Linear Accelerator

1. Introduction	10-1
2. Ion Source and Preaccelerator	10-2
3. Beam Transport from Preaccelerator to Linac	10-5
4. Linear Accelerator	10-5
References	10-10





## 10. LINEAR ACCELERATOR

C. D. Curtis, G. M. Lee, P. V. Livdahl, J. E. O'Meara,  
C. W. Owen, M. Palmer, R. Rihel, D. E. Young

### 1. Introduction

A linear accelerator provides protons of 200 MeV energy for injection into the booster synchrotron. A higher injection energy into the booster would improve its magnetic guide field at injection, would reduce the range of frequency over which its rf accelerating system was required to modulate, and would increase the booster's space-charge limit, and therefore its possible intensity. On the other hand, a higher booster injection energy would require a more costly injector. The injection energy of 200 MeV strikes a balance between these competing factors, and provides the desired intensity.

A different kind of accelerator could be utilized for injection into the booster, but it would be difficult for any other type to match the intensity capability of a linear accelerator, which can provide an output current of 100 milliamperes or more in pulse lengths adequate for booster injection.<sup>1</sup> Although no proton linear accelerator of an energy as large as 200 MeV has yet been operated, its principles are well established. A 200 MeV proton linear accelerator is now being constructed as a new injector for the Alternating Gradient Synchrotron at Brookhaven National Laboratory.<sup>2</sup> The design discussed here is purposely quite similar to that of the Brookhaven group. It is expected that this similarity will allow reductions both in design effort and in fabrication schedules. There will, of course, be some differences in the two linear accelerators arising from different design requirements. For example, there will certainly be differences in the accelerator housings, because of differences in topography and layout at the two sites.

The linear accelerator is made up of nine cylindrical cavities, each about 3 feet in diameter and about 50 feet long. A radio-frequency electromagnetic wave is set up in these cavities and its electric fields accelerate the protons. The electromagnetic wave alternates many times during the passage of a proton through one cavity, so that during part of the time the electric field would decelerate the protons. Cylindrical drift tubes are placed along the axis of the cavity to shield protons from these decelerating fields. A proton's speed changes along the accelerator, and each drift tube is therefore made of different length in order that a proton shall pass through it when the electric field is decelerating. There are altogether 286 drift tubes in the 9 tanks

of the 200 MeV linear accelerator. Inside the drift tubes are small quadrupole magnets to focus the beam around the axis during acceleration.

Protons for injection into the linear accelerator are provided by a 750 keV dc Cockcroft-Walton preaccelerator. At this energy, high-voltage supplies are well understood and commercially available. An ion source inside the Cockcroft-Walton accelerator initially produces the protons that are eventually to reach 200 BeV or more.

The linear-accelerator system then consists of the ion source, preaccelerator, linear accelerator, and auxiliary equipment to carry the beam to the booster and to operate the system.

A layout of the system is shown in Fig. 10-1. The linear accelerator is installed in a 14 by 12.5 ft housing with appropriate radiation shielding. RF power and mechanical equipment are in a parallel equipment bay. The emergent beam from the linear accelerator can be bent by a transport system either for injection into the booster or into beam dumps for studies of the performance of the linear accelerator. Drift space is provided to debunch the beam and a debunching cavity will reduce its energy spread.

## 2. Ion Source and Preaccelerator

A proton beam of 75 mA peak current from the linear accelerator allows four turns to be injected into the radial phase space of the booster injector at 70% efficiency to achieve the required  $3.85 \times 10^{12}$  particles per pulse in the booster (to give  $5 \times 10^{13}$  particles per pulse in the main-synchrotron ring when 13 pulses are injected). This linac current requires a total beam of about 220 mA from the preaccelerator, since this beam is not all protons that can be accepted in the linac. This current is within the limits of demonstrated performance with high-quality beams. Preaccelerator tests at Brookhaven indicate that it is possible to obtain a 200 mA current with an emittance of  $4\pi$  mrad-cm.<sup>3</sup> The CERN PS operates with a 540 keV beam of approximately 500 mA within an emittance of  $15\pi$  mrad-cm.<sup>4</sup> For somewhat lower beam currents, emittances less than  $1\pi$  mrad-cm have been achieved at these laboratories and in preliminary work at Saclay,<sup>5</sup> MURA-ANL,<sup>6</sup> and Rutherford.<sup>7</sup>

Although the design intensity can be achieved with a linac beam current of 75 mA, it is felt that the linac design should allow at least 100 mA to be accelerated with similar beam emittance. It is felt quite likely that advances in source technology will allow beams of higher brightness. Under these conditions, injection into the booster should be simplified, with some possible increase in intensity; space-charge limits at injection into the booster prevent larger intensity gains.

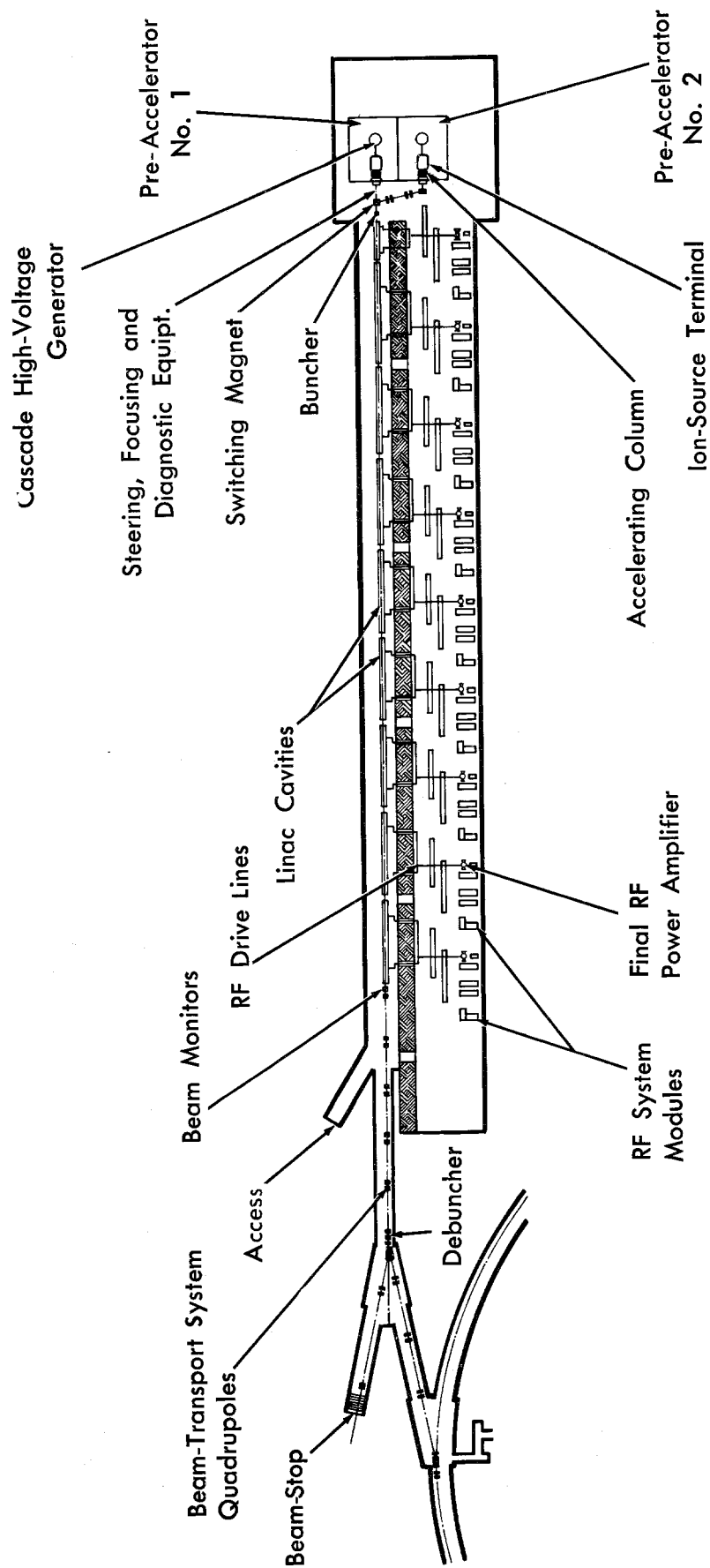


Figure 10-1 — Plan View of Linac

A preaccelerator emittance of  $5\pi$  mrad-cm will transform to a linac output emittance of about  $0.5\pi$  mrad-cm, with a factor 2 dilution in the linac. Four or more turns of the linac beam can then easily be accommodated in the  $5\pi$  mrad-cm radical acceptance of the booster. With four turns, a linac pulse length of about 12  $\mu$ sec. is required. For smaller emittances, it may be possible to inject a larger number of turns, so that it is useful to provide for longer pulse lengths in the linac and preaccelerator.

Recent development work on modified versions of the duoplasmatron source with plasma-expansion cups have resulted in high-current beams of high brightness. When particular care is given to the design of the cup and the extraction region of the source, as well as to the matching of the source to the high-gradient accelerating column, distortion in the transverse phase space occupied by the beam can be kept very small. A high-gradient accelerating column with a mean accelerating gradient of about 43 kV/cm has been used in operation at CERN.<sup>4,8</sup> High-gradient columns accelerate the beam quickly, reducing the effects of space-charge forces in the beam. It is proposed to develop and use a source-column system with fields up to 30 kV/cm in the accelerating column.

An ion-source dome containing source circuitry at high voltage will be air insulated to provide rapid access to the source for maintenance. Dimensions of the dome are 6 ft by 8 ft by 8.5 ft high. A 60-Hz, 15-kW generator for electric power in the dome will be driven from ground by an insulating shaft.

The dc high-voltage supply will have a rating of 850 kV at 12 mA with a nominal operating voltage of 750 kV at  $\pm 0.05\%$  stability including ripple. The high-voltage generator will be a 10-kHz-driven symmetrical voltage-multiplying circuit of the Greinacher-cascade type, with pulsed-load rating of 500 mA for 100  $\mu$ sec or a charge drain per pulse of  $5 \times 10^{-5}$  Coulomb.

In addition to the slow voltage-regulation system, a fast regulator is required during the pulse. This "bouncer" will correct for voltage droop along the accelerator column during the beam pulse.

A high-voltage protective resistor connected between the rectifier and the ion-source terminal will limit power dissipation in the accelerating column during arc-down and will aid in column conditioning and voltage holding.

Space will be provided in the preaccelerator building for two preaccelerators. One preaccelerator will be directly in line with the axis of the linac and will be considered the primary unit; the other unit will be offset so that its beam passes through a beam translation system into the linac. The short transport system of the primary unit will be designed to handle the high intensity-low energy beams without loss of beam quality. The second unit is provided for standby service and can also be used for preaccelerator development work.

Performance parameters of the preinjector are summarized in Table 10-1.

Table 10-1. Nominal Preaccelerator Performance Parameters

Voltage	750 kV
Voltage Stability	$\pm 0.05\%$
Ion-Beam Current	220-300 mA
Beam-Pulse Length	30-100 $\mu$ sec
Pulse-Repetition Rate	15 per sec
Beam Emittance (90% of Total Beam)	$5 \pi$ mrad-cm

### 3. Beam Transport from Preaccelerator to Linac

A transport distance is required for matching preaccelerator-beam emittance to linac acceptance, for beam observational equipment, and for prebunching. Quadrupole-focusing magnets will be used for matching to the linac and for focusing the beam. Beam steering will be accomplished by deflecting magnets. Beam-defining slits will stop particles that otherwise possibly would be lost in the linac. Viewing boxes built around the slits will contain beam-observation devices.

The prebunching will be accomplished by a single conventional cavity operating at the linac frequency (200 MHz). It will improve beam-capture efficiency by a factor 2 to 3 over the 20 to 25% dictated by phase acceptance of the linac. For a drift space of 1.5 m, a peak voltage on the buncher cavity of approximately 17 k V is required. The decision on using a second harmonic in addition to the fundamental buncher cavity, to approximate more nearly the ideal sawtooth-voltage waveform, will await further study.

### 4. Linear Accelerator

Performance parameters of the linear accelerator are given in Table 10-2 and a cavity-by-cavity description of the linac is given in Table 10-3 (as specified for the 200 MeV linac at Brookhaven). The drift-tube parameters appearing in Table 10-3 are defined in Fig. 10-2.

Table 10-2. Nominal Linear-Accelerator Performance Parameters

Output Energy	200.30 MeV
Output Energy Spread, Before Debuncher	$\pm 1$ MeV
Output Energy Spread, After Debuncher	$\pm 400$ keV
Peak Beam Current	75 mA
Beam Pulse Length	100 $\mu$ sec
Pulse Repetition Rate	15 pulses per sec
Emittance at 200 MeV (Each Transverse Mode)	$0.5 \pi$ to $1.0 \pi$ mrad-cm
RF Frequency	201.25 MHz
RF Pulse Length	300 $\mu$ sec
RF Duty Factor	0.5%
Peak RF Excitation Power	22 MW
Average RF Excitation Power	110 kW
Total Peak RF Power at 75 mA	37 MW
Number of Accelerating Cavities	9
Number of Drift Tubes	286
Total Length (including drift spaces between cavities)	145.8 m (478.3 ft)

Each of nine accelerating cavities is about 50 feet long, with the exception of the first. It is only about 20 feet long to allow greater design flexibility in this section of the linac. The lengths of the rest of the cavities are chosen to match the power capabilities of available 200 MHz power amplifiers. When beam loading is included, approximately 5 MW of 200 MHz power will be dissipated in each cavity. It is planned that this power will be furnished by an RCA 7835 super-power triode, whose performance and reliability has been proven on the 50 MeV linac injector for the Zero Gradient Synchrotron at Argonne National Laboratory<sup>9</sup> and in tests elsewhere. At the present time, this tube appears to be the best choice for this application.

The cavity and drift-tube dimensions have been chosen from the shapes extensively calculated in the MURA field-computational program, MESSYMESH,<sup>10</sup> and the cell-to-cell dimensions have been generated from the parameters supplied by that program. It has been shown<sup>11</sup> that the cylindrical drift tubes calculated in the MESSYMESH program, whose parameters are defined in Fig. 10-2, give values of shunt impedance nearly as great as other drift-tube shapes and are simpler to construct. The rounded faces of the drift tubes allow higher accelerating fields to be achieved without excessively high surface fields.

The linac geometry and accelerating fields can be chosen to strike a balance between length costs, including buildings, and the power costs.<sup>12</sup> The same output energy can be achieved by increasing the length of the structure and reducing the accelerating field and power, but with an increased cost arising from the added length of the structure. To reduce cost by increasing the accelerating field is not always possible because of sparking problems and consequent unreliable operation when the fields exceed some safe level. Fortunately, the cost optimum is a slowly varying function of geometry and field, so that small departures are not costly. In this design, departures from the optimum

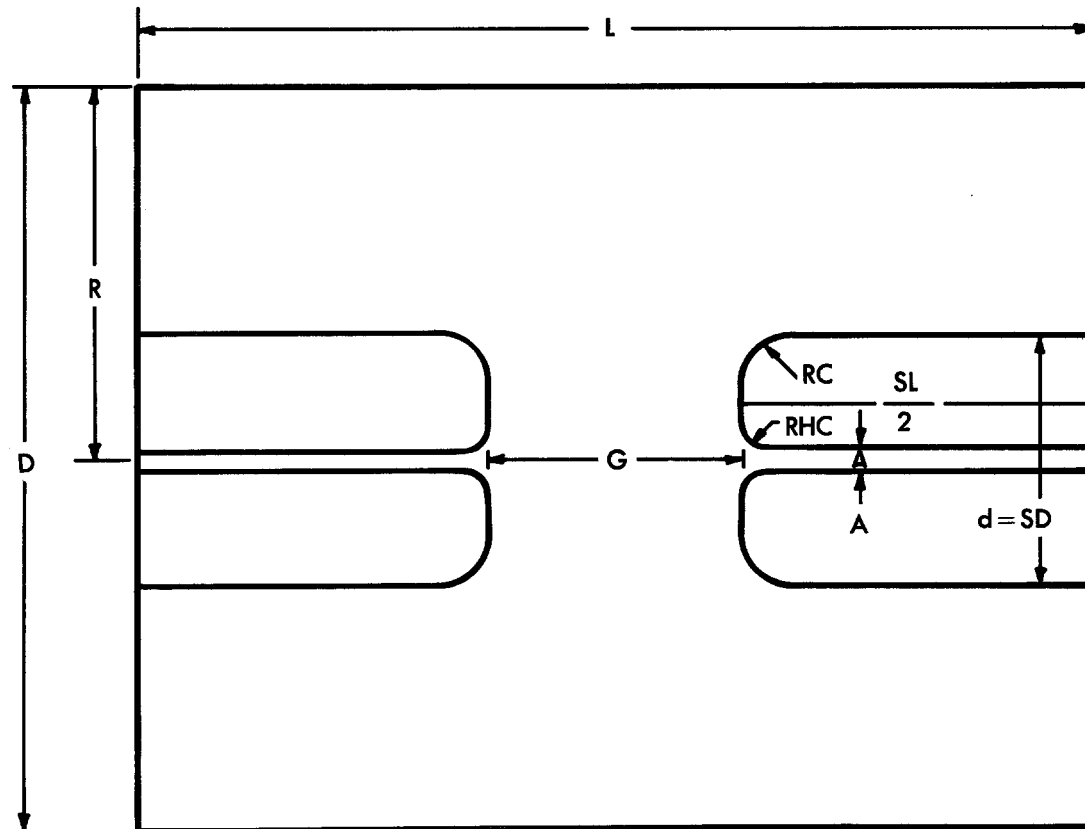


Figure 10-2 — Linac Unit-Cell Geometry

have been chosen to allow more reliable operation, greater uniformity of cavity and drift-tube shapes to simplify fabrication, and to give convenience in assembly.

The peak surface fields at the beginning and end of each cavity as obtained from the MESSYMESH program are listed in Table 10-3 for the average accelerating field chosen. The fields have been reduced at the beginning of the early cavities, where sparking has been observed on existing linacs.<sup>13</sup> Surface fields less than 15 MV/m should present no particular sparking problems, especially with ion-pumped vacuum systems and after proper rf conditioning of the surfaces.

The cavity excitation power has been calculated from the shunt impedance calculated in the MESSYMESH program increased by a factor ( $x$  in Table 10-3). This factor takes into account practical losses not included in the program, such as losses on loops, drift-tube stems and supports, tuners, rf contacts, and so forth.

Quadrupole focusing magnets are placed in each drift tube. They are pulsed in order to economize on power and cooling. To accommodate the large beam currents in this design, the first drift tube is designed with a 2.0-cm bore hole and a quadrupole strength of 10 kG/cm or greater. These fields have been achieved at Brookhaven<sup>14</sup> in model studies of the quadrupole in the most restricted space of

Table 10-3. Linear-Accelerator Specifications

Cavity Number	1	2	3	4	5	6	7	8	9
Proton Energy In (MeV)	0.75	10.42	37.54	66.18	92.55	116.54	138.98	160.53	181.01
Proton Energy Out (MeV)	10.42	37.54	66.18	92.55	116.54	138.98	160.53	181.01	200.30
Relative Proton Velocity In ( $\beta_{in}$ )	0.04	0.148	0.275	0.357	0.414	0.457	0.491	0.520	0.545
Relative Proton Velocity Out ( $\beta_{out}$ )	0.148	0.275	0.357	0.414	0.457	0.491	0.520	0.545	0.566
Energy Gain Per Cavity (MeV)	9.67	27.12	28.64	26.37	23.99	22.44	21.55	20.48	19.29
Cavity Length (m)	7.44	19.02	16.53	16.68	15.58	15.54	15.83	15.88	15.73
Cavity Diameter (cm), D	94	90	88	88	84	84	84	84	84
Drift-Tube Diameter (cm), d	18	16	16	16	16	16	16	16	16
Bore-Hole Diameter (cm), A	2.0 - 2.5	3.0	3.0	3.0	4.0	4.0	4.0	4.0	4.0
Drift-Tube Corner Radius (cm), RC	2.0	4.0	4.0	4.0	5.0	5.0	5.0	5.0	5.0
Bore-Hole Corner Radius (cm), RHC	0.5	1.0	1.0	1.0	1.0	1.0	1.0	1.0	1.0
Cell Length, L, (cm)	6.04 - 21.8	32.2 - 40.8	41.1 - 53.0	53.3 - 61.5	61.8 - 67.9	68.2 - 73.1	73.3 - 77.4	77.6 - 81.1	81.3 - 84.3
Gap Length, G, (cm)	1.3 - 6.7	4.4 - 12.7	12.2 - 19.3	19.5 - 25.1	22.6 - 26.9	27.1 - 30.8	30.9 - 34.2	34.3 - 37.1	37.3 - 39.7
G/L	0.21 - 0.31	0.20 - 0.31	0.30 - 0.36	0.37 - 0.41	0.37 - 0.40	0.40 - 0.42	0.42 - 0.44	0.44 - 0.46	0.46 - 0.47
Axial Transit-Time Factor	0.64 - 0.81	0.86 - 0.81	0.82 - 0.75	0.75 - 0.69	0.73 - 0.69	0.68 - 0.65	0.64 - 0.61	0.61 - 0.58	0.58 - 0.55
Effective Shunt Impedance (M $\Omega$ /m)	27.0 - 47.97	53.5 - 44.8	44.6 - 35.2	35.0 - 28.5	29.6 - 25.0	24.8 - 21.7	21.5 - 19.0	18.9 - 16.8	16.7 - 14.9
Drift Space Following Cavity (m)	0.22	0.6	0.75	1.0	1.0	1.0	1.0	1.0	---
Accumulated Length (m)	7.66	27.28	44.56	62.24	78.82	98.36	112.19	129.07	144.80
Number of Unit Cells	56	60	35	29	24	22	21	20	19
Number of Full Drift Tubes	55	59	34	28	23	21	20	19	18
Average Axial Field E <sub>0</sub> (MV/m)	1.60 - 2.31	2.0	2.60	2.60	2.56	2.56	2.56	2.56	2.56
Average Gap Field E <sub>g</sub> (MV/m)	7.62 - 7.45	10.0 - 6.45	8.7 - 7.2	7.03 - 6.3	6.9 - 6.4	6.4 - 6.1	6.1 - 5.8	5.8 - 5.6	5.6 - 5.4
Peak Surface Field E <sub>max</sub> (MV/m)	8.9 - 10.2	12.6 - 9.7	13.1 - 12.9	12.9 - 13.2	14.0 - 14.1	14.1 - 14.2	14.2 - 14.3	14.3 - 14.5	14.5 - 14.8
Cavity Excitation Power (MW)	0.51	1.40	2.36	2.57	2.75	2.91	3.13	3.19	3.24
Factor $\kappa^*$	1.30	1.30	1.35	1.40	1.45	1.50	1.55	1.55	1.55
Total Power Per Cavity for 75 mA (MW)	1.24	3.44	4.51	4.55	4.55	4.59	4.75	4.73	4.68

\* Cavity excitation power calculated as factor  $\kappa$  times theoretical power (to account for losses on stems, supports, contacts, increased surface losses, etc.)

Synchronous phase angle,  $\phi_s = -32^\circ$

Total Number of Unit Cells -- 286  
 Total Number of Full Drift Tubes -- 277  
 Total Cavity Excitation Power -- 22.1 MW  
 Total Linac RF Power for 75 mA -- 37 MW



the first full drift tube in the linac, using pulsed quadrupoles. Special problems arise in the early part of the linac in preserving the beam emittance from the preaccelerator. Work now in progress at Brookhaven<sup>15</sup> and CERN<sup>16</sup> is expected to improve this situation, so that output emittances from the linac of  $0.5\pi\text{mrad-cm}$  can be expected, which would improve the filling efficiency in the booster.

Conventional proton linacs operate in a mode similar to the  $\text{TM}_{010}$  mode in an empty cylindrical cavity; i. e., the direction of the electric field is primarily along the axis of the cavity being most intense near the axis and the magnetic fields have only an azimuthal component. In this mode the accelerating fields have a zero (or  $2\pi$ ) phase shift from accelerating cell to accelerating cell. It has been recognized that the field distribution of this particular cavity mode, although it has the desired field distribution for particle acceleration, is very susceptible to perturbations such as mechanical detuning and beam loading. This is primarily due to the poor energy-propagation characteristics of this mode. Work is in progress at Brookhaven,<sup>17</sup> Los Alamos<sup>18</sup> and CERN<sup>19</sup> to develop alternative structures or cell-to-cell coupling schemes that would reduce these difficulties. A multistem system has been developed at Brookhaven in which several additional stems of varying diameter are added to each drift tube. At Los Alamos, it is intended to use a single post at each drift tube position that is capacitatively coupled to the drift-tube and thereby tuneable by changing the capacity (called a post coupler). The basic linac specifications given in Table 10-3 are not greatly modified by either of these schemes; the power requirements in this table have been calculated on the basis of the multistem structure, in which the power losses on the additional stems are greater. We are in the process of studying both systems. The first cavity will be constructed using a conventional structure, because its reduced length tends to reduce these problems, and because the extreme change in cell length from beginning to end in the cavity make the tuning of these stabilization schemes specially difficult.

The cavities will be fabricated from copper-clad steel, 0.15-in copper on 0.75-in steel, to provide a stable high-Q cavity in which extraneous frequency shifts can be minimized and controlled.<sup>20</sup> The structure is mechanically rigid, so that the drift tubes, which are supported from the tank walls, will not be misaligned when the cavities are evacuated. Piston tuners are provided along the wall of the cavity to maintain the design frequency and to compensate for local variations of frequency. The cavities will be closely temperature-controlled by cooling channels welded longitudinally on the tank walls. The cavities will be initially evacuated by a mechanical roughing system and brought to an operating pressure of  $10^{-6}$  to  $10^{-7}$  torr by ion pumps.

The drift tubes are supported from a single stem, which carries the power for the enclosed quadrupole and cooling required to remove the heat generated by the quadrupole and the rf losses. Alignment is accomplished by an adjustment mechanism that positions the magnetic center of the quadrupole to the beam centerline. The drift tube is clamped in position after alignment. A back-up vacuum system is provided should a leak develop in the drift tube or support bellows.

Beam-diagnostic equipment will be installed ahead of the linac and between linac cavities, so that operation can be continuously monitored and controlled to preserve beam quality. It is expected that a debuncher cavity will be used to reduce the momentum spread from the linac. An access entry will be provided at the end of the linac. This access could serve later as an extra beam dump. A beam dump following the debuncher has been provided to allow the momentum spread of the beam to be measured conveniently during accelerator operation.

The linac cavities will be installed in a rectangular housing approximately 14 ft wide by 12.5 ft high, with working space on both sides of the cavities, as shown in Fig. 10-1. A 2-ton crane is provided to lift equipment over the linac. A single-story equipment bay parallels the linac housing. The equipment is in modular form. These modules can be removed with a 10-ton overhead crane to the service area provided on either end of the bay. Earth cover on the housing will provide radiation shielding when the linac is operated at full intensity, although several lateral openings are provided from the equipment bay to allow easy personnel entry during initial installation.

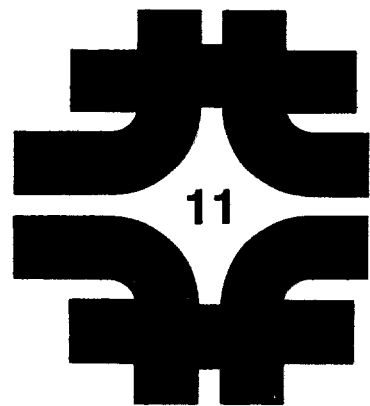
#### References:

1. M. Q. Barton, J. P. Blewett, E. D. Courant, A. W. Maschke, I. Polk, J. Spiro and G. W. Wheeler, "Design Study for a 1000-MeV Booster Synchrotron Injector for the Brookhaven AGS" BNL Internal Report AADD-127 (1966); S. C. Snowdon, E. A. Crosbie, "Study of High Intensity Injectors for the ZGS" ANL-MURA Internal Report, MHESG 12.6.1 (1966)
2. Staff, AGS Conversion Division, Brookhaven Accelerator Department, "Alternating - Gradient Synchrotron Conversion Program" BNL-9500 (1965); G. W. Wheeler, "Progress Report on the AGS Conversion Project" Proceedings of the VI International Conference on High-Energy Accelerators, Cambridge, Massachusetts (1967) (to be published)
3. Th. J. M. Sluyters and V. J. Kovarik, "Large Brightness Beams Up To 200 MA In A 750 kV High Gradient Preinjector" AGS DIV 67-6 (1967) Internal Report; T.J.M. Sluyters, V. Kovarik, R. Amari, S. Senator, "Development of a 750 keV High Gradient Preinjector" Proceedings of the VI International Conference on High Energy Accelerators, Cambridge, Massachusetts (1967) (to be published)
4. B. Vosicki, M. Buzic and A. Cheretakis, "The Duoplasmatron Source For The CERN-PS Linac" Proceedings of the 1966 Linear Accelerator Conference held at Los Alamos, LA-3609, Pg. 344 (1966)
5. P. Bernard, J. Faure and R. Vienet, "A 100 mA Ion Beam With a Large Brightness" IBID, Pg. 395 (1966)
6. J. A. Fasolo, C. D. Curtis, and G. M. Lee, "Duoplasmatron Source Performanc at MURA" ibid, Pg. 371 (1966); C. D. Curtis, G. M. Lee, and J. A. Fasolo, "Initial Test of the MURA High GradientColumn" ibid, Pg. 365 (1966)

7. H. Wroe, "A Note on Some Emittance Measurements" *ibid*, Pg. 394 (1966); H. Wroe, "Some Emittance Measurements With a Duoplasmatron Ion Source" *Nuclear Inst. and Methods* 52, 67-76 (1967)
8. J. Huguenin, R. Dubois, G. Visconti, R. El-Bez, "The New 500 keV Single-Gap Pre-Injector Tube for The CERN Proton Synchrotron Linac" LA-3609, Pg. 355 (1966)
9. J. Abraham, R. W. Castor, P. V. Livdahl, W. Meyers, R. Perry, "Operational Experience With The ZGS Injector". *Proceedings of the International Conference on High Energy Accelerators*, Dubna, U.S.S.R., U.S.A.E.C. CONF-114, Pg. 640, (1963)
10. T. W. Edwards, "Proton Linear Accelerator Cavity Calculations" MURA Report No. 622 (1961) (unpublished)
11. D. E. Young, R. S. Christian, T. W. Edwards, F. E. Mills, D. A. Swenson, and J. van Bladel, "Design of Proton Linear Accelerators For Energies Up To 300 MeV" *Proceedings International Conference on Sector-Focused Cyclotrons and Meson Factories*, CERN 1963, CERN 63-19, Pg. 372 (1963)
12. B. Austin, T. W. Edwards, J. E. O'Meara, M. L. Palmer, D. A. Swenson, and D. E. Young, "The Design of Proton Linear Accelerators For Energies Up To 200 MeV" MURA Report No. 713 (1965)
13. D. A. Swenson, *Informal Discussion of Sparking Phenomena*, 1964 Linear Accelerator Conference, MURA-714 (1964)
14. A. N. Otis and R. Damm, "Drift Tube Quadrupoles" *IEEE Transactions on Nuclear Science*, NS-14, No. 3, 420, (1967)
15. R. Chasman, "Numerical Calculations of Coupling Effects in a Low Energy Proton Linac" *Proceedings of the 1966 Linear Accelerator Conference held at Los Alamos*, LA-3609, Pg. 224 (1966); also R. Chasman, (Private Communication)
16. C. S. Taylor, D. J. Warner, F. Block and P. Tetu, "Progress Report on the CERN-P S Linac", *Proceedings of the 1966 Linear Accelerator Conference held at Los Alamos*, LA-3609, Pg. 48 (1966)
17. S. Giordano and J. P. Hannwacker, "Measurement on a Multistem Drift Tube Structure", *ibid*, Pg. 88
18. D. A. Swenson, E. A. Knapp, J. M. Potter, E. J. Schneider "Stabilization of the Drift Tube Linac by Operation in the  $\pi/2$  Cavity Mode", *Proceedings of the VI International Conference on High-Energy Accelerators*, Cambridge, Massachusetts (1967) (to be published)
19. G. Dome and J. White, "A General Theory of Multistem Drift Tube Structures Proposed for Proton Linacs", *ibid*.
20. P. Grand, "The Physical Design of a 200-MeV Linac Facility" *IEEE Transactions on Nuclear Science*, NS-14, No. 3, 860 (1967)

# Monitoring and Control System

1. Introduction	11-1
2. Control Computer	11-3
3. Data-Transmission System	11-5
4. Data Collection Stations	11-7
5. General Communications System	11-7
References	11-7



## 11. MONITORING AND CONTROL SYSTEM

L. C. L. Yuan (BNL)

R. Littauer (Cornell U.), K. B. Mallory (SLAC), M. W. Sands (SLAC)

### 1. Introduction

The function of a monitoring system is to provide information on the operating status of components of the accelerator and to indicate any malfunctions. A control system provides means to command operations and to transmit information and commands to components, in part on the basis of the status information supplied by the monitoring system. Since both systems involve communication to all parts of the accelerator, they are naturally combined into a single system.

Information obtained by the monitoring system can be classified into three categories: (1) status information tells whether a component is on or off or whether a circuit is open or closed; (2) analog information consists of signals proportional to measured quantities; and (3) video information provides monitoring of areas or actions by means of closed-circuit television. Control commands can be similarly classified into: (1) on-off command, which instructs a circuit to open or close, and (2) analog command, which sets an operating parameter to a predetermined value or function.

In addition, the monitoring system and the control system may be coupled together to form feed-back servo-loops that will then operate as an automatic control system.

A high-energy particle accelerator is a very complex system with a large number of monitor and control functions. As the design energies of accelerators have increased over the years, the distances between components, the complexity of components and systems, and the precision required in adjustment have all increased. The control and monitoring systems of the National Accelerator Laboratory must provide for operation of each of the four accelerators and must phase their operation so that proton beams can be successfully transferred from one accelerator to the next without appreciable loss. In addition, greater flexibility is required in the distribution of beams to experiment areas than was provided in the design of previous accelerators.

The size and complexity of the system can be appreciated from the data-transmission distances and the approximate number of control and monitoring functions listed in Table 11-1.

Table 11-1. Average Data-Transmission Distances and  
Number of Control Functions

	<u>Main Accelerator</u>	<u>Booster</u>	<u>Linac and Preaccelerator*</u>
<u>Average Distance (Feet)</u>	<u>6,000</u>	<u>1,200</u>	<u>600</u>
Number of Status Points	4,700	800	70
Number of Analog Monitoring Points	5,600	1,000	170
Number of Video Monitoring Points	1,200	20	50
Number of On-Off Controls	700	200	100
Number of Analog Controls	<u>500</u>	<u>100</u>	<u>170</u>
Total Signals	12,700	2,120	560

\*These numbers do not include approximately 1,000 analog and status points taken from the linac to its local control station.

The specification established for the design of the control and monitoring system for the NAL accelerator can be summarized as:

- (i) There should be one central control system such that the entire accelerator is operated by a single operating crew from a single location.
- (ii) Capability for future conversion to computer control of all routine operations should be provided. All equipment should be compatible with such a converted system.
- (iii) The system should provide the operator status information on all essential components of the accelerator at all times during operation. Some of the essential information will be displayed automatically at all times in the control room, whereas the rest of the information will be stored and can be displayed on demand by the operator.
- (iv) Alarm signals should be provided to warn the operator of malfunctions of components together with information giving their locations.
- (v) The system should provide safeguards to protect inter-related components from damage if one of the components should fail.
- (vi) The system should provide means for the operator to optimize performance of the accelerator.
- (vii) The system should be capable of executing preplanned beam program for maximum utilization of the experimental beams with reliable and consistent performance.

- (viii) The system should provide communication of appropriate data between the main control center and the various remote locations.
- (ix) The system should be able to organize and record operating data for maintenance records, for future reference and for improvements in performance.
- (x) The system should provide for autonomous operation of all equipment independent of the central control system of the accelerator. This assures continued operation while maintenance or repair of the central system is in progress, and allows testing and trouble-shooting of individual components without affecting the rest of the accelerator.

In the control and monitoring concept envisaged, most of the functions outlined above will be carried out by a control computer located in the control center in the central laboratory. Monitoring data will be collected at a number of stations around the accelerator and transmitted to the control center. Most of the transmission will be by time-shared multiplex systems, similar in design to those developed by Littauer<sup>1,2</sup> for the Cornell 10BeV electron synchrotron. The three major parts of the control system namely the control computer, the data-transmission system, and the data-collection stations, are described in more detail below.

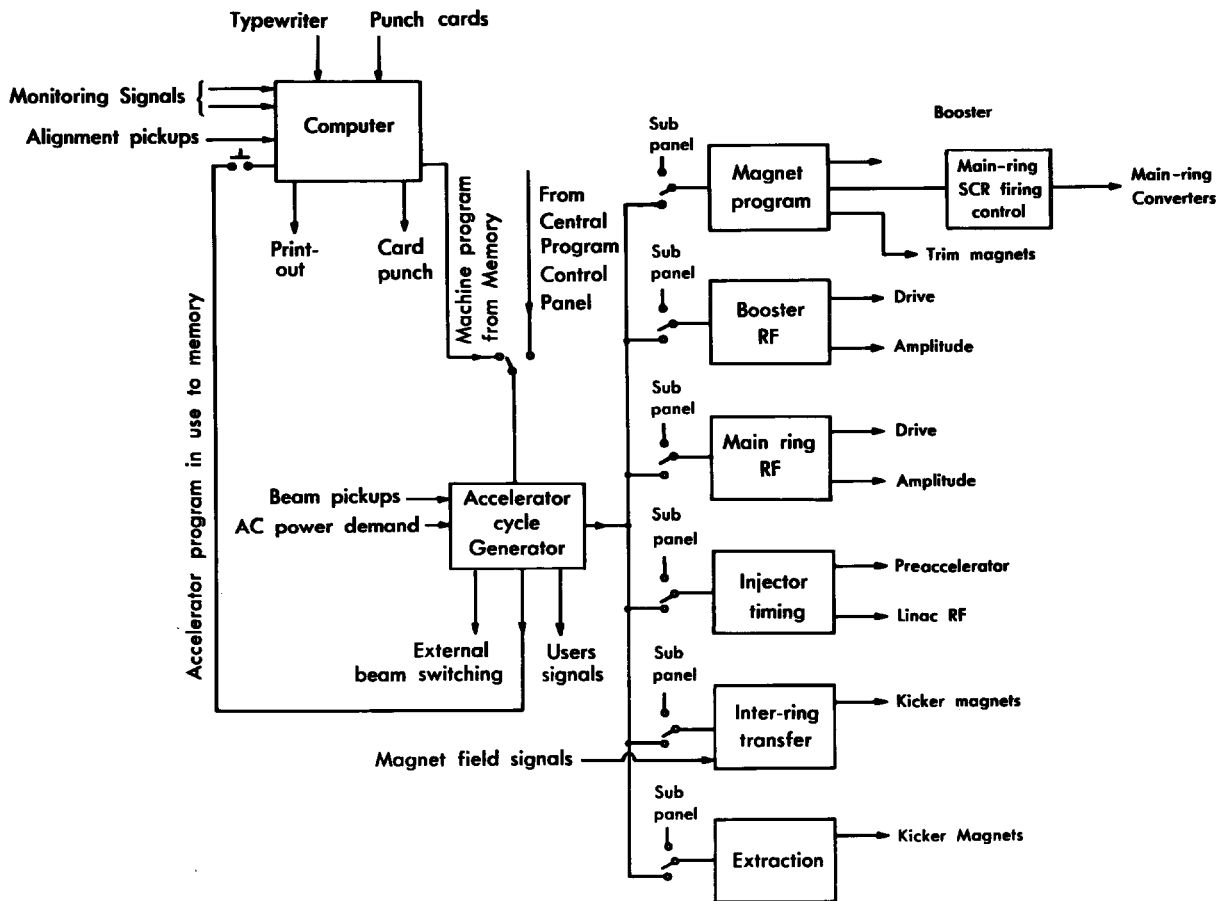
## 2. Control Computer

The computer is designed to perform the functions of:

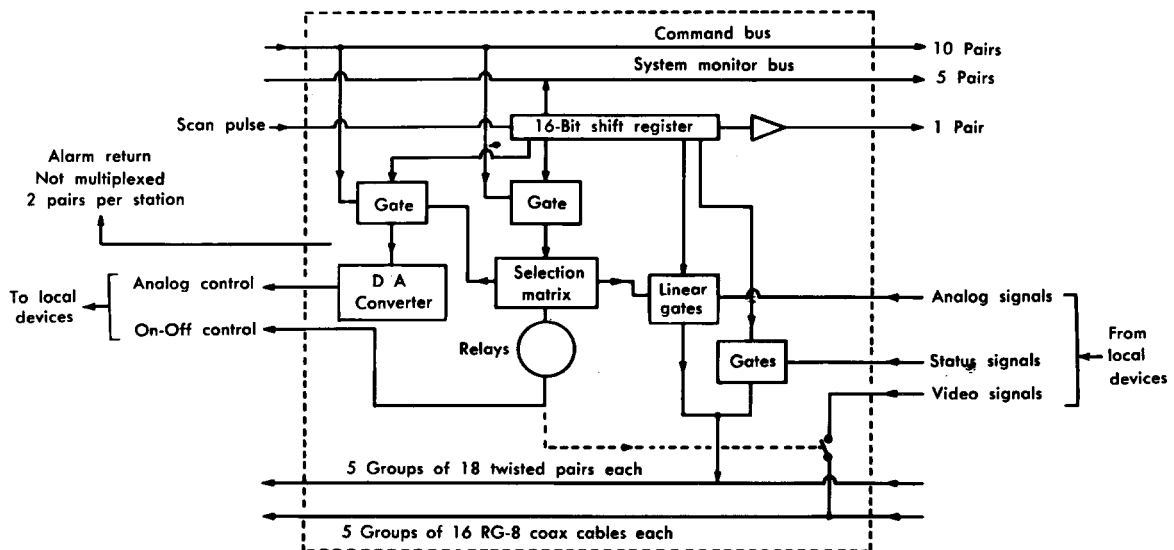
- (i) data logging, processing, and analysis, and information display, and
- (ii) transmission of control commands.

The upper part of Fig. 11-1 is a block diagram illustrating functions of the control computer. It can be programmed to provide specific data desired by the operator and to report signals from any source that are beyond preset limits. The computer can automatically protect inter-related components from damage in the event of a fault far more rapidly than a human operator, and can aid in the analysis of faults during trouble-shooting.

The operator will be able to select specific data for display as desired. For example, beam positions and intensities at different positions around the booster or the main accelerator can be displayed as an aid in centering the beam for optimizing intensity. Thus the operator can concentrate on particular aspects of the operation without the distraction caused by great masses of extraneous information. The control center will also monitor and program the distribution of extracted proton beams to different experimental areas.



Central Time and Function Generator



Multiplex System in Typical Data Station

Figure 11-1 — Control-System Schematic



The computer will provide means for encoding and transmission of commands by the operator and will be of great help in the complicated optimization of beam intensities, since it can carry out systematic studies of the effects of varying a large number of parameters. On the other hand, it is desirable that the operation should not be totally dependent on the central computer. Therefore, provision is made for manual and local operation of component accelerator systems for testing and in the event of a computer shutdown.

It may be noted that the memory needed for the computer is relatively large, but that the arithmetic and logic units required are relatively small. The requirement is therefore closer in concept to that for industrial control computers rather than the more familiar general-purpose data-processing computers.

### 3. Data-Transmission System

Experience<sup>1,2</sup> and previous studies<sup>3,4</sup> have shown the economic advantage of signal transmission by time-shared multiplex systems, in which different signals are sent in succession over the same cable. A frequency-multiplex system, in which signals are sent on different carrier frequencies over the same cable offers higher speed of data transmission, but at higher cost. In fact, high speed is not needed except for a few special functions, for which conventional direct-wire systems will be used. The lower part of Fig. 11-1 is a block diagram of a multiplexer located at a data station.

Except for transmission of very fast signals where special coaxial cables with wide-band frequency characteristics are needed, twisted-pair wires will be generally used in the system. Analog (adjustable parameters) and status (on-off) signals, and dc control and selection signals will be transmitted by twisted wire-pairs.

Information that cannot be time coded conveniently, such as video beam-pickup signals, will be transmitted by conventional coaxial cables. Selection of signals to be sent over specific cables will be made by reed relays. These relays will be controlled by time-coded pulses in the usual manner.

There are six major areas from which information is transmitted to the control system by direct-wire systems. These areas are:

- (i) The linear accelerator and the Cockcroft-Walton accelerator.
- (ii) The main-synchrotron and booster rf systems
- (iii) The beam-extraction system.
- (iv) The beam-transfer system between the booster and main ring.
- (v) Some components of the extracted-beam transport system.
- (vi) The radiation-protection and personnel-access systems.

Direct-wire systems are utilized for the first five because of their proximity to the control center. The radiation-protection and personnel-access circuits utilize direct-wire systems for maximum reliability.

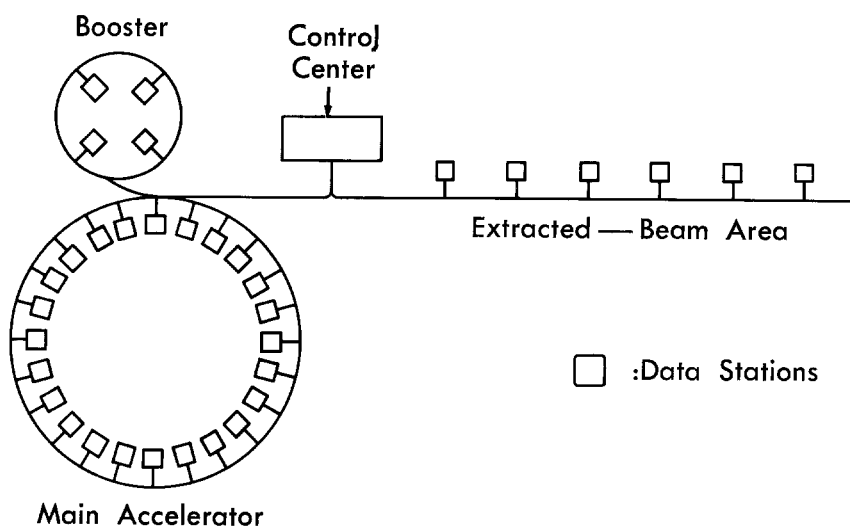
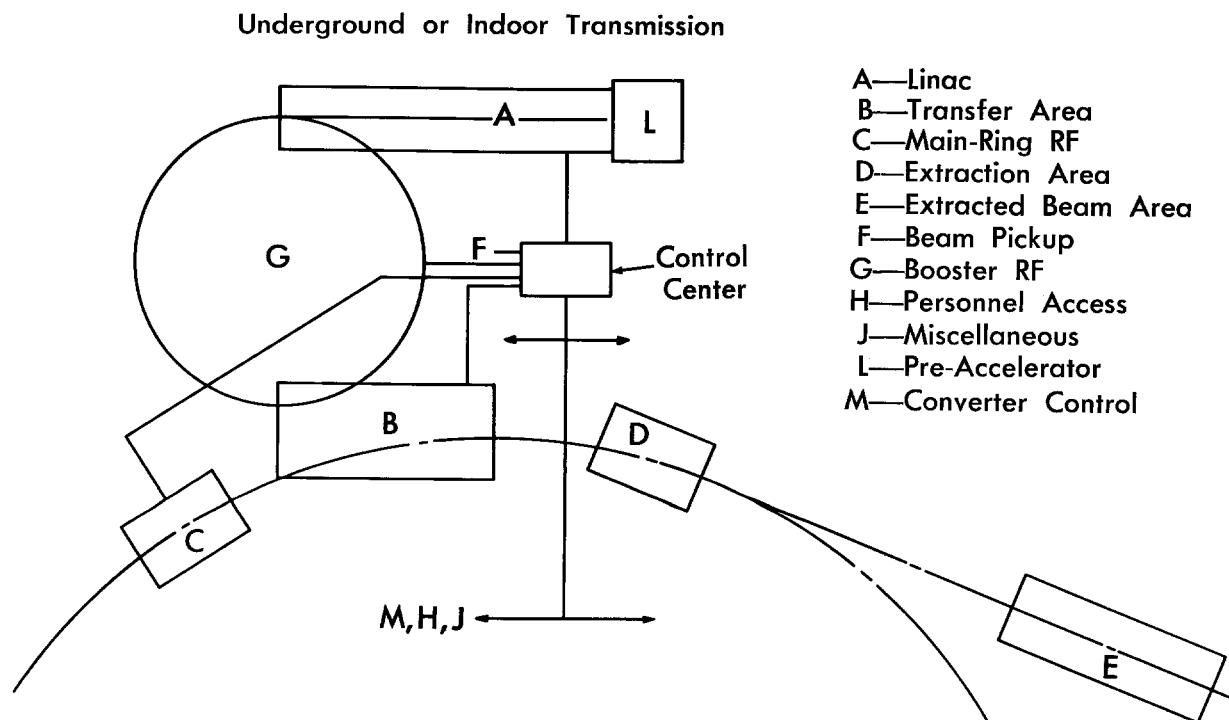


Figure 11-2 — Control-System Schematic

#### 4. Data-Collection Stations

Figure 11-2 shows the layout of data-collection stations. There are twenty-four stations for the main ring, located in the utility buildings, four stations for the booster, and six stations for the extracted-beam areas. The electronic equipment for multiplexing and transmission is located in these stations and shielded from the radiation in the enclosures.

#### 5. General Communications System

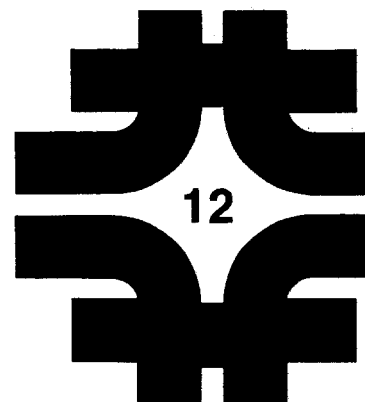
Conventional telephone and intercom communication will be provided between the control center and remote accelerator and experimental areas. A number of closed-circuit television sets with audio channels will also be used at different locations.

#### References:

1. R. Littauer, Multiplex Control and Monitoring of a Large Accelerator, IEEE Transactions on Nuclear Science, pp. 36-38 (June, 1965).
2. R. Littauer and H. Pfeffer, The Multiplex Control System for the Cornell 10 GeV Synchrotron, IEEE Transactions on Nuclear Science, pp. 1050-1052 (June, 1967).
3. CERN/563, Report on the Design Study of a 300 GeV Proton Synchrotron by the CERN Study Group on New Accelerators, Vol. I, (November, 1964).
4. 200 BeV Accelerator Design Study, Lawrence Radiation Laboratory Report UCRL-16000, (June, 1965).

# Radiation and Shielding

1. Introduction	12-1
2. Policy on Permissible Radiation Levels	12-2
3. Design of the Accelerator Biological Shields	12-3
3.1 Linac Shielding	12-3
3.2 Booster and Main-Ring Shielding	12-3
3.3 Shielding of Target Buildings	12-4
3.4 EPB Shielding	12-5
3.5 Shielding of Secondary-Particle Beams	12-5
4. Control of Residual Radioactivity	12-6
4.1 Wall Radiation	12-6
4.2 Beam-Loss Control	12-6
4.3 Beam Dumps	12-6
4.4 Air Activation in the Accelerator Enclosures	12-6
4.5 Cooling - Water Radioactivation	12-6
References	12-7



## 12. RADIATION AND SHIELDING

M. Awschalom, J. W. DeWire,  
M. S. Livingston, A. Maschke, A. L. Read,

R. Thomas (Rutherford Laboratory)

### 1. Introduction

If an accelerator is to be successful, the vast majority of the injected protons must be used for research. But some small fraction of the proton beam will inevitably be lost during acceleration and extraction. These lost protons constitute radiation against which people must be shielded. In addition these protons induce radioactivity in materials which they strike and the resultant radiation will continue after the accelerator is turned off. Plans for servicing the accelerator must take into consideration the exposure of maintenance personnel to this residual radiation. The lost-proton radiation can also damage components. Hence, care must be taken in the choice of materials both from the point of view of radiation damage and remanent radioactivity. The problem of radiation damage to magnet coil insulation is discussed in Sec. 3.2 of Chapter 5. In some locations, the judicious use of additional local shielding may avoid the use of massive earth shields on the outside of the enclosure and simultaneously reduce the remanent-radiation exposure dose rate.

In the experimental areas, where the protons are used for research, the problems are the same in quality but in quantity are from a hundred to ten thousand times greater.

These three facets of radiation problems -- shielding, residual radioactivity, and radiation damage -- are closely related to each other, because their effects are all proportional to the amount of beam lost. In particular, the presence of residual activity places a limit on the average proton current loss that will be permitted anywhere. In turn, this limits the shielding thickness that is actually useful. It is comparatively simple to increase the shield thickness to allow operation at higher proton current losses, but this higher intensity will generate a greater residual radioactivity that will increase the difficulties of maintenance and servicing. Unless relative beam losses are reduced or maintenance procedures developed that do not expose personnel, there is then a practical limit on the average intensity that can be usefully accelerated. Hence, beam intensities will be allowed to increase only as fast as the ability to control the beam itself improves.

Plans for this accelerator include the development of shielded vehicles to allow maintenance personnel to work on components in high levels of residual radiation. All the equipment is being designed for removal by remote manipulators operated from the shielded vehicle. The general practice will be to replace a component rather than to repair it in place. In the long range, it is hoped to develop completely remote servicing methods, so that people will not need to approach high radiation areas.

Present techniques make it difficult to reduce losses in beam extraction equipment, including beam scrapers, below the order of 1%; this loss will create a few localized high-radiation areas. It would, however, be intolerable to allow the entire circumference of the accelerator to become very radioactive, because servicing from a shielded vehicle will undoubtedly take much more time than would be needed by unshielded workers. The operational policy of the accelerator will therefore include limitation on intensity when beam is being lost at rates greater than those that will permit proper maintenance and improvements of the accelerator. In this way, approximately 95% of the main accelerator circumference will be accessible for useful work by unshielded personnel without exposure to a radiation dose beyond the maximum permissible levels set by the Federal Government.

## 2. Policy on Permissible Radiation Levels

The maximum permissible doses (MPD) for radiation workers and the general population are prescribed in the Federal Register, Title 10, CFR, Part 20. These MPD's are in agreement with those recommended by the National Committee on Radiation Protection and the Federal Radiation Council.

These MPD's are about twenty times the natural background dose and they contain adequate safety factors. Hence, all our radiation protection measures will be guided by these MPD's.

We will define three types of radiation areas on the site. Control requirements and occupancy times will differ in them.

1. Uncontrolled Areas. These are areas where the yearly dose with continuous occupancy will be less than 0.5 rem. This level is the MPD for the general population. Examples are offices, most shops, some developmental laboratories, open parking areas, off-site areas, and so on.

2. Controlled Areas. These are areas in which personnel may absorb doses greater than 0.5 rem year. Hence, they will require control of personnel access and, at times, limitation of occupancy times.

The radiation safety officer will control access, post and enforce occupancy times and maintain exposure records for the appropriate personnel.

The controlled areas are divided into two large classes, low and high radiation areas.

2.a. Low Radiation Areas. These areas will permit continuous occupancy, namely, 40 or more hours per week, without exceeding the MPD. Examples are: control room, peripheral equipment bays, parts of experimental areas, etc.

2.b. High Radiation Areas. These are areas in which the radiation levels are high enough that occupancy times must be less than 40 hours/ week. Personnel access and occupancy times will be strictly controlled. Personnel working in these areas may occasionally use special shielding and special tools to increase occupancy times. At times, heavily shielded vehicles may be used to protect the personnel working in these areas.

### 3. Design Of The Accelerator Biological Shields

Although, in principle, it is possible to provide enough shielding everywhere along the accelerator structures to maintain very small radiation levels on the outside of the shield even if there is continuous loss of a large fraction of the beam at any point, this approach is unnecessarily expensive.

The composition and energy spectrum of the lateral radiation are not very energy dependent for incident protons with kinetic energies of 30 BeV or more. Hence, the results of experimental studies performed at the Brookhaven AGS and at the CERN PS may be used to estimate the permitted proton loss rate, the remanent radioactivity and the biological dose rates outside various shielding configurations. The amount of radiation per incident proton is usually taken to be proportional to its momentum,<sup>1</sup> which at these energies is proportional to its energy. Hence, the rule of thumb is that the amount of radiation is proportional to the beam power lost.

3.1 Linac Shielding. The linear accelerator will be similar to the one being built for the Brookhaven AGS conversion. Hence, we use their shielding calculations. Wheeler and Moore<sup>2</sup> give a curve of required shielding thickness as a function of position along the linac. Their estimate is within 8% of the LRL design study once a correction is made for average beam current.

3.2 Booster and Main-Ring Shielding. In calculating the shielding required over the two circular accelerators, the relationship between the proton current on a target and the dose outside a 700 g/cm<sup>2</sup> shield was taken from Wheeler<sup>3</sup> and the AGS conversion proposal<sup>4</sup>. The relationship of proton current on a target and remanent exposure dose rate at the "hottest" spot downstream from it one hour after shutdown was taken from Distenfeld<sup>5</sup>. The mean free path adopted for the extension of the shielding is  $\lambda = 110 \text{ g/cm}^2$ , taken from Fortune et al<sup>6</sup>.

The results of these estimates are shown in Table 12-1. Here "Near" refers to areas near building occupied by non-radiation workers and "Far" to areas far from such buildings. Note that the dose rate on top of the shielding "Far" from buildings may be too conservative (2.5 mrem/hr) and that proper neutron-transport calculations of skyshine may allow for larger dose rates and thinner shields. Finally, no estimates have yet been made for neutron leakage through penetrations. Hence, present plans call for possibly too elaborate penetration labyrinths and plugging. However, neutron transport calculations will be made to adopt the simplest safe penetrations.

Table 12-1. Preliminary Estimate of Soil Cover Over Accelerator Enclosures\*

Accelerator	Exposure Dose Rate at 1 ft from Vac. Cham.	Max. Perm. Proton Losses Per Second	Biological Dose Rate on Surface (mrem/hr)	Soil Cover(115 lb/cu ft)-ft			
				Quiet Area	Hot Spot	Near	Far
Linac	25 mR/hr	1.3x10 <sup>10</sup> per foot	0.15	13**	-	-	-
Booster	25 mR/hr	1.5x10 <sup>9</sup> ***	0.25	21	-	-	-
			2.5	-	16	-	-
	10 R/hr	6x10 <sup>11</sup> ***	0.25	-	-	32	-
			2.5	-	-	-	28
Main Ring 200 BeV (400 BeV in paren- theses)	25 mR/hr	8x10 <sup>6</sup> *** (4x10 <sup>6</sup> )	0.25	21	-	-	-
			2.5	-	16	-	-
	10R/hr	3x10 <sup>9</sup> *** (1.5x10 <sup>9</sup> )	0.25	-	-	32	-
			2.5	-	-	-	28
	50R/hr (100 R/hr)****	1.5x10 <sup>10</sup>	2.5	-	-	-	31

\*It is assumed that the enclosure will have a 1-ft thick ordinary concrete shell.

\*\*Ordinary concrete ( $\rho=2.3$  g/cm = 145 lb/cu ft)

\*\*\*Per obstruction

\*\*\*\*Beam scraper area

3.3 Shielding of Target Buildings. In target buildings, a combination of steel and concrete shielding will be used. Steel will be used only when necessary, principally in locations close to the radiation source.

We have considered two orthogonal approaches to problems associated with servicing equipment that will be located close to one of the proton targets.



In accordance with one of these, the target and beam transport elements will be housed in a shielding enclosure made of movable blocks on ceiling, walls and floor. When a beam element must be replaced, the element itself, and its enclosure can be removed by remotely controlled handling equipment. A new assembly of "clean" enclosure blocks can then be assembled, and the replacement beam element can be put in place and aligned by usual means. This requires a residual dose rate, in the working space, of less than 40 mR/hr. The use of reusable iron blocks and boron-loaded concrete blocks will make it possible to achieve this level.

The second approach again contemplates that beam elements and shielding block configurations can be remotely unstacked. Beam elements are designed to be suspended from the shielding block immediately overhead and these assemblies are then further designed so that they can be positioned accurately by remote-handling equipment and precisely aligned by remote detection devices and remotely operated jacks.

Estimates for shielding required for beam stops, thick targets and beam collimators have been taken from Ranft's <sup>10</sup> work and are given below:

$$E_p = 200 \text{ BeV}, I_p = 1.5 \times 10^{13} \text{ p/sec}$$

Top shield = 6.5 ft Fe + 24 ft ordinary concrete

Lateral shield = 6.5 ft Fe + 2 ft boron-loaded concrete +  
22 ft ordinary concrete

Forward shield = 25 ft Fe + 350 ft of heavy concrete. The muon shield will be about 10 ft wide and will extend about 10 ft above the beam line near the target. It will taper appropriately away from the target.

The information for the muon absorber was taken from Kuhlmann and Wuster <sup>11</sup>. The actual material and dimensions will have to be calculated using cost analysis similar to that of Roberts <sup>12</sup> and Romano <sup>13</sup>.

**3.4 EPB Shielding.** The external proton transport system is essentially similar to the "quiet" areas of the main ring and it will be dealt with in a similar fashion.

**3.5 Shielding of Secondary-Particle Beams.** The secondary particle beams have to be studied individually since their relative hazard varies greatly. A secondary beam of diffraction-scattered protons could be only one or two orders of magnitude less hazardous than the primary beam itself. On the other hand, a large production angle charged-particle beam may be carried without lateral shielding and dumped in less than fifty feet of heavy-concrete back stop.

#### 4. Control of Residual Radioactivity

4.1 Wall Radioactivation. Nachtigall and Charalambus<sup>9</sup> have studied the use of boron-loaded concrete to reduce exposure dose rates in the tunnel. Their findings show that the use of boron could possibly reduce the exposure dose rate by a factor of two in the booster and main ring enclosures. A study of the applicability of their findings to our accelerators (closed-frame magnets) will be made. Surveys of the chemical content of concrete aggregates are now being made to find aggregates with low Na and Mn content. A cost analysis will be made to choose between low Na and Mn aggregates and ordinary aggregates with boron loading.

4.2 Beam-Loss Control. Since the design of the shield is based on continuous spill control, an elaborate fail-safe redundant system to monitor beam losses will be designed and incorporated in the accelerator controls. The outputs of this system will be interlocked with the ion source to stop acceleration in case of any abnormal beam spill.

4.3 Beam Dumps. The proton beam dumps will be water-cooled iron beam stops capable of dissipating about 0.5 MW of beam power in some two nuclear interaction lengths. Special precautions will be taken to control possible losses of the water coolant. The beam stops will be designed for removal to holding areas using only remotely operated manipulators.

4.4 Air Activation In The Accelerator Enclosures. The accelerator enclosures are designed to be sealed during normal operation to avoid continuous contamination of the atmosphere with radioactive argon and its radioactive spallation products.<sup>8</sup> Purging systems located in the utility buildings will be adequate to produce two complete changes per hour in the quiet areas and eight such changes per hour in the "hot" areas. These will be operated after an appropriate delay time, after the machine is shut down and before the entry of personnel. The radioactivity concentration released to the atmosphere in these purgings will be small. The small amount of air-borne radioactivity will be another benefit from the policy of proton-current loss limitations.

4.5 Cooling-Water Radioactivation. The magnet coils and yokes as well as other peripheral equipment will be cooled by deionized water flowing in closed loops. This water will contain radioactive nuclides mostly from the spallation of O<sup>16</sup>. These will be principally, O<sup>15</sup>, O<sup>14</sup>, N<sup>13</sup>, C<sup>11</sup>, Be<sup>7</sup> and H<sup>3</sup>. There will also be some spallation products of copper. Most of these radionuclides will be retained by the ion exchange resins of the water deionizers.

The temperature of the cooling water will be regulated by means of heat exchangers in which the secondary cooling water will flow in open loops. Radiation-monitoring equipment will be used to ascertain that no leaks occur from the closed system to the open one.

## References:

1. J. Ranft, CERN Report MPS/Int. MU/EP 67-5, June 20, 1967.
2. G. W. Wheeler and W. H. Moore, "Shielding Of The 200 MeV Linac", BNL. Memorandum AGSCD-10, May 18, 1966, and errata, AGSCD-10E, June 3, 1966.
3. G. W. Wheeler, "Shielding", BNL Int. memorandum, May 25, 1967.
4. BNL Report 7956, "A Proposal For Increasing the Intensity of the AGS At the Brookhaven National Laboratory", May, 1964.
5. Carl Distenfeld, private communication, December 14, 1967.
6. R. D. Fortune et al., "Shielding Experiment At The CERN-PS, CERN/LRL/RHEL Collaboration, 1966" UCID-10199.
7. J. Ranft, CERN 64-47, November 18, 1964.
8. M. Awschalom et al., "Air Spallation Products in the Vicinity of a Target Bombarded by 3 GeV Protons", Health Physics (to be published).
9. D. Nachtigall and S. Charalambus, CERN Report ISR Div. Rept. 66-28 (September 16, 1966).
10. J. Ranft, CERN/ECFA 67/WG2/U - SG5/JR 1.
11. P. E. Kuhlmann and H. O. Wuster, CERN/ECFA 66/WG2/US-SG5/pek-how-1 (October, 1966).
12. A. Roberts, NAL Note FN-70, September 6, 1967.
13. V. J. Romano, NAL Note FN-95 October 5, 1967.
14. 200 BeV Accelerator Design Study, Lawrence Radiation Laboratory Report, (June, 1965) Chapter XII, 2.6.4.

## **Provisions for Experimental Use**

13. Beam-Extraction and Transport System

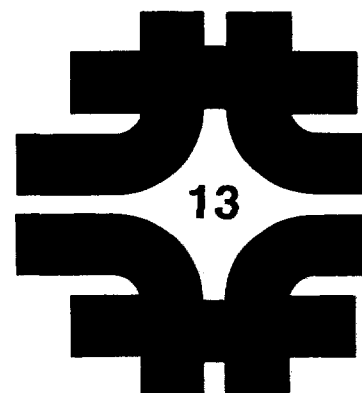


14. Experimental Areas and Program



# Beam-Extraction and Transport System

1. Introduction	13-1
2. Beam-Extraction System	13-3
3. Beam-Transport System	13-7
4. Loss-Control System	13-7
References	13-8



### 13. BEAM-EXTRACTION AND TRANSPORT SYSTEM

A. W. Maschke

K. R. Symon (Wisconsin)

#### 1. Introduction

The purpose of the beam-extraction and transport system is to take full-energy protons from the accelerator to targets, where they interact with the material of the target. In some cases, these reactions will be studied directly, in others they will be used to produce secondary beams of particles which experimenters will then use for a variety of studies. Very few experiments will require a full-intensity bombardment and virtually all experiments must go through periods of testing that can be carried out at low intensity. The system therefore includes provisions for splitting the extracted proton beam so that it can be shared among different targets.

The time distribution of protons on targets is of great importance. Some experiments, such as those utilizing resonant-expansion bubble chambers, require very short bursts repeated at definite time intervals. Others, such as those utilizing counters, can best use a continuous beam extending uniformly over as long a time as possible. Still other experiments require tightly bunched beams for time-of-flight measurements or modulation of the beam intensity at extremely high frequency for the separation of particles by an rf deflection technique.

In meeting these requirements, the beam-handling system must operate within the limits imposed by a number of constraints. Radiation levels produced around the accelerator by lost beam must be kept as low as possible. Although provision is made in the enclosure for shielded vehicles, their use for much of the necessary maintenance and modification would take substantially extra time. The extraction system must operate with maximum reliability and should therefore be as simple as possible, in order to minimize down-time.

On any one pulse of the accelerator, the beam-extraction and transport system may be required to deliver beam to three or four targets with varying kinds of spills. It is important to make the different functions of the system operate independently with a minimum of coupling between them.

The beam-extraction and transport system described below has been designed to meet all these requirements and constraints. It can

be described in two parts, the extraction system, which takes the proton beam out of the accelerator, and the beam-transport system, which carries the extracted beam to the targets.

Extraction of a short burst, or "fast extraction", is begun by kicking the beam sideways with a rapidly rising magnetic field. This kick induces an oscillation that carries the whole beam into a series of electrostatic and magnetic devices that bend it away from the accelerator. Such a device generally has a septum to separate its field from that of the accelerator, in order that protons will not be affected by extraction fields during injection and acceleration. Some protons will strike the septum and be lost, resulting in undesired radioactivity in and near the extraction system. To minimize this effect, and to permit the device to be brought very close to the orbit, the septum must be made as thin as possible.

Extraction of a long burst, or "slow-extraction," is begun by perturbing the beam by a small auxiliary magnet system so that its betatron oscillations around the central orbit become unstable and grow. This growth carries the particles into the same septum devices used for fast extraction to bend them away from the accelerator.

All the septum devices are located in one long straight section, immediately downstream from injection. All beams are extracted by this one system; different targets are fed by means of "switching magnets" in the beam-transport line. The positions of the switching stations are shown in Fig. 14-1. Conventional focusing systems utilizing strong-focusing quadrupoles, similar to those of the main accelerator, transport the beam approximately 1000 feet to the first switching station S1. This station contains a replica of the beam-extraction system, that is, a series of septum devices that split the proton beam into two. One beam is bent to target-station C, while the other is carried straight forward to a second switching station S2, where it is again split, with part being bent to target stations A and B and any remainder continuing straight to a beam dump.

The use of a single extraction point in the accelerator provides important advantages in the potential effectiveness of the system. In an accelerator with two extraction points, it is impossible in practice to match the accelerator orbit dynamics to give good efficiencies at both points simultaneously. In addition, if two extraction systems are used, the accelerator will in general be shut down for repair if either one of the extraction systems fails, even though the other could continue. Thus there is no greater reliability in two extraction systems. In fact, the average shutdown time could well be greater with two extraction systems.

At the same time, the use of external switching systems is advantageous in its own right. The radioactivity created in them will not affect the much larger number of components of the accelerator itself. A catastrophic failure in them, for example, a large water

leak into the vacuum system, will not damage the accelerator. The external systems can be made more reliable, because there is ample straight-section room to install redundant equipment.

External systems are also simpler. Their vacuum requirements are much less severe, because the proton beam traverses the system only once per cycle. They need not be pulsed or stroked into position, because their fields do not affect protons during acceleration.

Finally, additional switching and target stations can be constructed if needed without interference to the research program, whereas adding an extraction point in the main accelerator would require a shutdown.

## 2. Beam-Extraction System

The septum devices are the most important and difficult elements of the extraction system. They must provide enough bending to make the emergent beam clear the accelerator components at the downstream end of the long straight section. Their fields should not affect the beam during acceleration.

At the same time, the septa that separate extraction fields from main-accelerator fields must be thin enough that they do not intercept any significant fraction of the beam. The efficiency of the extraction system is inversely proportional to the thickness of the septum. For example, if in slow extraction the oscillation amplitude increases by 1 cm per revolution, 10% of the beam will strike a septum 0.1 cm thick and the extraction efficiency will be 90%.

Most extraction-system designs have utilized magnets with current-carrying copper septa cooled at the edges. The magnetic field achievable in this kind of magnet decreased with decreasing septum thickness. If the septum thickness is to be less than 0.005 to 0.010 in., the maximum attainable magnetic field is so low that an electrostatic deflector becomes more effective. The first septum device in the extraction system is therefore an electrostatic deflector with a septum 0.002 in. thick. All subsequent septa are designed to lie in the shadow of this first one.

Figure 13-1 shows this and the following magnetic elements. Their parameters are summarized in Table 13-1. The electrostatic deflector and the first two magnet elements are stroked or plunged into the aperture each cycle to avoid occupying aperture at injection. The length of the required stroke is 1 to 2 cm.



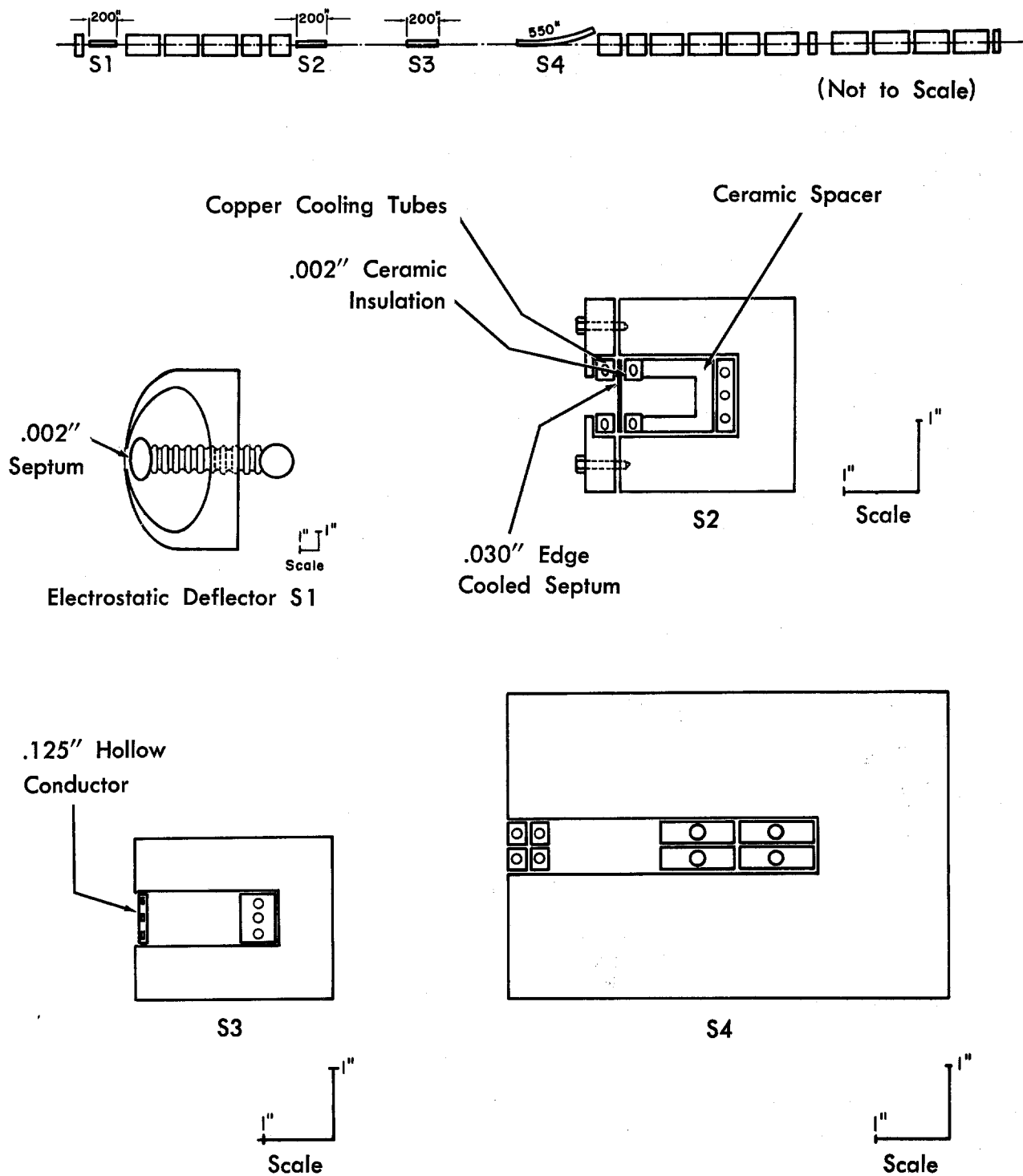


Figure 13-1 — Extraction-System Magnets

Table 13-1. Parameters For 200 BeV Extraction Elements

<u>Element</u>	<u>Type</u>	<u>Field</u>	<u>Septum</u>	<u>Length</u> <u>(in.)</u>	<u>Deflection</u> <u>(mrad)</u>
			<u>Thickness</u> <u>(in.)</u>		
1.	Electrostatic	40 kV/cm	0.002	200	0.1
2.	Magnetic	1-2 kG	0.03 - 0.06	200	1
3.	Magnetic	6 kG	0.2 - 0.4	200	5
4.	Magnetic	9 kG	1.0 - 2.0	480	16

This extraction system is designed for 200 BeV protons. For 400 BeV extraction, the first magnetic septum will be displaced downstream approximately 200 in. and another magnet of septum thickness 0.01 in. placed in the resulting space. The current densities in all the magnetic septa are low enough at 200 BeV that the fields can be doubled. It is not clear that the electrostatic deflector can be operated reliably at 80 kV/cm, but the added magnet will allow the system to operate at high efficiency without such high electric fields.

Figure 13-2 is a phase plot of computed extraction orbits. It shows the envelope of extraction trajectories with a time-varying tune. It is planned to make use of the third-integral resonance excited by the trimming sextupoles. Growth rates of approximately 1 cm per revolution are predicted by the computations, so that the system has a calculated efficiency of 99%. It is planned to have enough flexibility to allow, in addition, the possibility of extraction on the half-integral resonance, excited by quadrupoles or octupoles.

Slow extraction over the entire flat-top time of 1 second is planned. This requires that the main-accelerator guide field be held constant within very tight tolerances over this time. Variation or ripple in the guide field would have two deleterious effects:

(i) Changes in  $\nu$  value: Guide-field ripple modulates the  $\nu$  value and lowers the effective duty cycle. The modulation can be removed by energizing trim windings on the quadrupoles with a voltage picked-up from the rate of change of magnet current. A separate set of low-power quadrupoles will be used to control the change of  $\nu$  value with time and, consequently, the extraction rate. This will have the effect of "locking-in" the value of  $\nu$  as a function of radius, independent of variations in guide field.

(ii) Radial movement of the orbit: A radial motion of 1 mm is caused by a change of magnet voltage  $\delta V$  of magnitude

$$\delta V = f V \times 2.5 \times 10^{-3} ,$$

where  $V$  is the magnet voltage and  $f$  the ripple frequency. For

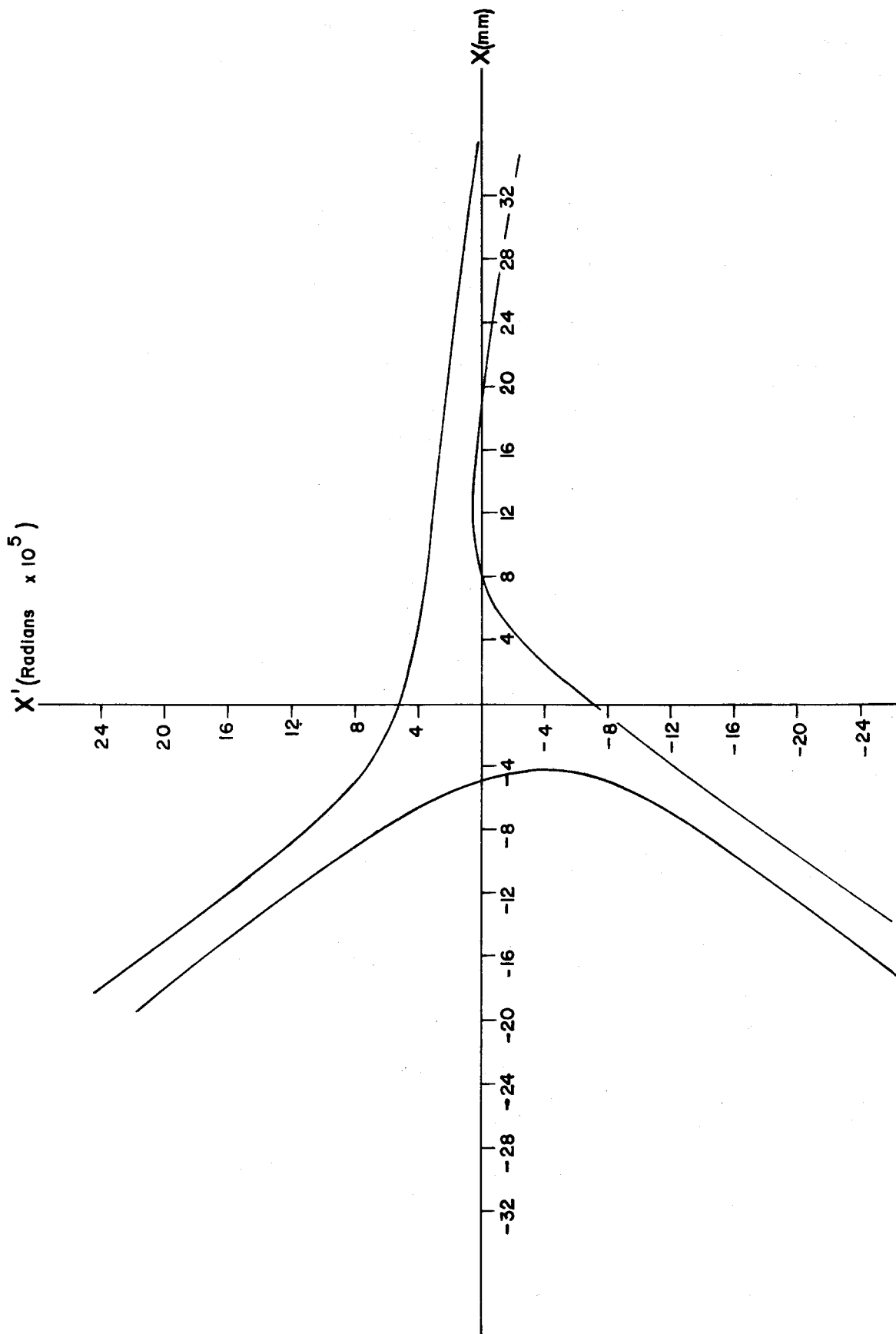


Figure 13-2 — Extraction-System Phase-Space Diagram

frequencies of 60 Hz or more, the guide-field regulation will be adequate. For low frequencies, a beam-position detector can be used to serve the power-supply voltage.

### 3. Beam-Transport System

The system that transports the proton beam to switching stations utilizes conventional strong-focusing quadrupoles. The beam will be transported in vacuum, but the system pressure can be as high as  $10^{-3}$  torr without creating any problems. This is true because protons make only one pass through the transport system, whereas they pass  $10^5$  times around the accelerator.

The switching-station components themselves are replicas of the extraction-system components described above in Table 13-1 and shown in Fig. 13-1. They need not be pulsed or stroked in normal operation. The proton beam will be formed into a horizontal ribbon at the splitting station, and it can be kicked onto or off the septum by a fast-rising kicker magnet. There are in addition steering magnets that are servo-controlled to keep constant the ratio of beams on the two sides of the splitting septum. Additional servo controls will lock the beam spot on the target.

It is also possible to reduce the losses in the neighborhood of the electrostatic septum by introducing a specially designed shield septum ahead of it.<sup>1</sup> This shield septum is made of a low-density, high-Z material; e. g., a line of 2-mil tungsten wires spaced at approximately 150-mil intervals, and a few feet long. Particles that enter the leading edge of the septum will tend to be Coulomb-scattered out of the shield septum before reaching the electrostatic septum. It is estimated that 95% of the protons will be scattered out before making a "strong" interaction in the material, thereby reducing radiation levels around the septum by a factor 20.

The beams will be raised in elevation from 728 feet above mean sea level at the switching stations to 745 feet at target stations A and C. The bending will be done by magnets identical to the main-ring bending magnets. The enclosure will have the standard cross section of the main ring.

### 4. Loss-Control System

Because of the large amount of energy stored in the beam (1.5MJ), the consequences of accidentally dumping the beam on equipment can be quite serious. An interlock system for the main ring is designed to keep radiation levels down in the quiet areas and to prevent component damage due to loss of beam control.

The major element of the beam-control system is the "abort" mechanism. Any one of a number of signals can trigger this, for example, detection of anomalous beam loss, power-supply failure,

rf failure, vacuum failure, and so on. A fast kicker in the ring will then be activated to bump the beam immediately onto a "clean-up" target in one of the medium straight sections.

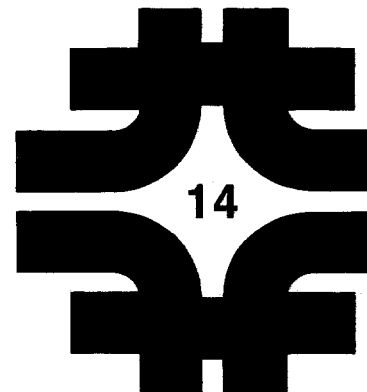
Some losses may occur during acceleration (at transition energy for instance), and the clean-up targets must, therefore, be adjusted to be the limiting aperture of the accelerator. Since the "position" of these clean-up targets should change during the cycle, it is proposed to build in orbit bumps around the aperture stops. In the particular design discussed here, this array of clean-up stops is able to collect more than 95% of the stray losses. Separate aperture stops are used for inside and outside, top and bottom. In addition, they should occur in pairs that are an integer plus a quarter betatron wavelength apart. At the nominal tune of the accelerator, medium straight sections B and C have this relation to D and E. In addition to being collection points for stray beam losses, these aperture stops will also define the phase of the resonant betatron oscillation during slow extraction. That is, the only particles that will be able to reach the septum will be those with the proper phase. This will then protect the septa from any possibility of being burned up by the beam slowly scraping on the septum.

#### References:

1. A. W. Maschke, On Casting Shadows of Septa, NAL Note FN-100, November 15, 1967.

# Experimental Areas and Program

1. Introduction	14-1
2. Number of Beams and Size of the Research Program	14-3
3. Description of the Target Areas	14-6
4. Secondary-Beam Areas	14-14
References	14-15



## 14. EXPERIMENTAL AREAS AND PROGRAM

A. W. Maschke, A. L. Read, A. Roberts, J. Sanford (BNL)

M. H. Blewett (ANL), L. J. Koester (Illinois), D. I. Meyer (Michigan)  
R. Rubinstein (BNL), T. G. Walker (Rutherford Laboratory)

### 1. Introduction

Full-energy protons are extracted from the accelerator and transported to targets by the systems described in Chapter 13. Most physics experiments will be concerned with the properties and behavior of secondary particles produced in the bombardments of these targets. Other experiments will be concerned with the primary interactions of the beam protons with the particles in these targets.

It is far too early to plan in any detail the experiments and the detailed experimental arrangements that will be laid out at the time the accelerator starts operation. Nevertheless, for the purposes of cost estimates and the establishment of a site plan it has been necessary to adopt, even at this early date, a plan for the initial experimental areas. In Chapter 18 are presented a number of options for their future modification, expansion, proliferation and diversification. Provision is made in the initial design for the future exploitation of any or all of these options, should that become desirable. The secondary-beam layout that has been developed is one that will probably never materialize, but it does provide, in number and variety of beams, for the full gamut of research potential for which one can now foresee an apparent need. Thus the plan presented here for the experimental areas must be considered as a model rather than a final design. It will undergo continuous review over the next several years by both Laboratory and university physicists in order to provide a final layout that will have been responsive to the interim developments in both physics and instrumentation.

In practically all cases, the targets will be external to the accelerator. An internal-target area, using protons directly inside the accelerator, is also planned, but will be used only at low beam intensities. The primary reliance will be on external targets in order to avoid building up radioactivity in the accelerator itself. Radioactivity will also be induced in the shielded housings surrounding external targets. It is, however, far easier to make special provisions for maintenance and repair of external-beam components than it is for components inside the accelerator enclosure.

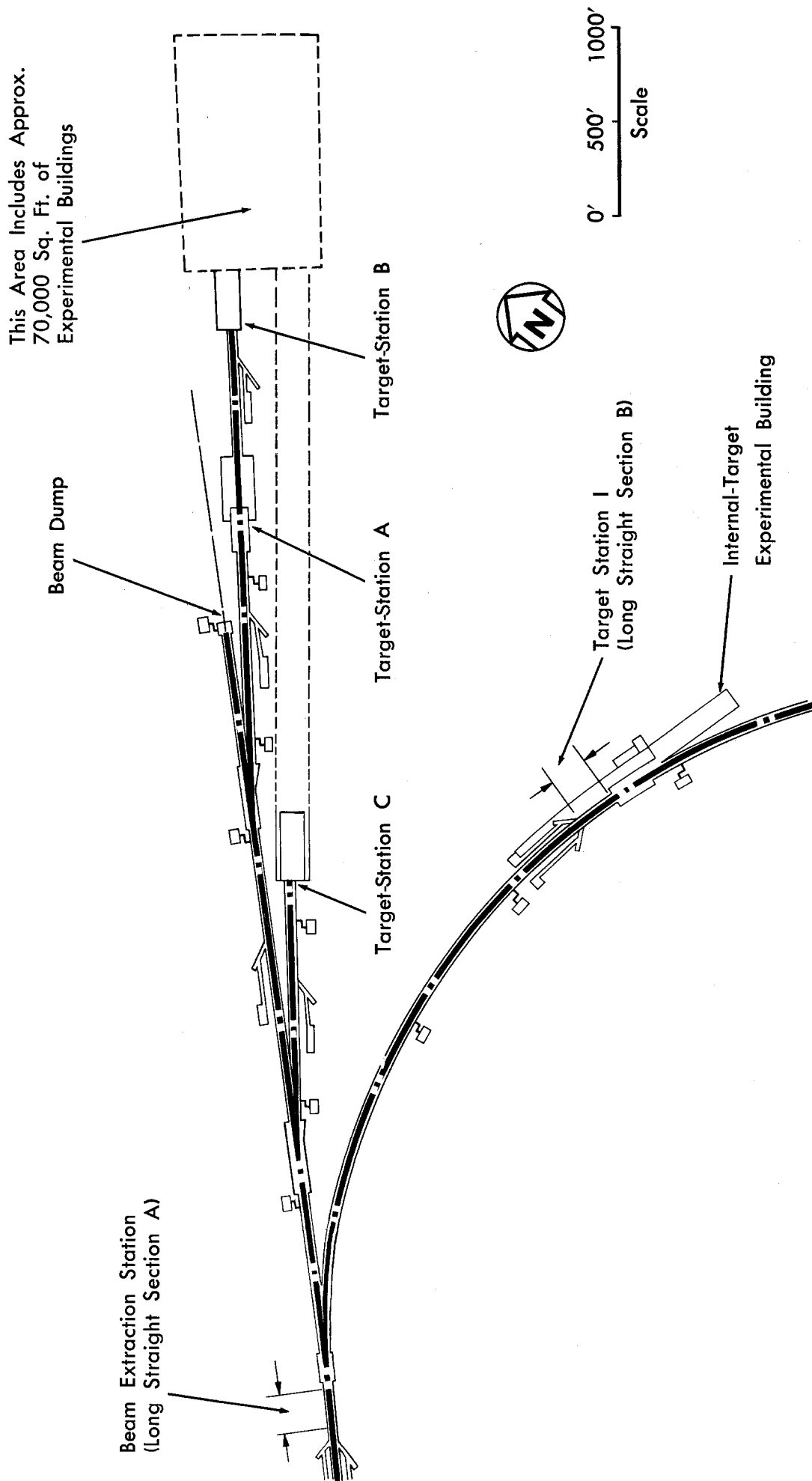


Figure 14-1 — Layout of Experimental Areas



Three external target stations and one internal-target station are planned. A general layout is shown in Fig. 14-1. Desired fractions of the beam will be deflected by switching magnets to the external-target stations as described in Chapter 13.

The external-target stations are denoted in Fig. 14-1 as A, B and C. Stations A and B are in series. Station A is designed for use with thin targets. Only a small fraction of the beam will interact in these thin targets and most of the beam in this line will be transported through A to B. Many secondary beams will be simultaneously available from Station B. Station C is similar to B, but will be specially designed to give secondary beams emerging from the target at or near 0 degrees with respect to the direction of the primary proton beam. This imposes constraints that limit the number of independent beams available at C to a smaller number than at B.

The internal-target station, also shown in Fig. 14-1, is planned to provide only two secondary beams. Its main advantages are its simplicity of design and operation, and a potentially greater efficiency in its use of protons. Its possible future use as a second proton extraction point, particularly for feeding the beam-bypass discussed in Sec. 3 of Chapter 18, is an important factor in its design. This area will also be useful during construction as a staging area where accelerator components can be prepared for installation in the main ring.

## 2. Number of Beams and Size of the Research Program

The design of the experimental areas is closely related not only to the kind of experiments to be done, but also to the number of experiments and thus to the size of the research program. It is therefore important to estimate these factors. This has been done by extrapolation from present-day experience.

The model layout that has been developed provides from external proton targets seven beams for electronic detectors, two more for bubble chambers, and a special set of beams for weak-interaction studies.

There were approximately 1,050 Ph. D. physicists actively engaged in High-energy physics research in 1964. They were divided roughly equally into three categories, theoretical physicists, experimental physicists working with electronic-detection (counter and spark-chamber) methods, and experimental physicists working with bubble chambers.

Several studies<sup>1,2,3</sup> have been made to estimate the future number of physicists engaged in high-energy physics. These have concluded that in 1975, when research with this accelerator is reaching full activity, there will be approximately 2,200 Ph. D. physicists in the field. By then there may well be important new detection methods, but at this time we can only assume that work will be divided roughly as it is today. This argument leads to an expectation that there will

be approximately 750 workers each in theory, electronic-detectors, and bubble chambers. The demand and the constraints imposed by experimentation at higher energies are likely to increase the fraction of the program that will be carried out using electronic techniques. It is assumed that about one quarter of the nation's total experimental high-energy physics program will be centered at the National Accelerator Laboratory.

Electronic-Detection Program. A principal demand for experimental beams is expected to be generated by physicists utilizing electronic-detection methods, such as scintillation and Cerenkov counters, spark- and streamer-chambers. If these techniques follow the present pattern, a typical group will divide its efforts into three approximately equal parts, one-third to the creation and instrumentation of new experiments, one-third to setting up apparatus and taking data, and one-third to the analysis and interpretation of the results. Then it can be expected that approximately twenty research groups will be occupied with work from seven beams. At present, the average research group has seven Ph. D. physicists. With the increasing complexity of equipment, groups may increase somewhat in size, and we therefore take the average group size to be ten Ph. D. physicists. With this assumption, approximately 200 physicists using electronic detectors can be expected to center their research activities around the facilities that are initially being planned at this accelerator.

Bubble-Chamber Program. Bubble chambers offer a powerful technique for exploratory investigations of the properties of elementary particles and their interactions, because the interaction point is visible and because they provide a view of the total solid angle for the detection of secondary particle tracks.

No specific plans have been made for construction of a very large hydrogen bubble chamber at the National Accelerator Laboratory, even though the need for such a chamber is recognized. The design of such a chamber should be considered very soon because the required lead-time is large, and this type of instrument would be very valuable for exploratory work at higher energies. However, further study is required before a firm proposal for construction is submitted.

At present, a 12-foot hydrogen bubble chamber is being constructed at Argonne National Laboratory and a 7-foot test chamber is being constructed by a group at Brookhaven National Laboratory. The Brookhaven group has also proposed the construction of a 14-foot hydrogen chamber for use with the AGS at Brookhaven.

In addition to the possible construction of an NAL chamber, consideration is also being given to the possibility of moving the Argonne 12-foot chamber or the Brookhaven 7-foot chamber or both to the National Accelerator Laboratory for use at an early date. A decision will be based in large part upon the judgment of qualified scientists about the availability and relative potential of those chambers to

contribute to significant research at the Argonne and Brookhaven National Laboratories and at the National Accelerator Laboratory. If it is decided that either or both of these chambers should be moved, authorization and funding for the housing and ancillary space required for operation of the chambers will be separately requested. If further study shows a new chamber to be desirable, its authorization and funding will be separately requested. Both the Argonne and Brookhaven groups have expressed a strong interest in participating in one or another phases of this three-pronged program.

The plans being developed for experimental areas include provision for two high-energy separated-particle beams and for an intense neutrino beam. Such beams are expected to be semi-permanent, operating for long periods without major changes. All of these beams will be suitable for bubble-chamber experiments, and if designed for that purpose, for electronic-detection experiments also.

Resident and Visiting Users. The planning for a proper mixture of research by resident and visiting users is of great importance to the laboratory. The National Accelerator Laboratory will be operated as a national facility, open for use by all on the basis of the scientific merit of the proposed experiments. Decisions regarding use of the facilities will be made by the Director with the advice of a nationally representative group of the best qualified high-energy physicists. Even within this context, the final disposition of research time will clearly be strongly influenced by the size of the resident NAL research staff. Thus the size and composition of that staff have far-reaching implications.

On the one hand, the resident staff provides continuity to the program. These people will also devote a fraction of their time and effort to the development of large facilities and complex experimental arrangements. Visiting users, on the other hand, bring diversity and vitality to a research program. It is therefore important that the program not be preempted by an overly large resident staff.

By way of contrast with the present situation, the small accelerators of two decades ago were exploited by a single, local research group. The programs of today's large accelerators appear to be matched to a resident staff that carries out about one-third of the research program. We estimate, by extrapolating this experience to the even larger program of the National Accelerator Laboratory, that about one-fourth of the research program should be carried out by resident staff and about three-fourths by visiting users. The Laboratory will provide technical assistance for visiting users. The number of Laboratory staff members providing this assistance is shown in the population estimate of Table 17-1.

Table 14-1 summarizes the estimated size of the research program, giving numbers of physicists and experiments approximately two years after turn-on, in FY 74 or 75. The size of the Laboratory has been planned to support this research program. Growth of the program in later years would necessitate construction of additional experimental areas; more laboratory and shop facilities would also be needed.

Table 14-1. Estimated Research Program

Number of Target Stations	4	
Number of Experiments Set Up	12	
Number of Experiments in Operation	9	
Number of "Electronic" Set Ups	10	
Number of "Electronic" Experiments per year	20	
Number of Bubble-Chamber Set Ups	2	
Resident Experimental Ph. D. Physicists	90	
Resident Theorist Ph. D. Physicists	<u>15</u>	
Total Resident Physicists		105
Non-resident Experimental Ph. D. Physicists (a)	300	
Non-resident Theorist Ph. D. Physicists (b)	<u>--</u>	
Total Non-resident Physicists		<u>300</u>
Total Physicists		405

(a) Non-resident participating experimentalists are those whose research is focused on this laboratory's program. They are not all at the laboratory at any one time.

(b) The number of non-resident participating theorists has no impact on experimental-area planning.

The average visitor population is expected to be approximately half of those participating, or 150 at any time, with "electronics" physicists spending more of their time at the Laboratory than bubble-chamber physicists. Although any large bubble chamber will be operated by an NAL operating crew, a large fraction of the analysis of film for visitors' experiments is expected to be carried out at their home universities. Thus the average population of bubble-chamber users at the laboratory will be smaller than that of electronic-detection users, even though the programs may be of roughly equal size. The total number of physicists involved is less than one-fourth of the national total because the university-centered theoretical-physics effort has not been included.

### 3. Description of the Target Areas

A general layout of the experimental areas is shown in Fig. 14-1. Specifications of some beams that can be provided in the four areas are given in Table 14-2. The specifications of the structures in these areas

Table 14-2. Characteristics of Some Possible Secondary Beams Produced by 200 BeV Protons\*

Target Station	Beam No.	Particle	No. of Interacting protons/sec	Lab. Solid Angle $\Delta\Omega$ (sr)	$\Delta p/p \pm \%$	Production Angle	Momentum (BeV/c)	Intensity (sec <sup>-1</sup> )
A	A1L	Protons	This is large-angle scattering channel for p-p scattering experiments.			Various: $\sim 10^\circ$ - $40^\circ$		
A	A1R	Protons	This is small-angle scattering channel for p-p scattering experiments.			Various: $\sim 0.5^\circ$ - $10^\circ$		
A	A2	$\pi^-$	$10^{11}$	$10 \times 10^{-6}$	1	10 mr	10 20 40	$3 \times 10^6$ $8 \times 10^6$ $6 \times 10^6$
B	B1	$\pi^-$	$3 \times 10^{12}$	$3 \times 10^{-6}$	1	7.5 mr	25 50 75	$10 \times 10^7$ $7 \times 10^7$ $2 \times 10^7$
B	B2	$\pi^-$	$3 \times 10^{12}$	$3 \times 10^{-6}$	1	2.5 mr	50 100 150	$3 \times 10^8$ $5 \times 10^7$ $4 \times 10^6$
B	B3	K	$3 \times 10^{12}$	$3 \times 10^{-6}$	0.1	2.5 mr	50 100 150	$3 \times 10^6$ $5 \times 10^5$ $3 \times 10^4$
B	B4	K	$3 \times 10^{12}$	$3 \times 10^{-6}$	0.1	7.5 mr	25 50 75	$10 \times 10^5$ $7 \times 10^5$ $2 \times 10^5$ **
C	C1	K	$3 \times 10^{12}$	$10 \times 10^{-6}$	0.1	0	50 100 150	$1.6 \times 10^7$ $6 \times 10^6$ $1 \times 10^6$
C	C2	$\pi^-$ (decays to $\mu^-$ and/or $\nu$ beam)	$3 \times 10^{12}$	$10 \times 10^{-6}$	5	0	10 20 40	$1 \times 10^9$ $4 \times 10^9$ $10 \times 10^9$ ***
C	C2D	$\mu^-$	$3 \times 10^{12}$					
C	C3	$\pi^-$	$3 \times 10^{12}$	$10 \times 10^{-6}$	0.1	0	50 100 150	$1.6 \times 10^8$ $6 \times 10^7$ $1 \times 10^7$

\*Estimated secondary beam production yields are based on the empirical formula given by Koester (L. J. Koester, NAL Note FN-72, 9/18/67).

\*\*K decay in flight along beam path is not taken into account; we assume K/ $\pi$  production ratio  $\approx 10\%$ .

\*\*\* $\mu^-$  and  $\nu$  beams (C2D), obtained from decay of  $\pi^-$  beam C2, based on  $\mu^-$ - $\nu$  channel described by Toohig (UCRL 16830, Vol. 1, p. 409), yield typically (number of  $\mu^-$ )/(number of  $\pi^-$ )  $\approx 0.2$ , and (number of  $\nu$ )/(number of  $\pi^-$ )  $\approx 0.5$ .

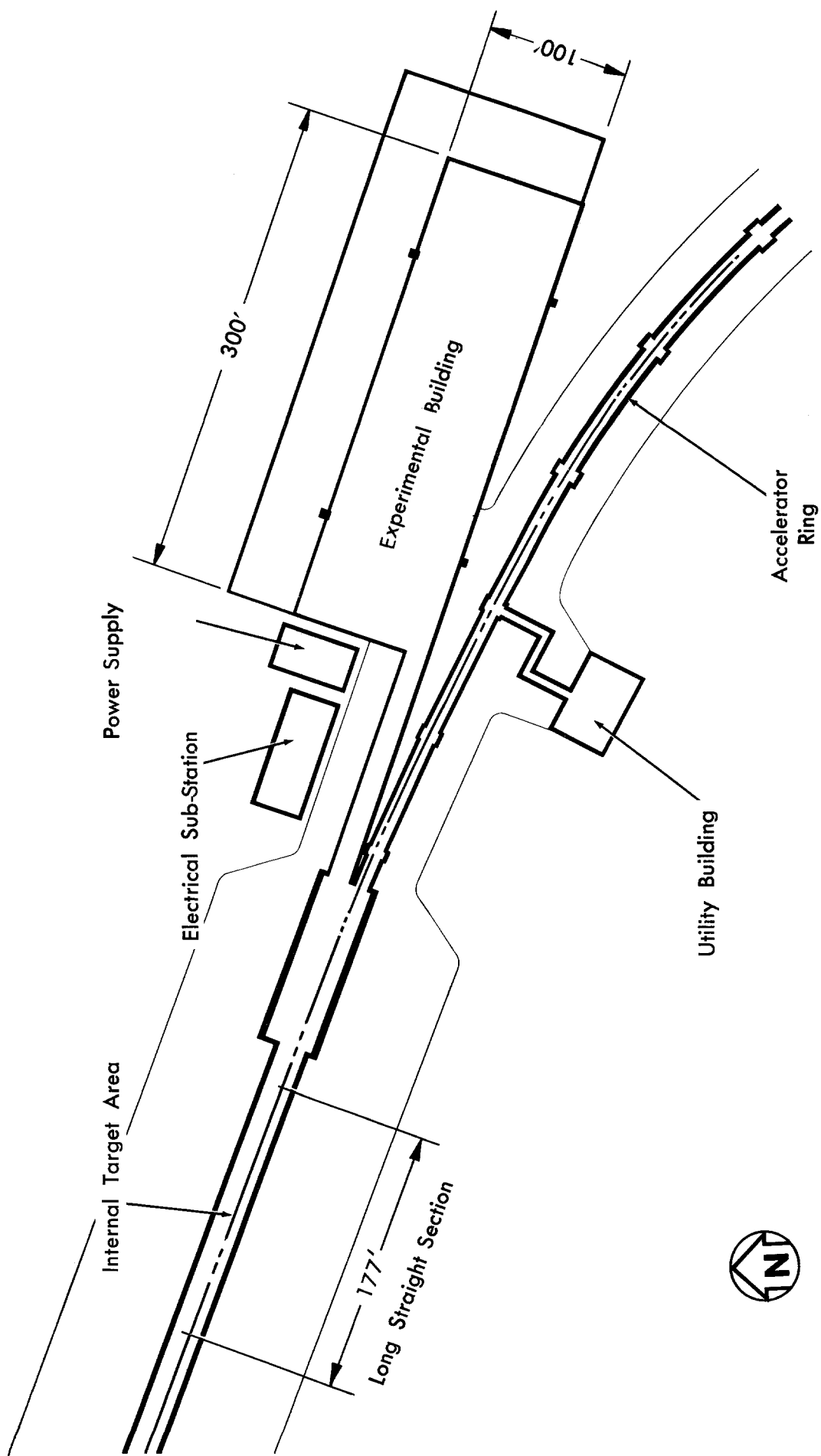


Figure 14-2 — Internal-Target Experimental Area

are given in Chapter 15. The discussion here is confined to the potential exploitation of the target areas for physics experiments.

Target Station I (Internal-Target Station). A layout of the internal-target facility, including an associated experimental building, is shown in Fig 14-2. Primary proton bombardment intensity must be kept at a relatively low level at this target in order to limit the radioactivity induced in accelerator components immediately downstream from the target.

The internal-target station is designed to become a second beam-extraction point, possibly to feed the external beam bypass that is discussed in Chapter 18.

Target Station C (Target Area for Production of Highest Intensity Secondary Beams.) Target Station C is intended for the production of beams for experiments in which rare processes are studied. These experiments will require very high secondary-beam intensities. Among them are investigations of neutrino interactions,  $\mu$ meson interactions, and production of separated beams of rare particles for bubble-chamber bombardment. In such cases, it is advantageous to obtain the most intense secondary beams, and these are found at or near a 0 degree production angle.

In order to exploit beams of secondary particles produced at 0 degrees, bending magnets must be placed in the 0-degree beams to separate the desired secondaries from the intense residual primary proton beam. These magnets then disperse the intense flux of particles produced at all momenta at 0 degrees. This dispersion in turn creates a need for somewhat increased shielding. If the dispersed background is allowed to travel a great distance before it is stopped, the lateral spread and the number of decay  $\mu$ 's become appreciable. The required mass of shielding then becomes very costly.

One possible method of operation of such a target station is to divide the external proton beam with septum splitting devices, as is done in the main transport system, so that separate proton beams impinge upon separate targets, one for each of the 0-degree beams. Independent control of the 0-degree beams then becomes possible. The relative intensities of the secondary beams can be controlled by adjustments of the septum splitter systems. Even when the maximum intensity is required for a single experiment, it is still advantageous to be able to switch the beam from one to another of several independent experiments.

It is not clear from existing data that the angular distribution of secondary particles is as sharply peaked as present empirical formulas suggest. It may be possible to obtain the desired secondaries at small, but non-zero, angles. In this case, it would be possible to avoid the expensive problems of 0-degree dispersion magnets and shielding. Experiments now in preparation will test this angular distribution at proton energies between 12 and 76 BeV.

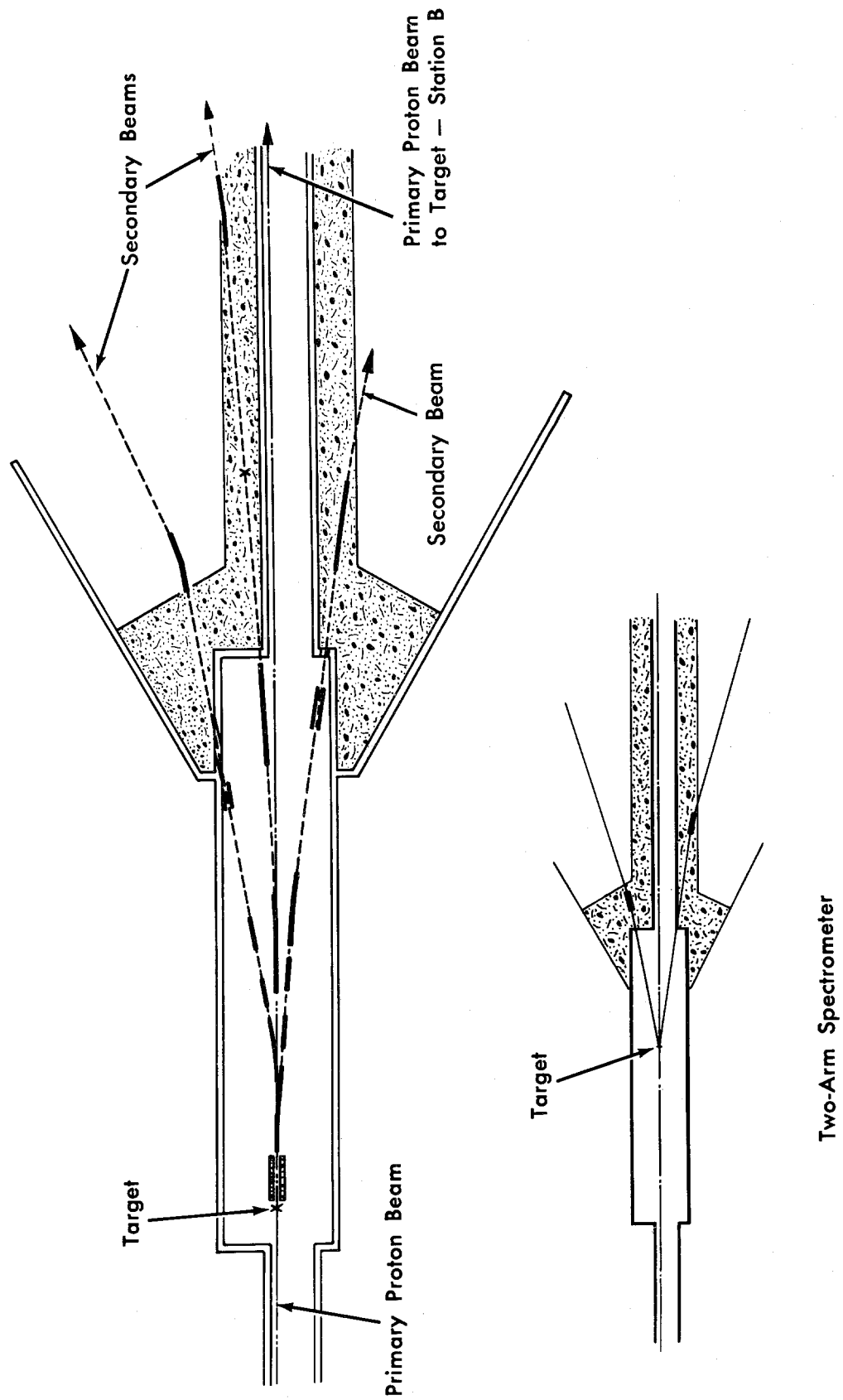


Figure 14-3 — Target — Station A



Target Station A (This Target Station). Target Station A is shown in Fig. 14-3. This target station is designed for a relatively low proton interaction rate; the target thickness will be established to limit the rate to about  $10^{11}$  interactions per second, a very small fraction of the incident beam. The non-interacting protons can be transported to a second target which is located in Target Station B.

One possibility for Station A is to use liquid hydrogen for the thin target. This permits the performance of proton-proton scattering experiments in this area. Simultaneous detection of the two scattered particles will be possible in some cases, as shown schematically in the inset of Fig. 14-3.

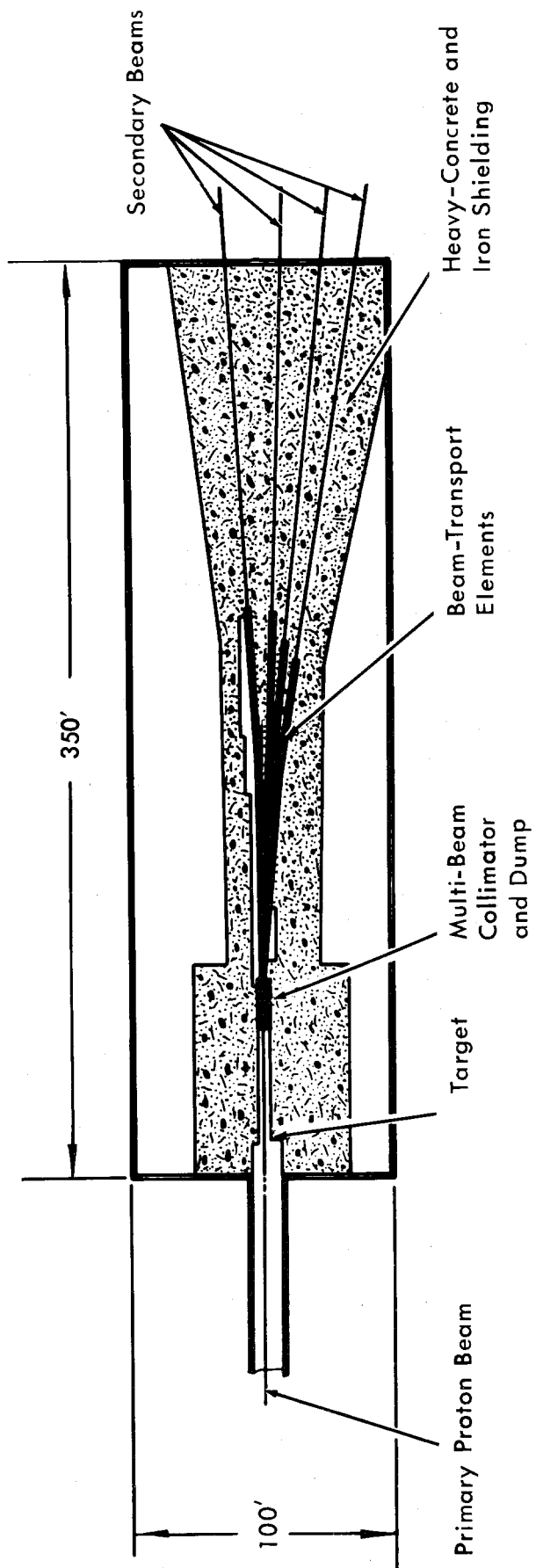
Target Station B (Multi-Beam Target Area). A large number of experiments will require secondary beams of only moderate intensity, say  $10^6$  particles per pulse. Using production angles other than 0 degrees, this intensity can be achieved for many kinds of beams and a number of advantages can simultaneously be realized. The plan for Target Station B, which provides such beams, is presented in Fig. 14-4.

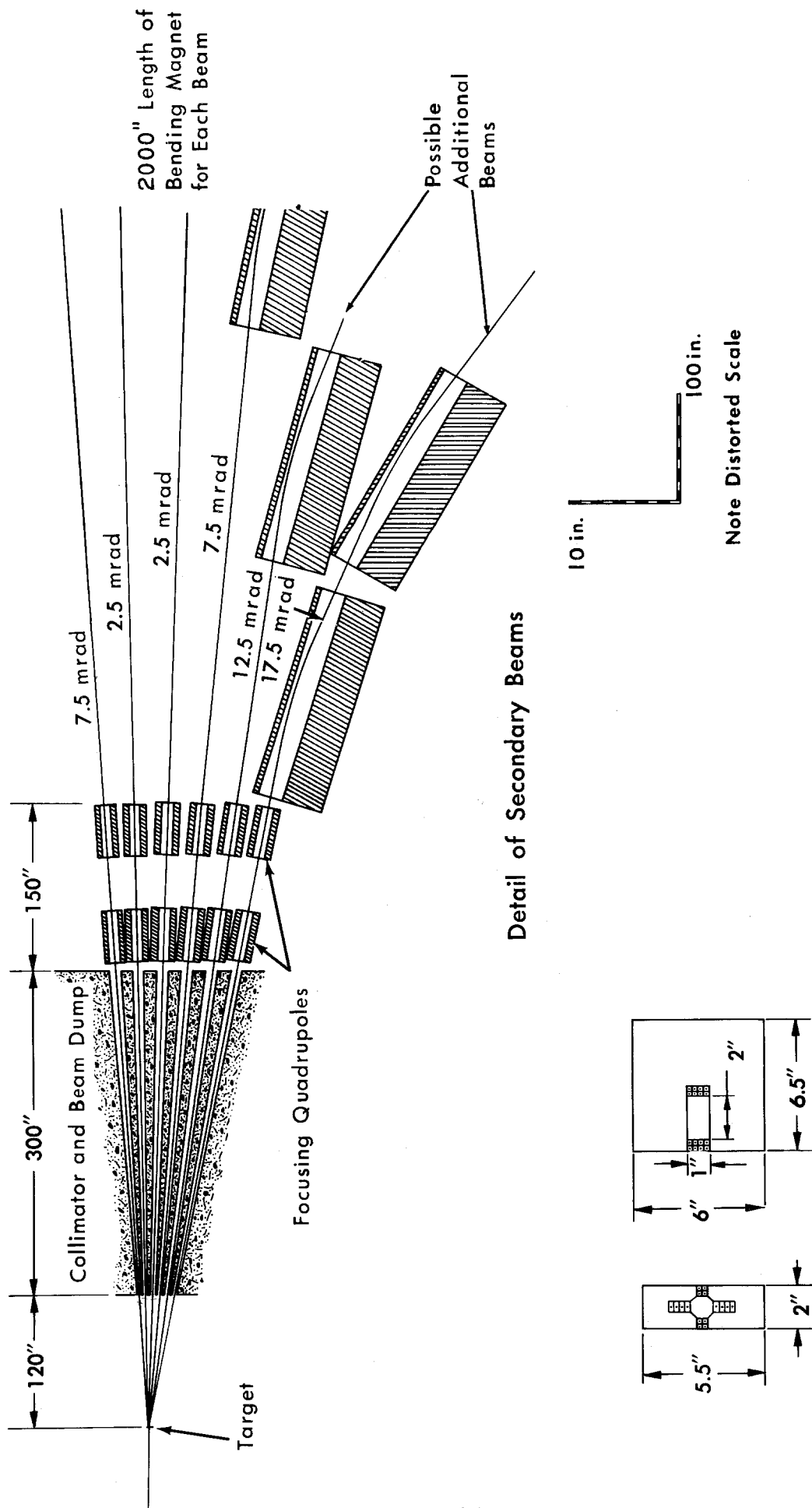
Secondary beams can be produced at angles other than 0 degrees by providing a drift space downstream from the target so that secondaries can separate from the intense proton beam and then be focused and analyzed. In this configuration, the residual unscattered proton beam can be disposed of in a beam dump close to the target.

A major shielding problem stems from the high muon fluxes arising from the decay of pions and kaons produced at the targets. The muons are produced in a concentrated cone around the forward direction, particularly the medium and high energy muons that require the largest thickness of shield. In the absence of a dispersion magnet, such as that required for formation of a 0-degree beam, a long thin beam stop in the forward direction will help to reduce the muon flux emerging from a target area into the experimental areas. Furthermore, if this beam stop is located close to the target, only a small fraction of the forward pions will decay into the more penetrating muons. This is the arrangement that has been designed for Target Station B, as indicated in Fig. 14-4.

This arrangement has the further advantage that totally independent control of secondary-particle sign and momentum can be achieved in each secondary beam. In contrast, when several beams are produced at 0 degrees from the same target, they all pass through a single dispersion magnet and are therefore interdependent.

The four beams illustrated in Fig. 14-4 for Target Station B have production angles of 2.5 mrad and 7.5 mrad. At 100 BeV/c, the number of pions in the 2.5 mrad beam is estimated to be at least one-quarter the flux that would be obtained in the corresponding 0-degree beam<sup>4</sup>. For many experiments, this factor may not be important, especially since with this small loss of flux, beams can be simultaneously and independently operated. Eight or more beams of moderate intensity can be





Cross Sections of Focusing and Bending Magnets

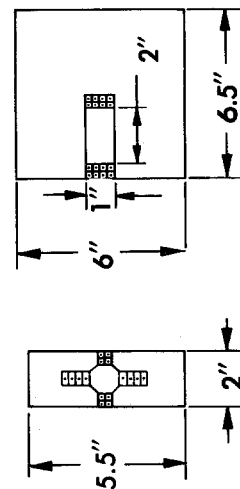


Figure 14-4 — Target — Station B

accommodated at Target Station B.

All of the beams envisioned for Target Station B could likewise be established at Station C. The choice between these two stations will be dictated by intensity requirements and economy. The basic structures that efficiently house these two stations are essentially identical and provision of utilities and other services will be approximately the same for both.

#### 4. Secondary-Beam Areas

Many of the beams produced in Target Stations A, B and C will extend for hundreds of feet beyond the target-station buildings. A variety of configurations of apparatus for physics experiments will be placed at the ends of these beam-transport lines. The details of the experiments and experimental arrangements that will be laid out will not be definitely established for several more years.

Preliminary design and cost estimates for facilities for experiments have included an enclosed area of approximately 70,000 square feet for experimental work with secondary beams from external proton beam targets. As is the case with the experiments themselves, an exact configuration of the desired enclosures cannot yet be finally determined. In fact, the configuration will change during the course of future research work at this accelerator. In the single building that has been developed for the purposes of making cost estimates, the floor slabs are designed to support heavy shielding loads, for example for a neutrino-interaction facility. Full floor coverage by a 30-ton bridge crane is provided, with a clear height to the bridge crane girder of 25 feet. There is a plan for a paved heavy-duty apron along each side of the building. As can be seen in Fig. 14-1, such a building could be located in the vicinity of the large partly-open paved area immediately downstream of Target Station Building B.

Further design work may well develop a plan for several experimental area buildings totaling approximately the same area as the one whose cost has been estimated.

At present, consideration is also being given to the use of inflatable housings to provide cover for some of the experimental areas. In addition, simple, portable shelters for the housing of long secondary beam runs, such as a separated beam for a bubble chamber, are being considered.

Finally, it should be noted in Fig. 14-1 that the relative positions of target areas B and C are so arranged that a single experimental station, perhaps a major fraction of the approximately 70,000 square feet of enclosed experimental space, can be located on the large paved area downstream of Target Area B so as to exploit either short, low-energy secondary beams from Target B or long beams from Target C.

References:

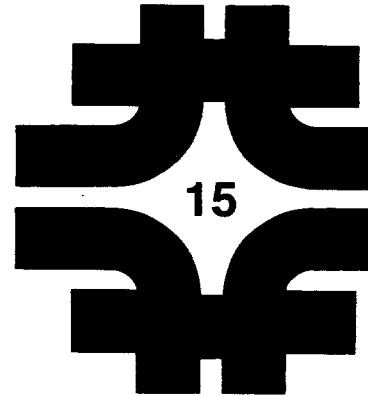
1. Report of the Panel on High Energy Accelerator Physics of the General Advisory Committee to the Atomic Energy Commission and the President's Science Advisory Committee, April 26, 1963.
2. Elementary-Particle Physics. Chapter in Reports on the Subfields of Physics Supplementing the Report of the Physics Survey Committee, NAS/NRC, 1966.
3. High Energy Physics Program: Report on National Policy and Background Information, Joint Committee on Atomic Energy, Congress of the United States, February 1965.
4. L. J. Koester, Fluxes of particles in secondary beams, NAL Note FN-72, September 18, 1967.

## Physical Plant



# Physical Plant

1. Master Plan	15-1
1.1 Site Description	15-1
1.2 Planning Consideration	15-1
1.3 Site Utilization	15-2
2. Accelerator Enclosures	15-3
2.1 Main Accelerator	15-3
2.2 Booster Synchrotron	15-7
2.3 Linear Accelerator	15-8
3. Experimental Areas	15-9
3.1 Description	15-9
3.2 Mechanical Equipment	15-10
3.3 Power Distribution	15-10
4. Support Facilities	15-11
4.1 Area Breakdown	15-11
4.2 Design Considerations	15-13
4.3 Preliminary Concept	15-13
5. Utilities	15-14
5.1 General	15-14
5.2 Utilities - Systems Interfaces	15-14
5.3 Site Utility - System Descriptions	15-14
5.4 Site Utilities Distribution	15-22
6. Site Roads and Walks	15-23
6.1 Typical Road Design	15-23
6.2 Pedestrian Walkways	15-23
7. Central Plants and Site Distribution Systems	15-23
7.1 Central and Individual Heating and Cooling Energy Plants	15-23







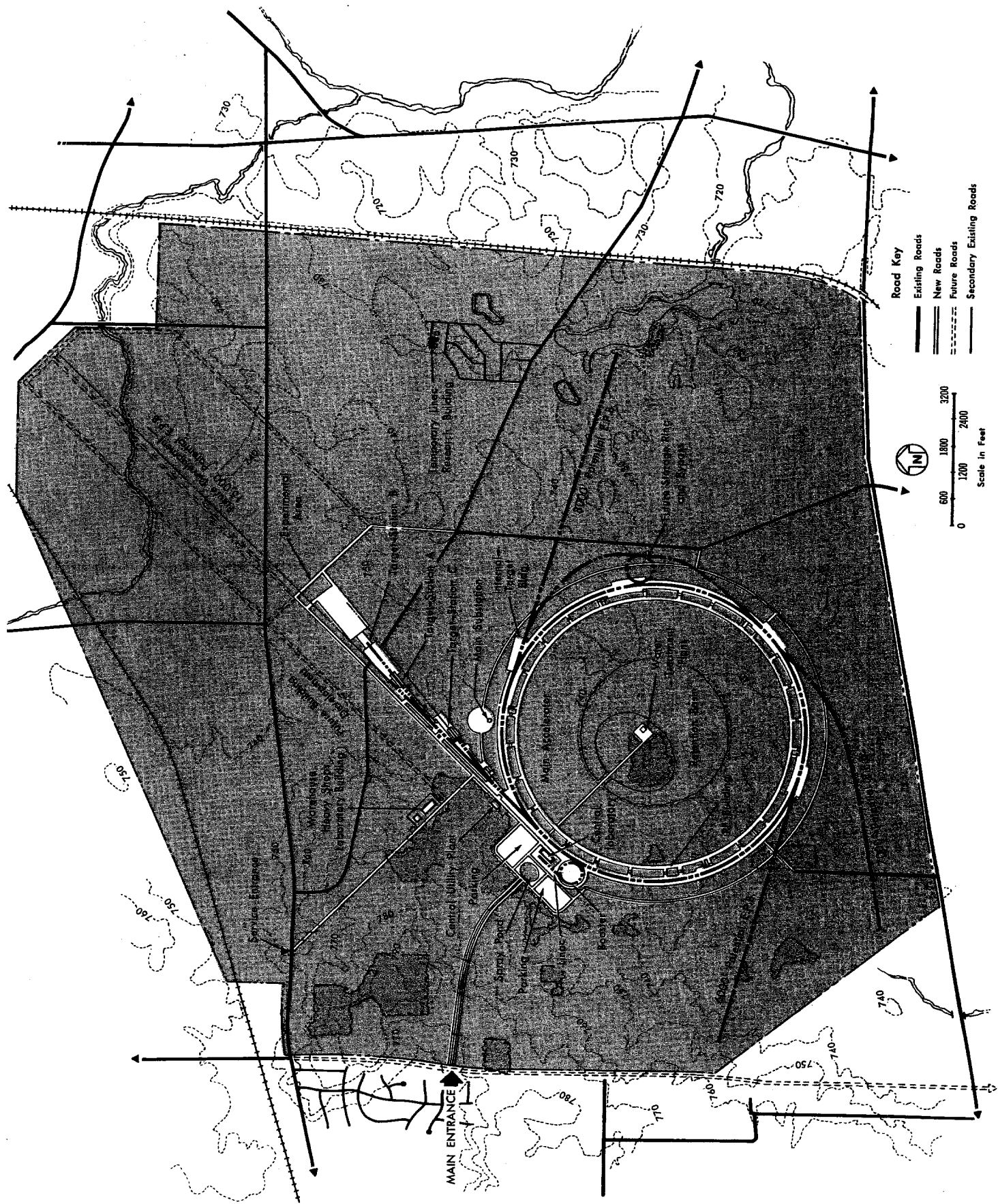


Figure 15-1 — Master Plan



## 15. PHYSICAL PLANT

T. L. Collins, DUSAF

### 1. Master Plan

#### 1.1 Site Description:

Real Property. The site of the National Accelerator Laboratory is a land area of approximately 6800 acres in DuPage and Kane Counties, State of Illinois. The general site boundaries are shown in Fig. 15-1.

Physical Features of the Site. Maximum relief over the entire site is approximately 70 feet. High ground at the northwest corner slopes gently to a swamp area at the southeast corner. The general character is gently rolling farm land with scattered wooded areas. Subsurface soils consist of wind-deposited silt over glacial clays. Lower strata are block conglomerate over a gently sloping limestone bedrock approximately 70 feet below the surface.

The Village of Weston and numerous farmsteads lie within the site boundary. Two railroads, one a belt-line trunk, the other a single-track spur, serve the site along the northern and eastern boundaries. State Highway 56 traverses the southern boundary and nearby routes parallel the north, east and west boundaries. Three county roads pass through the site, providing adequate access for construction operations.

1.2 Planning Considerations. The master plan should locate the accelerators, experimental areas, and support facilities so as to promote economical construction and operation, to provide good communication and circulation patterns, to utilize and enhance the natural environment, and to provide capability for expansion of the Laboratory, particularly the experimental areas. The master plan must also provide for utility supplies and distribution, sewerage, drainage, and radiation shielding.

The master plan, which is shown in outline in Fig. 15-1, has as its most important elements the central location of research offices and laboratories with respect to the accelerator and experimental areas and the vertical planning of the central laboratory.

These special considerations have been given preliminary study in the development of the proposed master plan. Studies will be continued in depth during Title I design.

### 1.3 Site Utilization.

Main Accelerator. The land area required to accommodate the main accelerator dominates site utilization. Five basic solutions are possible on the nearly square proposed site. These five would place the main accelerator, respectively, in one of the four corners or near the center of the site.

The primary advantages of the proposed main-accelerator location shown in Fig. 15-1 are: (i) uniformity of subsurface soil conditions, (ii) greatest potential capacity for development of future external proton beams (EPB's), (iii) most favorable utilization of the prime northwest portion of the site, and (iv) best opportunity to utilize the low swampy area along the east side of the site for drainage and waste disposal.

Booster. The smaller diameter of the booster (150 m versus 2000 m for the main accelerator) permits a wider choice of potential sites for the booster, insofar as utilization influences the choice. The site proposed is based on planning considerations: (i) It is desirable to keep the main-ring injection and extraction points close to one another. (ii) it is desirable to keep the booster close to the office and laboratory support core, and (iii) the booster should be outside the main accelerator ring for ease of access.

Linear Accelerator. Based on siting constraints imposed by the locations adopted for the main accelerator and the booster, two potentially workable Linac sites result: (1) as shown in Fig. 15-1 or (2) south of the booster injecting into the booster, also in a counterclockwise direction. The chosen configuration results in a more compact overall site plan without penalty to accelerator performance.

Experimental Area. A primary objective of the master plan is maximum site capacity for target stations in an extracted external proton beam. This requirement has been satisfied by two features of the master plan:

- (i) The initial EPB has been located on the site to allow extension diagonally to 15,000 feet of length.
- (ii) Additional potential EPB's of 8,000, 9,000 and 6,000 feet may be added around the ring as needed plus a future storage ring and bypass. These are indicated in Fig. 15-1.

A second planning objective is the location of experimental areas in close proximity to supporting shops and supplies.

Shops. There is a requirement for on-site industrial support, including heavy shops, heavy (high-bay) laboratories and assembly areas, shipping and receiving, storage and salvage. A heavy shop, a heavy laboratory, a warehouse and a canteen have been provided in the master plan to accommodate these functions. The gradual evolvement of a storage and salvage yard must be included in the final detailed master plan.

Existing wooded areas have been employed in the master plan as a natural screen for these industrial-activity areas. A separate service entrance road has also been planned.

By placing the shop area near the central laboratory, physicists can benefit by convenient access to shop support, while other activities in the support center are effectively insulated from distractions by the screening and separated traffic patterns.

Central Laboratory. Office and light-laboratory functions have been developed, in formulation of the master plan, into a single support center serving as a hub for personnel activity for the entire site.

The Director of the laboratory and his working staff will maintain their headquarters in this central laboratory. Resident and visiting physicists will work here. They will often have limited available time, so that lost time resulting from extended circulation distances of the absence of needed support services must be minimized.

The operational aspects of the support-center planning concept will be studied in detail during Title I design.

Site Utilities. Each of the principal site facilities requires roads, parking, power distribution, water supply, sewerage system, heating and cooling capability and other specialized types of utility support. The master plan has been based on preliminary studies of central versus individual systems for each required utility service. Utility centers serving more than one activity have been located for minimum distribution costs.

Each utility system has also been planned to accept future accelerator growth as an "add-on" without disruption of the existing system.

## 2. Accelerator Enclosures

### 2.1 Main Accelerator.

Physical Description. The main-accelerator enclosure will be a horizontal ring approximately 20,600 feet in circumference. A typical cross section through the ring will be a horseshoe-shaped magnet enclosure 10 feet in diameter, as shown in the right-hand part of Fig. 15-2, with a floor elevation of 725 feet. This elevation is from 15 to 22 feet below natural grade. Protection from radiation emission will be provided by a cover of earth shielding fill.

The main accelerator will also include the internal proton beam (IPB) target station and adjacent experimental area (Fig. 14-1).

The main-accelerator circumference will be subdivided into six equal superperiods. The magnet lattice within each superperiod has different parts that will require different enclosure cross sections. These parts are:

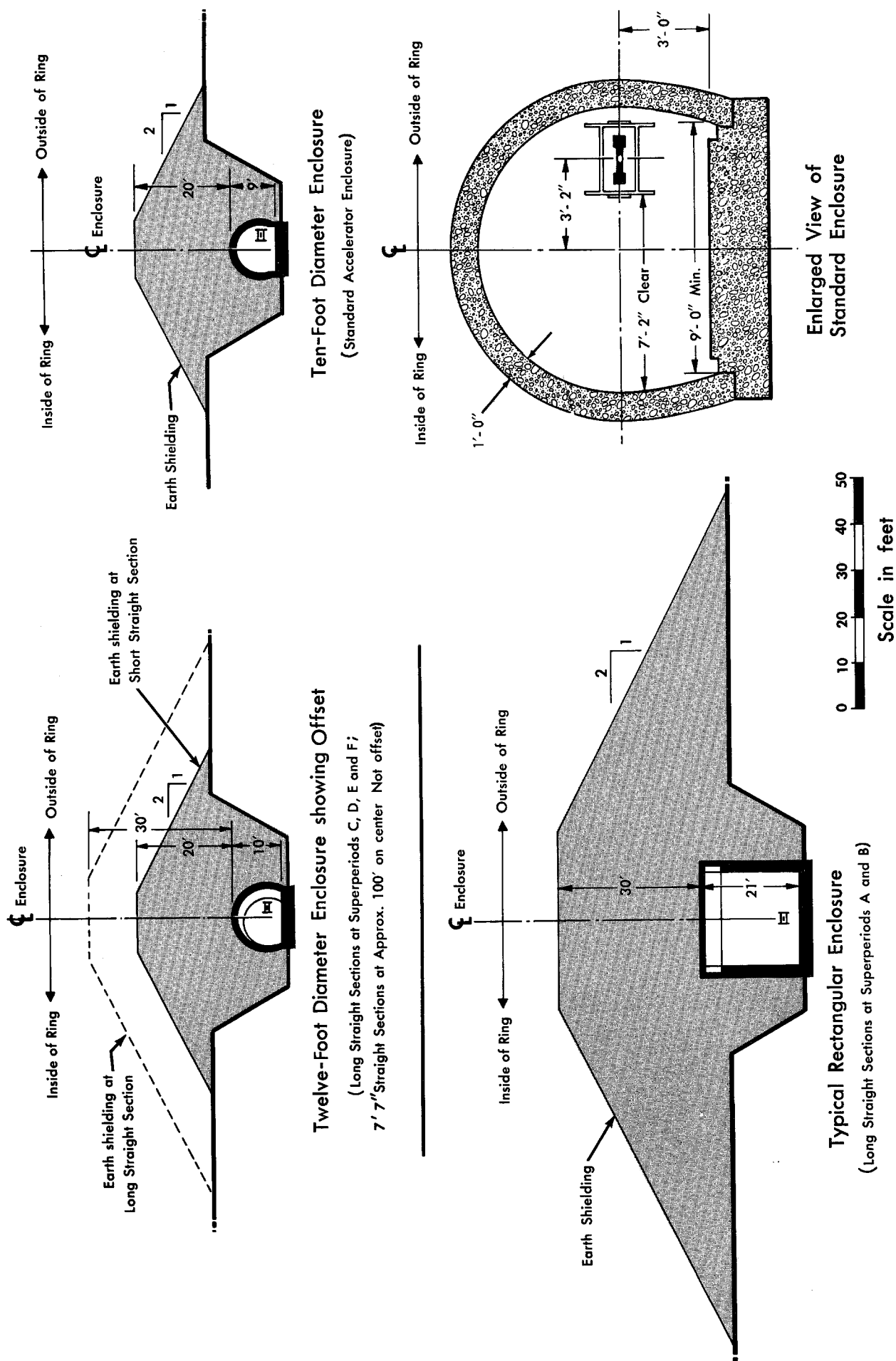


Figure 15-2 — Main-Ring Enclosure Cross Sections

- 1) A typical series of bending magnets spaced to provide a 1-foot straight section between each two magnets. The required enclosure will be the typical 10-foot diameter section of Fig. 15-2.
- 2) An arrangement of magnets (both bending magnets and quadrupoles) spaced to form a 7-foot straight section. The required enclosure will be an enlarged 12-foot diameter section as in the upper right of Fig. 15-2.
- 3) A special arrangement of magnets (omitting four bending magnets) forming a medium straight section. The required enclosure will be the enlarged 12-foot diameter horseshoe section.
- 4) A special arrangement of bending and quadrupole magnets providing a long straight section.  
The typical enclosure for a long straight section will be the enlarged 12-foot diameter horseshoe section with the centerline offset one foot to the outside. This offset enlargement is shown at the upper left in Fig. 15-2. It will be used in long straight sections C, D, E and F, the accelerating-system straight section.
- 5) The long straight sections in superperiods A and B will be used for external proton beam (EPB) extraction and for the internal proton beam (IPB) target station respectively.  
The additional working space required will be provided by a rectangular section varying from 20 to 35 feet in width and 21 feet in height, with a bridge crane. This section is shown at the lower left in Fig. 15-2. A plan view of the extraction straight section is given in Fig. 15-3, while the IPB area was shown in plan view in Fig. 14-2. The accelerator ring position in the enclosure is also shown in Fig. 15-2.

Utility support will be provided to the main-accelerator components by the facility support systems discussed in Sec. 5 of this chapter. These systems will include power, cooling water, ventilating air, and communications.

Access. Access will be required into the main-accelerator enclosure for special maintenance vehicles, equipment and personnel. Two types of access are provided:

- 1) Personnel access passages from utility buildings located at 24 points around the periphery. Passage will be 3 feet by 9 feet in cross section.
- 2) Vehicle and equipment access from a vehicle-access building and passage located in each superperiod.

Auxiliary Buildings. Auxiliary buildings for the main accelerator will include:

- 1) Utility Buildings. Power, LCW, air-purge systems. Total number: 24, with 6 major (includes a cooling tower) and 18 minor.
- 2) Vehicle-Access Buildings. Total number: 8



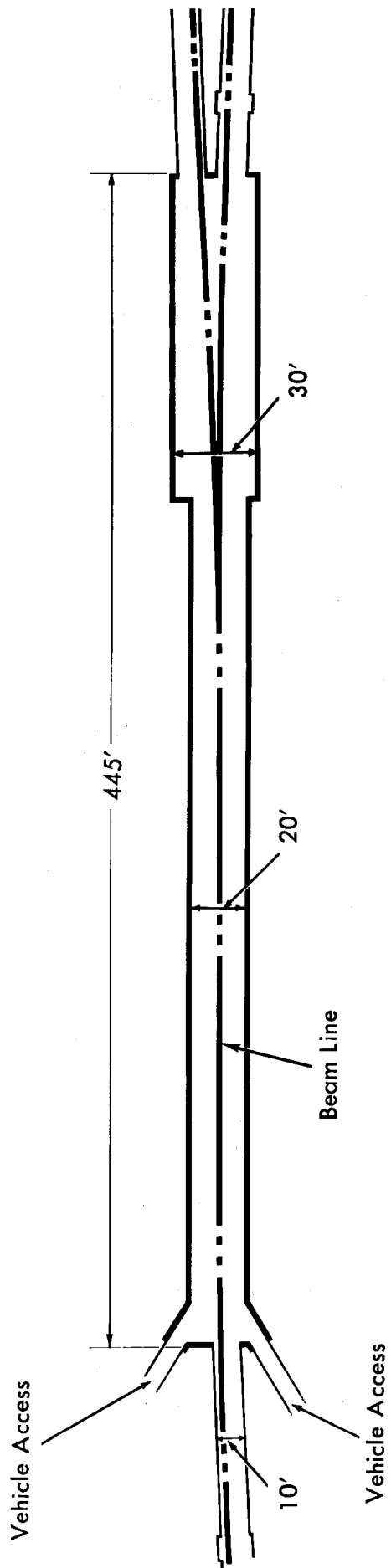


Figure 15-3 — Extraction Straight Section

- 3) Substation Pads. 12 for facility power  
24 for pulsed magnet power  
1 for rf power

Support for the main accelerator will also include a road system, a domestic-water system, and a sanitary system.

Internal-Target Area. The internal-target area includes a beam-transport housing 35,000 square feet of enclosed experimental floor space, a power-supply building, an electrical substation and a paved staging area outside the experimental building. It is shown in Fig. 14-2.

## 2.2 Booster Synchrotron.

Description. The booster will consist of a standard 12-foot diameter concrete horseshoe-section magnet enclosure, circular in layout, with an approximate diameter of 500 feet. It will be located at the end of the linear accelerator and connected to it by a beam-transport enclosure. A rectangular concrete segment of the booster ring will be designed to connect to the beam-transport enclosure at the injection point. A similar rectangular segment lying diametrically opposite the injection point will accommodate the extraction point. The extraction system for the booster will include a beam dump, a small spur of standard 10-foot diameter enclosure containing a very high density beam-stop material. The floor elevation of the booster ring along with its injection and extraction network will be 725 feet.

The booster magnet enclosure will be shielded for radiation emission by earth fill. For access and safety, four underground stair exits from the booster through the earth shielding will be provided. One of these exits will be equipped with a hydraulic elevator for vehicle access to the booster from the outside. The booster accelerator ring is close to the inner radius of the enclosure.

A continuous ring utility gallery will be constructed on top of the earth shielding about 20 feet above the booster ring and concentric with it. This gallery will house the power equipment and necessary utilities for the booster ring below. Interconnection of utilities from the gallery to the booster will be by way of sleeves through the earth shielding at various points around the circle. The gallery itself will be a visible architectural element and reflect the functional character of the total design. In cross section, the gallery will be basically rectangular, about 12 feet wide and 14 feet high. It will widen at one point to accommodate heating and ventilating equipment, toilet and emergency shower.

Booster Supporting Systems. Electrical power will be distributed underground at 13.8 kV, 3 phase, 60 Hz from the main substation to unit load substations, located around the utility gallery, that supply power for the accelerator components at 480 V, 3 phase, 60 Hz. The ac and dc power equipment will be supplied with regulated power at 13.8 kV, 3 phase, 60 Hz, and the interface occurs at the connecting points to this equipment.

### 2.3 Linear Accelerator.

Description. The linear accelerator will have three principal parts: (1) a chamber for the preinjector proton source, (2) a linac housing approximately 550 feet in length, and (3) an equipment bay for accelerator power supplies, controls, and supporting equipment. These are shown in Fig. 10-1.

Beam transport between the linac and the booster synchrotron will include a beam dump upstream of beam debunching and a final beam dump upstream of the entry to the booster synchrotron.

Preinjector chambers for two preinjectors and their associated equipment are planned. Accommodation for preinjectors and the associated laboratory space will require a 10,000-square foot area, including preinjector pits 60 feet by 70 feet, with a clear height of 35 feet. The floor elevation of the pit is depressed 13 feet below the linac housing floor.

The linac housing, a shielded enclosure for the linac cavities, has a rectangular cross section 14 feet by 12.5 feet high. A 2-ton bridge crane will be installed for transferring equipment from one side of the linac to the other. Earth shielding will be used for protection from radiation from the linac housing.

The equipment bay, 40 feet in width and approximately 19 feet in clear height, will parallel the linac housing. It will have a length of 575 feet. This area will have full bridge-crane coverage with a minimum lifting capacity of 10 tons.

Linac Support Systems. Electrical power will be distributed underground at 13.8 kV, 3 phase, 60 Hz, from the main substation to unit load substations located adjacent to the linac, which supply power for linac components and building facilities at 480 V, 3 phase, 60 Hz.

Equipment cooling, using low-conductivity water (LCW), will be supplied from a central utility plant at 96° F. For equipment cooling in the beam-transport enclosure and in the preinjector-transport area, LCW at 75° F. will be supplied by a heat exchanger using a chilled-water source from the central utility plant.

Room air temperature, filtration, and humidity control required for proper equipment operation will employ air-handling units uniformly distributed within the areas served. Absolute filters will be provided in the preinjector and laboratory area. Hot water and chiller water will be supplied from the central utility plant, shown in Fig. 15-1.

Fire protection will include smoke detectors for actuation of the alarm system, fire-hose stations and fire extinguishers, including CO<sub>2</sub> and foam-type extinguishers.

### 3. Experimental Areas

3.1 Description. The initial external experimental areas are planned to include three target stations plus experimental buildings.

Beams from the accelerator will be carried through a beam-transport enclosure of the standard 10-foot diameter cross section to two switching stations. At Switching Station S1, a primary proton beam will be extracted at an angle of 7 degrees from the EPB. An additional primary beam will be extracted at an angle of 5 degrees at Switching Station S2. These switching stations and beams are shown in Fig. 14-1.

Beam-transport enclosures between switching stations and the respective target stations will be inclined, so that target stations and related experimental areas are located at a natural grade elevation of approximately 740 feet. These beam-transport enclosures will utilize the standard 10-foot cross sections.

In general, the experimental area does not require all-weather protection. Experimental programs requiring the establishment of beam paths during unfavorable seasons can be accommodated by Target Stations B and C, each of which is protected by a building having enough functional flexibility to permit a wide range of potential secondary-beam paths.

Target Station A requires a shielded target area, 30 by 160 feet, served by a bridge crane of 20-ton capacity. Experimental-area pads for secondary-beam paths will be provided. The primary beam will continue to Target Station B.

Target Stations B and C will be similar in concept. Each will require a Target Building which is shown in Fig. 14-4 imposing a minimum restraint on research operations. The building slab will be designed to support modular shielding block loads of 4,000 pounds per square foot. Special slabs will be used in the areas where the shielding load may be increased to 7,500 pounds per square foot. A 30-ton bridge crane with a clear height of 35 feet to the bridge-crane girder will handle shielding blocks and other live loads associated with research operations.

There will be a paved area of approximately 80,000 square feet outside each target building.

Section 4 of Chapter 14 discusses the status of the concepts of structures for secondary-particle beams and experiments. For planning purposes, an enclosed area of approximately 70,000 sq ft has been used. Floor slabs will be designed to support shielding loads. Full floor coverage by a 30-ton bridge crane is proposed, with a clear height to the bridge-crane girder of 25 feet. Paved aprons along the buildings are planned.

### 3.2 Mechanical Equipment.

General. Mechanical-equipment requirements for the experimental areas include conditioned-air purge for beam-transport enclosures, switching stations and Target Station A. Heating and ventilation will be required for Target Stations B and C and the experimental building. Cooling water for magnets and other equipment will be distributed throughout the experimental areas. Domestic water will be distributed for fire protection and toilet rooms.

LCW Systems. A distributed low-conductivity water (LCW) system for experimental-area equipment cooling will be designed on a local cooling basis. The planning concept will employ seven cooling tower stations supplying 96° LCW sized for local demand.

Air-Purge Systems. Equipment will be local, using package systems. These systems will be located in typical utility buildings, similar to those of the main accelerator, located at convenient points along the beam line.

Building Heating and Ventilating. Winter heating for target-station and experimental-area buildings will be by hot-water systems supplied by boilers located within the respective buildings served.

Ventilation will be supplied by louvered air intakes and roof exhaust fans. Local ventilation for hazardous gas fumes will be provided by separate roof exhaust fans and flexible duct runs.

3.3 Power Distribution. Electrical power will be distributed underground at 13.8 kV, 3 phase, 60 Hz, from the master substation to stationary unitload substations and plug-in stations located near the switching stations, target stations and experimental areas supplying power for the dc magnets at 480 V, 3 phase, 60 Hz. The distributed power capacity for experimental use is approximately 100 MW, the maximum power demand for experimental use at the main substation is limited to 60 MW.

Several additional portable substations rated at 2500 kVA will be provided in addition to supply power to non-fixed experimental loads.

Electrical power for facility requirements will be supplied by separated feeders connected to a number of unit load substations appropriately located for distribution at 480/277 V for motor and lighting loads. Dry transformers will be used for 120/208 V power requirements. Power capacities for service to the experimental areas are given in Table 15-1.

Table 15-1. Experimental-Area Power Capacities

Location	Component Power	Facility Power
Target Station A	5 MW Stationary Sub-station 10 MW Plug-in*	1.5 MW
Target Station B	10 MW Stationary Sub-station 20 MW Plug-in*	1.5 MW
Target Station C	10 MW Stationary Sub-station 20 MW Plug-in*	1.5 MW
Experimental Building	10 MW Stationary Sub-station 20 MW Plug-in*	1.5 MW
Internal-Target Experimental Area	5 MW Stationary Sub-station 10 MW Plug-in*	1.5 MW

\*Plug-in to accommodate portable substation

#### 4. Support Facilities

The support facilities will be designed to provide shelter, service fabrication and research support for the entire Laboratory. These facilities will house a population of 2000 people in structures having a gross area of 600,000 square feet. Figure 15-4 gives an overall view of the support facilities.

A breakdown of the estimated population of the Laboratory is given in Table 17-1. In that table, the category "Other Support" lumps together the following activities: administration, accounting, personnel, technical information, public information, motor pool, protection and fire departments, plant-engineering services, utilities services, custodian, groundskeepers, medical, cafeteria and auditorium services.

4.1 Area Breakdown. The planned gross area of 600,000 square feet for Support Facilities will be allocated to provide 440,000 square feet in the central laboratory and 160,000 square feet in the industrial area.

The central laboratory will house approximately 1550 people. Functions will include reception for visitors, office of the Director, office and light laboratory facilities for resident and visitor physicists, engineering, laboratory support services, accelerator operations and control center, electronics and materials-testing shops, computer center, film processing laboratory, library, auditorium, cafeteria for 450 people, dining facilities for 250 people, canteen and lounge centers, and medical-first-aid facilities.

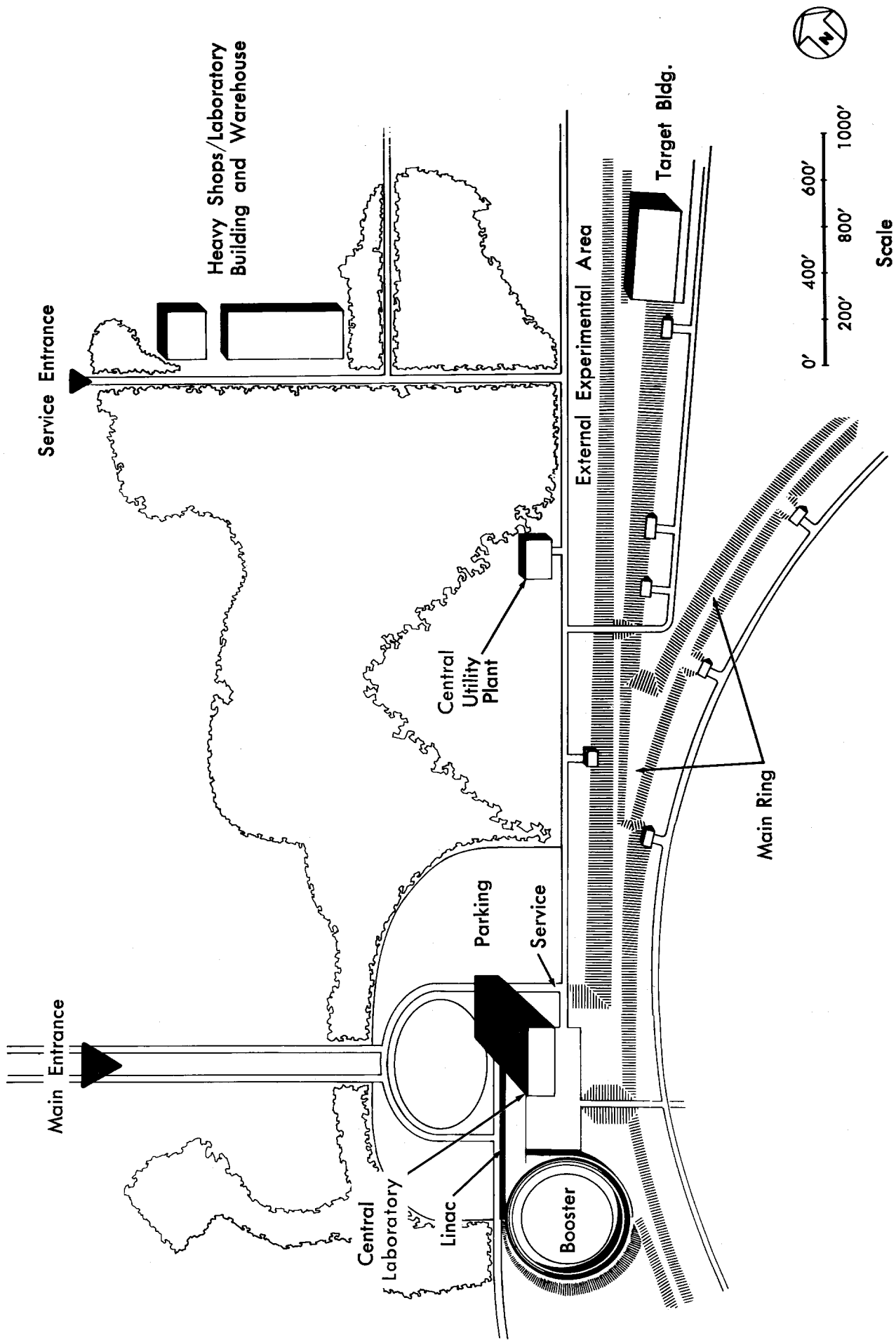


Figure 15-4 — Support-Facility Areas

The industrial area will house approximately 450 people. Functions will include heavy shops (machining, welding, electrical and painting), receiving, shipping and storage warehouse, heavy-laboratory, staging and assembly facility, motor-pool dispatch and service area, garage for emergency vehicles and a cafeteria-canteen facility.

4.2 Design Considerations. The relation of the control center to the accelerators and to accelerator operations is of prime importance. The acceleration operations center in turn has a strong direct relationship to the balance of the resident physics and general service group. The ideal would be to be able to go from one's office (resident physics, engineering, administration or visitor physics) to accelerator operations and the control center easily, quickly, and directly without going outside. In turn, an individual should also be able to reach any of the other physics, general, industrial, accelerator and experimental-service groups easily, preferably by a reasonably short walk. The industrial, accelerator, and experimental-service facilities should have convenient pedestrian and vehicle access to the experimental areas themselves.

As a result, the ideal scheme is one that, because of the prime relationships of the accelerator and the climate, will have an extremely high population and building-area density. These facilities should be located between the linac and the experimental areas on the outside of the main ring. They should be so designed and distributed that one has free and direct access to his colleagues and the Laboratory services through visual, vocal and pedestrian communication.

4.3 Preliminary Concept. As conceived, the control laboratory will provide a closely grouped arrangement comprising offices, light laboratories, control center, electronic shop, computer center, film processing, medical, dining and auditorium facilities. A multi-level structure is planned of concrete-frame or steel-frame construction with precast concrete exterior walls. Unit masonry and metal lath and plaster will be used for fixed interior partitions. Movable partitions will be used consistent with need and safety regulations. Exposed ceilings are planned for laboratories, shops and equipment rooms. Other areas will have suspended ceilings, acoustical or non-acoustical. Floor will be resilient tile, ceramic tile or precast terrazzo. Full air conditioning, separate passenger and freight elevator service and both 120 and 480 V power distribution will be provided.

The preliminary concept for the industrial area envisions a grouping of industrial support separated and visually screened from the central laboratory, but convenient to each activity served. As a preliminary concept, the architectural approach for the industrial area will use high-bay industrial construction, with a clear span of 100 feet for industrial functions other than warehouse. Bridge-crane coverage of 20-ton capacity of the entire floor area is planned. Warehouse space will be planned for forklift handling of stored materials. A minimum column spacing of 40 feet is planned.



Exterior treatment of industrial-area buildings will be designed for site unity with the central laboratory, accelerator and experimental buildings. Air conditioning will be provided for areas involved in precision work.

## 5. Utilities

5.1 General. Development of the site will include the following utility systems:

- Main substation and primary power distribution
- Water treatment and distribution
- Storm-drainage system
- Waste-water collection and treatment plant
- Site roads and sidewalks
- Central plant and distribution systems for chilled water, hot water and Low Conductivity Water
- Outside lighting
- Landscape sprinkler systems

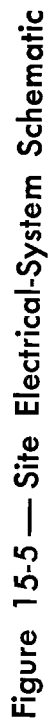
5.2 Utilities-Systems Interfaces. Site utility systems considered in this section include those systems serving more than one major building or activity. The typical interface will be the construction limits of a building or activity or five feet outside such a building.

5.3 Site Utility-System Descriptions.

Main Power Substation and Primary Power Distribution. Electrical power supplied to the National Accelerator Laboratory will be from the Commonwealth Edison Company transmission lines passing along the east boundary of the site at 345 kV and 138 kV, 3 phase, 60 Hz. Power supply reliability will be provided by means of a switching station capable of selecting one of the two transmission lines in each system, 138 and 345 kV.

The distribution system on the site is shown schematically in Fig. 15-5. A double 3-phase transmission line will carry the power from the switching station to the main substation, a distance of approximately 4 miles. The main-substation location is shown on the master plan Fig. 15-1.

Main Substation. This will be arranged in two sections: (1) 345/34.5kV, 90 MVA transformer capacity "OA" 3 phase, 60 Hz, delta-wye connected,  $\pm 10\%$  LTC, oil-filled transformers, fully protected by means of oil circuit breakers capable of interrupting the maximum available short-circuit current. This section will supply power to the pulsed magnet load in the main-ring enclosure and the rf station equipment. (2) 138/13.8 kV, 124 MVA transformer capacity "FOA", 3 phase, 60 Hz, delta-wye connected 10% LTC, oil-filled transformers, fully protected by means of oil circuit breakers capable of interrupting the maximum available



short-circuit current. This section will supply: (1) the conventional power to the entire project, (2) power for the booster accelerator, (3) power for linear-accelerator components, and (4) the entire dc magnet power supply for the IPB and EPB experimental facility.

The main substation will provide for expansion at both sections to fulfill electrical power requirements for 400 and 500 BeV Accelerator power demands.

Primary Power Distribution. The 34.5 kV 3-phase 60 Hz system will distribute power to the static converter stations for the pulsed magnet load. There will be three circuits employed around the main accelerator ring. Two of the circuits will be connected through 3-phase autotransformers, one to one ratio but with 5 electrical degrees phase displacement. The third circuit will be connected through a 3-phase series reactor. Power factor and voltage-stabilization correction will be applied on the 34.5 kV bus at the master substation by the use of the step-down transformers and synchronously switched SCR-controlled capacitors.

The 13.8 kV, 3 phase, 60 Hz, power distribution will be installed throughout the project with RINJ type cable.

Unit load substations of various sizes, 3-phase, oil-cooled, will be connected to this system to step down the power to 480/277 V and 208/120 V, whichever is required in each particular facility, with the exception of the large chiller motors, where the power will be stepped down to either 2400 or 4160 V, depending on the exact size of the motors.

Electrical power for all power supplied to accelerator components and magnets in the booster, linac and experimental facilities will be 480 V, 3 phase, 60 Hz solidly grounded neutral.

Integral-hp motors will be supplied power at 480 V, 3 phase, while fluorescent lighting will be 277 V, with phase-to-neutral connection of the 480 V supply.

Dry transformers will be used to step down power to 120/208 V for fractional-hp motors, receptacles, incandescent lighting, controls and instrumentation power. Voltage regulators will be used to limit voltage fluctuation for instrumentation and control equipment to within 2%.

The low-voltage distribution will be with "RHW" type cable installed in rigid conduit and concealed wherever possible.

#### Water Supply, Treatment and Distribution.

Supply Sources. The supply of water to meet laboratory, domestic and accelerator demands will be obtained from three principal sources: (1) Ground water from shallow wells, (2) Runoff from on-site precipita-

tion, (3) Surface water from Fox River during periods of flow in excess of 200 cubic feet per second, as measured at Algonquin, Illinois. The on-site water-supply system is shown schematically in Fig. 15-6.

Transmission and Storage Facilities. The focal point of the raw-water supply will be a 100 acre-foot (325-million gallon) capacity reservoir, serving as a combination regulatory and catchment facility. Water will be pumped from the Fox River through a transmission line, a distance of 14,000 feet, to the on-site raw-water reservoir. At this point it will be mixed with runoff water from the site. The reservoir will provide a retention time of approximately three months during periods of peak accelerator demand, assuming that on-site well water is not being utilized during the same period.

Assuming full utilization of on-site water resources, planning studies indicate that the proposed storage reservoir can provide water supply for approximately 180 days without pumping from the Fox River.

Treatment Plant. Water will be pumped from the reservoir, blended with on-site well water and supplied to the treatment plant. Treatment will consist of clarification, softening, filtering chlorination and pH control.

Treated water will be stored in a 3.0-million gallon covered reservoir and pumped directly into the distribution system.

Distribution System: System demands have been estimated to be as follows:

- (1) Domestic requirements of approximately 420 gallons per minute, based on average daily use per peak month, for a 2000-person resident population, 1000 average daily visitors plus a 25% initial expansion factor, for a total equivalent design population of 2600 persons.
- (2) Makeup water for cooling systems should peak at approximately 2000 gallons per minute or 2.9 million gallons per day. This will provide the cooling requirements for the full-intensity 200 BeV accelerator and support facilities.
- (3) Fire flows for various areas of the site will vary from a minimum of 1000 gallons per minute to a maximum of approximately 1750 gallons per minute with a duration of four hours.
- (4) Irrigation requirements as now planned will be limited to an area of 100 acres in the vicinity of the central laboratory. A total demand of 3 inches per annum, based on four applications during the four summer months, has been used to establish a peak flow of 370 gallons per minute.
- (5) Miscellaneous water requirements, including losses due to evaporation, filter backwash, etc., are estimated at approximately 280 gallons per minute.

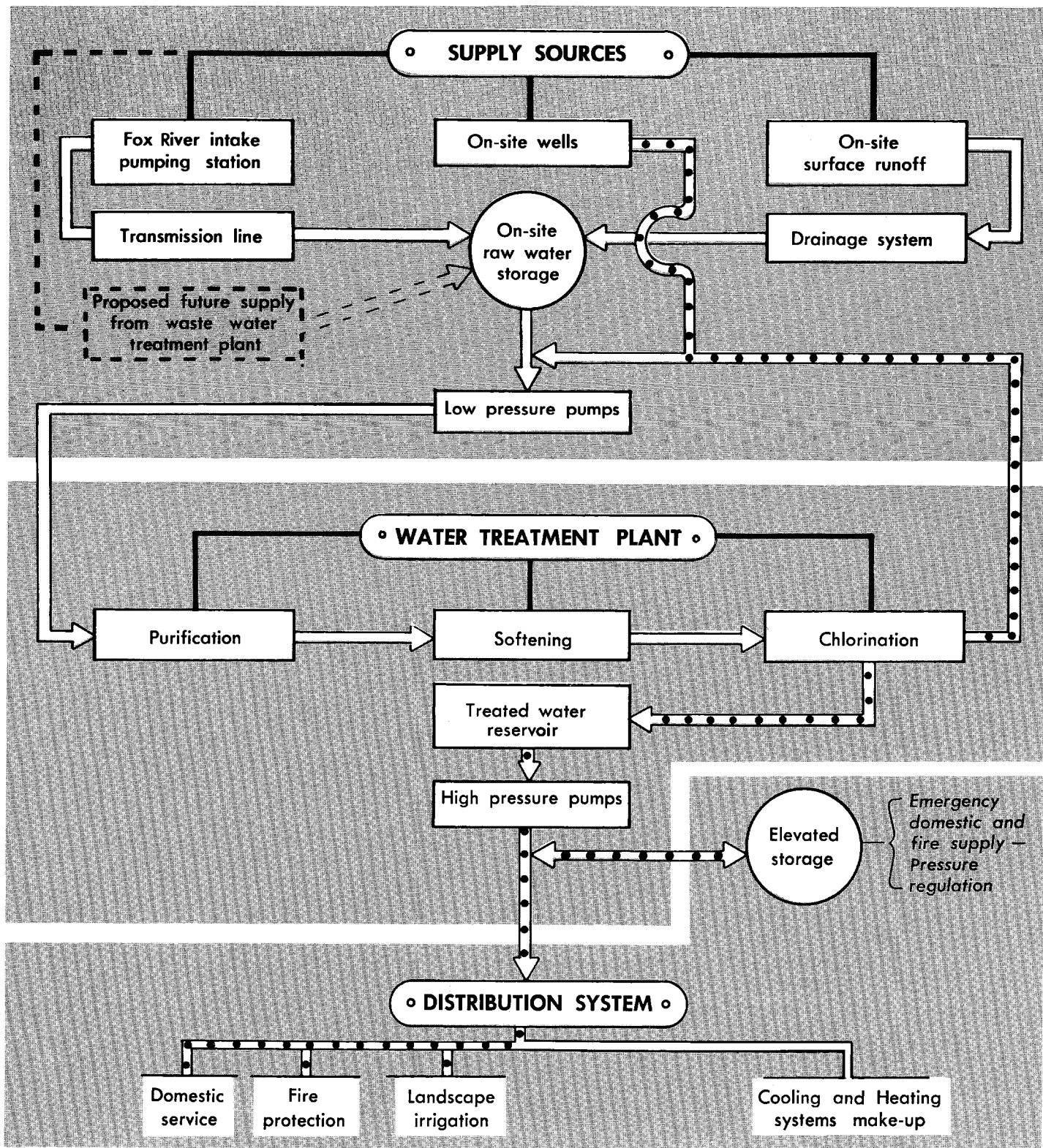


Figure 15-6 — Water Supply System

Water-main sizes are based on summation of the various demands appropriate for a given area. Pressure regulation will be accomplished by using a 500,000-gallon elevated storage reservoir which will "float" on the entire system. Generally, emergency demands will be met by gravity flow from the elevated reservoir. Fire flows during periods of peak system demand will be met by supply from both the elevated reservoir and high-pressure water pumps at the water treatment plant.

Future Expansion. Possible future increases in system demands, (in excess of the 25% domestic-demand expansion factor) may be readily accomplished without on-site service interruption as follows:

- (1) Additions to Fox River pumping facility.
- (2) Enlargement of on-site regulatory storage and pumping facilities.
- (3) Extension and additional looping of distribution system.
- (4) Reclamation and recycling of waste-water treatment plant effluent, as indicated schematically in Figs. 15-6 and 15-7.

Drainage System. The elevation of above-ground facilities will be set to permit maximum utilization of on-site drainage courses. Controlled ponding of runoff will be utilized at various locations to reduce the size of the outfall facilities.

Site Drainage Plan. A principal drainage pond will be located in the center of the main-ring area. A system of drainage swales, channels, and culverts will transport the runoff from the perimeter of the main-ring road to the pond. In addition to control of peak flows, detention in the pond will clear the water of silt and other suspended matter. A major culvert at the westerly side of the ring will transport the pond overflow to the raw-water storage reservoir. The size of this culvert will be chosen to protect the ring interior from a 100-year storm when working in conjunction with the storage effect of the pond.

Because of the flat grades on the site, extensive use of turfed swales and drainage channels will effectively satisfy erosion control and esthetic considerations while minimizing the need for concrete-lined channels and under-ground piping.

Improved areas without an effective overflow outlet will be designed for protection against a flood occurrence of once in 100 years. All other areas will have a minimum protection against floods of a frequency of once in 25 years.

An underdrain system of perforated-pipe and aggregate-filter media will be provided to control ground-water levels in the vicinity of all major structures and heavy-duty paved areas. Where adverse elevations preclude free gravity drainage, subdrainage flows will be directed to a central collection point and pumped into the gravity drainage system.



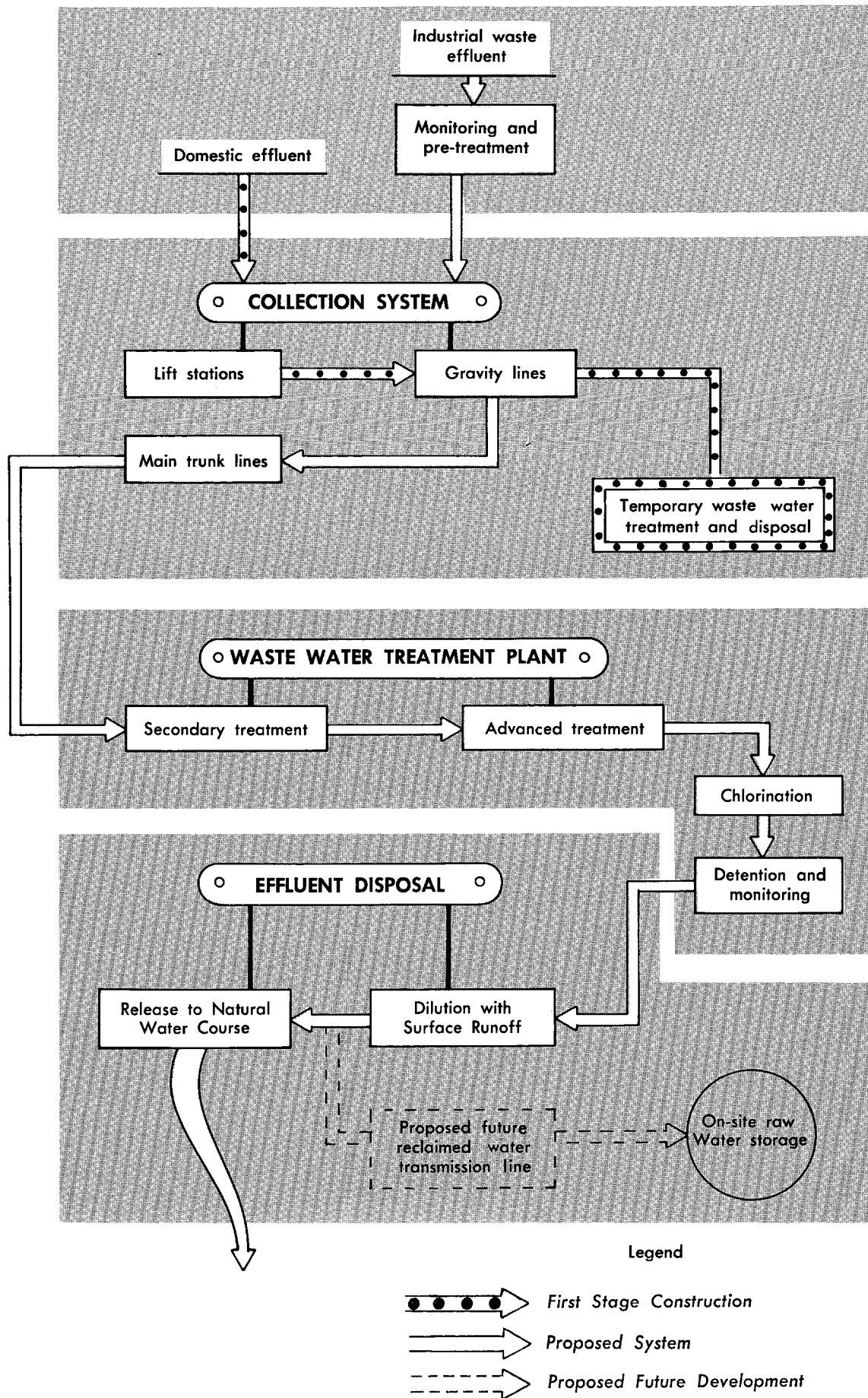


Figure 15-7- Waste Water System

### Sewerage System.

Effluent Collection. Waste waters will be principally a combination of domestic sewage, effluent from cooling tower blow-down and a small amount of demineralizer backwash and rinse water. Since current planning does not foresee major wet-laboratory or manufacturing facilities, industrial wastes have not been considered as a significant factor. Combined waste waters will be collected in a typical underground system of asbestos-cement sewer pipe and transmitted by gravity flow to the treatment plant.

Where trench cuts become excessive or floor elevations preclude gravity flow, the effluent will be collected at central locations and pumped to the nearest point of gravity outfall.

Provisions for monitoring and detection will be made in areas of high potential radioactivity, prior to releasing the effluent to the main system. The collection system will be designed to handle a flow from 2600 persons and a cooling-tower blow-down rate of approximately 500 gallons per minute.

Waste-Water Treatment. The combined waste waters will be treated in a secondary-treatment plant, as shown schematically in Fig. 15-7. Additional polishing of the effluent will be required to meet the requirements of the Illinois Sanitary Board for release to natural surface streams. Such advanced treatment will be performed by detention in oxidation ponds and final chlorination of the effluent.

Study will be needed to establish the actual make-up of cooling tower blow-down, but it is expected that it will contain up to five times the concentrations of dissolved solids compared with original cooling water. This will require pretreatment before the effluent is passed through the sewage-treatment plant. It is expected that within the main ring, cooling-tower blow-down may be sufficiently diluted by the under-drain water from the accelerator housing. Cooling-tower effluent from the experimental area will, however, require pretreatment before being discharged in the sewage-collection system. Additional study will establish the relative economy of providing individual pretreatment at each cooling tower, or a central demineralization plant adjacent to the experimental area.

Effluent Disposal. Upon completion of the required treatment process, and ultimate disinfection of the effluent, the treated waste waters will be released to the existing water course near the easterly edge of the site. Prior to the eventual flow beyond the boundary of the site, the effluent will be further retained and diluted with surface runoff. In this way, both chemical and radioactive pollution will be effectively monitored and treated before release to a public water course.

Because of the high level of treatment proposed for the waste waters from the site, reclamation of the sewage effluent for use as a secondary source of water supply will be considered at a future time.



#### 5.4 Site Utilities Distribution.

Low-Conductivity Water-Distribution System. LCW piping between structures will be distributed underground below the frost line.

The piping will be wrapped and waterproofed if either lined steel or aluminum is used. If lined cement-asbestos pipe is used, flexibility will be provided to withstand anticipated earth settlement. The pipe casing will be designed to resist the earth load and pressure exerted from above ground.

Chilled-Water Distribution System. Chilled-water piping between buildings will be underground below the frost line. The chilled-water supply line will be insulated and wrapped for moisture protection. Cathodic protection will be considered for steel piping. When cement asbestos pipe is used, extra-heavy pipe casing and flexibility will be employed to withstand the earth load and possible settlement.

High-Temperature Water (HTW) and Hot-Water (HW) Distribution Systems. HTW and HW piping on site will be underground. HTW and HW piping will be insulated 85%-magnesium type insulation and placed in buried conduit below frost line. Manholes will be placed at desired intervals for service access. Piping and conduits will have cathodic protection.

Gas-Distribution System. The system will be connected to an uninterrupted supply source of pressure not less than 50 psig.

Below-grade gas lines will be suitably protected. One coat of coal-tar primer followed by a hot coal-tar enamel into which shall be bonded an asbestos felt wrapper, and finished with kraft paper or one coat of water-resistant coating is currently planned. Gas distribution pressure will be not less than 20 psig.

### 6. Site Roads and Walks

The site road plan is shown on the master plan, Fig. 15-1. The road pattern provides for access throughout the site without exposure to radiation hazard except for those whose assigned tasks may require limited exposure on a controlled basis.

6.1 Typical Road Design. New roads indicated on the master plan will be designed to accommodate a program of staged construction to be coordinated with the proposed project schedule.

Principal access roads and heavy duty paved areas will be designed for H20-S16 truck loading as defined by the American Association of State Highway officials. Roads and parking areas subject to less traffic and infrequent heavy loads will be designed to handle the appropriate anticipated loading conditions.

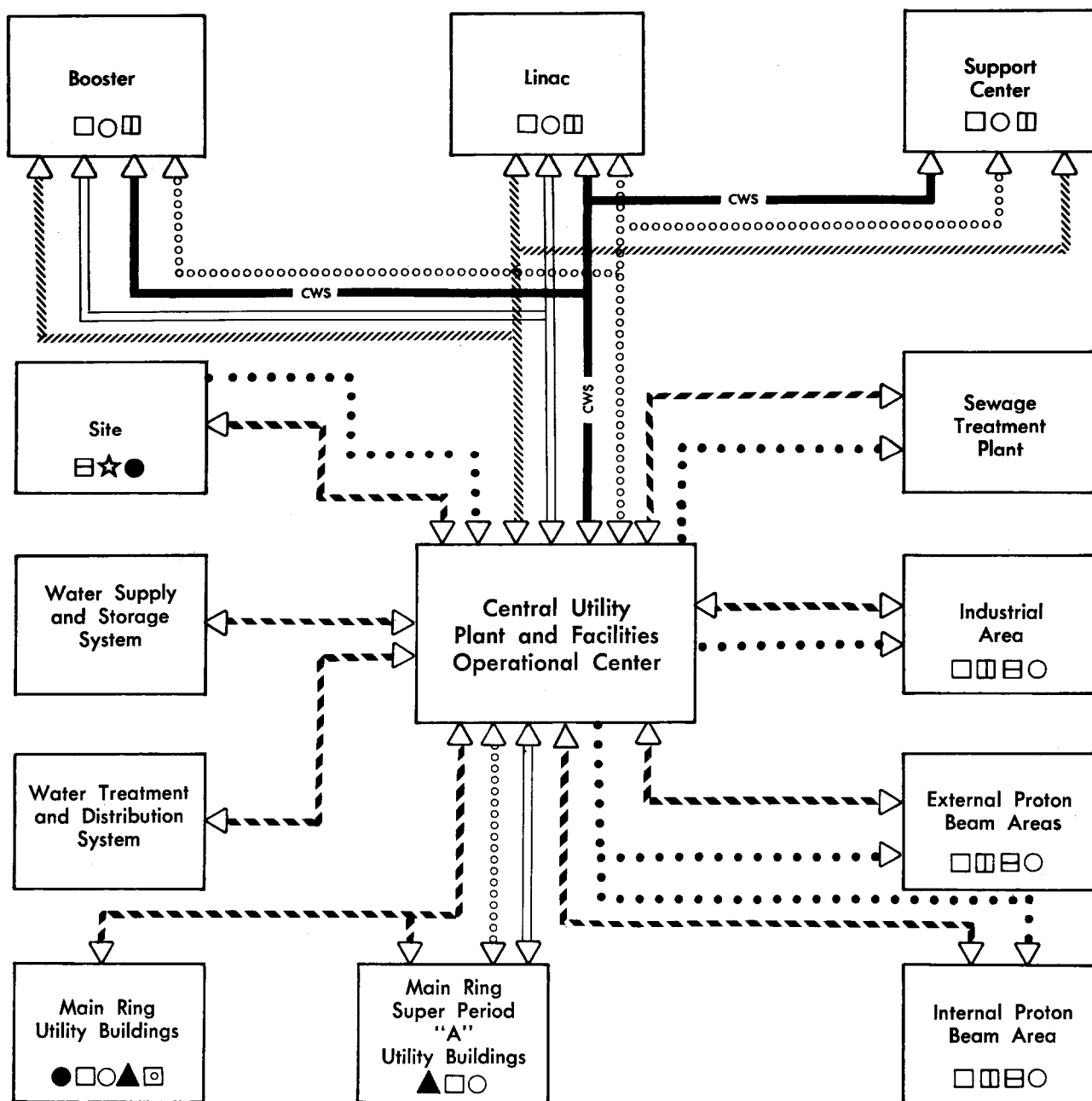
The typical design section will have a 24-foot wide roadway with 8-foot wide shoulders. The structural section of the traveled roadway will include a subbase course of select native granular soils, a stabilized-aggregate base-course and a wearing surface of asphaltic concrete.

Roadway and shoulder width and pavement thickness will vary according to individual traffic and loading classifications. Where special considerations such as snow removal, surface abrasion and grade stability are anticipated, portland-cement concrete surfacing will be substituted for asphaltic concrete.

6.2 Pedestrian Walkways. Pedestrian walkways will be provided where required for adequate pedestrian circulation. The typical walkway will be 5-foot wide concrete construction.

## 7. Central Plants and Site Distribution Systems.

7.1 Central and Individual Heating and Cooling Energy Plants. A central plant is planned to serve an area including the central laboratory, linac, booster, the external proton-beam extraction area and one major utility building of the main synchrotron. A heat generating capacity of 50 million BTUH through four package-unit high-temperature water boilers and refrigeration load of 4500 tons is planned. In addition, there will be a 25 MW capacity central low-conductivity-water cooling system to serve the area designated above. A central control station will be provided. The location of the central plant is shown in the master plan. Its operation is diagrammed in Fig. 15-8.



#### Legend

- HVAC
- LCW System
- ▤ Fire Alarm
- ▲ Air Purging
- Snow Melting
- ▣ Electrical Heating
- ▢ Security
- ★ Lighting

- CWS Chilled Water System
- ..... Gas Distribution System
- ==== LCW System
- oooooooo High Temperature Water System

- Control System
- Monitoring ————
  - Monitoring and Operation ————

Figure 15-8 — Central Utility Plant and Facilities Operational Center

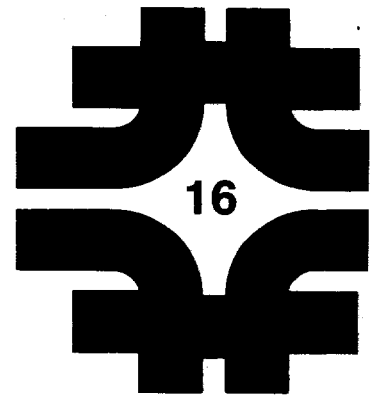
## **Costs and Schedules**

16. Construction Cost Estimate and Schedule 

17. Estimates of Operating Program 

# Construction Cost Estimate and Schedule

1. Methods of Cost Estimation	16-1
2. Cost Summaries	16-2
3. Cost Estimate	16-3
4. Construction and Obligation Schedules	16-11



## 16. CONSTRUCTION COST ESTIMATES AND SCHEDULES

W. M. Brobeck and Associates, DUSAF, R. C. Juergens

### 1. Methods of Cost Estimation

The cost estimates and schedules presented in this chapter are inter-related. If the schedule is stretched out in time, the costs will increase, because the staff costs included in EDIA (Engineering, Design, Inspection, and Administration) will also stretch out and because escalation will increase component and conventional-facilities costs.

The costs of technical components have been estimated by W. M. Brobeck and Associates. The costs of conventional facilities have been estimated by DUSAF, the architectural-engineering group who have been carrying out the conventional-facility design. In all cases, the cost estimates given for specific items are those developed by these groups. The Laboratory has developed EDIA, contingency and escalation figures, and takes responsibility for the entire estimate.

EDIA costs on technical components have been estimated at 25% of component costs. Installation costs of technical components have been estimated separately by W. M. Brobeck and Associates and are shown explicitly as part of component costs. Contingency on technical components has been estimated at 25% of component and EDIA costs.

Architect-engineering-management (AEM) costs on conventional facilities have been estimated at 20% of facilities costs. Contingencies on conventional-facilities have been estimated at 15% of facilities and AEM costs.

The estimate also includes items of standard equipment falling into two classes. The first class is laboratory, office and administrative equipment for the planned Laboratory. The second is movable shielding. EDIA and AEM costs are included in the items, because they are largely stock items. On all standard equipment, a contingency of 10% is estimated on item and AEM costs. This lower percentage reflects the conventional and repetitive nature of the standard equipment.

Escalation has been estimated at approximately 4% per year of the uncommitted balance of construction, EDIA and AEM costs. The average commitment time is approximately 3.5 years and we have therefore used a total escalation figure of 14%.

We have shown separately the item of \$1,705,000 of Construction Planning and Design funds already expended in preliminary phases of this project. Without these funds, the total construction cost of the National Accelerator Laboratory is estimated to be \$248,295,000. With these funds included, the total cost is estimated to be \$250,000,000. No contingency or escalation are taken on these items, since they have already been spent.

These estimates do not include the cost of research equipment needed to carry out experiments with the beams produced in targets. They include the costs of the areas in which these experiments will be done and the costs of providing utilities for research equipment.

## 2. Cost Summaries

It is interesting to summarize the cost estimates in different ways to observe the costs of different parts of the construction. Table 16-1 summarizes the costs of different elements of the Laboratory, with EDIA, contingency, and escalation included.

Table 16-1. Construction Cost Estimate Summary By Function  
(all amounts in millions of dollars)

---

I. Accelerators		
A. Technical Components	111.5	
B. Enclosures and Utilities	34.5	
II. Experimental Areas		
A. Technical Components	2.3	
B. Enclosures and Utilities	21.6	
III. Support Facilities and Site Utilities	65.8	
IV. Standard Equipment	<u>12.6</u>	
	248.3	= \$248.3M

---

By way of contrast, Table 16-2 summarizes costs by items, showing EDIA, contingency and escalation explicitly. It is a direct summary of the detailed cost estimate of Table 16-3.

Table 16-2. Construction Cost Estimate Summary  
(all amounts in millions of dollars)

---

I. Construction Costs	
A. Technical Components	65.5
B. Conventional Facilities	78.4

C. Standard Equipment	10.2	
D. Construction Bond	<u>0.4</u>	
Subtotal		154.5
II. EDIA (Engineering, Design, Inspection and Administration)		
A. Technical Components (25%)	16.4	
B. Conventional Facilities (20%)	<u>15.7</u>	
Subtotal		32.1
III. Contingencies		
A. Technical Components (25%)	20.4	
B. Conventional Facilities (15%)	14.1	
C. Standard Equipment (10%)	<u>1.0</u>	
Subtotal		35.5
IV. Escalation (Approximately 14%)		
A. Technical Components	11.5	
B. Conventional Facilities	13.3	
C. Standard Equipment	<u>1.4</u>	
Subtotal		<u>26.2</u>
Total		248.3 = \$248.3M

### 3. Cost Estimate

Table 16-3 gives the detailed breakdown of the construction cost estimate. Items IA, IIA1, and IIB1 have been estimated by W. M. Brobeck and Associates, the remainder of the construction costs by DUSAF, and the EDIA, contingency and escalation by the National Accelerator Laboratory.

Table 16-3. Construction Cost Estimate  
(All amounts in thousands of dollars)

#### I. 200 BeV Proton Synchrotron

##### A. Accelerator Technical Components

1. Main Accelerator Magnets	20,945
a. Bending Magnets	16,320
b. Quadrupoles	1,881
c. Collins quadrupoles	444
d. Trim quadrupoles	97
e. Sextupoles	505
f. Water and power manifolds	1,115
g. Magnet installation	553
h. Vertical steering magnets	30



2.	Main-accelerator magnet power supplies	6,221	
a.	Rectifier-inverter, filter, pf correction	2,368	
b.	Power supplies for auxiliary and trimming magnets	2,972	
c.	Wiring for main and auxiliary magnets	881	
3.	Main accelerator rf system (16 cavities, 1 spare)	2,778	
a.	Accelerating modules	604	
b.	Anode modulators	595	
c.	Power supplies (anode, screen voltage, ferrite, filament)	1,202	
d.	Control and safety interlocks, fences	101	
e.	Amplifiers	114	
f.	Wiring, water distribution	154	
g.	Installation	8	
4.	Main-accelerator vacuum system	2,632	
a.	Vacuum chamber	380	
b.	High-vacuum pumps, power supplies, connections and cables	759	
c.	Roughing pumps, trucks, connections	345	
d.	Remotely operated joints, sector valves, pneumatic-valve operating system	1,128	
e.	Power distribution	12	
f.	Vacuum gauging	8	
5.	Main-accelerator magnet adjustment and alignment	945	7 Apr 68
6.	Inter-ring transfer	55	
7.	Inter-ring transfer magnets	420	
8.	Inter-ring transfer magnet power supplies	1,390	2395
9.	Booster accelerator magnets	1,167	1825
a.	Magnets	1,004	
b.	Trim and auxiliary magnets	52	
c.	Water manifolding	59	
d.	Installation	52	
10.	Booster-magnet power supplies	4,979	3810
a.	Capacitors	877	
b.	Reactors	2,072	

c. Excitation power supplies and controls	1,320	
d. Wiring	710	
11. Booster-magnet adjustment system		128
12. Booster beam-dump		5
13. Booster-accelerator vacuum system		818 975
a. Vacuum chamber	257	
b. High-vacuum pumps, power supplies, cables	238	
c. Roughing pumps	144	
d. Remotely operated joints, sector valves, pneumatic-valve operating system	159	
e. Power distribution	13	
f. Vacuum gauging	7	
<i>Total Booster w/o rf, transfer</i>		7097
14. Booster-accelerator rf system (18 cavities and 1 spare)		4,807
a. Accelerating modules	1,945	
b. Anode modulators	441	
c. Power supplies (anode, screen voltage, ferrite bias, filament)	1,480	
d. Control and safety interlocks	105	
e. Amplifiers	126	
f. Wiring, water distribution	700	
g. Installation	10	
<i>Total Booster w/o transfer</i>		11,904
15. Linear accelerator		10,492
a. Preaccelerator system; (including preaccelerator-linac beam transport)	1,088	
b. Tanks and supports	1,390	
c. Drift tubes, tuners, quadrupole	1,030	
d. Beam transport between tanks	120	
e. Alignment system	31	
f. Vacuum systems	726	
g. Cooling system and controllers	53	
h. Installation	1,324	
i. RF system, pulsed power supply, high-power amplifier	1,954	
j. Driver chain and transmission lines	853	
k. Cooling system	37	
l. Local controls	257	
m. Installation	817	
n. Beam transport, linac to booster	812	1104
<i>Total Booster incl Transp, not rf</i>		9744 9609

16. Accelerator control system		3,913	
a. Direct-wire system	398		
b. Multiplex system	2,906		
c. Main accelerator rectifier control	47		
d. Beam sensing devices, controls, display, console	489		
e. Communication	40		
f. Central time and function generator	33		
17. Beam-extraction magnets		1,199	
18. Beam-extraction magnet power supplies		899	
19. Special handling devices		353	
a. Trucks and battery chargers	212		
b. TV camera and receiver	22		
c. Guide rail	119		
Subtotal, accelerator technical components		64,146	
EDIA (25%)		16,037	
Accelerator technical components			80,183

#### B. Accelerator Housing and Auxiliary Structures

1. Main accelerator		16,576	
a. Earthwork and yardwork	2,300		
b. Accelerator enclosure	3,660		
c. Magnet foundations, enclosure floor slab	167		
d. Straight sections	1,039		
e. Penetrations and utility structures			
(i) Utility and control access	1,794		
(ii) Service buildings	1,866		
(iii) Drainage system	409		
(iv) Survey monuments	14		
f. Utilities			
(i) Electric-power distribution, lighting, wiring	993		
(ii) Power regulation, controls	157		
(iii) LCW cooling	2,822		
g. Heating, ventilating, and air conditioning	1,129		
h. Material handling equipment	131		
i. Fire protection and sanitary facilities	95		
2. Booster accelerator		3,623	
a. Earthwork and yardwork	242		
b. Accelerator enclosure and gallery	1,509		

c. Utilities		
(i) Electric-power distribution wiring, lighting	261	
(ii) Power regulation, controls	78	
(iii) LCW cooling	875	
d. Drainage system	53	
e. Survey monuments	6	
f. Heating, ventilating and air conditioning	439	
g. Fire protection and sanitary facilities	42	
h. Fixed dense shielding	118	
3. Linear accelerator		1,931
a. Earthwork and yardwork	42	
b. Structure, foundation, cranes	1,260	
c. Utilities		
(i) Electrical distribution, lighting	209	
(ii) Power regulation, controls	55	
(iii) LCW cooling	167	
d. Heating, ventilating and air conditioning	132	
e. Drainage system	16	
f. Survey monuments	2	
g. Fire protection and sanitary facilities	48	
Subtotal, accelerator conventional facilities		22,130
AEM (20%)		4,426
Accelerator conventional facilities		26,556
Accelerator Total		106,739

## II. Experimental Facilities

### A. External Proton-Beam Areas

1. Technical components		1,198
a. Pumping stations, valves, and valve-operating system	535	
b. System magnet vacuum chamber	53	
c. Remotely operated joints	85	
d. Power distribution	5	
e. Vacuum gauges	9	
f. Beam pipe	130	
g. Targets and beam dumps	381	
2. Conventional facilities		11,598
a. Earthwork	885	
b. Heavy-duty paving	1,038	

c. Structures	
(i) 6000 ft enclosure	1,223
(ii) Switching stations and utility buildings	478
(iii) Vehicle entrances (4)	209
(iv) Target areas A, B and C	2,758
(v) Experiment building	2,229
(vi) Beam dump	52
d. Utilities	
(i) Electric-power distribution, wiring and lighting	867
(ii) Controls, power regulation	78
(iii) LCW cooling	1,568
e. Drainage system	181
f. Survey monuments	4
g. Fire protection	28

(Shielding included in another part of estimate. Heating, ventilation, and air conditioning, material handling equipment included in structures above.)

#### B. Internal-Target Area

1. Technical components	107
a. Internal target mechanisms	107
2. Conventional facilities	2,316
a. Structures	
(i) Enlargement in main accelerator ring	609
(ii) Crane in enlargement	78
(iii) Experiment building, including crane and apron	1,222
b. Utilities	
(i) Electrical power distribution	110
(ii) Controls	26
(iii) LCW Cooling	255
c. Fire protection and sanitary facilities	16

(Shielding included in another part of estimate. Heating, ventilating and air conditioning included in structures. Drainage facilities included in main accelerator.)

Subtotal, experimental-area technical components	1,305	
EDIA (25%)	326	
Technical components		1,631

Subtotal, experimental-area conventional facilities	13,914	
AEM (20%)	2,783	
Conventional facilities		<u>16,697</u>
Experimental Facilities Total		18,328

### III. General Plant and Utilities

#### A. Facilities Control System 1,934

#### B. Site Development

1. Roads and Parking, walks	3,359
2. Fencing	222
3. Site earthwork, landscaping and erosion control	1,463
4. Access to interior of accelerator	105
5. Railroad siding	132

#### C. Site Utilities

1. Main water system and distribution	2,740
2. Electrical system	11,330
a. Main substation	3,318
b. Site distribution	5,731
c. Paging system, protection alarm system	575
d. Emergency-power system	1,045
e. Street and area lighting	400
f. Over-all installation and tuneup	261
3. Main utility equipment, steam plant and distribution system	3,574
4. Sewage systems	2,147
a. Storm drainage	983
b. Sanitary-sewer system	1,164

#### D. Support Facilities

1. Main support building (420,000 sq ft) housing resident and visitor physics offices, computer center, film processing, library, auditorium, cafeteria, medical center, light laboratory and light service and maintenance shops, and general laboratory and administrative offices	11,128
2. Heavy service shops (50,000 sq ft)	1,536
3. Heavy laboratory (50,000 sq ft)	1,568
4. Service and maintenance building and motor pool (9,000 sq ft)	160
5. Receiving, stores and warehouse (60,000 sq ft)	585

6. Fire-protection building, site security (11,000 sq ft)	184	
7. Main utility building (12,000 sq ft)	188	
Subtotal, general plant and utilities	42,355	
AEM (20%)	8,471	
General Plant and Utilities Total		50,826
IV. Standard Equipment and Shielding		
A. Standard Equipment	3,900	
1. Specialized laboratory equipment	1,860	
2. Furniture and office equipment	480	
3. Film-processing equipment	298	
4. Food-service equipment	98	
5. Machine-shop equipment	342	
6. Medical-facility equipment	141	
7. Mobile equipment (trucks, fork lifts, etc.)	482	
8. Translation equipment and miscellaneous equipment	199	
B. Shielding (fixed and movable, both normal and high-density concrete and steel)	6,300	
Standard Equipment and Shielding Total		10,200
Technical Components Total	81,814	
Conventional Facilities Total	94,079	
Contractors' Bond on Conventional Facilities	425	
Standard equipment Total	<u>10,200</u>	
TOTAL ESTIMATED CONSTRUCTION AND ENGINEERING COST		186,518
Contingencies		
Technical Components (25%)	20,454	
Conventional Facilities (15%)	14,112	
Standard Equipment (10%)	<u>1,020</u>	
Total Contingency		35,586
Escalation (Approx. 14% of Construction and Engineering)		<u>26,191</u>
		248,295
Expended Construction Planning and Design Funds (No Contingency or Escalation)		1,705
TOTAL ESTIMATED PROJECT COST		250,000

#### 4. Construction and Obligation Schedules

It is our objective to construct the synchrotron so as to obtain a beam of protons by June 30, 1972, and so that a modest experimental program can be started soon thereafter. The laboratory should be in full operation in 1975. The obligation schedule shown in Table 16-4 and the Construction Schedule on pages 16-12 and 16-13 show how this is to be done. We originally planned for completion of construction in 1973. The total cost for that schedule was \$243.6 million instead of \$250 million but it required a very high initial rate of funding. At the present time, because of a general scarcity of funds, it seems unrealistic to strive for the faster schedule. The schedule shown represents the smallest obligation rate for FY 69 that would still allow us to achieve our objective of having initial operation in 1972. This schedule will result in a serious delay in the availability of support buildings. More significantly, it will mean that few experimental facilities will be available at the time the synchrotron goes into operation. We will have the capability of building at a more rapid rate, and we would hope that a period of greater availability of research funds would allow us to increase substantially the rate of construction above that indicated in Table 16-4.

Table 16-4. Construction Obligation

<u>Fiscal Year</u>	<u>Obligations (thousands of dollars)</u>
1968	4,633
1969	27,700
1970	90,000
1971	80,000
1972	25,000
1973	<u>20,962</u>
	248,295



# CONSTRUCTION SCHEDULE

	FISCAL YEARS						
	1968	1969	1970	1971	1972	1973	1974
<u>GENERAL PLANT &amp; UTILITIES</u>							
<u>SITE DEVELOPMENT</u>							
Site Grading, Rough Roads & Drainage	CD	Title I Title II Bid Construction					
Finished Roads, Lights, Fencing, Landscaping	CD		Title I		Title II	Bid Construction	
<u>UTILITIES</u>							
Advanced Procurement - Electrical	CD	Title I Title II Bid Procurement					
Water, Power & Sewage Distribution							
(To Five Feet Outside of Structures)							
a. All Areas Except EPB Area	CD	Title I Title II Bid Construction					
b. EPB to Target-Station C	CD	Title I	Title II	Bid Construction			
c. EPB to Target-Station A & B	CD	Title I	Title II	Bid Construction	Title I	Bid Construction	
Central Utility Plant (Incl. Equipment)	CD	Title I	Title II Bid Construction				
Main Substation	CD	Title I	Title II Bid Construction				
Water & Sewage Plants	CD	Title I	Title II Bid Construction				
Instrumentation, Control, Fire, Paging Systems							
a. All Areas Except EPB Area	CD	Title I Title II Bid Construction					
b. EPB Area	CD	Title I	Title II Bid Construction				
Emergency-Power Facility	CD	Title I	Title II Bid Construction				
<u>SUPPORT</u>							
Receiving & Stores Warehouse	CD	Title I Title II Bid Construction					
Service-Maintenance & Fire-Security Buildings	CD	Title I Title II Bid Construction					
Heavy Service Shops & Heavy Laboratory	CD	Title I	Title II Bid Construction				
Central Laboratory Building	CD	Title I	Title II Bid Construction				
Standard Equipment	CD	Title I	Title II Bid Construction				
<u>LINEAR ACCELERATOR</u>							
Tanks, Supports, Drift Tubes	R&D Title I & II Bid	Procurement		Assembly in Linac Bldg.			
Linac RF System	R&D Title I	Title II Bid Procurement		Assembly & Test			
Other Technical Components	R&D Title I	Title II Bid Procurement		Installation			
Linac Building	CD Title I	Title II Bid Construction		Assembly & Test			

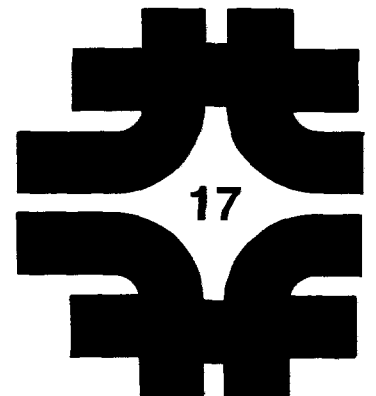
FISCAL YEARS							
	1968	1969	1970	1971	1972	1973	1974
<u>BOOSTER SYNCHROTRON</u>							
Magnets	R&D Title I	Title II	Bid Title II	Procurement	Procurement Assemble & Test		
Power Supplies	R&D Title I	Title II	Bid Title II	Procurement	Install & Test		
RF System	R&D Title I	Title II	Bid Title II	Procurement			
Vacuum System	R&D Title I	Title II	Bid Title II	Procurement			
Enclosure	C D Title I	Title II	Bid Title II	Construction			
<u>MAIN SYNCHROTRON</u>							
Primary Magnets	R&D Title I	Title II	Bid Title II	Procurement	Install & Test		
Secondary Magnets	R&D Title I	Title II	Bid Title II	Procurement	Install & Test		
Magnet Power Supplies	R&D Title I	Title II	Bid Title II	Procurement			
RF System	R&D Title I	Title II	Bid Title II	Procurement	Install & Test		
Vacuum System	R&D Title I	Title II	Bid Title II	Procurement	Install & Test		
Enclosure (Superperiod "A")	C D Title I	Title II	Bid Title II	Construction			
Enclosure (Balance of Construction)	C D Title I	Title II	Bid Title II	Construction			
<u>EXPERIMENTAL AREAS</u>							
<u>INTERNAL-TARGET AREA</u>							
Technical Components	R&D	Title I	Title I	Title II	Bid Procurement	Install	Test
Internal-Target Buildings (Ext. to Ring)	C D	Title I	Title I	Title II	Bid Construction		
<u>EXTERNAL BEAM</u>							
Technical Components (To Target Sta. C)	R&D	Title I	Title II	Procurement	Install & Test		
Technical Components (To Target Sta. A & B)	R&D	Title I	Title I	Title II	Procurement	Install & Test	
Beam-Transport Buildings (To Target Sta. C)	C D	Title I	Title II	Bid Construction			
Beam-Transport Buildings (To Target Sta. A & B)	C D	Title I	Title I	Title II	Bid Construction		
<u>EXTERNAL EXPERIMENTAL AREAS</u>							
Target-Station C Buildings	C D	Title I	Title II	Bid Construction			
Target-Station A & B Buildings	C D	Title I	Title I	Title II	Bid Construction		
Experiment Buildings & Pads	C D			Title I	Bid Construction		

— Test Protons Available

LEGEND  
C D - Criteria Development  
R&D - Research & Development

# **Estimates of Operating Program**

- |                                 |      |
|---------------------------------|------|
| 1. Introduction                 | 17-1 |
| 2. Personnel and Cost Summaries | 17-1 |



## 17. ESTIMATES OF OPERATING PROGRAM

R. C. Juergens

J. H. Fregeau (NSF), P. J. Reardon, (MIT)

### 1. Introduction

It is necessary to estimate the effects of the size of the research program, discussed in Chapter 14, on the size of the Laboratory in order to plan the facilities. The size of the staff and facilities in turn affect the estimated budgets during operation.

Approximately 75% of operating time will be used for high-energy physics research by visiting groups. Because many visitors will also work at other installations, spending only part of their time at this Laboratory, the total number of physicists involved in any one year will be considerably greater than the number present at any one time.

It is expected that visiting groups from universities and other laboratories will derive the majority of their financial support from their home institutions, in accord with the current policy of government funding agencies. Facilities will be provided for visiting users, including office and laboratory space, the accelerator, major experimental facilities such as bubble chambers and other major instruments, as well as beam transport and experimental set-up costs. Additional support will be provided users in areas including design, fabrication and testing, operation of experiments, the use of shops, technicians and computer facilities. On the other hand, aside from large bubble chambers and similar apparatus, visitors will be expected to supply the special apparatus and equipment required to conduct their particular experiments.

The resident research staff will use approximately 25% of available research time. It will also be the responsibility of the resident staff to develop the accelerator and experimental facilities and equipment.

### 2. Personnel and Cost Summaries

Laboratory population and cost projections follow here. Visitors appear here only as their number contributes to the size of the facility. Their wages and the cost of their special experiment apparatus are not included in the cost data. Table 17-1 gives a breakdown of personnel in FY1975, two years after turn-on. Table 17-2 shows the manner in which the laboratory is expected to grow to this population. Table 17-3 gives the estimated annual budget in FY1975 and Table 17-4 summarizes the yearly budgets. It should be noted that this last table includes estimated requirements for the preoperating program, including funds for the development of major research equipment.

Table 17-1. Estimated Laboratory Population in 1974

	Ph. D Physicist	Professional (a)	Technical (b)	Other (c)	Total
<u>Directorate</u>					
Director's Office	5	8		12	25
Planning Group	1	5	3	2	11
Safety	2	6	10	1	<u>19</u>
					55
<u>Resident Research Groups (d)</u>					
Electronic Detection	25	40	60	14	139
Bubble Chamber	20	35	30	8	93
Theoretical Physics	15	5		3	<u>23</u>
					255
<u>Visiting Research Groups</u>					
Experimental Physics	150	50 (e)	10		210
Theoretical Physics	15			2	17
Visitor Support (f)		60	40	18	<u>118</u>
					345
<u>Operations and Development</u>					
Technical Operations	10	30	100	25	165
Experimental Support	5	20	80	30	135
Accelerator Development	20	30	25	10	85
Research-Equipment "	45	65	80	20	<u>210</u>
					595
<u>Technical Support</u>					
Engineering Group		60	45	9	114
Machine Shops		1		110	111
Materials Laboratory		1		20	21
Craft Shops		1		35	36
Electronics		2		40	42
Computer Center		30	20	10	60
Film-Processing Center			10	1	11
Library		6		4	<u>10</u>
					405
<u>Other Support</u>					
		63	39	243	345
	313	518	552	617	2,000

(a) Includes engineers, B.A. physicists, graduate students, and programmers

(b) Includes accelerator, electronic and mechanical technicians, operators and scanners

(c) Includes machinists, building trades and crafts, clerical, custodial, and administrative personnel

(d) Approximately half the resident research physicists are also listed under "research equipment development"

(e) Includes visiting graduate students

(f) NAL personnel who provide assistance to visiting users

Table 17-2. Population at End of Fiscal Year

Fiscal Year	<u>1968</u>	<u>1969</u>	<u>1970</u>	<u>1971</u>	<u>1972</u>	<u>1973</u>	<u>1974</u>	<u>1975</u>
Resident Research	10	20	30	50	100	150	200	255
Visitor Research	0	0	0	0	20	100	200	345
Accelerator R & D	70	85	200	190	130	20	0	0
Accelerator Design and Construction	50	100	200	300	250	200	100	0
Operation and Development	0	0	0	50	200	300	500	595
Technical Support	35	75	120	160	200	250	350	405
Administration*	<u>35</u>	<u>70</u>	<u>100</u>	<u>150</u>	<u>200</u>	<u>280</u>	<u>350</u>	<u>400</u>
	200	350	650	900	1,100	1,300	1,700	2,000

\*Includes directorate

Table 17-3. Estimated Annual Budget in FY 75(all amounts in thousands of dollars)

<u>Operating Costs</u>		
Wage Expense (1195 full-time equivalents)	17,900	
Supplies	5,200	
Major procurements:		
Film	2000	
Power	2000	
Computer	1000	
Other	<u>800</u>	5,800
Engineering and shop burden (includes department administration, services, clerical and similar costs)	<u>6,100</u>	
Total direct costs		35,000
Indirect costs (includes general administration and services)		6,000
Total operating costs		<u><u>41,000</u></u>
<u>Other costs</u>		
Equipment	7,500	
Accelerator-improvement and General-plant projects	9,000	
		<u><u>16,500</u></u>
<u>Total annual budget</u>		<u><u>57,500</u></u>

Table 17-4. Budget Summary

		(All amounts in thousands of dollars)						
		Fiscal Year						
		1968	1969	1970	1971	1972	1973	1974 1975
<u>Construction Project</u>								
Obligations	6,338(a)	27,700	90,000	80,000	25,000	20,962		(Total 250,000)
Costs	3,705(a)	4,500	20,000	50,000	70,000	60,000	30,000	11,795 (Total 250,000)
<u>Preoperation Program</u>								
Operating	2,650	5,400	8,000	10,300	16,650			
Equipment	300	900	11,000	15,600	20,200			
<u>Operation Program</u>								
Operating						30,000	35,000	41,000
Equipment						15,000	7,500	7,500
<u>Post Project Construction (b)</u>							3,000	9,000
(a) Includes 1,705 CP & D funds already expended								
(b) Accelerator-improvement and general-plant projects								

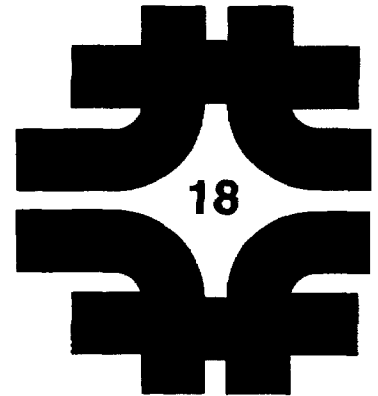
## Provisions for Future Expansion

18. Provisions for Future Expansion



# Provision for Future Expansion

1. Introduction	18-1
2. Options for Future Accelerator Improvements	18-1
2.1 Increase of Peak Energy	18-1
2.2 Increase of Intensity	18-4
2.3 Other Accelerator Improvements	18-5
3. Options for Future Expansion of Research Facilities	18-5
3.1 Expansion of Existing Experimental Areas	18-5
3.2 Addition of a Beam Bypass, Storage Rings and Colliding Beams	18-7
References	18-10



## 18. PROVISIONS FOR FUTURE EXPANSION

R. Billinge, A. W. Maschke, A. L. Read, A. Roberts

E. D. Courant (BNL), L. W. Jones (U. of Michigan),

B. W. Montague (CERN), E. M. Rowe (U. of Wisconsin)

R. Serber (Columbia U.), A. M. Sessler (LRL)

### 1. Introduction

The problems of greatest interest in high-energy physics and the methods used to attach them experimentally are both constantly changing. Experiments performed at the National Accelerator Laboratory will inevitably generate new problems and new experimental techniques. Furthermore, because this is an instrument to investigate a new range of physics, there is no unique guide to the choice of major parameters. These uncertainties must be recognized in the design and a facility provided with enough flexibility to meet later needs.

In the conceptual design work discussed in this report careful consideration has been given to the future possibilities. Features have been included that, at quite small additional present cost, provide "options" for future expansions of the high-energy physics capability of the laboratory, without undue cost and with as little interruption of the research program as possible.

These options can, for descriptive purposes, be separated into two kinds, those that permit improvements in the performance of the accelerator and those that permit expansion of facilities for a larger research program or for a new way of doing physics experiments. Accelerator improvements for which options have been built in include both greater energy and intensity. The options for a larger research program include expanding the experimental areas along the beam-transport run from the main extraction point, adding separate new extracted-beam positions around the main ring, and adding a beam bypass and storage ring outside the ring. The bypass and storage ring can be utilized for new ways of doing physics by means of colliding beams. These are described in more detail below.

### 2. Options for Future Accelerator Improvements

**2.1 Increase of Peak Energy.** The accelerator design provides for future conversion to a higher energy. The main-ring magnets have been designed to give approximately 500 BeV when powered to their maximum possible field. In addition, adequate magnet cabling and water piping for the higher power operation have been provided so that a conversion

program can proceed without extensive work in the magnet enclosure and thus without a major shutdown of the facility. Most components of the accelerator outside the enclosure are designed for 200 BeV only and this section discusses the nature and approximate cost of their conversion for higher energy operation.

The cycles chosen for acceleration to 400 BeV are shown in Fig. 3-4. The normal 200 BeV cycle has a 1-second flat-top and a 4-second total period. The 400 BeV cycle has a 2-second flat-top and an 8-second period. Both cycles therefore have a 25% duty cycle. The 400 BeV cycle has a 1.6 second filling-time instead of the 0.8 second of the 200 BeV cycle, allowing twice the charge per cycle, so that the average current could be the same in both cases. The booster would inject two turns into the main ring in the longer filling time, but is not otherwise affected by the conversion to higher energy.

The nature of the conversion depends strongly on this choice of the new cycle time for the higher energy. For example, the repetition frequency could be lowered enough that the average power into the magnets was not increased at the higher energy. This slow-cycle mode of operation would require only modest improvement of a few components, such as the rectifiers in the magnet power supply, but it would give a considerably lower average current and duty cycle. Thus, the intensity would be reduced by a factor of approximately four. The slow-cycle mode will be used for occasional operation to extend the range of some important experiment, perhaps to 300 BeV, but it is not a true conversion.

For routine operation at higher energy, average current and duty cycle should be the same as before conversion. The cycle chosen will do this at 400 BeV. It may also be noted that after conversion, 200 BeV operation can have an increased current and a better duty cycle. After conversion the slow-cycle mode can be used for occasional operation at 500 BeV, should this prove practical. With the same average power loss and a 2-second flat-top, the intensity at 500 BeV will be reduced by a factor of 2.5 from the 400 BeV intensity.

The accelerator components that require modification in the conversion program are: magnet power supply, cooling system, injection, radio-frequency accelerating system, extraction, external-beam handling and controls. In addition some provision is necessary for increased target shielding and experiment space. The major effort and cost will be for conversion of the magnet power supply.

The average magnet power must be increased by a factor of four, from 17 to 68 MW. Some modification to the existing supplies will be required, but most of the power increase will come from the installation of additional units, including additional filtering and power-factor correction. These units are outdoor equipment, so that installation requires pads, conduits, etc., and only minor building modifications. The increased load on the substation will be handled by the installation

of forced-oil, forced-air cooling on existing units. It is now believed that this increased load can be connected directly to the power line. The costs would not be substantially different if motor-generator sets were used.

The greater magnet power will increase the magnet heating. During the conversion the magnet cooling-water pressure will be doubled by additional pumps to increase the water flow. Nevertheless the magnet temperature rise will be more than doubled, from 6°C to 16°C, still well within normal practice. The magnet system has excess cooling capacity for 200 BeV operation in anticipation of the conversion. The number of accelerator cooling towers must be increased substantially to handle the heat load and some enlargement of the water-treatment and handling system may be necessary.

The radio-frequency accelerating system must also be enlarged considerably. The present design has a beam loading of about two-thirds, that is, two-thirds of the rf power is transferred to the beam of protons, with the rest being dissipated in the rf system. For 400 BeV operation, we will load twice as many protons into the main ring, so that rf power capability must be doubled to maintain this ratio. We believe, however, that more efficient transfer of power to the beam will be possible at higher intensity. Whether this is done by increasing the number of units or their individual power or both is best determined after experience with the rf system.

Both the injection and extraction systems will require extensive modification. The injection system will be changed to a two-turn system and the slow-extraction system must work at twice the energy for twice as long. Although both conversions present some technical difficulty, neither is very costly.

The magnets in the external beam run are copies of the main-ring magnets and can therefore be used without modification. The power supplies for these magnets must be increased.

The general control system of the accelerator must be enlarged to provide monitoring and control of the new equipment and to provide new timing circuits.

Some provision for using the extracted 400 BeV beam must also be included. The estimate includes the cost of improving one target station to a 400 BeV standard by increasing the shielding and extending the length of the secondary beam buildings and services. The target muon shielding, in theory, must be twice as long, but no thicker. This is a very expensive part of the conversion and one would not like to do it before actual experience with 200 BeV shielding problems. It can, however, be predicted with confidence that the accelerator itself will not need any extra shielding.

Table 18-1 is a cost-estimate summary for the conversion. The costs are given separately for accelerator components and for conventional construction. EDIA is estimated at 25% for the first and 20% for the second, except for shielding, which is estimated at 5%. An overall contingency of 25% is added on both accelerator components and conventional construction. This larger contingency on conventional items is judged to be appropriate in view of the relatively early stage of the conversion design. No sensible estimate of escalation is possible; these figures represent present-day (1967) costs. If the conversion project were started six years from now and completed in 1-1/2 years, the costs would obviously increase, perhaps by as much as one-third.

Table 18-1. Estimated Conversion Costs (millions of 1967 dollars)

<u>Component</u>	<u>Accelerator</u>	<u>Conventional</u>
Magnet Power	7.0	2.2
AC Service		0.4
Cooling		3.0
Water System		0.5
Radio Frequency	1.4	
Injection and Extraction	0.5	
Beam Handling	1.0	
Controls	0.3	
Targeting		
Shielding		2.0
Building Extension		2.0
Subtotal	10.2	10.1
EDIA	2.6	1.7
	12.8	11.8
		24.6
Contingency		6.1
Total (without escalation)		\$30.7 M

2.2 Increase of Intensity. The intensity is limited by space-charge forces. Within these limitations, the intensity can be increased by raising the repetition rate. Since the space-charge limit is approached most closely in the booster, it would be possible to increase the intensity by loading more charge into the main ring from the booster, by increasing the injection time or by increasing the booster cycling rate. It would also be possible to increase the formal limit by a factor of approximately 2.5 by interposing a "supercharger", a 500 MeV synchrotron, between the 200 MeV linear accelerator and the booster. Space has been reserved for this eventuality. It may also be possible to increase the space-charge limit in the main accelerator by adjusting the focusing fields to compensate the space-charge forces. The separated-function design is particularly advantageous for this purpose. It can be expected that operational experience and the understanding gained from beam experiments will aid greatly in increasing the intensity, as has been the case with all previous accelerators.

If increased intensity is to be useful in day-to-day operation, either the efficiency of beam extraction must be improved at the same time, as the estimates of Chapter 12 show, or maintenance and access problems in the presence of higher induced radioactivity levels must be solved. Otherwise, higher intensity will only be useful for special experiments of short duration.

2.3 Other Accelerator Improvements. A number of other accelerator improvements will be possible. One will be prebunching of full-energy beams for use in time-of-flight experiments and for rf separation. Ample straight-section length is available for the special rf cavities needed.

The possibility of accelerating polarized proton beams in a strong-focusing accelerator appears to be highly unlikely, because of the depolarizing effects of the magnetic-field gradients. If methods to preserve polarization of the beam could be found, these polarized high-energy beams would be of great interest.

### 3. Options for Future Expansion of Research Facilities

3.1 Expansion of Existing Experimental Areas. Figure 18-1 is a sketch showing various methods of adding to the experimental areas now planned. Two branch points and three external target stations are shown as solid lines. The possible additions, shown as dashed lines, are:

- (i) At a: The addition of branches to secondary beams. The efficiency of many secondary beams may be appreciably increased, according to current experience, if two experiments are simultaneously set up to use a beam that can be readily switched between them. This relieves each group of the obligation to be operative all the time, and reduces down-time while experiments are installed.
- (ii) At b: The addition of new secondary beams at existing targets. The number of beams that can be produced at a target is often limited by budgetary rather than technical considerations. Both the foregoing methods increase operating efficiency without decreasing the share of the beam given to any one experiment.
- (iii) At c: Additional branches may be taken off the existing external proton beam, by moving the beam stop back and installing new branch points, transport enclosures, targets and experimental areas. This procedure divides the available beam among more targets, and is thus indicated when beam currents have reached satisfactory operating values.

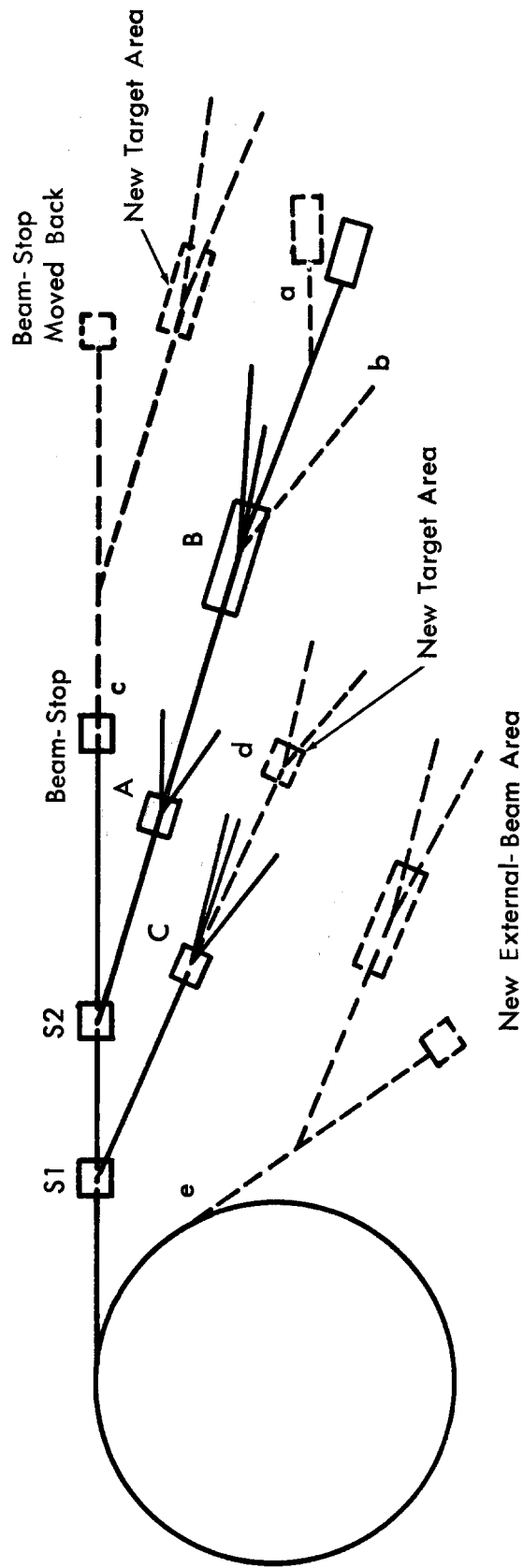


Figure 18-1 Possible Expansions of Existing Experimental Areas

- (iv) At d: A variant of this procedure adds a new target area to an existing branch by retrieving the proton beam after it has gone through a target and carrying it through the existing area to a new one.
- (v) At e: Additional external proton beams may be desirable. There is some question, on technical grounds, whether the simultaneous extraction of two independent proton beams is as efficient as extracting one beam, with many branches. However, since there may be other overriding considerations (for example, possible interference between short and long pulse extraction, need for large or isolated areas, etc.), this possibility should not be foreclosed.

Figure 18-2 shows, in addition to the options discussed in the next section, the 16,000-foot length available on the site for these extensions of existing experimental areas. One of the extensions discussed above may well be an efficacious way to develop a 400-500 BeV experimental area.

### 3.2 Addition of a Beam Bypass, Storage Rings and Colliding Beams

Figure 18-2 shows a possible alignment of the site of additional facilities to enter a new energy range.<sup>1</sup>

At long straight-section B, the present internal-target area, the full-energy beam can be extracted and taken around a "beam bypass" to be reinjected in the ring at long straight-section D. The bypass would substitute its own arc for the 120-degree arc of the main ring between B and D; the remaining 240 degrees of the circumference would continue to be used by the circulating protons. The bypass could be used as another extraction point and would have advantages as an internal-target location, because the radioactivity generated would not contaminate the main accelerator and because it offers more flexibility for setting up experiments without interrupting operation. It could also be used to feed either of two possible types of storage rings.

- (i) Large Intersecting Storage Rings. In case future research should demonstrate its desirability, space on the site has been reserved for concentric intersecting storage rings of the same radius as the main accelerator. Protons would be injected into the rings from the extracted beam associated with the external by-pass. The storage facility might well utilize superconducting magnets. It could provide 200-200 BeV collisions, with an equivalent laboratory energy of 80,000 BeV. Further, slow acceleration might be carried out in it to proton energies of 1000 BeV.
- (ii) The Bypass Storage Ring. A small single storage ring of radius about 100 m that might contain energies up to 50 BeV, could be located between the bypass and the main accelerator as sketched in Fig. 18-2. It could be loaded from the accelerator. In fact, it could be loaded to quite high intensity at 50 BeV by a number of pulses from the main accelerator. Half of this cir-



culating beam could then be reinjected from the storage ring into the main accelerator to achieve higher intensity in it (since the space-charge limit would be higher at 50 BeV than at conventional 10 BeV injection). Colliding-beams experiments could then be performed with the storage-ring protons interacting with the main-accelerator protons in the bypass.

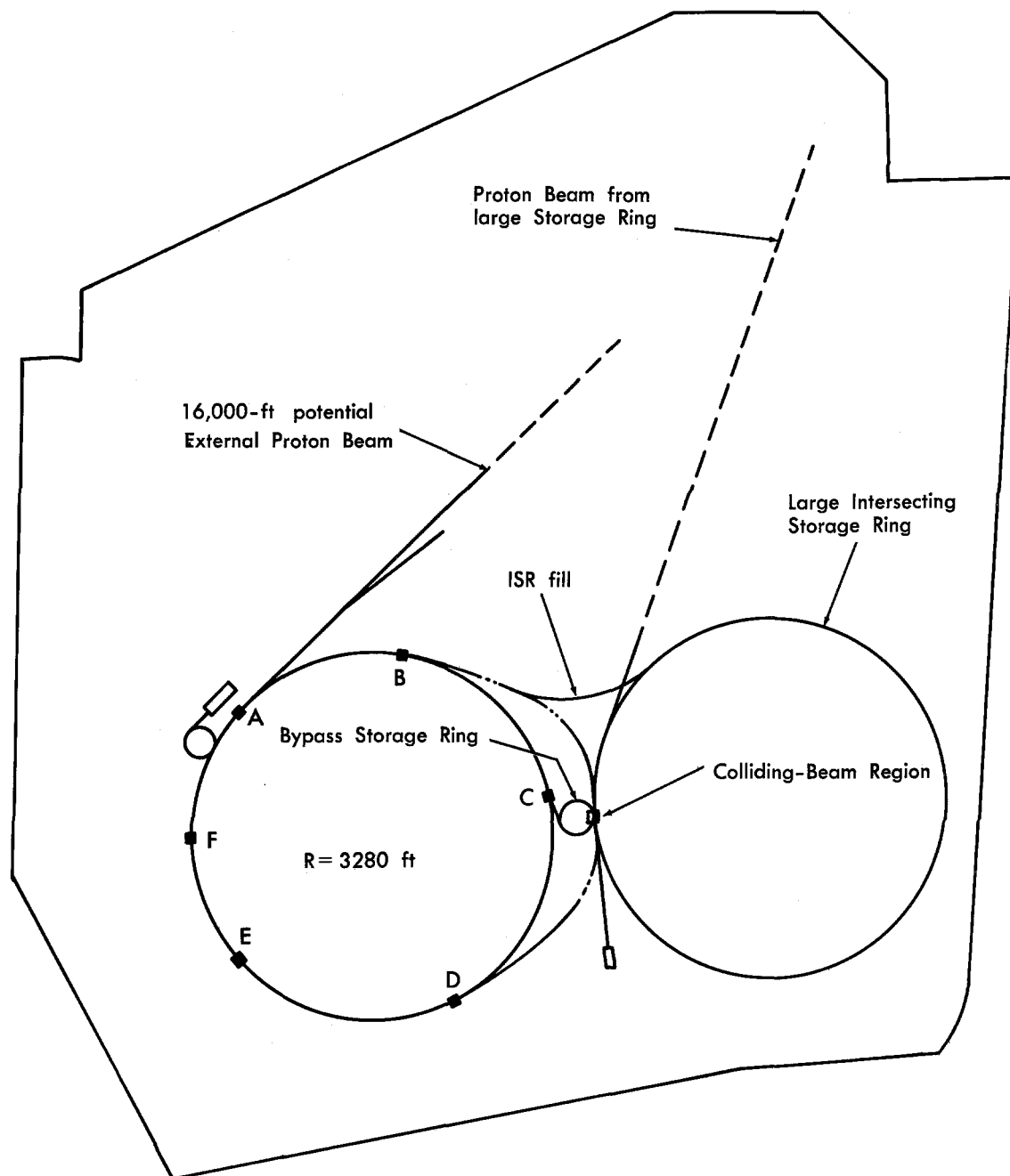


Figure 18-2 — Options for Future Expansions

Colliding-Beam Interactions. In colliding-beam interactions, much more energy is available than in the interaction of a proton with a stationary target. It is difficult to study colliding-beam interactions because they are relatively rare compared with interactions between either of the proton beams and the background gas, even with a very good vacuum. Furthermore, the interaction itself, because it occurs inside two intense beams, cannot be directly observed, but must be inferred from observation of the emergent particles. Consequently, it would not be prudent to propose complete dependence on colliding beams at this time, but experience gained with the 30 BeV intersecting storage ring now being constructed at CERN might well demonstrate that colliding beams are the best way to approach super-high energies.

Tests of great significance for physical theories can be envisaged with 200 BeV storage rings. For example, Serber has suggested <sup>2</sup> that the cross sections for large momentum-transfer events at proton-proton center-of-mass energies of the order of 200 BeV may well be quite large and that a quark model would predict them to be appreciably larger than a non-quark model. Thus studies of such interactions might give results bearing directly on the structure of the neutron and proton. Were the cross sections observed to fall off exponentially, this might have the most radical implications for physics. A question would be raised about the measurability of very small distances, and our basic concepts of space and time would be challenged.

Table 18-2 gives center-of-mass and equivalent laboratory energies for the bypass storage ring at various energies. The center-of-mass energy is the amount available in a nuclear interaction. The CERN Intersecting Storage Ring (ISR) is included for comparison.

Table 18-2. Energies of Bypass Storage Ring

	<u>Kinetic Energy</u> <u>(BeV)</u>		<u>Center-of-Mass</u> <u>Energy</u>	<u>Equivalent</u> <u>Laboratory</u>
	<u>Beam 1</u>	<u>Beam 2</u>	<u>(BeV)</u>	<u>Energy (BeV)*</u>
NAL Accelerator	200	0	20	200
	400	0	28.3	400
CERN ISR	30	30	60	1,800
Bypass Storage Ring	200	25	141	10,000
	200	50	200	20,000
	200	100	283	40,000

\*Energy of a proton giving the same center-of-mass energy in a collision with a stationary proton (zero energy in Beam 2).

Other Uses of Bypass and Storage Ring. A bypass and storage ring provide additional features that increase their experimental utility:

a. The storage ring can be used to store stable (or nearly stable) particles. Thus it could be used to store muons. Stored muons would permit much improved measurements on muon properties; the muon g-factor, scattering cross sections, etc.

b. It can also store antiprotons produced at a target in the bypass enclosure. Such operation, at say 30 BeV, might allow antiprotons at, say 10 BeV to be stored for many pulses. These stored antiprotons could then be reinjected into the main ring and accelerated to 200 BeV. This opens up the field of study of high-energy anti-particle interactions.

c. The storage ring can be used to extend the duty-cycle capabilities of the accelerator. As a storage device, it can filter out all discontinuities and provide a uniform dc beam output. It can also store many pulses and then emit all the stored particles onto a target to make one very large pulse; this could be useful for certain types of experiments.

References:

1. E. D. Courant et al, Bypass-Storage Ring Option for NAL, National Accelerator Laboratory Report NAL-5, August 30, 1967.
2. R. Serber, Cross Sections at Large Momentum Transfer, National Accelerator Laboratory Report NAL-8, November 28, 1967.

## Appendix



## APPENDIX A

### ACCELERATOR PARAMETERS

Compiled by L. C. L. Yuan

#### I. MAIN ACCELERATOR

##### A. Principal Parameters

1. Final energy	200 BeV
2. Intensity	$5 \times 10^{13}$ protons/pulse ( $1.5 \times 10^{13}$ protons/sec)
3. Average Radius (circumference/ $2\pi$ )	1 km (3281 ft)
4. Magnetic radius	2434 ft (742 m)
5. Circumference	20614 ft (6283 m)
6. Lattice type	Separated function with matched long straight sections
7. Injection energy	10 BeV
8. Space-charge limit	$3 \times 10^{14}$ protons
9. Betatron-oscillation wave number	20.25
10. Synchrotron oscillation wave number	0.002
11. Transition kinetic energy	17.4 BeV
12. Rise time	1.6 sec
13. Flat-top time	1 sec
14. Repetition rate	
a. without flat-top	20 pulses/min
b. with 1.0 sec flat-top	15 pulses/min
15. Duty factor	0-25%
16. Beam emittance at 200 BeV	
a. vertical	$0.09\pi$ mm-mrad
b. horizontal	$0.23\pi$ mm-mrad
17. Energy resolution $\Delta E/E$	0.01%

##### B. Lattice Structure and Orbit Parameters of Main Accelerator

1. Normal cell (C)	
a. Length of bending magnet (B1 and B2)	19 ft 11 in (6.07 m)
b. Length of cell quadrupole magnet (QF and QD)	7 ft (2.13 m)
c. Length of minimum separation between magnets (S)	1 ft (0.305 m)

- d. Length of short straight section (SS) 6 ft 11 in (2.11 m)
  - e. Cell structure (QF)SS(B1)S(B1)S(B2)S(B2)S-(QD)SS(B2)S(B2)S(B1)S(B1)S  
(8 bending magnets - 4 B1 and 4 B2)  
(2 quadrupole magnets - QF and QD)
  - f. Total length of cell 195 ft 2 in. (59.49 m)
  - g. Total number of normal cells 84
2. Cell with medium straight section (M)
    - a. Length of medium straight section (MS) 63 ft 9 in. (19.43 m)
    - b. Cell structure (QF)SS(B1)MS(QD)SS(B2)S(B2)-S(B1)S(B1)S
    - c. Total length of cell 195 ft 2 in. (59.49 m)
    - d. Total number of cells with MS 6
3. Cell with matched long straight section (L)
    - a. Length of end matching quadrupole magnet (QFE and QDE) 3 ft 10 in. (1.168 m)
    - b. Length of outer matching quadrupole magnet (QFO and QDO) 9 ft 9 in. (2.97 m)
    - c. Length of inner matching quadrupole magnet 11 ft 10.85 in. (3.628 m)
    - d. Length of end straight section next to QFE (FS) 31 ft (9.449m)
    - e. Length of end straight section next to QDE (DS) 4 ft 2 in. (1.27 m)
    - f. Length of separation between outer and inner matching quadrupole magnets (TS) 4 ft 10.44 in. (1.484 m)
    - g. Length of long straight section (LS) 169 ft 4.68 in. (51.63 m)
    - h. Cell structure (QFE)FS(B1)S(B1)S(B1)S(QFO)-TS(QDI)LS(QFI)TS(QDO)SS(B2)S-(B2)S(B2)S(B2)DS(QDE)SS(B2)S-(B2)S(B1)S(B1)S
    - i. Total length of cell 508 ft 2.25 in. (154.9 m)
    - j. Total number of cells with LS 6
4. Superperiod
    - a. Structure C C C C C C M C C L C C C  
C C C
    - b. Total length of superperiod 3435 ft 8.25 in. (1047.2 m)
    - c. Total number of superperiods 6

5. Orbit Functions	
a. Betatron wavelength	310.3 m
b. Betatron amplitude function $\beta$	
Normal cells and Medium straight sections	
$\beta_x$ max.	98.8 m
$\beta_z$ max.	99.0 m
Long straight sections	
$\beta_x$ max.	115.2 m
$\beta_z$ max.	115.0 m
c. Momentum compaction $X_p$ per ( $\Delta p/p$ )	
Normal cells (max)	5.59 m
Medium straight sections (max)	4.59 m
Long straight section (max)	3.89 m
Average	2.62 m
d. Revolution period	
injection	21.04 $\mu$ sec
final energy	20.96 $\mu$ sec

#### C. Magnet System of Main Ring

1. Rise time	1.6 sec
2. Flat-top time	1.0 sec
3. Bending magnets	
a. Type B1 magnets	
i. Number of units	384
ii. Length	19 ft 11 in. (6.07 m)
iii. Aperture	1.5 in. (high) x 5 in.
iv. Injection field	490 G (10 BeV)
v. Peak field	9.03 kG (200 BeV) 18.02 kG (400)
vi. Number of turns of coil	12
vii. Current	2300 A (200 BeV) approx. 5000 A (400)
b. Type B2 magnets	
i. Number of Units	384
ii. Length	19 ft 11 in. (6.07 m)
iii. Aperture	2 in. (high) x 4 in.
iv. Injection field	490 G (10 BeV)
v. Peak field	9.03 kG (200 BeV) 18.02 kG (400)
vi. Number of turns of coil	16
vii. Current	2300 A (200 BeV) approx. 5000 A (400)

4. Normal-cell quadrupoles	
a. Number of units	180
b. Length	7 ft (2.13 m)
c. Gap size	2 in. (high) x 5 in.
d. Injection field gradient	6.8 kG/m
e. Peak field gradient	125 kG/m
	250 kG/m
5. Matching quadrupoles	
a. Number of units	
i. Outer matching quadrupoles	12
ii. Inner matching quadrupoles	12
iii. End matching quadrupoles	12
b. Length	
i. Outer matching quadrupoles (QFO, QDO)	9 ft 9 in. (2.97 m)
ii. Inner matching quadrupoles (QFI, QDI)	11 ft 10.85 in. (3.63 m)
iii. End matching quadrupoles (QFE, QDE)	3 ft 10 in. (1.17 m)
c. Peak field gradient	125 kG/m (200 BeV)
	250 kG/m (400 BeV)
6. Correction magnets	
a. Closed-Orbit Deflecting Magnets	
i. Field Strength	$\pm 3$ kG
ii. Length of each unit	1 ft
iii. Number of units	1 per cell
iv. Total number of units	96
b. Trimming quadrupoles	
i. Field gradient	$\pm 7$ kG/m
ii. Length of each unit	0.5 ft
iii. Number of units	2 per cell
iv. Total number of units	192
c. Sextupoles	
i. Field gradient	$\pm 2000$ kG/m
ii. Length of each unit	1 ft
iii. Number of units	2 per cell
iv. Total number of units	192
7. Magnet weight (Total of all Units)	
a. Core Steel	8900 tons
b. Copper	850 tons
8. Power Supply	Rectifier-Inverters (no rotating machine)
a. Inductance of magnet circuit	5.37 H
b. Resistance of magnet circuit	6.01 $\Omega$ (at 40° C)



9. Power Input
  - a. Peak 53 MW
  - b. Mean 16 MW
  - c. Reactive voltamperes approx. 10 MVAR (max)
  - d. Total voltamperes 28 MVA (max)

D. Magnet Support, Adjustment, Foundation, Survey and Enclosure

1. Magnet support and adjustment
  - a. Support Magnets supported at ends by adjustable pedestals. No support beams.
  - b. Adjustment Jacks equipped with gears which can be adjusted by coupling to remote controlled traveling device
2. Foundation Slab on ground. No piles.
3. Survey Cross wires and position pick-ups attached to pedestal.
4. Enclosure
  - a. Size
    - i. Cool sections 10-ft diameter horseshoe-shaped precast-concrete
    - ii. Hot sections (straight sections A and B) 16 ft 6 in. high x 20 ft wide rectangular poured-in-place concrete.
    - iii. Straight sections C, D, E, F, and medium straight sections 12 ft diameter horseshoe-shaped precast concrete sections, 11 ft wide at base.

E. Vacuum System of Main Accelerator

1. Vacuum chamber
  - a. Material and wall thickness < 50 mil stainless steel
  - b. Size
    - i. Type B1 magnets 3.5 cm x 12 cm (inside dim.)
    - ii. Type B2 magnets 5 cm x 10 cm oval (inside dim.)
  - c. Length
    - i. Type B1 and B2 magnets (as integral unit of each magnet) 21 ft
    - ii. Quadrupole magnets (as integral unit of each magnet) 8 ft
2. Pumping System
  - a. Number of sputter-ion pumps
    - i. Vacuum envelope (50 l/sec) 400
    - ii. RF cavities (200 l/sec) 16

iii. Long straight sections (100 $\ell$ /sec)	12
iv. Special tanks (2000 $\ell$ /sec)	3
b. Number of roughing-pump stations	6 permanent plus portable units

#### F. Radio-Frequency System of Main Accelerator

1. Injection energy	10 BeV
2. Final energy	200 BeV
3. Main accelerator magnet rise time	1.6 sec
4. Acceleration Cycle Time	
a. Injection (no acceleration)	0.8 sec (0-0.8 sec)
b. Rise time from 10-16.3 BeV	0.1 sec (0.8-0.9 sec)
c. Rise time from 16.3-200 BeV	1.5 sec (0.9-2.4 sec)
5. Average	5.69 kG/sec
6. Synchronous phase - programmed	50° max
7. Peak rf voltage per turn	3.47 MV
8. Energy gain per turn	2.66 MeV
9. Average circulating beam current	0.382 A
10. Harmonic number	1120
11. Injection frequency	53.24 MHz
12. Final frequency	53.44 MHz
13. Relative frequency change	0.37%
14. $R_b$ (beam shunt resistance)	7 M $\Omega$
15. Total number of accelerating cavities	16
16. Length of individual cavity	68 in.
17. Required straight-section length	91 ft
18. Orbit frequency range	47.54-47.71 kHz
19. Total rf power input	
a. Peak	2 MW
b. Mean	1 MW
20. Total rf-system stored energy	12 J

## II. BOOSTER SYNCHROTRON

### A. Principal Parameters

1. Output energy	10 BeV
2. Injection energy	0.2 BeV
3. Transition kinetic energy	4.48 BeV
4. Beam intensity	$3.8 \times 10^{12}$ protons/pulse
5. Orbit radius	75 m
6. Magnetic radius	43.7 m
7. Lattice type	FOFDOOD, combined function
8. Cycling rate	15 Hz
9. Guide field at injection	490 G
10. Peak guide field	8.32 kG
11. Betatron oscillation wave number	6.75

## B. Lattice Structure and Orbit Parameters

### 1. Cell Structure

a. Number of cells	24
b. Cell length	19.63 m
c. Number of gradient magnets per cell	4
d. Length of long straight section	5 m
e. Length of short straight section	2 m
f. Length of intermagnet straight sections	0.6 m
g. Circumference factor	1.72

### 2. Orbit Parameters

a. Betatron wavelength $\beta$	69.8 m
b. Betatron amplitude function gradient magnets,	
$\beta_F$ (max) horizontal	30.7 m
$\beta_F$ (max) vertical	11.6 m
$\beta_D$ (max) horizontal	15.5 m
$\beta_D$ (max) vertical	22.6 m
c. Momentum compaction, $X_p$ per ( $\Delta p/p$ )	
F (max)	2.9 m
D (max)	2.1 m
d. Phase advance per cell	0.28(2 $\pi$ )
e. Synchrotron oscillation wave number (max.)	0.1
f. Revolution period	
at injection	2.78 $\mu$ sec
at ejection	1.58 $\mu$ sec

### C. Beam-Transfer Parameters

1. Typical injection operational mode	75 mA, 4 turns (75% <del>4/6</del> )
2. Charge injected into main ring, nominal (13 booster cycles)	$5.0 \times 10^{13}$ protons
a. Injector transverse emittance area	$\pi$ cm-mrad
b. Transverse emittance area, after stacking (nominal)	
horizontal	$5\pi$ cm-mrad
vertical	$2\pi$ cm-mrad
c. Booster transverse emittance area at ejection (nominal)	
horizontal	$0.3\pi$ cm-mrad
vertical	$0.12\pi$ cm-mrad
d. Injector momentum spread after debuncher, ( $\Delta p/p$ )	$\pm 1.1 \times 10^{-3}$

e. Booster momentum spread for bunched beam at injection	$\pm 2.5 \times 10^{-3}$
f. Bunching factor	0.44
g. Longitudinal phase-space area at injection	2.22 eV-sec
h. Bucket area at injection	3.00 eV-sec
i. Booster momentum spread at ejection	$\pm 0.9 \times 10^{-3}$
j. Booster bunching factor at ejection	0.14

#### D. Aperture Requirements

1. Vacuum envelope, internal dimensions (approx. elliptical)
  - a. Gradient magnets, F, horizontal 5.5 in.  
                                     F, vertical 1.75 in.  
                                     D, horizontal 4.0 in.  
                                     D, vertical 2.5 in.
  - b. Long straight section  
     horizontal 2.25 in.  
     vertical 2.5 in.
  - c. Vertical magnet gap (F) 2.25 in.  
                                     (D) 3.0 in.

#### E. Magnet System

- |  |                |
|--|----------------|
| 1. Number of gradient magnets                | 48 (D), 48 (F) |
| 2. Effective length of (F) unit              | 2.86 m         |
| 3. Effective length of (D) unit              | 2.86 m         |
| 4. Magnet cross section                      | 25 x 18 in.    |
| 5. Profile parameter<br>in F unit            | 2.36 /m        |
| 6. Profile parameter<br>in D unit            | 2.48 /m        |
| 7. Number of correcting sextupole components | 24             |
| 8. Number of tune-correcting quadrupoles     | 24             |
| 9. Number of skew-quadrupole elements        | 48             |
| 10. Number of closed-orbit deflectors        | 48             |

#### F. Magnet Power Supply

- |                                |                                       |
|--------------------------------|---------------------------------------|
| 1. Magnet excitation           | sinusoidal by biased resonant circuit |
| 2. Number of resonant sections | 24                                    |
| 3. Magnet current at injection | 124 A                                 |
| 4. Peak magnet current         | 2100 A                                |
| 5. Bias current                | 1100 A                                |

6. Magnet stored energy (max.)	1.6 MJ
7. Magnet inductance	0.7 H
8. Dc magnet coil resistance	0.8 $\Omega$
9. Number of magnets	96
10. Number of resonant cells	24
11. Peak power-supply voltage (ac)	2.9 kV
12. AC voltage per cell (rms)	2.0 kV
13. Max. voltage to ground	1.6 kV
14. Capacitance per cell	7260 $\mu$ F
15. Choke inductance per cell	0.03 H
16. Peak capacitor stored energy	720 kJ
17. Choke stored energy, total	1.64 MJ
18. Total ac power losses	1.1 MW
19. Total dc power losses	1.9 MW
20. Losses	
magnets (dc)	980 kW
(ac)	510 kW
chokes (dc)	980 kW
(ac)	510 kW
capacitors (ac)	91 kW

#### G. Booster Acceleration System

1. Frequency range	30.256 - 53.242 MHz
2. Harmonic number	84
3. Number of cavities	18
4. Maximum energy gain per turn	0.76 MeV/turn
5. Peak rf voltage	0.85 MV/turn
6. Maximum voltage per cavity (2 gaps)	48 kV
7. Peak total rf power	0.7 MW
8. Peak power to beam	0.3 MW
9. Cavity length	2.4 m

#### Ferrite Tuners - Total for two tuners/cavity

10. Ferrite Density	5 gm/cm <sup>3</sup>
11. Ferrite Weight per cavity	1200 lb
Ferrite Volume	110,000 cm <sup>3</sup>
12. Maximum H <sub>dc</sub>	30 kA/m
13. Minimum H <sub>dc</sub>	5 kA/m
14. Ferrite $\mu_{\Delta}$ Injection	7.2
15. Ferrite $\mu_{\Delta}$ Ejection	1.5
16. Axial Field strength in gap	0.32 MV/m
17. Cavity rf current (at current maximum)	1200 A
18. Cavity Z (tapers from 80 $\Omega$ at gap to 20 $\Omega$ at center)	60 $\Omega$
19. H <sub>rf</sub> (at location of ferrite)	0.78 kA/m
20. RF stored energy/ cavity at maximum voltage	0.03 J

### III. LINEAR ACCELERATOR

#### A. Energy

1. Input energy	0.75 MeV
2. Output energy	200.30 MeV
3. Output energy spread, $\Delta E$	
a. Before debuncher	$\pm 1 \text{ MeV}$
b. After debuncher	$\pm 0.4 \text{ MeV}$

$$\frac{\Delta p}{p} = 2.8 \times 10^{-3}$$
$$1.1 \times 10^{-3}$$

#### B. Beam Characteristics

1. Peak Beam Current	75 mA
2. Beam pulse length	100 $\mu$ sec
3. Pulse rate	15/sec
4. Duty cycle (max)	0.15%
5. Beam emittance at 200 MeV (each transverse mode)	0.5 $\pi$ to 1.0 $\pi$ cm-mrad

#### C. RF Characteristics

1. RF frequency	201.25 MHz
2. RF pulse length	300 $\mu$ sec
3. Repetition rate (max)	15 pps
4. RF Duty factor	0.5%
5. Peak rf excitation power	22 MW
6. Average rf excitation power	110 kW
7. Total peak rf power (at 75 mA)	37 MW

#### D. Physical Characteristics

1. Number of Accelerating Cavities	9
2. Total length including drift space between cavities	145.8 m
3. Number of drift tubes	286
4. Aperture	
a. Input at Tank 1	2 cm
b. Output at Tank 9	4 cm

### IV. PREACCELERATOR

1. Voltage	750 kV
2. Voltage stability	$\pm 0.05\%$
3. Ion-beam current	220-300 mA
4. Beam pulse length	30-100 $\mu$ sec
5. Pulse repetition rate	15/sec
6. Beam emittance	50 $\pi$ mm-mrad
7. Power-supply type	Cockroft-Walton
8. Accelerator-tube length	11.8 in. (30 cm)
9. Accelerator-tube aperture	2.5 in.

